An Integrated Analysis of the Extended Hippocampal System Across Species

Kathleen Yolande Faye Christiansen

A Thesis submitted to the Senate of Cardiff University in Partial Fulfilment of the Requirements for the degree of Doctor of Philosophy

School of Psychology

Cardiff University

September 2016

Summary

The objective of this thesis was to investigate functional differences within the extended hippocampal system by 1. analysing its connectional topography and 2. looking at evidence for differential functions within its component structures. The main areas under examination were A. the subiculum and B. its diencephalic targets, along with C. the fornix, the principle white matter tract connecting these structures.

Retrograde tracer experiments in rodents and primates revealed consistent topographies in the subiculum projections to these diencephalic target sites, with distinctions occurring primarily along the proximal-distal and laminar subicular axes in rodents and primarily along the anterior-posterior and laminar subicular axes in primates. Based on different input patterns to the proximal subiculum (principally from sites processing object information) and distal subiculum (principally from sites processing spatial/context information) it was predicted that this proximal-distal axis would show functional activation differences in rodents for matched object:spatial tasks. Immediate early gene imaging (using *zif268* expression) did not, however, reveal clear-cut gradient differences, although there were indications of the expected bias to object memory in the proximal subiculum.

Diffusion MRI was used to study the fornix by separating its precommissural and postcommissural connections in a healthy older and cognitively impaired human population. Reliable topographic differences were found for the precommissural and postcommissural fornix in each group but cognitive function proved difficult to differentiate between the tracts for the tasks used. Lastly, fornix reconstructions were also found to be separable according to their links with either the anterior or posterior

hippocampus in a healthy population. These distinctions provide another way of studying the fornix in terms of relating different functional properties with different sets of hippocampal connections. It is assumed that different populations of fornical fibres should underlie different aspects of memory/ cognitive tasks involving the fornix, making their segregation informative in future studies researching this tract. detailing the nature of the connections within the extended hippocampal system, this thesis lays the groundwork for future studies investigating the relative roles of its component structures in cognitive function.

“We never say anything unless it is worth taking a long time to say”

- *Treebeard*

List of Publications

Research presented in Chapters 2 and 4 of this thesis has been included in the following publications:

Christiansen, K., Aggleton, J. P., Parker, G. D., O'Sullivan, M. J., Vann, S. D., & Metzler-Baddeley, C. (2016). The status of the precommissural and postcommissural fornix in normal ageing and mild cognitive impairment: An MRI tractography study. *NeuroImage, 130*, pp 35-47.

Christiansen, K., Dillingham, C. M., Wright, N. F., Saunders, R. C., Vann, S. D., & Aggleton J. P. (2016). Complementary subicular pathways to the anterior thalamic nuclei and mammillary bodies in the rat and macaque monkey brain. *The European Journal of Neuroscience, 43*, pp 1044-1061.

Research presented in Chapter 5 of this thesis is currently under review for the following publication:

Christiansen, K., Metzler-Baddeley, C., Parker, G. D., Muhlert, N., Jones, D. K., Aggleton, J. P. & Vann, S. D. (2016). Topographic separation of fornical fibres associated with the anterior and posterior hippocampus: an MRI-diffusion study. *Brain and Behaviour,* (under review).

Acknowledgements

I have never been particularly adept at expressing the insurmountable gratitude I feel to those who have helped me through these past four years. In any case, I will attempt to acknowledge both the scientific contributions and emotional and moral support that went into this body of work.

First and foremost, thank you to my primary PhD supervisor, Professor Seralynne Vann. You are my role-model, both as a woman leading cutting-edge research in the field of neuroscience, and as an all-around amazing human being. I know I cannot have been the easiest of students; I have had a lot of life-events outside of academia putting strain on my performance and overall well-being during this PhD, but you have always been there for me, with scientific aspiration, motivation, and support beyond measure. My ability to write scientifically also leaves a lot to be desired, but you have persevered with me nonetheless and your advice and wisdom are and always will be greatly appreciated. I have been very blessed to have you as my supervisor, and I can honestly say I do not think I would have gotten past the first hurdle without you, let alone be where I am now. On top of this, the ethical complications with my original PhD project would have left me lost to the wind without you leading the way.

Professor John Aggleton, thank you so much for taking me on as a volunteer when I had finished my undergraduate degree in Psychology and wanted experience in research in the neuroimaging/neuroscience fields. My spark of enthusiasm had just been lit having done the final year modules in memory and neuroimaging, and you provided the fuel to keep that fire burning, which continues to this day. Your passion and optimism for the study of the brain are nothing short of inspirational, and needless to say you are a legend

in your field – a recognition acknowledged across the world. As my secondary supervisor, the knowledge you have imparted on me in terms of not only neural anatomy but how to conduct oneself in science is beyond measure and I will be forever in your debt.

To my unexpected tertiary supervisor, Dr Claudia Metzler-Baddeley, how lucky I was to get a third supervisor also so renowned in my area of interest and with enough passion, determination and wisdom for an army of scientists! Without your neuroimaging expertise and extreme generosity, the latter two experimental chapters of this thesis simply would not have been possible. While I wish it was not an important aspect still, I have to reiterate how lucky I have been to have another astounding female scientist providing me with support and guidance. You are a prime example of what is possible for women to achieve in science, if we set our minds to it. There is still a huge discrepancy between the number of men and women pursuing these topics, and you and Seralynne are part of the movement pushing to destroy this inequality.

Continuing on the academic note, a huge thank you to Chris Dillingham, Eman Amin, Nick Wright, Nils Muhlert, and Derek Jones.

Chris Dillingham – thank you for your help statistically and for the figures provided by you for our published paper and which I have used in Chapters 2 and 6 of this thesis (acknowledged there also). Your illustration skills and expertise know no bounds!

Eman Amin – thank you for being my mentor in all things neuroscience methods-wise, you taught me so much and were so generous with your time and patience, I have no

clue how I could ever repay you! You made everything much less stressful than it could have been, and are a general pleasure to be around and talk to.

Nick Wright – thank you for all your help in the early days when I was still volunteering, you showed me the ropes with the microscope and cell-counting techniques and were so kind with sharing/digging up prior collected brain tissue. You were a brilliant and thorough teacher and certainly made those days where my learning-curve was at its steepest a lot more tolerable!

Nils Muhlert – you are the omniscient neuroimaging guru, that is all there is to it! There is no question I asked that you did not have some kind of solution to. I cannot thank you enough for taking the time out of your busy schedule for helping a poor, naïve PhD student when you really had no obligation to whatsoever. You were my encyclopaedia of imaging knowledge and were always only an e-mail away. Thank you for taking the pressure off, especially before I had Claudia as my third supervisor and so was at a loss with neuroimaging dilemmas.

Derek Jones – where would I be without the Jedi master of all things diffusion imaging? I am eternally grateful for all the time and effort you put into me when I was volunteering before my PhD with you and John. You are always striving for greatness and your endless desire for improvement helped spur me on whenever I was at the end of my tether with the constantly evolving world of imaging. Your informal, modest and hilarious personality put me at ease - a feeling I do not often get when in the presence of brilliant minds!

An additional acknowledgement goes to Nick Wright, Chris Dillingham, John Aggleton and Richard Saunders for providing the data for Chapter 2, and Eman Amin, Anna Powell and Liad Baruchin for the data used in Chapter 3. Furthermore, thank you to Mike O'Sullivan, John Evans, Derek Jones, and Claudia Metzler-Baddeley for providing the data for Chapter 4, and Derek Jones, Karen Caeyenberghs, Sonya Foley and Claudia Metzler-Baddeley for the data in Chapter 5.

On a more personal note now, thank you to my best friend, brain-mate, and partner, Liam Reynolds. You have essentially been with me through the thick of it all, you poor thing! Thank you for putting up with me throughout my determined and inspired Daenerys Targaryen moments, and also throughout my stressed-out and callous Cersei Lannister moments. You provided light in my darkest hours, and an unwavering overtone of logic and reason when I was over-reactive and logically impaired. I genuinely do not think I will meet another person so like-minded, with our warped sense of humour and view of the world in general. I know that whatever the future holds, we will always be comrades.

To my wife (if only I was a man), best friend, my everything, Hayley Van-de-Burgt, thank you for being you. You have been my rock for not just the last four, but 15 years, and are the only person who, when I have been in my lowest moments, kept me laughing and smiling. That being said, during the more serious times, you have always pulled me through, and I hope I have done the same for you. I am thankful beyond words to have you in my life.

To my mother – thank you for pushing me to the furthest point of my intellectual capabilities, despite still not knowing what a PhD entails! Thank you to my Nan, Janet

Jackman, who is sadly unable to witness this achievement, but who always showed pride in me for pursuing an academic path, and helped me out on many occasions. I wish you were here to see my graduation. Likewise, thank you to my second family, the Van-de-Burgts, who have supported me when I was in need, despite having so much on their plates already. Thank you especially to Linda and Nick - proof that family is much more than blood.

To Christina Crosby/Mama Llama – thank you for being my second mother and for your guidance in all things PhD and existential crisis related. I have always felt I can be myself around you. Thank you for letting me talk your ear off about the labour of academia and never getting fed up (or at least never showing it!). Melissa Reynolds – thank you for being that unjudging voice of openness and kindness in my life, and a beautiful person inside and out. You will always be my sestra.

Thank you to Julie Perkin, my team leader, and Karen Kirk my general manager – you have been extremely understanding and patient with me while I finished writing my thesis whilst working full-time in a completely unrelated job. I doubt many others would put up with me!

As for the rest of my friends and colleagues – too many to list separately here – thank you for not letting me become a hermit crab. I can be closed off at the best of times and your persistence to get me out of my shell and generally get some vitamin D is greatly appreciated. Thank you for your patience with me, here's to the good times ahead!

Contents

List of abbreviations

abFornix:	anterior body of the fornix
AC:	anterior commissure
ACE:	Addenbrooke's Cognitive Examination
AD:	anterodorsal nucleus and axial diffusivity
aHPC:	anterior hippocampus
AM:	anteromedial nucleus
aMCI:	amnestic Mild Cognitive Impairment
Amyg/TSX:	ventroamygdalofugal pathway transection
ANOVA:	analysis of variance
A/P:	anterior/posterior
ATN:	anterior thalamic nuclei
AV:	anteroventral nucleus
BC:	Behavioural Control
BOLD:	blood oxygen level dependent
CA:	cornu ammonis
CHARMED:	composite hindered and restricted model of diffusion
CSF:	cerebrospinal fluid
CT:	computed tomography
CUBRIC:	Cardiff University Brain Research and Imaging Centre
Cy:	cynomolgus monkey
DAB:	diaminobenzidine
DBS:	deep brain stimulation
DG:	dentate gyrus
D-KEFS:	Delis and Kaplan Executive Function System
dRL:	damped Richardson-Lucy
DTI:	diffusion tensor imaging

D/V: dorsal/ventral

DY: Diamidino Yellow

EPI: echo-planar imaging

f: tissue volume fraction

FA: fractional anisotropy

FB: Fast Blue

FCSRT: Free and Cued Selective Reminding Test

fMRI: functional magnetic resonance imaging

FMRIB: Oxford Centre for Functional MRI of the Brain

FnX: fornix transection

fODF: fibre orientation density function

FSL: FMRIB Software Library

FSPGR: fast spoiled gradient echo

FWE: Free Water Elimination

GE: General Electric

H2O2: hydrogen peroxide

HARDI: high angular resolution diffusion imaging

HCC: Home-Cage Control

HMOA: hindrance modulated orientational anisotropy

HRP: horseradish peroxidase

HYPOTH: hypothalamus

IAM: interanteromedial nucleus

IBM: International Business Machines Corporation

ICE: Image Composite Editor

IEG: immediate-early gene

LC: locus coeruleus

LD:	laterodorsal thalamic nucleus
LM/lMB:	lateral mammillary body
LTP:	long term potentiation
MB:	mammillary bodies
mc:	pars magnocellular
MCI:	Mild Cognitive Impairment
MD:	mean diffusivity and medial dorsal nucleus
Mid:	midline
M/L:	medial/lateral
ML/MML:	medial mammillary body pars lateralis
MM/MMM:	medial mammillary body pars medialis
mMB:	medial mammillary body
MMSE:	Mini-Mental State Examination
MNI:	Montreal Neurological Institute
mPULV:	medial pulvinar nucleus
MRI:	magnetic resonance imaging
mRNA:	messenger ribonucleic acid
MTT:	mammillothalamic tract
N. ACC:	nucleus accumbens
NART:	National Adult Reading Test
NeuN:	neuronal nuclear antigen
NIH:	National Institutes of Health
NIMH:	National Institute of Mental Health
OR:	Object Recognition
PAL:	Paired Associate Learning
Para:	parasubiculum

PB:	phosphate buffer
PBS:	phosphate buffered saline
PBST:	phosphate buffered saline with added Triton X-100
PCC:	posterior cingulate cortex
PET:	positron emission tomography
PFA:	paraformaldehyde
PFC:	prefrontal cortex
PHA-L:	Phaseolus vulgaris
pHPC:	posterior hippocampus
Post:	postsubiculum
Pre/PreS:	presubiculum
RAM:	radial arm maze
RD:	radial diffusivity
Rdg:	dysgranular retrosplenial cortex
RE:	nucleus reuniens
Rga/b:	granular retrosplenial cortex a/b
Rh:	rhesus monkey
ROI:	region of interest
S.D.:	standard deviation
SM:	Spatial Memory
SPSS:	Statistical Package for the Social Sciences
Sub:	subiculum
SUM:	supramammillary nucleus
TBS:	Tris buffer solution
TE:	echo time
TI:	inversion time

TMB:	3,30,5,50-tetramethylbenzidine
TR:	repetition time
V:	ventricle
VA:	ventral anterior nucleus
WAIS-III UK:	Wechsler Adult Intelligence Scale - Third UK Edition
WGA:	wheatgerm agglutinin
WGA-HRP:	horseradish peroxidase conjugated to wheatgerm agglutinin
WMS-III:	Wechsler Memory Scale - Third Edition

Chapter 1: Introduction

1.1 Research focus of thesis

This thesis describes research into the connectivity and activity of brain areas involved in learning and memory. The principal focus is on the hippocampal formation (the hippocampus proper and subiculum), given the structure's long-established links with learning and memory. This introduction considers findings from studies of rodents, nonhuman primates, and humans, reflecting the species involved in the research to be described in this thesis. Much of the rationale for this research concerns understanding how the hippocampus is organised with respect to its connections with other sites also critically involved in learning and memory. The overall goal is to further our knowledge about those connections thought to be required for human episodic memory.

1.2 Episodic memory and the extended-hippocampal system

Episodic memory was described by Tulving (1972), who said it "receives and stores information about temporally dated episodes or events, and temporal-spatial relationships among these events". In other words, episodic memory encompasses the "what" "when" and "where" of those individual day-to-day events that are remembered explicitly. Reflecting these demands, Tulving (1972) also included the active search for information linked to past time as part of this definition. In contrast, semantic memory refers to explicit information that lacks a specific context, and so it typically relates to factual information. Consequently, we "remember" episodic memories but "know" semantic information. A distinction is also made with those types of memory that are not explicitly recalled but are revealed by changes in subsequent behaviour, e.g. priming, habituation, procedural learning, and classical conditioning (Schacter, 1987). Because recognition memory is "explicit", i.e. the person can state whether they do or do not recognise an event, this form of memory is usually placed in the former category (with episodic and semantic memory).

The present series of experiments focus on the substrates of episodic memory. The rationale for concentrating on the hippocampal formation and its connections originally derives from neuropsychological studies of anterograde amnesia, where the dominant symptom is a failure of episodic memory (Corkin, 2002; Spiers et al., 2001; Zola-Morgan et al., 1986). For over a hundred years, hippocampal damage has been linked with anterograde amnesia (Bechterew, 1900; Scoville and Milner, 1957; Spiers et al., 2001). This hippocampal focus has more recently been supported by human functional magnetic resonance imaging (fMRI), as well as animal studies that have revealed specific hippocampal contributions to spatial and event memory (Astur et al., 2002; Jarrard, 1993; Maguire et al., 2001; Rugg et al., 2012; Vann et al., 2000b).

Rather than just examine the hippocampal formation, the present experiments also look at its connections to other sites also strongly implicated in episodic memory, most notably sites in the medial diencephalon (this term refers to the thalamus and hypothalamus). The medial diencephalon stands out as, like the hippocampal formation, damage to this region has repeatedly been associated with anterograde amnesia (Aggleton et al., 1995, 1996; Van der Werf et al., 2003; Vann and Aggleton, 2003; Victor et al., 1971). Within the medial diencephalon, neuropsychological studies have repeatedly highlighted the especially close links between pathology in the mammillary bodies, the anterior thalamic nuclei, and their interconnecting tract, the mammillothalamic tract, in diencephalic amnesia (Aggleton and Brown, 1999; Barbizet, 1963; Carlesimo et al., 2011; Delay and Brion, 1969; Harding et al., 2000; Parker and Gaffan, 1997a, b; Van der Werf et al., 2003).

The term “extended hippocampal system” (Aggleton and Brown, 1999) was introduced to highlight the close anatomical and functional ties between the hippocampal formation

and certain medial diencephalic nuclei, e.g. the mammillary bodies and anterior thalamic nuclei. While the dense hippocampal inputs to the mammillary bodies are unidirectional, there are reciprocal connections between the anterior thalamic nuclei and the hippocampal formation (Aggleton and Brown, 1999; Amaral and Cowan, 1980; Poletti and Creswell, 1977; Vann and Aggleton, 2004, Figure 1.1). The numerous hippocampal formation projections to these diencephalic nuclei arise in the subiculum, with a large majority of fibres joining the fornix before reaching their diencephalic targets (Aggleton et al., 1986, 2005b; Dillingham et al., 2015; Poletti and Creswell, 1977; Poletti and Sujatanond, 1980; Saunders and Aggleton, 2007; see Figure 1.1 on page 19). For these reasons, the experiments described in this thesis largely focus on two brain structures, one comprising grey matter (the subiculum) the other comprising white matter (the fornix).

The next few sections describe techniques that have helped to uncover features and actions of the hippocampal formation that relate to either the fornix, the medial diencephalon, or both. These same techniques are used in experiments described in this thesis.

1.2.1 Techniques for investigating the extended hippocampal system across species

1.2.1.1 Anatomical tracers

In order to investigate hippocampal connections in precise detail it is necessary to use invasive techniques that actively track the pathways between target structures. The most common approach has been to inject anterograde or retrograde anatomical tracers, which rely on axoplasmic flow for transport (Lanciego and Wouterlood, 2011). Retrograde flow ensures that axons can transport various materials from where an axon ends (the axon terminal) to the soma of the cell, so revealing its origin. With

anterograde tracers the flow is *vice versa* (from cell-soma to cell tip), while some tracers travel in both anterograde and retrograde directions. The direction of transport depends on the molecular properties of the label such as weight and size, however, mechanisms of transport are the same for both methods. The tracer is transported through active transport in vesicles and lateral diffusion in cell membranes. The most obvious limitation with these methods is that post mortem tissue is required to visualise the locations of the tracer while the injections are in living tissue. For this reason, such methods are not applicable to humans.

One of the most widely used axonal tracers is horseradish peroxidase (HRP), a plant enzyme that can be taken up by axons at their terminals and transported retrogradely to their corresponding cell somas. The activity of this enzyme is then used to stain the cells that the enzyme reached (Kristensson and Olsson, 1971). In the late 1970s a number of fluorescent dyes were developed, as it was discovered that injection of these dyes also resulted in a retrograde fluorescence signal (Akintunde and Buxton, 1992). In addition, a number of tracers that travel in an anterograde direction, e.g. radioactively labelled amino acids have been used to track efferent projections from particular brain sites.

1.2.1.2 Functional imaging

While anatomical tracer studies can reveal the topography of connections between brain areas under investigation, these methods can only indirectly suggest the functional properties of those same regions. A multitude of other methods have, therefore, been applied to provide more direct information about function. One example, already mentioned, involves the testing of patients with particular patterns of brain injury. The assumption is that this approach, e.g. when applied to amnesia, can help define those brain structures necessary for particular aspects of memory.

Other approaches now widely used with humans include functional magnetic resonance imaging (fMRI). In this technique, the blood oxygen level dependent (BOLD) response is measured via the diamagnetic properties of deoxygenated haemoglobin. This response is informative as it is assumed that the more energy consumed by the brain, the more blood flow there will be to the relevant areas using the most energy. One of the major attractions of this method is that it can be used to look, non-invasively, at the activity of a normal brain. This same method is, however, limited by both its anatomical and temporal resolution, although advances are being made rapidly on both fronts (Muftuler and Nalcioglu, 2000; Petridou et al., 2013; Shi et al., 2015; Uğurbil et al., 2013).

One aim of the present research was to use a form of functional imaging that might reveal the same degree of anatomical resolution as that provided by axonal anatomical tracers, i.e. at the level of single neurons. In this way, the two classes of data (anatomical and functional) might best be aligned. For this reason, it was necessary to use animals. Information came from measuring how the activity of immediate-early genes (IEG) reflect different classes of learning. IEGs are genes that are transiently and rapidly transcribed following recent neuronal activity, due to trans-synaptic stimulation, cell membrane electrical activity and neurotrophic growth factors (Sheng and Greenberg, 1990). It has been proposed that IEGs form two distinct classes of genes: regulatory transcription factors, which affect cell function via the genes further downstream that they regulate, and effector factors, which directly control specific cellular functions. Two examples of regulatory transcription factors are c-*fos* and *zif268*, both of which are thought to play a part in long term plasticity (Guzowski, 2002; Tischmeyer and Grimm, 1999). Regulatory transcription factors encode regulatory

proteins that are responsible for late response gene expression, which then serve more specific neuronal response functions. Their initial expression is rapidly prompted at the transcriptional level within minutes of extracellular activity, is transient, and occurs independently of new protein synthesis. IEGs can therefore be described as cellular proteins that are created rapidly following extracellular stimulation of a resting cell.

Of the many IEGs, one of the most commonly used in research is c-*fos*. This IEG is widely spread across the brain and has a relatively rapid rise and fall time after induction (Chaudhuri, 1997; Zangenehpour and Chaudhuri, 2002). Other IEGS include *zif268* [also known as early growth response protein 1 *(EGR1*)], which encodes a zinc-finger transcription factor. The IEG *zif268* has a higher resting level than c-*fos* and shows a more prolonged expression once regulation is increased (Kerr et al., 1996; Zangenehpour and Chaudhuri, 2002). In addition to using IEGs to examine neuronal responses to new learning, changes in IEG activity can also be used to look at the downstream consequences of specific brain injury, e.g. within the rodent extended hippocampal system (Albasser et al., 2007; Dumont et al., 2012; Jenkins et al., 2006).

While the mapping of IEG expression can provide anatomical resolution to the level of a single neuron, it is however limited by its temporal expression. The level of temporal resolution varies depending on the method used to visualise IEG expression (*in situ* for mRNA or immunochemistry for protein products). In the case of IEGs like *c-fos* and *zif268*, peak production of the protein following a stimulating event can lag by as much as 1-2hrs (Aggleton et al., 2012a; Guzowski, 2002; Zangenehpour and Chaudhuri, 2002). This lag inevitably restricts the temporal resolution of the method with regard to defining the specific event that promoted the change in IEG expression.

1.2.1.3 Diffusion MRI tractography

As mentioned at the outset, the experiments described in this thesis involve comparisons across species, with the ultimate goal of better understanding the human brain in health and disease. A fundamental start point involves an improved knowledge of human brain connectivity. There has, for a long time, been an enormous gulf in the depth of knowledge we have about the connectivity of the human brain and that of various species used in experiments. This gulf principally reflects the inability to use *in vivo* methods, such as axonal tracers, with human tissue. Progress has, however, been made using MRI-based methods to reveal new insights into human brain white matter.

Diffusion MRI provides a means of extracting information about white matter micro- and macrostructure within the human brain *in vivo*. It does this by utilising information about Brownian motion – the random diffusion of water molecules in an open space. This is done using a variant of a conventional spin-echo pulse sequence typically used in MRI, with added strong magnetic field gradients in order to gain diffusion information. A number of diffusion weighted and non-diffusion weighted images are acquired, the more diffusion direction gradients included, the more detailed the map of directionality will be, and the more accurate the diffusion derived values. The diffusion of water molecules is particularly informative in biological systems as it tends to be hindered by cell membranes and macromolecules, causing it to travel more so in certain directional planes than others, a property known as anisotropy. This anisotropy is very evident in white matter, where axonal fibres are wrapped in a myelin sheath in order to promote signal transmission and bound tightly in parallel bundles, which results in diffusion being hindered along a particular direction within the axons and provides information about the anatomy of the tract. The pathway perpendicular to the long axis of axons, however, will have much weaker diffusion weighted signal strength, as the

motion of water molecules is hindered in this direction. Areas where water diffusion is free and unhindered are known as isotropic, as water is distributed evenly in all directions.

The initial stages of diffusion MRI tractography involve diffusion tensor imaging, using an algorithm whereby tensors are generated for every voxel in a diffusion weighted image (Basser et al., 1994). These tensors, which can be represented by spheres elliptical or non-elliptical in shape depending on their level of anisotropy, contain information about the diffusion properties of a voxel (Jones et al., 1999). The algorithm for performing tractography on diffusion weighted MRI data works by considering the diffusion tensor fields of voxels alongside their neighbours, and connecting only those where the directions of the principal eigenvectors of the tensors (the direction of fastest diffusion) are compatible (Basser, 1995). The criterion for terminating a tract is based on its fractional anisotropy (found to be the most robust measure for estimating anisotropy of a tract), and is most commonly marked as below 0.15, along with the angle through which it subtends being anatomically implausible (Jones, 1999a).

While this method has provided a break-through in visualising white matter fibres, there are various limitations and pitfalls to the original diffusion tensor imaging technique. One limitation concerns its inability to identify the direction of white matter, i.e. whether it is afferent or efferent to a given site. A further problem concerns the task of unpicking crossing fibres, due to only having a single maximum diffusion tensor (Tournier et al., 2007). This also means that the diffusion direction derived from the tensors in voxels containing multiple fibre orientations is inaccurate, as it will provide the average direction of diffusivity - this will be between the main peaks in the fibre orientation if there is more than one. For this reason, the new commonly used protocol

for tractography involves a technique known as constrained spherical harmonic deconvolution (Farquharson et al., 2013; Tournier et al., 2007). This technique uses high angular resolution diffusion imaging (HARDI) to estimate the fibre orientation distribution within each voxel, thus allowing for the detection of crossing fibre pathways (Farquharson et al., 2013, Tournier et al., 2007, 2008). This is particularly important given that one study estimated a third of white matter voxels to contain multiple fibre populations (Behrens et al., 2003). Since the invention, development, and application of diffusion MRI tractography, numerous studies have utilised it to investigate white matter structures in healthy and clinical populations (Catani and Thiebaut de Schotten, 2008; Ciccarelli et al., 2008; Thiebaut de Schotten et al., 2011).

1.2.2 The hippocampus

Having described the techniques to be used, as well as some of their individual limitations, it is appropriate to describe in more detail the studies that provide the rationale for the experiments that were conducted. As the hippocampal formation is the centre-point of the research, the next section will consider functional evidence about the importance of this structure for aspects of memory. As already noted, the term "hippocampal formation" is used for the hippocampus proper and the subiculum. For this reason, the hippocampal formation includes the dentate gyrus, subfields CA1, CA2, CA3, as well as the subiculum. The latter area includes the prosubiculum, that part of the subiculum at the junction with CA1, but not the parasubiculum or presubiculum.

1.2.2.1 Human studies

Historically, one of the first brain areas implicated in memory and memory loss was the hippocampus (Bechterew, 1900). Interest in this structure was considerably stimulated by the widely known research conducted into patient H.M. (Corkin, 2002). Patient

H.M., who suffered from epilepsy, underwent a bilateral medial temporal lobectomy in order to try and reduce his seizures (Scoville and Milner, 1957). Following the surgery, H.M. suffered from a persistent anterograde amnesia (the inability to recall events that happened post-surgery) and partial retrograde amnesia (the inability to recall events prior to the surgery). It was concluded that these severe memory impairments were due to the loss of key medial temporal lobe structures. Comparisons with other patients strongly suggested that the hippocampus was required for episodic memory (Corkin, 2002; Scoville and Milner, 1957, but see Aggleton, 2013). Other aspects of H.M.'s cognition such as language and skill learning remained intact, and his personality was thought to be little affected. The initial notion that the hippocampus was necessary for long term memory was further supported by another case that had received a left medial temporal lobectomy, but had also suffered undetected, prior tissue damage in the right hippocampus (Penfield and Milner, 1958).

Since these early studies, many more reports have supported the conclusion that memory deficits are found in clinical populations with neurological damage to the hippocampus. Examples include patients with herpes encephalitis, hippocampal sclerosis associated with epilepsy, traumatic brain injury, Alzheimer's disease, schizophrenia, and Mild Cognitive Impairment (MCI) (Aizenstein and Klunk, 2015; Burgess et al., 2002; Dickerson et al., 2005; Heckers et al., 1998; Jessen et al., 2003; Mueller and Weiner, 2009; Petersen et al., 2000; Scoville and Milner, 1957; Trenerry et al., 1993, Tulving and Markowitsch, 1998; van de Pol et al., 2006). A persistent problem, however, has been in confirming whether particular patients have pathologies that are truly confined to the hippocampal formation. This problem is linked to the related problem of finding patients with damage confined to the hippocampal formation.

In such cases, there is a loss of explicit memory while implicit memory can be spared. The most striking deficits relate to the recall of episodic memory. More contentious have been the ways in which recognition memory is disrupted in these examples of amnesia following hippocampal damage. While some cases studies indicate that recognition memory is relatively spared, reflecting a loss of recollective-based recognition but a sparing of familiarity-based recognition (e.g. Aggleton et al., 2005a; Turriziani et al., 2008), other reports fail to see this dissociation (Jeneson et al., 2010; Wixted and Squire, 2010).

The benefit of using neuroimaging techniques in human populations is that it can non-invasively provide information about various structural and functional properties in a normal population as well as those with cognitive impairments associated with structural abnormalities. Functional and structural MRI and positron emission tomography (PET) studies in healthy populations have reported associations between hippocampal size and activation in episodic memory retrieval and recognition for item and context memory, with studies in humans and other animals linking the posterior hippocampus to spatial episodic memory (Good, 2002; Greicius et al., 2003; Lepage et al., 1998; Maguire et al., 2000; Mundy et al., 2013; Rugg et al., 2012). A limitation is that these MRI studies are correlational and need not identify the primary cause of individual variations in memory.

1.2.2.2 Animal studies: Rats

An enormous number of studies have examined the role of the rodent hippocampus in memory. Advantages include the ability to make selective manipulations within the target structure and subsequently confirm their location. An obvious disadvantage concerns the difficulty of determining whether rats have a form of memory closely akin

to episodic memory, as they cannot be directly challenged by asking them to recall day-to-day events. Even so, much attention has gone into the development of behavioural tasks that tax aspects of "what", "when" and "where". While multiple techniques have been used to infer hippocampal function, for the sake of brevity and comparability with clinical studies the focus will be on the outcome of lesion studies.

Many studies have looked at the effects of hippocampal ablation in rats across a broad spectrum of tasks. These studies repeatedly show that the hippocampus is necessary for a number of memory processes, namely involving context, navigation and spatial aspects of memory, often in contrast to seemingly preserved non-spatial learning (Faraji et al., 2008; Good, 2002; Jarrard, 1993; Morris et al., 1982). One suggestion for how the hippocampus supports spatial learning is through the ability to discriminate between overlapping features and experiences though a process known as "pattern separation" (Kesner, 2013; Kesner and Hopkins, 2006; Norman, 2010; Yassa and Stark, 2011). It is argued that the dentate gyrus is of prime importance for this ability, although proximal CA3 (near to dentate gyrus) may also be involved (Lee et al., 2015; Leutgeb et al., 2007; Neunuebel and Knierim, 2014). In a complementary manner, the hippocampus, in particular area CA3, has also been shown to play a role in "pattern completion", which is the ability to reconstruct memory context associations based on degraded or minimised cues (Gold and Kesner, 2005; Neunuebel and Knierim, 2014). For instance, in the study of Gold and Kesner (2005), rats were able to recall a food-well location when 0 to 3 of the four external cues used to initially locate the food well were removed. Following CA3 lesions, the more cues that were removed the more errors that were accrued, whereas control animals exhibited excellent pattern completion in this task. Once again, CA3 does not appear homogeneous in this role as a gradient exists, whereby the distal end of CA3 (closest to CA2) appears to be more involved in pattern

completion than the proximal end (Lee et al., 2015). Moreover, blocking specific receptors in CA3 seems to result in different patterns of spatial memory impairments, i.e. blocking glutamate results in general short-term memory deficits whereas blocking mu-opioid receptors disrupts pattern completion (Kesner and Warthen, 2010).

Memory for temporal order also appears to rely on the hippocampus. Evidence comes from behavioural studies that have tested recency judgements for objects, spatial locations, and odours (Agster et al., 2002; Albasser et al., 2012; Bray, 2014; Ezzyat and Davachi, 2014; Fortin et al., 2002; Hoge and Kesner, 2007; Hsieh et al., 2014; Kesner et al., 2002; Sakurai, 2002). The dorsal hippocampus, particularly CA3 and CA1, also appears to be important for temporal sequence pattern completion (Hoang and Kesner, 2008). Unsurprisingly, fear conditioning appears to be partially dependent on the hippocampus when contextual information is important (Lehmann et al., 2013).

Electrophysiological studies have also revealed cells in the rodent medial temporal lobe that respond specifically to place or grid location within an environment (Moser and Moser 2008; Muller and Kubie, 1989; O'Keefe, 1979). In addition, "time" cells can fire at distinct temporal intervals during an empty time gap, as well as code for spatial and behavioural information (MacDonald et al., 2011). As noted above, another method by which the role of the hippocampus can be examined is through IEG imaging. This technique has been used in rats to show that increased hippocampal IEG activity (such as c-*fos* and *zif268*) follows spatial learning. Of the various IEGs, *zif268* and *Arc* appear to be especially linked to spatial tasks, while c-*fos* expression is often less sensitive (Barry and Commins, 2011; Guzowski et al., 2001; Penke et al., 2013; Toscano et al., 2006, although see Zhang et al., 2002). At the same time, hippocampal IEG expression appears to be relatively insensitive to object-based recognition tests, where rats must

discriminate novel from familiar stimuli (Zhu et al., 1995b). Consequently, a double dissociation exists as the perirhinal cortex can show the opposite pattern of IEG activation, i.e. greater for object-based tasks than spatial tasks (Hall et al., 2001; Kubik et al., 2007; Vann et al., 2000b; Zhu et al., 1995b).

1.2.2.3 Animal Studies: Monkeys

Monkeys show memory impairments similar to those seen in rats following hippocampal lesions, for example in spatial relational learning and the use of allocentric spatial representations in a food foraging paradigm (Lavenex et al., 2006), in scene/place discrimination abilities and for object-in-place associations (Gaffan, 1994; Mishkin, 1978; Parkinson et al., 1988). Moreover, lesions in the monkey hippocampus result in much milder deficits in object recognition memory than those associated with perirhinal cortex lesions, which result in persistent deficits on such tasks (Alvarez et al., 1995; Beason-Held et al., 1999; Murray and Mishkin, 1998; Zola et al., 2000; Zola-Morgan et al., 1992). Consequently, the relationship between the hippocampus and recognition memory is not straight-forward. For example, monkeys with hippocampal ablations that follow the surgical approach used by Scoville for H.M. do show severe impairments in object recognition memory (Mishkin, 1978). It is the case, however, that this approach also damages adjacent white matter and cortex. When the hippocampus is damaged by a neurotoxin which selectively targets neurons and spares surrounding white matter, monkeys appear not to be impaired on object recognition tasks (Murray and Mishkin, 1998). This suggests that the hippocampus itself is most likely not crucial for this type of memory in monkeys, presumably because the monkeys can rely on preserved familiarity information.

There is also electrophysiological evidence to support the role of hippocampal neurons in primates forming new associative memories, providing allocentric spatial co-ordinates, and responding to view, body motion and head direction (Georges-François et al., 1999; O'Mara et al., 1994; Rolls and O'Mara, 1995; Rolls et al., 1997; Wirth et al., 2003). Spatial-view responsive neurons delineate where the monkey is looking, and can be updated by self-directed eye movements (idiothetic input), and in object-place associations some neurons respond to object memories while the place is being recalled (even while the object is not visible), while some units respond only to the place being remembered (Rolls and Xiang, 2006). Differential responses in the primate brain to recognition memory problems are much less frequent in the hippocampus as compared to the perirhinal cortex (Brown and Aggleton, 2001; Brown et al., 1987; Miller et al., 1993; Sobotka and Ringo, 1993; Xiang and Brown, 1998), however, the hippocampus shows a much stronger encoding component when information about a stimulus is related to a particular spatial location (Eichenbaum, 2000; Rolls et al., 1989). The anterior hippocampus, in particular, may show increased neuronal firing to the spatial location of a preferred reward, relative to less preferred reward locations (Rolls and Xiang, 2005).

1.2.3 The topography of connections within the extended-hippocampal system

Before one can understand the functions of the various substrates involved in learning and memory, it is important to know the topography of the connections between these areas, in order to infer how the properties of one area may affect those of the areas it connects with, and *vice versa*. Direct evidence of these topographies comes from anatomical tracer studies in rodents and non-human primates, and, to a lesser extent, in human post-mortem anatomical studies. The connections of the hippocampus will

initially focus on those within the temporal lobe and those with structures outside the temporal lobe.

Many of the connections to and from the hippocampus beyond the temporal lobe were initially considered part of a circuitry involved in emotion, known as the Papez circuit (Papez, 1937). Subsequent neuropathological studies changed the emphasis to memory processes, as atrophy of the mammillary bodies is consistently found in the amnesic Korsakoff's syndrome (Benedek and Juba, 1940, 1941; Delay and Brion, 1969). The main pathway for hippocampal afferents and efferents is the fornix. This tract connects the hippocampus directly with diencephalic areas such as the anterior thalamic nuclei and mammillary bodies, in both rodents and primates (Aggleton, 2012; Aggleton et al., 1986, 2005b; Krayniak et al., 1979; Meibach and Seigel, 1977a, b; Poletti and Creswell, 1977, see Figure 1.1). The laterodorsal thalamic nucleus appears to be jointly innervated by fornical and non-fornical inputs from the subiculum (Aggleton et al., 1986). The various diencephalic regions are reached via the postcommissural columns of the fornix, which descend posterior to the anterior commissure (Poletti and Creswell, 1977, Figure 1.2). In the rat, there is an additional non-fornical route from the hippocampal formation to some parts of the anteroventral nucleus, the anterodorsal nucleus and the laterodorsal nucleus, which involves the internal capsule (Dillingham et al., 2015).

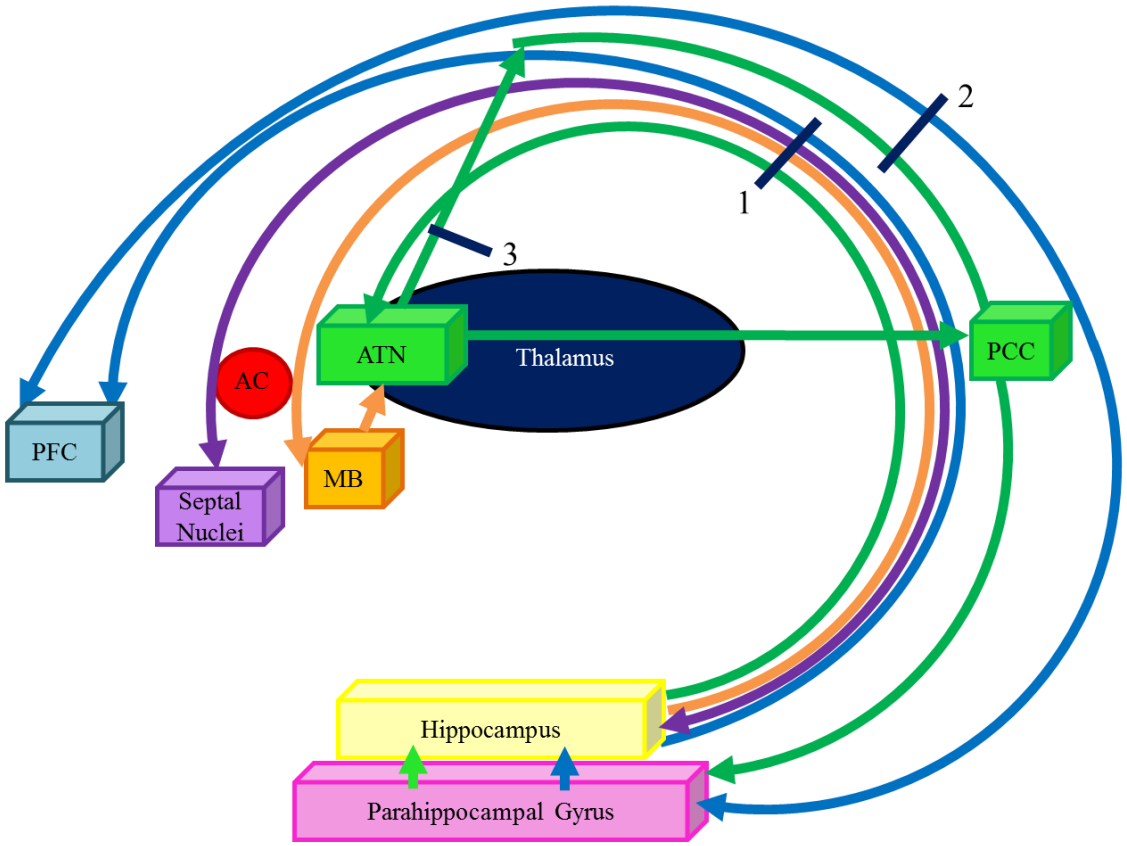

Figure 1.1 *Schematic diagram of the main connections of the extended hippocampal system. These same, principal connections are found in both the primate and rat brain. The arrows depict the direction of efferents. Abbreviations: AC = anterior commissure; ATN = anterior thalamic nuclei; MB = mammillary bodies; PCC = posterior cingulate cortex (the retrosplenial cortex is included in PCC); PFC = prefrontal cortex. Tracts; 1 = the fornix; 2 = the cingulum bundle; 3 = the internal capsule. (Note the depicted projections from the anterior thalamic nuclei are thought to occupy both the cingulum and the internal capsule.)*

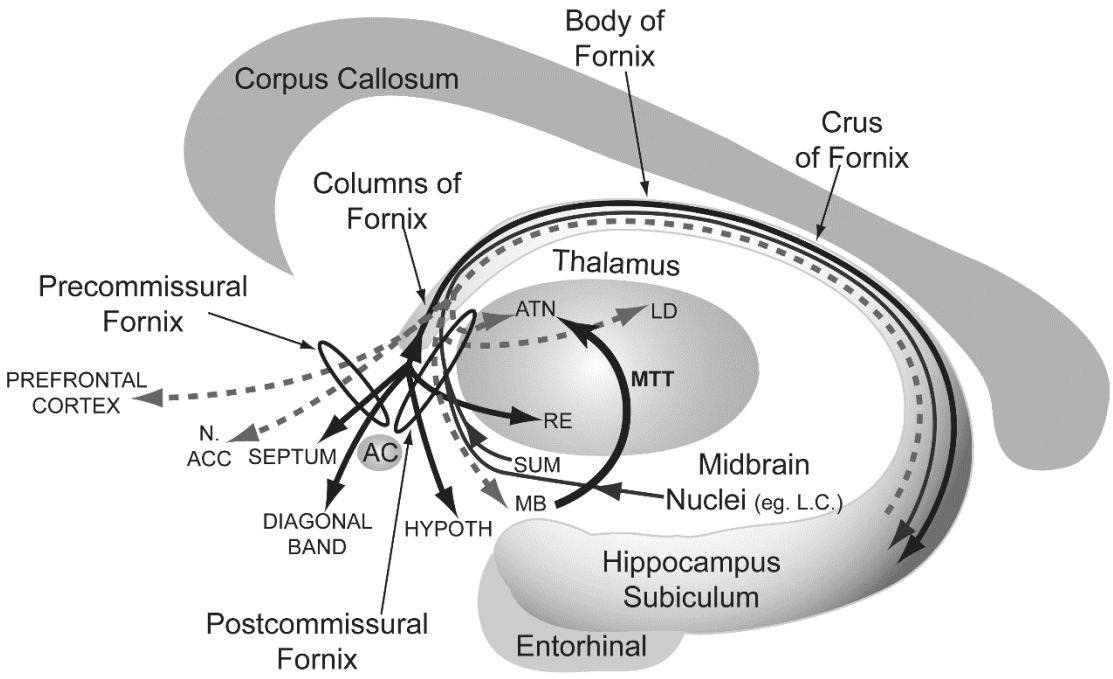

Figure 1.2 *Diagrammatic representation of the location of the fornix and its divisions. The dashed arrows show fornical connections that are solely efferent from the hippocampal formation, the narrow, solid arrows show fornical connections that are solely afferent to the hippocampal formation, and the wide, solid arrows show reciprocal connections within the fornix. Abbreviations: AC = anterior commissure; ATN = anterior thalamic nuclei; HYPOTH = hypothalamus; LC = locus coeruleus; LD = laterodorsal thalamic nucleus; MB = mammillary bodies; N. ACC = nucleus accumbens; RE = nucleus reuniens; SUM = supramammillary nucleus. (Modified from Aggleton, 2008.)*

The precommissural fornix connects the hippocampus reciprocally with the diagonal band of Broca and the septal nuclei (Figure 1.2). In addition, the precommissural fornix contains hippocampal efferents to nucleus accumbens and the medial and orbital prefrontal cortices, in both rodents and primates (Aggleton et al., 1987, 2015; Barbas and Blatt, 1995; Friedman, et al., 2002; Gaykema et al., 1991; Goldman-Rakic et al., 1984; Jay and Witter, 1991; Kitt et al., 1987; Koliatsos et al., 1988; Mesulam, 1995; Saunders and Aggleton, 2007; Swanson, 1977, Figure 1.2). While research in humans is not as detailed, due to methodological limitations, post-mortem dissections indicate that the fornix once again connects to the anterior thalamus, mammillary bodies, basal forebrain, septal area, and prefrontal cortex in the human brain (Shah et al., 2012).

In addition to the direct projections from the hippocampal formation to the anterior thalamic nuclei, there is also a well-known indirect projection via the mammillary bodies and the mammillothalamic tract (Kwon et al., 2010; Kwon et al., 2014; Watanabe and Kawana, 1980; Vann, 2013; Vann et al., 2007, Figures 1.1 and 1.2). The anterior thalamic nuclei then project back to the hippocampus via the internal capsule and the cingulum bundle, which first enters the parahippocampal gyrus, and then finally reaches the hippocampus (Agster and Burwell, 2013; Amaral and Cowan, 1980; Domesick, 1970; Heilbronner and Haber, 2014; Mufson and Pandya, 1984; Schmahmann and Pandya, 2006; Shibata, 1993a, b; van Groen and Wyss, 1990a, b, Figure 1.1). The anterior thalamic nuclei also project more indirectly to the hippocampal formation via the posterior cingulate region (Vann et al., 2009a, Figure 1.1). This series of connections extending from, and then returning back to, the hippocampus, constitutes Papez circuit.

As already noted, the basal forebrain has reciprocal projections back to the hippocampus via the fornix (McKinney et al., 1983; Mesulam et al., 1983; Segal and Landis, 1974; Rye et al., 1984, Figures 1.1 and 1.2). In contrast, the prefrontal cortex appears to have largely indirect projections back to the hippocampus. One route for these indirect prefrontal projections back to the hippocampus is via the cingulum bundle, passing firstly through the perirhinal, parahippocampal, or entorhinal cortices (Goldman-Rakic et al., 1984; Nauta, 1972; Takagishi and Chiba, 1991; Sesack et al., 1989; Wall and Messier, 2001, Figure 1.1). A more direct route from the prefrontal cortex to the hippocampus may also exist by means of the uncinate fasciculus (Fuster, 2008; Goldman-Rakic et al., 1984). Other indirect routes are via midline thalamic nuclei, e.g. nucleus reuniens and via the cingulate cortices.

In rat and monkey brains it is often possible to identify, with precision, the origin of particular hippocampal efferents. Some hippocampal efferents arise from the subiculum, adding to parallel projections from CA1, e.g. efferents to the prefrontal cortex, nucleus accumbens and amygdala. In other instances, the hippocampal efferents seem to solely arise from the subiculum, e.g. efferents to the thalamus, mammillary bodies and retrosplenial cortex (Aggleton, 2012; Aggleton and Christiansen, 2015). In addition, the subiculum receives dense inputs from other hippocampal areas. The realisation that the subiculum contributes to almost all extrinsic hippocampal efferents makes it a site of especial interest.

1.2.4 The fornix

The strategic position of the fornix, linking the hippocampal formation to regions beyond the temporal lobe raises the question of what the consequences of fornix damage on cognition are. Answering this question should not only tell us about hippocampal function but also about the potential roles of the various sites that are connected via this pathway. Further information has more recently come from looking at the status of the fornix using diffusion MRI methods.

1.2.4.1 Human studies

In the past there appeared to be much uncertainty about the consequences of fornix disruption. In an influential review (Garcia-Bengochea and Friedman, 1987) it was reported that out of 193 cases of fornix section, only four cases revealed a persistent memory loss. In a careful critique, Gaffan and Gaffan (1991) highlighted many shortcomings with the studies in that review, including the lack of detailed neuropsychological testing and the failure to monitor the pre-surgical cognitive status of the many epilepsy patients. More recent studies, which have typically focused on fornix

damage associated with colloid cyst and their removal (Aggleton et al., 2000; Hodges and Carpenter, 1991; McMackin et al., 1995; Vann et al., 2008), have found that fornix damage typically produces a severe impairment in the recall of episodic information. In some of these same studies there appeared to be a contrast as recognition memory was less affected than recall (Aggleton et al., 2000; Vann et al., 2008). Meanwhile, some studies have found a deficiency in both recollection and recognition following fornix damage (Park et al., 2000; Poreh et al., 2006). These differences in recognition abilities may be due to variations in the extent of fornix damage or additional damage both before and following surgery (Vann et al., 2008).

In a study that involved numerous colloid cyst patients (Tsivilis et al. 2008), it was found, once again, that those patients with the greatest fornix damage were most clearly impaired on the general memory index of WMS-III (Wechsler Memory Scale Third Edition). Of additional interest was the finding that across the entire cohort of colloid cyst patients, mammillary body volume was most consistently correlated with the recall of episodic information. This significant correlation was found for many individual tests of episodic memory. Intriguingly, the same correlations were not found for recognition memory (Tsivilis et al. 2008), suggesting a division between these two forms of memory. Follow-up studies provided convergent evidence that the mammillary body damage in these colloid cyst cases was associated with a loss of recollective-based recognition memory but a sparing of familiarity-based recognition (Vann et al., 2008).

Research into the fornix in humans has benefitted from the ability to reconstruct this tract using methods based on diffusion magnetic resonance imaging (Catani, 2008). In recent years, a number of diffusion MRI studies have provided information about this structure in humans. These studies consistently indicate that structural properties of this

tract are related to learning and memory. For instance, short-term learning appears to result in plasticity changes in the fornix (Hofstetter et al., 2013), while loss of fornical volume and increases in axial diffusivity (representing tract incoherence) are predictors of cognitive impairments, a key component of which is memory problems (Fletcher et al., 2013). It is striking that in healthy adults, fornix microstructure (fractional anisotropy; FA) is related to recollection but not familiarity memory (Rudebeck et al., 2009), a distinction sometimes observed in patients with damage to either the fornix or the hippocampus (Aggleton et al., 2000, 2005a; Vann et al., 2008; Tsivilis et al., 2008; Turriziani et al., 2008). Healthy older participants also exhibit this correlation between fornix FA and episodic memory, particularly immediate free recall, although this is undoubtedly mediated by age, which also correlates with FA (Metzler-Baddeley et al., 2011). Moreover, the reduction in recall associated with fornix FA contrasts with two other temporal lobe tracts (the parahippocampal cingulum and uncinate fasciculus), which showed no such involvement (Metzler-Baddeley et al., 2011). Further, a study by Metzler-Baddeley et al (2012a) found that, in healthy subjects following comparisons of the fornix, parahippocampal cingulum and uncinate fasciculus, only fornix tissue volume fraction (reflecting the amount of tissue of the white matter tract remaining after cerebrospinal fluid (CSF) contamination has been removed) was found to correlate with free recall.

Structural changes in the fornix, as revealed by MRI, have also been associated with memory loss in patients with Mild Cognitive Impairment (Zhuang et al., 2012). Furthermore, fornix FA measures, which symbolise tract coherence, can distinguish Alzheimer's disease from normal control participants, and predict conversion from normal cognition to amnestic mild cognitive impairment (aMCI), and from aMCI to Alzheimer's disease (Oishi et al., 2012). Meanwhile, tissue volume fraction in the left

parahippocampal cingulum was the only tract in aMCI patients that correlated with recall, with no such relationship for the fornix in these patients (Metzler-Baddeley et al., 2012a). This result may indicate a forced switch in the reliance of different pathways in these patients, following pathology in the fornix. Consistent with this view, tissue volume fraction was reduced in the fornix in aMCI compared to control participants (Metzler-Baddeley et al., 2012a). The authors, therefore, suggest that following degradation of the fornical route for episodic memory in aMCI (as revealed by the lack of correlations between fornix microstructure and memory measures in this group, which are seen in healthy participants), there might be compensation by another temporal lobe tract in this patient group – namely, the left parahippocampal cingulum (Metzler-Baddeley et al., 2012a). The mechanism for recruiting this alternative pathway may be enabled by cholinergic signalling inputs from the basal forebrain (Ray et al., 2015).

1.2.4.2 Animal studies: Rats

It is easier to quantify the effects of more focused fornical damage in non-human animal studies, as surgical lesions can be restricted to this structure. At the same time, careful thought has to go into those hippocampal connections that do or do not use this pathway (Dillingham et al., 2015). Lesion studies in rats have revealed that complete fornix ablations consistently produce robust spatial memory deficits and can sometimes disrupt object discriminations (Aggleton and Brown, 2002; Aggleton et al., 1995; Wible et al., 1992). For example, a study by Aggleton et al. (1995) compared fornix lesions with lesions in the mammillary bodies and anterior thalamic nuclei on a spatial T-maze alternation task. They found that the rats with fornix lesions showed a severe spatial memory impairment, which was similar to that seen after anterior thalamic lesions but more severe than that associated with mammillary body damage. In contrast, configural

learning can appear unaffected by fornix lesions (Bussey et al., 1998; McDonald et al., 1997; Sziklas and Petrides, 2002; Sziklas et al., 1998), with such sparing sometimes extending to biconditional spatial discrimination tasks (Sziklas and Petrides, 2002; Sziklas et al., 1998). This latter result seems surprising given the spatial demands of the tasks, although this sparing may to be due to the very protracted acquisition of the particular problems (Dumont et al., 2015). Of particular note is evidence that, like the human hippocampus, the rat fornix may be selectively important for recollective-like processes but not for recognition memory based on familiarity (Easton et al., 2009).

When trying to understand the role of the fornix in learning and memory, direct comparisons with hippocampal lesions become of particular interest. There are several learning/memory tasks that appear to be similarly affected by both fornix and hippocampal lesions, for instance fear conditioning has been shown to be equally impaired by lesions to either site, and a number of spatial tasks, such as the Morris water maze and radial arm maze tasks, also produce similar impairments (Aggleton and Brown, 2002; Cassel et al., 1998; Maren and Fanselow, 1997). Likewise, fornix and hippocampal lesions produce comparable deficits on an automated delayed nonmatching-to-position task that used retractable levers (Aggleton et al., 1992).

However, on the basis of other tasks, the functions of the hippocampus in spatial learning have also been shown to be partially dissociated from the fornix. For example, lesions in the hippocampus impaired performance of a spatial-visual conditional learning task, whereas fornix-lesioned rats appeared unaffected (Dumont et al., 2007). Furthermore, a study by Cassel et al. (1998) investigated the differences between fimbria-fornix and hippocampal lesions 4.5 months after surgery using the Morris water maze and radial-arm maze, with particular emphasis on working and reference memory

tasks. Hippocampal lesion animals were slower than fornix lesion animals to learn the platform location in the water maze and had larger impairments in the radial-arm maze task when working memory demands were more taxing. Rats with hippocampal lesions also tended to have higher locomotor activity than both the fornix lesion and sham lesion groups (Cassel et al., 1998). Post-surgical recovery period may also play a crucial role in these differences. While reference memory appears equally affected in fornix and hippocampal lesion groups at a 1 month and 6.5 month follow-up, working memory, which is initially impaired, appears to show some improvement in the hippocampal lesion group at 6.5 months, an improvement that was is not apparent in the fornix lesion group (Galani et al., 2002). These examples all highlight how, for some demands, the hippocampus can function without its many fornical connections.

1.2.4.3 Animal studies: Monkeys

In monkeys, fornix transections produce a noticeable, but rather mild, deficit in memory for the spatial arrangement of scenes (Gaffan, 1992; Gaffan, 1994; Gaffan and Harrison, 1989a; Gaffan et al., 2001). For example, lesions of the fornix seem to selectively impair the ability to use the arrangement of objects within a scene, which the authors suggest is due to the fornix providing "snapshot" scene memory (Gaffan and Harrison, 1989b). Moreover, the fornix has also been found to be important for spatial working memory in particular, but less so for general place learning (Murray et al., 1989). The fornix also appears to be involved in learning the significance of the monkey's actions with respect to the location of a visual stimulus associated with a reward (Rupniak and Gaffan, 1987). Related deficits are found for conditional visuomotor learning, in which a specific visual stimulus directs a specific motor response (Brasted et al., 2002). The impact of fornix lesions is not, however, restricted to tasks with a spatial component, as impairments were found for an object discrimination task that required flexible learning

(Wilson et al., 2007). Finally, in view of the mixed effects of hippocampal lesions in monkeys on visual matching and nonmatching-to-sample tests (e.g. Beason-Held et al., 1999; Heuer and Bachevalier, 2011; Murray and Mishkin, 1998; Zola et al., 2000), it is not surprising that fornix lesions also have varied effects, as most studies report little or no deficit on recognition memory (Bachevalier et al., 1985a, b; Gaffan et al., 1984a, b; Zola-Morgan et al., 1989).

Taken together, the findings imply that fornix connections help to encode information not only about the location of stimuli but the animal's own location as well. Some studies have shown that visual-visual associations are not impaired to the same extent as visual-spatial associations, and in fact can show an initial enhancement following fornix transection, which may reflect the monkeys being biased away from spatial strategies following fornix damage (Kwok and Buckley, 2009). It has also been suggested that this visual-spatial deficit affects the encoding process more than retrieval (Buckley et al., 2004, 2008; Gaffan, 1993). Furthermore, the effects of fornix damage on delayed nonmatching-to-sample in a T-maze task (similar to that used in rat studies) showed similarities with those from rats (Murray et al., 1989), suggesting similar functions across species. However, in the second experiment of Murray et al.'s (1989) study, fornix lesions did not create an impairment for conditional tasks where various spatial cues for objects were associated with reward i.e. if an object was located on the left, a reward would appear there, but not if that same object was presented on the right. This is contrary to the findings of Rupniak and Gaffan (1987), who did find a fornix lesion deficit on a similar conditional task, however in the latter study, monkeys had to learn different locomotor activities associated with the objects when in different spatial locations (rather than just approach where the reward appears), so perhaps this additional locomotor association was crucial for involvement of the fornix.

In a manner similar to rats, there are some aspects of memory in monkeys which appear to be reliant on the hippocampus but not the fornix. For example, initially fornix and hippocampal lesions produced similar levels of impairment on a delayed matching-to-place task, however after 18 months the fornix lesion group appeared no longer affected while for the hippocampal lesion group the impairment endured (Zola-Morgan et al., 1989). This difference might, however, be due to the increased likelihood of additional temporal lobe white matter damage in the latter group. Another study found that hippocampal lesioned monkeys were impaired on a visual concurrent discrimination task, whereas fornix lesioned monkeys were not (Moss et al., 1981). There was, however, extraneous damage to the inferotemporal cortex in the hippocampal lesion group, which might have exacerbated the deficit. This interpretation was ruled out in a second experiment comparing hippocampal and inferotemporal lesions, which found hippocampal lesions to impair both visual and tactile modes of this task, whereas inferotemporal lesions only impaired performance in the visual mode (Moss et al., 1981). Therefore, the effects of hippocampal lesion on delayed matching-to-place appears to last longer than that for fornix lesions, while visual discriminations may be more reliant on the hippocampus than the fornix. In both examples we should consider those hippocampal connections that do or do not depend on the fornix. The largest group that do not rely on the fornix relate to connections within the temporal lobe, which are with sites already linked with the same kinds of tasks as those seemingly less affected by fornix lesions. Consequently, these connections could help to explain hippocampus versus fornix lesion differences.

1.3 Outline of thesis

One issue that is apparent from previous research into the extended-hippocampal system is that studying each brain region as a single, independent structure is far too simplistic. In order to get a more complete picture of how this system functions it is important to study the system at different levels, from large scale connections to more detailed connections between subregions within structures. For example, do different connections across the same regions support different functions? Are these different connections equally affected by disease processes? These are all questions which this thesis aims to address, utilizing different methods across species, and taking advantage of the benefits of each.

The first experimental chapter (Chapter 2) looks at the organisation of the outputs of the hippocampus from the subiculum to the mammillary bodies and anterior thalamic nuclei, using retrograde tracer studies in primates and rodents. The organisation of the brain takes place along three planes (laminar (inferior-superior), longitudinal (anterior-posterior) and transverse (medial-lateral)) and has important, potential implications for the seclusion or congregation of function. The pathways to and from the proximal and distal ends of the subiculum may prove to be quite separated, suggesting functional gradients whereby one pathway (e.g. leading towards the distal subiculum) is more involved in spatial memory processes and the other (leading towards the proximal subiculum) is more involved in object recognition memory. However, the topographic arrangement of efferents arising from subiculum remains poorly understood, thus serving as a key focus of Chapter 2.

The second experimental chapter (Chapter 3) looks at functional differences within the subiculum in rats, based on a separation of those inputs and outputs as analysed in

Chapter 2. Chapter 3 uses IEG imaging, in particular, the visualisation of *zif268*. Based on what is currently known about hippocampal and parahippocampal connectivity, it is predicted that the proximal subiculum is more involved in object based memory, while the distal subiculum is preferentially involved in spatial memory. This difference is investigated by comparing activity associated with a spatial radial-arm maze task (RAM) and an object recognition task. Two other conditions are included [maze locomotion and home cage (baseline) controls].

Chapter 4 then turns to human imaging and investigates the two subdivisions of the fornix, the precommissural fornix and postcommissural fornix, and whether these fornical subdivisions are equivalently affected in healthy ageing and amnestic mild cognitive impairment (aMCI, the predominantly amnestic form of mild cognitive impairment as opposed to the more generalized cognitive deficits that can occur; Metzler-Baddeley et al., 2012a) . This study also investigates the effects of ageing on these fornical subcomponents and how these subcomponents relate to cognitive functions that are associated with the different precommissural and postcommissural efferents. One important aim was to provide an anatomical protocol for the reconstruction of these tracts. Following on from the previous two chapters, these *in vivo* neuroimaging methods made it possible to look for topographic connections within the human extended-hippocampal system.

Chapter 5 looks at another way of investigating the topography of the fornix, via its input from anterior and posterior hippocampal divisions, in a healthy young sample. This study principally sought to determine if it was feasible to reconstruct separate portions of this tract, with the information guiding future research into changes of hippocampal function along its various axes. This research was again based on the

supposition that the hippocampus possesses gradients of function along the longitudinal (anterior-posterior) axis, based on differences in connectivity with other brain sites. The anterior hippocampus, for example, is thought to be more connected with processes relating to anxiety and emotion. In contrast, the posterior hippocampus and its connections may more strongly reflect a role in spatial memory. Both Chapters 4 and 5 used diffusion MRI tractography to investigate white matter microstructure in the human brain *in vivo*.

The final Chapter (6, General Discussion) attempts to link these cross-species findings, discuss the limitations of the current techniques, and consider what potential future studies could be performed to elaborate upon these findings. The overall goal is to understand how the extended hippocampal system supports cognition.

Chapter 2: The proximal-distal and rostral-caudal organisation of dorsal subicular efferents to the anterior thalamic nuclei and mammillary bodies in the rat and non-human primate

2.1 Introduction

Research linking hippocampal anatomy with its various functions has often targeted its individual subfields, namely the CA1-4 fields, the dentate gyrus, and the subiculum (Chinnakkaruppan et al., 2014; Hitti and Siegelbaum, 2014; Hunsaker et al., 2008; Kesner, 2007a, b; Lee et al., 2005; O'Mara, 2005; Schlichting et al., 2014; Tyler et al., 2012; Wintzer et al., 2014). Related research has also targeted specialisations along the long axis of the hippocampus (Aggleton, 2012; Bannerman et al., 1999; Chase et al., 2015; Colombo et al., 1998; Fanselow and Dong, 2010; Moser et al., 1995; Poppenk et al., 2013; Poppenk and Moscovitch, 2011; Strange et al., 2014). [Note that in the rodent, the temporal (ventral) hippocampus is homologous with the primate anterior hippocampus, while the septal (dorsal) hippocampus is homologous with the primate posterior hippocampus (Strange et al., 2014); see Figure 2.1].

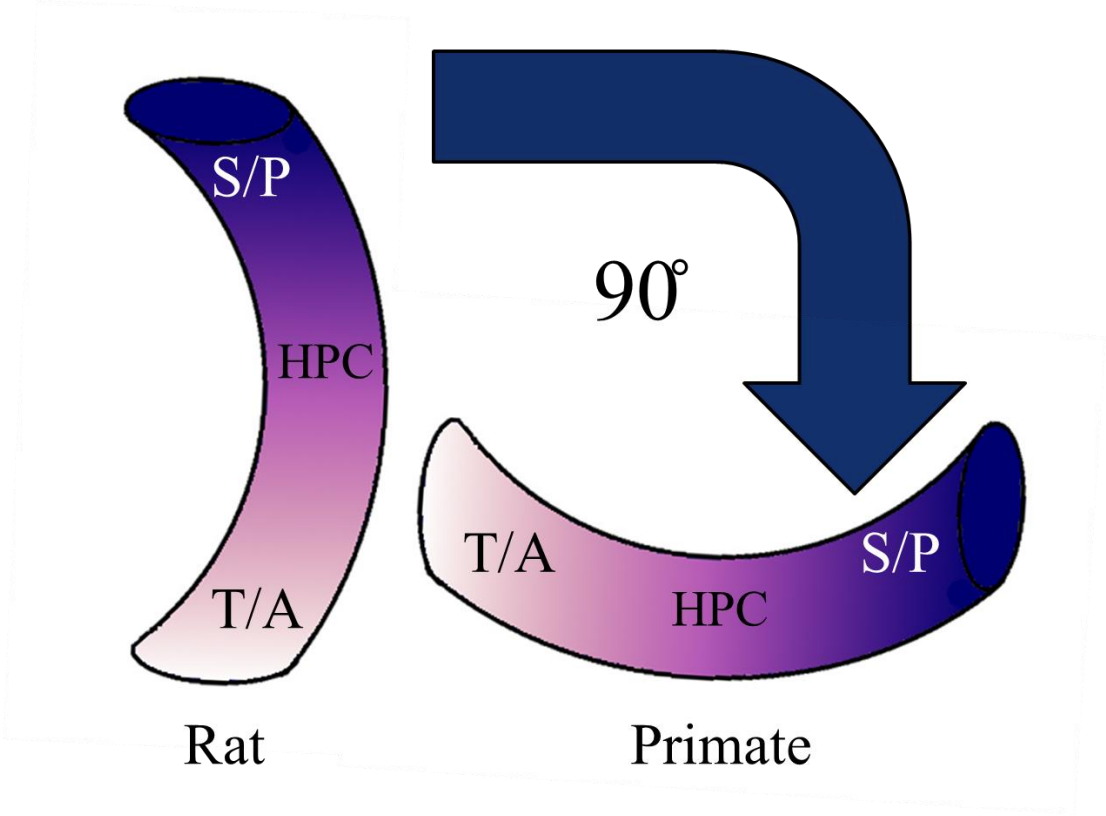

Figure 2.1 *Diagram depicting the relationship between septal/posterior (S/P) and temporal/ anterior (T/A) hippocampus (HPC) in the rat and primate brain, whereby the septal hippocampus of the rat brain is equivalent to the posterior hippocampus of the primate brain, and the temporal hippocampus of the rat brain is equivalent to the anterior hippocampus of the primate brain, via an angle of approximately 90°.*

While this is a productive way to view potential differences in the layout, role and interactions of various hippocampal sub-regions, a further distinction exists, between the "proximal" and "distal" portion of each hippocampal subarea, where "proximal" is closest to the dentate gyrus and "distal" is furthest from the dentate gyrus. For the subiculum, the chief output structure of the hippocampus (Witter, 2006), this means that the proximal portion is closest to CA1 and the distal portion is furthest from CA1, adjacent to the presubiculum. The presence of specific intrinsic and extrinsic connection patterns based on their proximal-distal locations (Naber et al., 2000, 2001a, b; van Strien et al., 2009; Witter, 2006) provides a new perspective on how hippocampal functions might be segregated (Henriksen et al., 2010; Kim et al., 2012; Nakamura et al., 2013).

One way to investigate potential topographies in the proximal-distal axis is through the use of retrograde and anterograde tracers. For this technique, injections of a particular tracer are made into a specific brain area, where the tracer travels either forwards from the injection site to the target site (anterograde), or backwards to the site of origin (retrograde) of the axonal projections (see Chapter 1). The following studies, which describe what is known about the topographies of hippocampal connections, all employ these techniques.

A proximal-distal topography has already been found in a number of intrinsic hippocampal connections in the rat. For instance, distal CA1, which receives input from proximal CA3, projects to proximal subiculum, whereas proximal CA1, which receives input from distal CA3, projects to distal subiculum (Naber et al., 2000; Nakamura et al., 2013; Van Strien et al., 2009; Witter, 2006). Extrinsic hippocampal connections that show a proximal-distal profile in the rat also exist. For instance, proximal CA1 and

distal subiculum share connections with the postrhinal cortex via the medial entorhinal cortex, and distal CA1 and proximal subiculum share connections with the perirhinal cortex via the lateral entorhinal cortex. The subiculum also receives these projections indirectly through CA1, as mentioned above (Amaral et al., 1991; Kloosterman et al., 2003; Kosel et al., 1983; Naber et al., 1997, 2000, 2001a; Witter et al., 2000a, b; Witter, 2006). One study by Witter et al. (1990), which used both anterograde and retrograde tracers to determine the organisation of subicular efferents, found a clear differentiation of proximal and distal efferents. Proximal efferents innervated the infralimbic and rhinal cortices, the nucleus accumbens and the rostral end of the medial mammillary nuclei. In comparison, the distal subiculum projected to the postrhinal and retrosplenial cortices, the anterior thalamic complex and caudal parts of the medial mammillary nuclei.

In the primate hippocampus, proximal-distal organisation also exists between CA1/subiculum and other temporal and non-temporal areas. One example concerns the hippocampal projections to the prefrontal cortex, which arise from distal CA1 and proximal subiculum. Another concerns the reciprocal connections between distal CA1/proximal subiculum and the rostral/medial entorhinal cortex and the perirhinal cortex. In contrast, proximal CA1 and distal subiculum share reciprocal connections with caudal/lateral entorhinal cortex, and also with area TH of the parahippocampus (Aggleton, 2012; Barbas and Blatt, 1995; Blatt and Rosene 1998; Carmichael and Price, 1995; Chrobak and Amaral, 2007; Insausti and Munoz, 2001; Jay and Witter, 1991; Saunders and Rosene, 1988; Witter and Amaral, 1991).

The other, previously mentioned gradient along which hippocampal connections are arranged is described as septal-temporal in the rat or longitudinal, i.e. anterior-posterior, in primates. The existence of graded connections along this axis has been demonstrated

for a number of extrinsic hippocampal connections in the rat. For instance, a lateral to medial gradient in the rat entorhinal cortex corresponds in turn to a septal to temporal gradient in regions of CA1, CA3, DG and subiculum (Dolorfo and Amaral, 1998; Ruth et al., 1982, 1988; Witter, 1989). Furthermore, more rostral parts of the perirhinal cortex project preferentially to more septal parts of CA1 and the subiculum, whereas caudal portions of the perirhinal cortex project more so to temporal parts of CA1 and the subiculum. This is similar for the postrhinal cortex, for which the rostral portion projects to septal subiculum, but the caudomedial region projects to temporal parts of the distal subiculum (Witter et al., 2000a, b).

Thirdly, laminar topographies also add further complexity to the numerous pathways connecting the hippocampus with external areas. In rats, for instance, anteroventral thalamic nucleus inputs arise chiefly from deeper layers of the subiculum, whereas mammillary body inputs arise from more superficial layers. This separation of outputs is confirmed by double-labelling studies (Ishizuka, 2001; Meibach and Siegel, 1975; Sikes et al., 1977; Wright et al., 2010). Projections to the nucleus accumbens also arise from a superficial layer of the subiculum that is separate from thalamic nuclei and mammillary body projections (Ishizuka, 2001). The same laminar arrangement of anterior thalamic nuclei and mammillary body connections is also found in the monkey brain, with anterior thalamic projections arising from the deepest subicular layers (Aggleton et al., 1986; Krayniak et al., 1979). Meanwhile, both mammillary body and retrosplenial projections arise from more superficial layers of the subiculum (Kobayashi and Amaral, 2003).

Of these three axes, changes along the longitudinal axis have been most fully described in the primate brain, indeed, it is possible that all hippocampal extrinsic connections are

organised in this manner. Examples include projections to the amygdala, the nucleus accumbens, and prefrontal areas which arise from the anterior hippocampus (Aggleton, 1986; Barbas and Blatt, 1995; Carmichael and Price, 1995; Insausti and Munoz, 2001). Meanwhile, projections to the mammillary bodies and the retrosplenial cortex arise predominantly from the posterior hippocampus, in particular the subiculum (Aggleton et al., 2005b; Krayniak et al., 1979; Rosene and Van Hoesen, 1977). Some of these topographies appear more complex as, for example, the anterior subiculum projects to area 29 and the posterior subiculum to remaining areas of retrosplenial cortex (Kobayashi and Amaral, 2003).

A lot of these aforementioned studies have focused on inputs to the subiculum and CA1, some of which are reciprocal, from other medial temporal sites or prefrontal areas. The subiculum is one of the principal output sites of the hippocampus, along with CA1, with which it is interconnected (O'Mara et al., 2001; Witter, 2006). The study in this thesis focuses, however, on the diencephalic connections of the hippocampus, in particular the anterior thalamic nuclei and mammillary bodies, which originate from the subiculum (Aggleton et al., 1986, 2005b; Meibach and Siegel, 1977a, b; Rosene and Van Hoesen, 1977; Saunders et al., 2005; Sikes et al., 1977; Swanson and Cowan, 1977). Figure 2.2 shows a comparison of coronal sections of these diencephalic substrates and the subiculum within the hippocampus between rat and monkey.

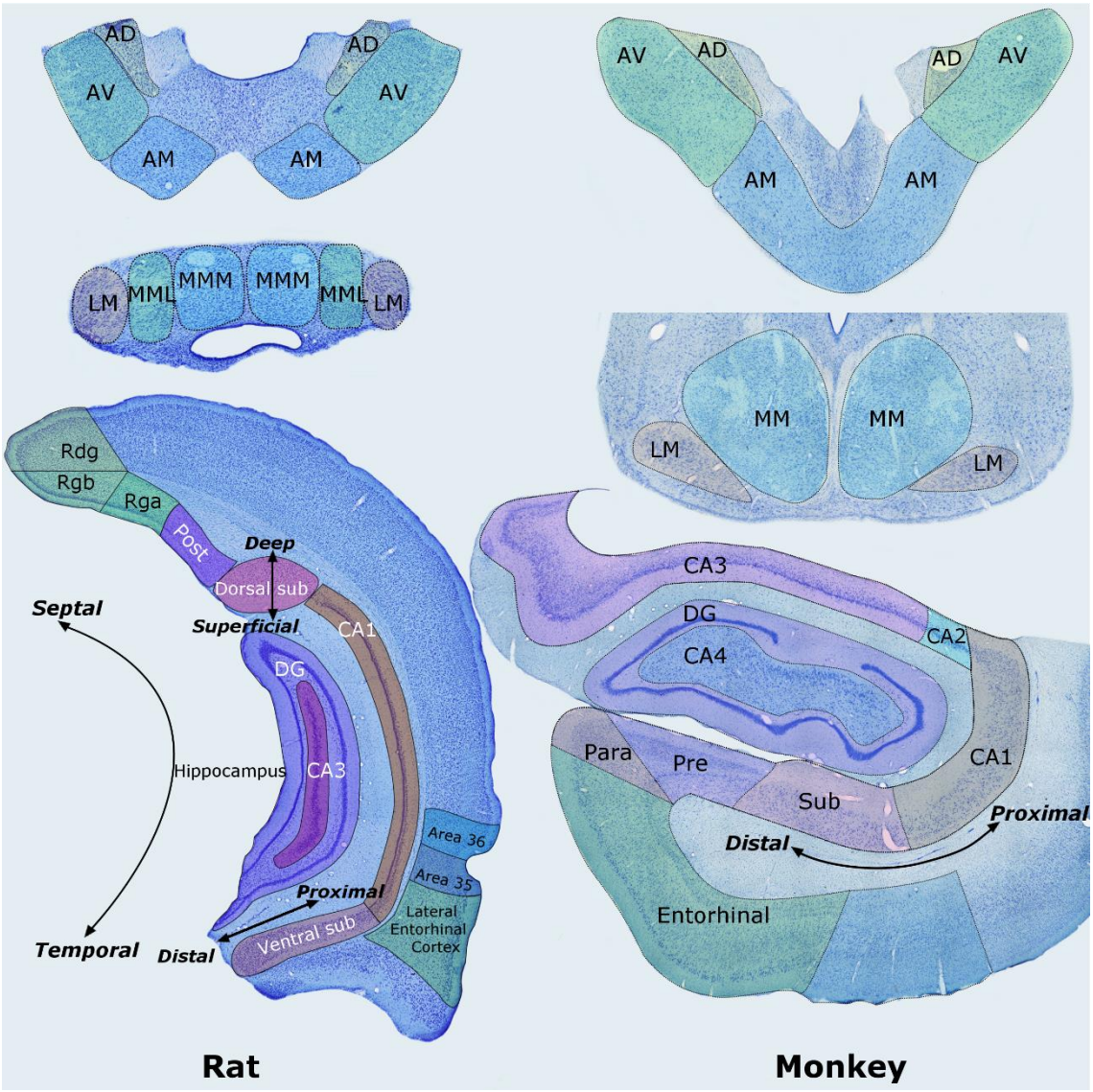

Figure 2.2 *Coronal cresyl violet-stained section of a (left) rat brain from the Paxinos and Watson (2004) brain atlas, and (right) rhesus monkey brain from the Paxinos et al. (2009) brain atlas, demonstrating the topography of the anterior thalamic (top) and mammillary body (middle) nuclei, alongside the location of the subiculum within the medial temporal lobe and its proximal to distal axis in relation to the dentate gyrus (bottom). Bregma co-ordinates for rat: ATN = -1.56mm; MB = -4.44mm; hippocampus = -.600mm. Bregma co-ordinates for monkey: ATN = -9.00mm; MB = -9.00mm; hippocampus = -10.35mm. Abbreviations: AD = anterodorsal nucleus; AM = anteromedial nucleus; ATN = anterior thalamic nuclei; AV = anteroventral nucleus; CA = cornu ammonis (1-4); DG = dentate gyrus; LM = lateral mammillary body; MB: mammillary bodies; MML = medial mammillary body lateral nucleus; MMM = medial mammillary body medial nucleus; Para = parasubiculum; Post = postsubiculum; Pre = presubiculum; Sub = subiculum; Rdg = dysgranular retrosplenial cortex; Rga/b = granular retrosplenial cortex a/b. Taken from Bubb et al. (submitted).*

Research thus far on subicular connections to these diencephalic areas in the rat has shown that connections with the anterior thalamic nuclei appear to follow a proximal-distal arrangement. Tracer studies indicate that the proximal subiculum projects mainly

to the anteromedial thalamic nucleus, whereas the distal subiculum projections terminate in the anteroventral, anterodorsal and laterodorsal thalamic nuclei (Meibach and Siegel, 1977a; Wright et al., 2010). While the numerous mammillary body inputs arising from the subiculum have been repeatedly examined (e.g. Meibach and Siegel, 1975; Wright et al., 2010), the proximal-distal gradient of these same connections has received less detailed attention. Referring to the study by Witter et al. (1990), it is apparent that both proximal and distal subiculum project to the mammillary nuclei, however, further differentiation was not described. These studies reveal that projections to the mammillary bodies are dense and may arise from across the proximal-distal extent of the subiculum. A septal-temporal gradient also exists for the anterior thalamic nuclei outputs from the subiculum. Retrograde tracers show that these connections arise predominantly from the septal subiculum and significantly less so from the temporal subiculum (e.g. Wright et al., 2010). This same gradient is also revealed by anterograde tracer injections into the temporal subiculum, which labelled few to no terminals in the anterior thalamic nuclei (Meibach and Siegel, 1977b; Wright et al., 2010). As previously mentioned, laminar topographies also exist for these connections, in which anterior thalamic nuclei projections arise from deeper subicular layers and mammillary body projections from more superficial layers (Ishizuka, 2001).

Current reports indicated that in the primate, anteromedial thalamic, anteroventral thalamic, and mammillary body projections all appear to originate from across the proximal-distal extent of the subiculum, however with a slight increase in the distal portion for mammillary body projections (Aggleton et al., 1986, 2005b). These diencephalic efferents are also organised along the anterior-posterior axis, with connections to the mammillary bodies showing the greatest concentration of cells from the posterior region of the subiculum and prosubiculum (Aggleton et al., 2005b). As

was previously mentioned, these diencephalic outputs also have a laminar arrangement similar to the rat, whereby mammillary body projection cells are more superficial than anterior thalamic nuclei projection cells (Aggleton et al., 1986; Krayniak et al., 1979). Hence, it would appear that in the primate brain, anterior-posterior and laminar gradients underpin hippocampal-diencephalic connections, whereas proximal-distal columnar organisation seems to be less evident.

As noted in Aggleton (2012), the level of analysis of diencephalic subicular projection topography in the rat remains to be applied to primate studies. Current primate studies typically treat these gradients in a qualitative rather than quantitative manner. This is why the present study re-examined the organisation of subicular projections in the rat and macaque monkey, paying particular attention to proximal-distal columnar and anterior-posterior/septal-temporal organisation. Many studies that have noted different proximal-distal arrangements for subicular afferents and efferents treat these differences as either one or the other (proximal or distal), i.e. in a dichotomous manner. The main aim of this study was, therefore, to examine systematically the full extent of proximal-distal subiculum topographies relating to the origins of anterior thalamic nuclei and mammillary body projections. A key step was to quantify the sources of these projections.

These particular projections are of interest as both the anterior thalamic nuclei and mammillary bodies are functionally linked and are thought to be important for episodic memory in humans and spatial and object memory in rodents and primates (Aggleton and Brown, 1999; Aggleton and Sahgal, 1993; Byatt and Dalrymple-Alford, 1996; Carlesimo et al., 2011; Harding et al., 2000; Henry et al., 2004; Parker and Gaffan, 1997a, b; Sutherland and Rodriguez, 1989; Tsivilis et al., 2008; Warburton et al., 2001).

While previous tracer studies have provided initial information for both the rat (e.g. Ishizuka, 2001; Meibach and Siegel 1977a, b; Naber and Witter, 1998; Wright et al., 2013) and monkey (Aggleton et al., 1986, 2005b; Krayniak et al., 1979; Saunders et al., 2005; Xiao and Barbas, 2002b) concerning these connections, there have been no direct cross-species comparisons.

To address these issues, A. rats with injections of retrograde tracers targeted at 1. the medial mammillary nucleus, 2. the anteromedial thalamic nucleus, and 3. the anteroventral thalamic nucleus were first examined (Experiment 1). This analysis was followed by a study of B. macaque monkeys with injections of retrograde tracers in the same diencephalic nuclei (Experiment 2). The underlying rationale was to ascertain the potential for parallel, high-resolution information streams to the medial diencephalon (Aggleton et al., 2010). The study did not examine inputs to the anterodorsal thalamic nucleus or the lateral mammillary nucleus, both part of the head direction system (Taube, 2007), as they have very different patterns of hippocampal inputs, which largely arise from the postsubiculum and presubiculum (Van Groen and Wyss, 1990a, b; Yoder and Taube, 2011). Both nuclei also offer difficult injection targets, given their size and location.

2.2 Methods

The author (K.C.) performed the cell counts and subsequent analyses but did not carry out the surgeries or the tracer reactions. These are described in full to help judge the validity of the methods and resulting data. The surgeries/histology were carried out by Nick Wright and Chris Dillingham for Experiment 1 and Richard Saunders and John Aggleton for Experiment 2.

2.2.1 Experiment 1: Rats

2.2.1.1 Anatomical nomenclature

The flexure of the rat hippocampus makes the terms "anterior" and "posterior" potentially misleading. As already noted, the rat temporal (or ventral) hippocampus corresponds to the primate anterior hippocampus, while the septal (or dorsal) hippocampus corresponds to the posterior hippocampus (Strange et al., 2014; see Figure 2.1). To maintain consistency with primate studies, the temporal-septal plane of the rat hippocampus is described as anterior-posterior.

Unless otherwise specified, anatomical names and borders essentially follow Swanson (1992). The anterodorsal, anteromedial, and anteroventral thalamic nuclei make up the principal anterior thalamic nuclei. In the rat, unlike the monkey, there is an additional midline area, the interanteromedial nucleus (Swanson, 1992). The major division within the mammillary bodies consists of the lateral and medial nuclei, with the latter further subdivided in the rat into pars lateralis, pars medialis, pars basalis, pars posterior, and pars medianus (Allen and Hopkins, 1988; Vann, 2010). Of these divisions, pars medialis and pars lateralis are the largest. The limits of the subiculum (Figure 2.3), presubiculum, parasubiculum, and postsubiculum follow Swanson et al. (1987). The laminae descriptions for the rat subiculum match Kloosterman et al. (2003), so that the subiculum consists of a superficial molecular layer and a deeper, thick layer of pyramidal cells. The term "intermediate subiculum" (Bast, 2007; Strange et al., 2014) describes the region of the subiculum where the septal subiculum and temporal subiculum converge, i.e. at the flexure of the hippocampus.

2.2.1.2 Subjects

A total of 17 lister hooded rats and two dark agouti rats were used in the experiment. Fourteen male Lister Hooded rats (270-300g; Harlan, Bicester, UK) and two male Dark

Agouti rats (180-220g; Harlan, Bicester, UK) were injected with retrograde tracers into either a unilateral anteromedial nucleus, the anteroventral nucleus, or the pars medialis or pars lateralis of the medial mammillary body/bodies. The eleven mammillary body injection cases involved nine Lister Hooded and two Dark Agouti rats. The five anterior thalamic nuclei cases all involved Lister Hooded rats. Eleven rats were used from previous experiments describing the inputs to the anterior thalamic nuclei and mammillary bodies (Wright et al., 2010, 2013). Five additional new cases of tracer injections into the mammillary bodies were also included. A further three male Lister Hooded rats (220-270g; Harlan, Bicester, UK) were also used for coronal sections stained for neuronal nuclei antigen (NeuN) (Jongen-Rêlo and Feldon, 2002). The purpose of these cases was to count an estimate of total neuronal numbers within the proximal-distal subdivisions of the subiculum, in order to provide normalised cell counts of the retrograde tracer labelled cells.

		MB			ATN			Total cell counts
Case	Sp	Location (hemisphere)	Tracer	Volume (µl)	Location (hemisphere)	Tracer	Volume (µl)	Stain
26_4	LH	MML (right)	WGA	0.04				
26_5	LH	MML (right)	WGA	0.04				
26_7	LH	MML (left)	WGA-HRP	0.04				
26_8	LH	MML (left)	WGA-HRP	0.04				
31_6	LH	MML (left)	WGA	0.04				
31_11	LH	MML (left)	WGA	0.04				
33_7	LH	MML (left), MMM (left)	FB, WGA	0.04				
58_1	LH	MML (left and right)	FB	0.04				
58_2	LH	MML (left and right)	FB	0.04				
86_1	DA	MMM (right)	FB	0.04				
86_9	DA	MMM (right)	FB	0.04				
41_5	LH				AVv (right)	FB	0.05	
42_2	LH				AVd, AM (left)	DY, FB	0.05	
45_11	LH				AVv, AM (left)	FB, DY	0.05	
45_14	LH				AV, AM (left)	DY, FB	0.05	
45_15	LH				AV, AM (left)	DY, FB	0.05	
39a_7	LH							NeuN
39_12	LH							NeuN
39a_14	LH							NeuN

Table 2.1 *List of injection sites, tracer types, and hemisphere (where relevant) for all rat cases. Abbreviations: AM = anteromedial nucleus; ATN = anterior thalamic nuclei; AV = anteroventral nucleus; DY = Diamidino Yellow; FB = Fast Blue; MB = mammillary bodies; MML = medial mammillary nucleus, pars lateralis; MMM = medial mammillary nucleus, pars medialis; Sp = species; WGA = wheatgerm agglutinin; WGA-HRP = horseradish peroxidase conjugated to wheatgerm agglutinin.*

2.2.1.3 Surgical methods

Rats were anaesthetised with 6% sodium pentobarbital (Sigma-Aldrich, Gillingham, UK). The corneas were protected with Chloramphenicol eye ointment (Martindale Pharmaceuticals, Romford, UK). Animals were then placed in a stereotaxic frame (Kopf, Tujunga, CA), with the nosebar set at +5.0mm. The scalp was incised on the

sagittal plane and a craniotomy made above the target site whilst the rat was under aseptic conditions. Injections of tracer were made with 1µl Hamilton syringes (Hamilton, Bonaduz, Switzerland) of 0.5µl of 3% Fast Blue (FB: Polysciences Inc., Eppelheim, Germany) or 3% Diamidino Yellow (DY: Sigma-Aldrich, Gillingham, UK) both diluted in phosphate buffered saline (PBS). 0.4µl injections of 1% wheat germ agglutinin (WGA: Vector Labs, Peterborough, UK) were made with a 0.5µl Hamilton syringe. Injections of 0.04-0.05µl volume of 40mg/ml concentration horseradish peroxidase conjugated to wheat germ agglutinin (WGA-HRP: Vector Laboratories, Peterborough, UK) were also used.

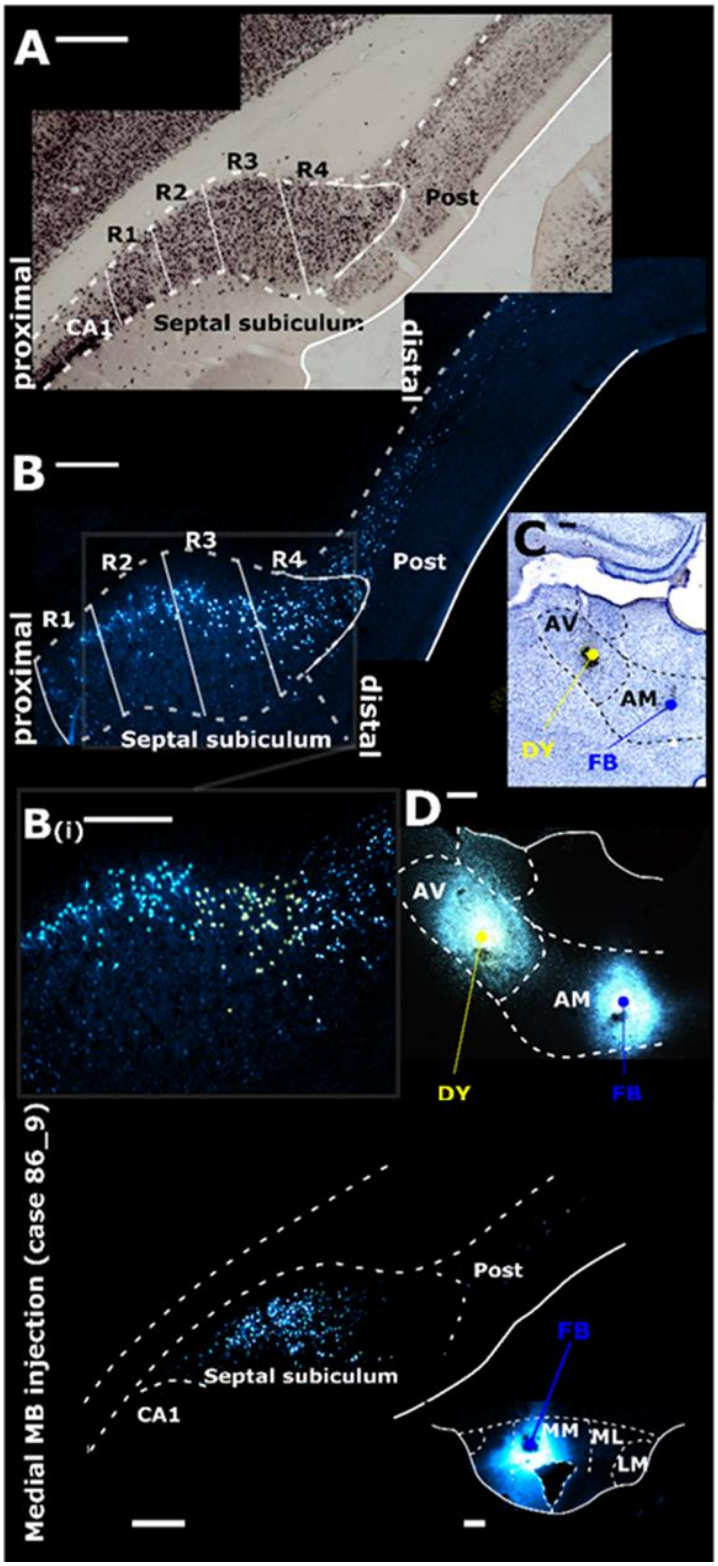

Figure 2.3 *The rat septal (dorsal) subiculum was divided into four regions of interest (A) with region 1 (R1) most proximal to the CA1 subfield of the hippocampus and region 4 (R4) most distal. The top photomicrograph (A) is a coronal section from the left hemisphere (NeuN immunostaining). (B, C, D – case 45_14) Example of neuronal tracer injections into the anteroventral nucleus (AV) of Diamidino Yellow (DY) and into the anteromedial nucleus (AM) of Fast Blue (FB). The anteroventral nucleus injection labelled relatively more neurons in the distal subiculum, extending into the postsubiculum (Post) – (marked in yellow in inset B(i)). Conversely, the anteromedial nucleus injection labelled more proximally situated neurons (marked blue in inset B(i)). (E) Example of FB injection into pars medialis (MMM) of the medial mammillary body. Other abbreviations: MML = pars lateralis of the medial mammillary body; LM = lateral mammillary body. Scale bars = 250µm. Taken from Christiansen et al., (2016b); courtesy of Chris Dillingham.*

Injections were targeted at the following co-ordinates for the mammillary bodies, relative to bregma: anterior/posterior (A/P) -2.1; medial/lateral (M/L) +/-0.8; dorsal/ventral (D/V) -10.4. For the anteroventral nucleus, the injections were placed at A/P -0.4; M/L +/- 1.5; D/V -6.2 from bregma. For injections into the anteromedial nucleus, the co-ordinates were A/P -0.2; M/L +/-0.7, D/V -6.8 from bregma. Once lowered to the target location, the syringe was left in place three minutes before the injection of the tracer gradually over ~40 seconds. After this it was left in place for another seven minutes to avoid any tracer travelling back up the syringe tract. For all cases, a 5ml subcutaneous injection of 5% glucose in 0.9% saline was given after completion of surgery (Baxter Healthcare, Norfolk, UK). Aureomycin antibiotic powder (FortDodge Animal Health, Southampton, UK) was applied over the closed sutured scalp post-surgery. Animals were then allowed to recover in a thermostatically controlled container before returning to individual housing with *ad libitum* food and water. Their drinking water contained paracetamol (500mg/l) and sucrose (2%) for 3 days after surgery. Each animal's health was monitored daily.

After a variable post-operative period, dependent on tracer (WGA: 12-24h; WGA-HRP: 2 days; FB: 4 days), animals were deeply anaesthetised with sodium pentobarbital (Euthatal, Merial, Harlow, UK). All animals were initially intracardially perfused with 0.1 M PBS at room temperature. For those that received fluorescent tracer injections or injections of unconjugated WGA, the PBS was followed by 4% paraformaldehyde in 0.1 M PBS at 4°C. Cases receiving WGA-HRP injections received a fixative comprising 1.5% paraformaldehyde and 1.5-2% glutaraldehyde, also at ~4°C.

Three different tracers were used for the eleven mammillary body injections (WGA, WGA-HRP, and Fast Blue). Four of these involved unconjugated WGA, two involved

WGA-HRP, two involved FB into both hemispheres, two involved FB into one hemisphere, and one involved both WGA and FB in the same hemisphere (Figure 2.5). Anterior thalamic nuclei injections comprised of FB and DY (Sigma, St Louis, MO, USA) separately into the anteromedial and anteroventral nucleus respectively for three cases, with the tracers reversed in the fourth case, and the fifth case consisting of a single FB injection into the anteroventral nucleus (Figure 2.5). A summary of all injection types and locations is shown in Table 2.1.

2.2.1.4 Histology

Brains were removed from the skull and post-fixed for four hours in the fixative with which they were perfused before being transferred to a cryoprotectant solution containing 25% sucrose in 0.1 M PBS for 24 hours. Brain sections were cut at 40µm in the coronal plane using a Leica 1400 freezing microtome. Two 1-in-3 series of sections were mounted directly onto gelatine-subbed slides, before being dried in the dark at room temperature. For localising injection sites, one series was stained with cresyl violet while the second series was rehydrated and coverslipped with either Hydromount (National Diagnostics UK, East Riding, UK) or DPX (Sigma-Aldridge, Gillingham, UK).

2.2.1.5 Immunohistochemistry (unconjugated WGA and NeuN)

NeuN and unconjugated wheat germ agglutinin (WGA; Vector Labs, Peterborough, UK) were localised immunohistochemically (Horikawa and Powell, 1986). Initially, sections were washed (3x ten minutes) in 0.1 M PBS, followed by two further washes in 0.1 M phosphate-buffered saline containing Triton X-100 (PBST). Sections were then incubated for 48 hours in a primary solution (anti-WGA raised in goat: 1:2000 dilution, Vector Labs, Peterborough, UK; anti-NeuN: 1:5000 dilution, Chemicon, Chandlers

Ford, UK) with 2% normal horse serum in 0.1 M PBST. Following incubation, sections were washed (3 x 10 minutes) in 0.1 M PBST before being incubated in a secondary antibody solution (for WGA: biotinylated rabbit-anti-goat at a 1:200 dilution; for NeuN: biotinylated horse-anti-mouse at a 1:250 dilution; both from Vector Labs, Peterborough, UK) for 2 hours. Following further washes in PBST, sections were incubated in the Vectastain ABC solution (Vector Labs, Peterborough, UK) for 2 hours, then washed in PBST twice for 10 minutes each followed by a further three washes in 0.1 M PBS. Sections were then reacted with diaminobenzidine (0.05% with 0.01% H_2O_2; DAB; Sigma Aldrich). Once the desired level of staining was achieved, the reaction was stopped with washes in 0.1 M PBS (3 x 10 minutes). Sections were then mounted, dehydrated and coverslipped, as above.

2.2.1.6 Histochemistry

Following tissue sectioning at 40µm, one of the 1-in-3 series was mounted directly onto gelatin-subbed slides while the remaining series were collected in 0.1 M PBS (pH 6.0) for the subsequent 3,30,5,50-tetramethylbenzidine reaction (TMB) for visualisation of anterogradely transported WGA-HRP. For the TMB reaction, sections were incubated, with agitation, in a fresh 0.1 M phosphate buffer (PB, pH 6.0) solution before being incubated at room temperature in a solution containing 0.25% ammonium molybdate in 0.1 M PB and 0.002% 3,30,5,50- tetramethylbenzidine, dissolved in 100% ethanol, for 30 minutes. Following incubation, a hydrogen peroxide solution in distilled water was added in three stages, at 30 minute intervals, until the final concentration of hydrogen peroxide was 0.3%. Sections were then incubated in the same solution overnight at 4ºC. The TMB reaction precipitate was stabilised through subsequent incubation of sections in a 5% ammonium molybdate solution in 0.1 M PB (pH 6.0) for 30 minutes (see Marfurt et al., 1988). Following incubation, sections were washed in 0.1 M PB (pH 6.0)

before being mounted on gelatine subbed slides and left to dry overnight at room temperature. The sections were then dehydrated, coverslipped and mounted, as above.

2.2.1.7 Imaging

A Leica DM5000B microscope with a Leica DFC310FX digital camera and Leica Application Suite image acquisition software was used for brightfield and fluorescence microscopy. Images were then montaged using Microsoft Image Composite Editor (ICE).

2.2.1.8 Cell counts for different components of the subiculum

Sections stained with the neuronal marker NeuN (Jongen-Rêlo and Feldon, 2002) were used to estimate relative neuronal counts in different proximal-distal sectors of the subiculum. The purpose was to ensure that differences in the numbers of subicular cells containing retrograde tracer did not merely reflect the presence of more neurons in that same area. The cell counting procedures were not designed to give precise absolute counts, for which stereology would be needed. Instead, it provided relative counts with which to compare levels of labelled cells within each subicular region of interest.

Prior to cell counting, the subiculum was divided along its proximal-distal axis into four equally sized columnar regions of interest (Figure 2.3). These four regions (R1-4) created a template for cell counting. In the case of NeuN, both hemispheres were counted, while for the retrograde tracers the cell counts were confined to the hemisphere ipsilateral to the injection site. For those cases that received anterior thalamic injections, eight coronal sections were examined per rat, each 240µm apart. The sections began from close to where the septal subiculum first appears, and ended as the dorsal and ventral subiculum fuse to form the intermediate subiculum, i.e. just before the structure

flexes at 90^0 (Strange et al., 2014). Counts were not made in the temporal subiculum as very few cells originate from here to innervate the anterior thalamic nuclei (Meibach and Siegel 1977b; Sikes et al., 1977; Swanson and Cowan, 1977; Wright et al., 2010, 2013). For the mammillary body injections, cell counting (which followed the same procedure as for dorsal subiculum) continued in the ventral (temporal) subiculum, with five coronal sections analysed per case. Seven such cases had staining in the ventral subiculum.

For the fluorescent tracers (FB and DY), each labelled cell was marked by hand using an ImageJ Cell Counter Plugin (Schneider et al., 2012). The cell counts based on the NeuN stain, WGA, and WGA-HRP tracers were made using an automated method. Firstly, NeuN, WGA, and WGA-HRP tracer images were converted into 8-bit greyscale images. The image was then manually thresholded to encompass all particles that were considered stained and any conjoined cells were split using the watershed tool. The acceptable particle size was set in the range 30-120μm^2 to limit the inclusion of glial cells or artefact. Stained cells were counted using ImageJ software (Schneider et al., 2012).

2.2.1.9 Statistical comparison of cell counts in the subiculum

Statistical comparisons were confined to within-subject analyses, which contrasted the cell counts in the four proximal-distal regions (Figure 2.3) or the various anterior-posterior levels. The data for these analyses come from the estimates of the proportion of labelled cells from the total neuron population in each subicular subregion. Comparisons were not made between cases as there are many individual factors that could affect the overall numbers of labelled cells in each animal, e.g. type and amount of tracer. All statistical and graphical analyses were performed in SPSS

(version 20) and Microsoft Excel (2010), respectively. Region of interest (i.e. R1-4) along the proximal-distal axis was treated as a categorical variable and studied within each injection group separately using univariate analyses of variance (ANOVAs; with Bonferroni-adjusted alpha levels for any follow-up pairwise comparisons). Distance along the septal-intermediate axis was treated as a continuous variable and analysed using linear regressions whereby anterior-posterior level acted as predictor for normalised cell counts.

2.2.2 Experiment 2: Monkeys

This experiment made use of archival anatomical data involving cynomolgus (*Macaca fascicularis*) or rhesus (*Macaca mulatta*) monkeys. All surgical procedures were carried out by John Aggleton and Richard Saunders. The tracer injections were performed between ten and forty years before the present analysis. Cases ACy1, Acy2 and Acy26 are all 35 years old; cases MB1-3 are 32 years old; BRh3 and BRh5 cases are approximately 15 years old; and the NeuN case (BB) is approximately 27 years old. Given the age of the brain tissue it is inevitable that the tracer signal will have somewhat faded over this time frame, however comparisons made with drawings taken shortly after the injection show that the overall distribution of retrograde tracer label has been fundamentally unaffected. The HRP injections into the mammillary bodies showed a similar level of retrograde label to when originally detected.

2.2.2.1 Anatomical nomenclature

The hippocampal nomenclature is taken from Lorente de Nó (1934). The subicular region is made up of four allocortical areas from proximal to distal: the prosubiculum, subiculum, presubiculum, and parasubiculum (also see Saunders and Rosene, 1988). The prosubiculum is a transitional region directly adjacent to field CA1 (Lorente de Nó,

1934), and is defined as the most proximal region of interest in this study (Figure 2.4). The distal end of the subiculum is distinguished by dense cells forming layer II of the presubiculum, although subicular cells may underlie the layer II cells of the most proximal subiculum. Three distinct laminae exist within the subiculum; a superficial molecular layer, a pyramidal cell layer, and a deep polymorphic cell layer (Lorente de Nó, 1934).

The mammillary body descriptions follow those of Veazey et al. (1982) for the cynomolgus monkey, dividing the medial mammillary nucleus, separate from the lateral mammillary nucleus, into pars basalis, pars medialis and pars lateralis. The thalamic nomenclature is taken from the description of the thalamus of the rhesus monkey by Olszewski (1952); the anterior thalamic group is composed of three nuclei: anterior medialis, anterior ventralis, and anterior dorsalis.

2.2.2.2 Subjects

The tracer data came from eight adult monkeys (six cynomolgus and two rhesus monkeys). All experimental procedures were in strict adherence to the NIH Guide for Care and Use of Laboratory Animals, in accordance with the "Principles of Laboratory Animal Care" (NIH Publication No. 86-23, revised 1985). An additional adult rhesus monkey provided coronal sections for NeuN analysis.

2.2.2.3 Surgical methods

Mammillary bodies

Subjects were three male cynomolgus monkeys ranging in weight from 4.0kg to 5.6kg at the time of surgery (MB1-3). In all three cases a 0.15µl injection of 35% horseradish

peroxidase (HRP) (Boehringer, Mannheim) in 2% dimethyl-sulphoxide solution was placed in the region of the left mammillary body. Full descriptions of the surgical procedures have been given elsewhere (Saunders et al., 2012). In brief, monkeys were sedated with ketamine hydrochloride (10-15mg/kg, intramuscular injection), then given intravenous pentothal, before being placed in a stereotaxic apparatus. After removal of a bone flap, a 1µl Hamilton syringe (Bonaduz, Switzerland; 25 gauge) was lowered into the mammillary region using coordinates determined from X-ray skull landmarks (Aggleton, 1985). After 48 hours the monkeys were perfused intracardially with physiological saline followed by 1L of a solution of 2.5% paraformaldehyde and 1.5% glutaraldehyde in phosphate buffer (pH = 7.2). The brains were blocked in the coronal plane and then cryoprotected in cold 30% sucrose in 0.1 M phosphate buffer solution for three days. Frozen sections (50µm) were cut in the coronal plane and collected in phosphate buffer.

The series of sections examined in this study was processed according to a modified Hanker-Yates technique (Hanker et al., 1977; Perry and Linden, 1982). The Hanker-Yates procedure was as follows: The brain sections were incubated in 700ml of a 0.1 M sodium cacodylate buffer solution (pH 5.1) containing 2.4g cobalt chloride, 1.6g ammonium nickel sulphate, 700mg catechol and 350mg p-phenylenediamine for 15 minutes and then washed in phosphate buffer for 3-5 minutes. The sections were then transferred into a fresh solution of 700mg catechol, 350 mg p-phenylenediamine and one drop of hydrogen peroxide (H2O2) and incubated for 15 minutes. Sections were mounted on glass slides, counter-stained with cresyl violet and coverslipped. Cells labelled with HRP were charted and counted on coronal sections at 1mm intervals.

Anterior thalamic injections

HRP cases: Three adult cynomolgus monkeys (ACy1, ACy2, ACy26) weighing from 3.5-6.8kg received a single injection of HRP into the anteromedial thalamus under visual guidance. The initial surgical procedures were identical to those for the mammillary body injections. Next, dorsal bone and dural flaps exposed the midline. The wall of one hemisphere was then gently retracted and a 5-10mm portion of the corpus callosum and the underlying fornix were split longitudinally to expose the thalamic midline. The largest HRP injection (case ACy1) involved a single, stereotaxic injection of 0.22µl (40% HRP, Sigma, type IV) delivered via a 1µl Hamilton syringe (25 gauge). Case ACy2 received a single injection of 0.13µl of 40% HRP, while in case ACy26 a stereotaxic injection of 0.8µl of a 4% solution of HRP (Sigma, type IV), conjugated with WGA, was targeted at the anterior thalamic region. Following injection of the tracer, the dura and skin were sutured in anatomical layers, while antibiotics and analgesia were given according to NIH veterinary guidance (see Aggleton et al., 2014). Recovery was without incident. After 48 hours, the monkeys were anaesthetised, perfused, and the brain treated exactly as described for the mammillary body injections except that the perfusion used a solution of 1% paraformaldehyde and 1.25% glutaraldehyde in 0.1 M phosphate buffer (pH 7.2). A 1-in-5 series was then treated with tetramethyl benzidine according to the protocol of Hardy and Heimer (1977). Alternate sections were dehydrated, counterstained with thionine, and coverslipped, while the remaining sections were just dehydrated and coverslipped.

Fluorescent tracer injections (FB): Additional information came from two adult rhesus monkeys with FB injections into the anterior thalamic nuclei (BRh3, 4.9 kg; BRh5, 4.7kg). This information is used selectively as in both cases there are complications concerning the tracer injections. In case BRh3, FB was injected into the left anterior

thalamic nuclei at the same time as a surgical transection of the ventroamygdalofugal pathway in the same hemisphere (Saunders et al., 2005). It is most unlikely that this tract surgery would disrupt direct inputs from the subiculum to the anterior thalamus (see Aggleton et al., 1986; Saunders et al., 2005). In the same case (BRh3), FB was also injected into the right mediodorsal thalamic nucleus, i.e. in the opposite hemisphere. The subiculum does not project to the mediodorsal nucleus. Furthermore, the fornix was sectioned in that same hemisphere, so disconnecting hippocampal inputs (see Saunders et al., 2005).

In case (BRh5), FB was injected into the caudal left anterior thalamus. Although a second FB injection was located in the right laterodorsal thalamic nucleus, i.e. in the contralateral hemisphere, the projections from the hippocampus (subiculum) to the laterodorsal nucleus are almost exclusively ipsilateral (Aggleton et al., 1986). For the reasons explained, the tracer in the left subiculum in both BRh3 and BRh5 should overwhelmingly reflect the ipsilateral anterior thalamic injection. Nevertheless, greater reliance is placed on those cases with HRP injections in the thalamus.

The initial surgical procedures followed those described for HRP except that surgical anaesthesia was maintained with isoflurane (1% to 4%, to effect). Under visual guidance, an injection of FB (Sigma; St Louis; 3% suspension in distilled water) was made through a 5µl Hamilton syringe fitted with a 28-gauge needle. Following the tracer injection (~1µl), the dura and skin were sutured in anatomical layers, while antibiotics and analgesia were given according to NIMH veterinary guidance (see Aggleton et al., 2014). In both cases recovery was without incident.

After a post-operative period of between 5 and 10 days, the animals with FB injections were deeply anaesthetised with sodium pentobarbital. They were then perfused intracardially with saline followed by 4-6% paraformaldehyde in 0.1 M cacodylate buffer (pH 7.4). The brains were then removed and placed in a series of cryoprotectant solutions consisting of first 10% and then 20% glycerol in 0.1 M cacodylate buffer with 2% dimethylsulfoxide and 4-6% paraformaldehyde (pH 7.4, 4˚C). Four to six days after perfusion, the brains were rapidly frozen by immersion in -75˚C isopentane, and then cut at 40µm in the coronal plane on a freezing microtome (Rosene et al., 1986). Three 1-in-10 series of sections were mounted immediately onto gelatine-subbed slides, dried, coverslipped, and stored in the dark at 4°C. A summary of species, injection site, tracer and hemisphere, stain, and ipsilateral surgery, where relevant, is shown in Table 2.2.

Case	Species	Injection Site	Ipsilateral surgery	Tracer (Hemisphere)	Stain
MB1	Cy	MB	None	HRP (right)	
MB2	Cy	MB	None	HRP (left)	
MB3	Cy	MB	None	HRP (left)	
ACy1	Cy	AM Mid Re (MD)	None	HRP	
ACy2	Cy	AM Mid	None	HRP	
ACy26	Cy	AM Mid Re	None	HRP	
BRh3	Rh	*MD*	*FnX*	*FB (right)*	
		AM	Amyg/TSX	FB (left)	
BRh5	Rh	AV (AM)	None	FB (left)	
		LD	*None*	*FB (right)*	
BB	Rh				NeuN

Table 2.2 *List of injection sites, surgeries, tracer types, and hemisphere (where relevant) for all primate cases. Abbreviations: AM = anteromedial nucleus; Amyg/TSX = ventroamygdalofugal pathway transection; AV = anteroventral nucleus; Cy = cynomolgus monkey; FB = Fast Blue; FnX = fornix transection; HRP = horseradish peroxidase; LD = laterodorsal nucleus; MB = mammillary bodies; MD = mediodorsal nucleus; Mid = midline; Re = nucleus reuniens; Rh = rhesus monkey.*

<u>NeuN staining</u>

Staining was conducted in a male adult rhesus monkey (BB; 10.2kg) that had received tracer injections into the auditory cortex (Scott et al., 2015). Following a survival period of 14 days, the animal was deeply anaesthetised with pentobarbital and perfused

transcardially with 0.5L of saline, followed by 0.5L of 1% paraformaldehyde and 8L of 4% paraformaldehyde, both in 0.1 M phosphate buffer (pH 7.4) at room temperature. The brain was then removed from the skull, cryoprotected through a series of glycerols (Rosene et al., 1986), blocked in the coronal plane, and frozen in −80°C isopentane. Sections were cut in the coronal plane on a sliding microtome at a thickness of 40μm.

For NeuN immunohistochemistry, a 1-in 5 series was retained. The sections were rinsed three times in Tris buffer solution (TBS) and subsequently agitated for 60 minutes in a blocking solution composed of 10% normal rabbit serum, 0.2% Tween-20 in TBS, before additional TBS rinses. The sections were then incubated for 24 hrs in mouse anti-NeuN (1:500; Chemicon, MAB377) at room temperature. The next day sections were repeatedly rinsed with TBS and then incubated with pooled highly cross-adsorbed secondary antibodies (anti-mouse Alexa Fluor 568, 1:250; Life Technologies, Grand Island, NY). Sections were then mounted onto slides and coverslipped with PVA-DABCO (Sigma).

2.2.2.4 Cell counts for different components of the subiculum

Coronal sections taken from along the length of the hippocampus were stained with the neuronal marker NeuN (Jongen-Rêlo and Feldon, 2002). The sections analysed came from an adult male rhesus monkey. As in the rat, the goal was to estimate relative neuronal counts in different proximal-distal sectors of the subiculum. The procedure for dividing the subiculum into four equidistant proximal-distal regions and for counting the NeuN cells was the same as that described for rats, i.e. automatic (Figure 2.4). These sections were then matched to the tracer section at the most comparable anterior-posterior level.

In all cases with tracer injections, cell counting was manual, to address the variable fading of the signal (least in the three mammillary body cases with HRP injections, but most in the three thalamic cases with HRP injections). For the three mammillary body injection cases and the two fluorescent (FB) thalamic injections, a total of 12-13 sections per animal were imaged and counted. The proximal and distal boundaries of the subiculum (along with R1-4) were first marked on the image. Cell counts were confined to the hemisphere ipsilateral to the injection site. For the three cases with anterior thalamic HRP injections, the number of remaining coronal sections through the subiculum varied, from eight (ACy2) to 27 (ACy26). Each section was treated as separate, except in case ACy26, where the cell counts from adjacent slides were combined and the mean computed. Cell counting in these three thalamic HRP cases was conducted at a higher magnification than in the other cases, in response to the fading of the HRP positive reaction product.

Figure 2.4 (page opposite) *Retrograde label in the cynomolgus monkey subicular cortices following injections of horseradish peroxidase (HRP) into either (C-F) the left medial mammillary nucleus (cases MB2 and MB3) or (G-H) the anteromedial nucleus. A-B: Low (A) and higher (B) magnification photomicrographs of a NeuN-stained coronal section through the rhesus monkey hippocampus. Dashed lines indicate the boundaries of the subiculum while solid lines depict the boundaries of the four subiculum regions of interest (R1–4). R1 corresponds to the prosubiculum (ProS; most proximal to CA1) while R4 is most distal to CA1, i.e. next to the presubiculum (PreS). Following injections into the medial mammillary nucleus (MB2, MB3), retrograde label was concentrated in the more superficial pyramidal cells of R3 and R4 (distal subiculum), tapering off into deeper pyramidal cells when going more proximal (C-F). Inset D(i) shows retrograde label in more superficial R4 at higher magnification. G-H: low (G) and high (H) magnification photomicrographs showing retrograde label in the deep layer of the subiculum following an injection of HRP into the anteromedial nucleus (case ACy1). In ACy1 the label is in deep polymorphic cells (black arrows) and pyramidal-like cells (purple arrows) nearer the upper border of this deep layer. (Note, sections G and H have been left-right reversed to aid comparison with the other cases.) The black rectangle and inset in G shows the region of high magnification shown in H. Other abbreviation: DG = dentate gyrus. Scale bars, 500lm (A–G), 100lm (H). Taken from Christiansen et al., (2016b); courtesy of Chris Dillingham.*

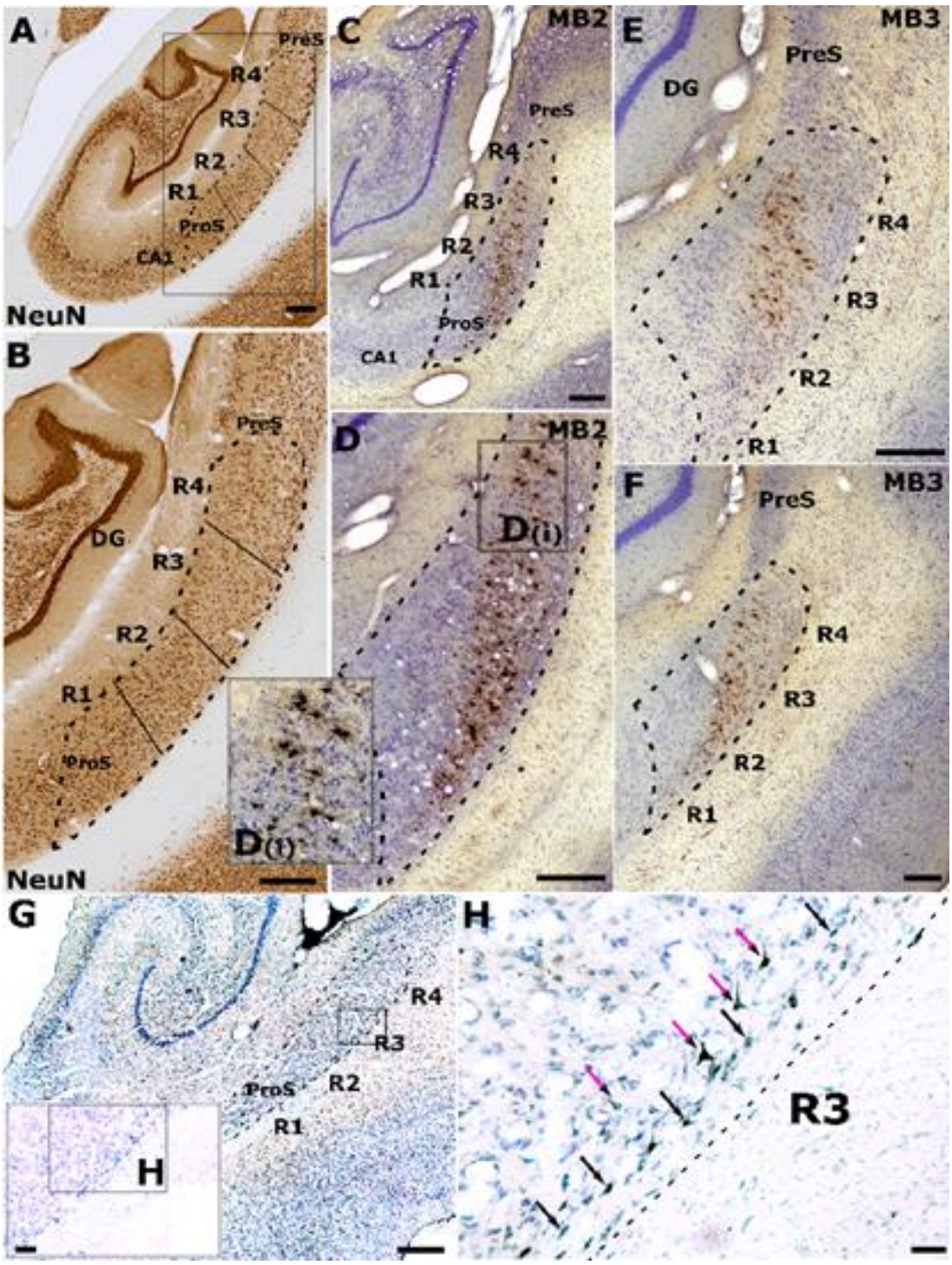
A
PreS
R4
R3
R2
R1
ProS
CA1
NeuN
B
PreS
R4
DG
R3
R2
R1
ProS
D(i)
NeuN
C
MB2
PreS
R4
R3
R2
R1
ProS
CA1
D
MB2
D(i)
E
MB3
PreS
DG
R4
R3
R2
R1
F
MB3
PreS
R4
R3
R2
R1
G
R4
R3
ProS
R2
R1
H
H
R3

2.3 Results

2.3.1 Rats

Eleven cases, with a total of fourteen injections, provided the quantitative data for the inputs to the mammillary bodies (Table 2.1 and Figure 2.5). The five anterior thalamic injection cases used for cell counts were those in which the tracer injection was most clearly centred in either the anteroventral nucleus or anteromedial nucleus (Table 2.1 and Figure 2.5). Cells projecting to the medial mammillary nucleus, the anteroventral nucleus and the anteromedial nucleus all displayed different topographies in the proximal-distal plane (Figures 2.3 and 2.6). There were also clear differences in the anterior-posterior plane when the findings from the mammillary body injections were compared with those in the anterior thalamic nuclei (Figure 2.7).

2.3.1.1 Rat injection sites

Figure 2.5 contains detailed depictions of the injection location for each case. Of the eleven mammillary body injection cases consisting of fourteen injections in total, the majority of the tracer injections were centred on the lateral part of the medial mammillary nucleus (pars lateralis, n = 9). Two cases contained some tracer spread into the medial part of the medial mammillary nucleus (WGA, 86_1, 86_9), and one had overlap into the lateral mammillary nucleus. The anterior thalamic nuclei cases were all selected for their clearly centrally located injections in either the anteroventral, or anteromedial thalamic nucleus (Figure 2.5). None of these injections appeared to cross the midline, but the anteromedial injections often spread medially to the edge of the interanteromedial nucleus. Most cases consisted of unilateral injections, however, for cases 58_1 and 58_2, which were bilateral, both hemispheres were counted and the mean computed of the two.

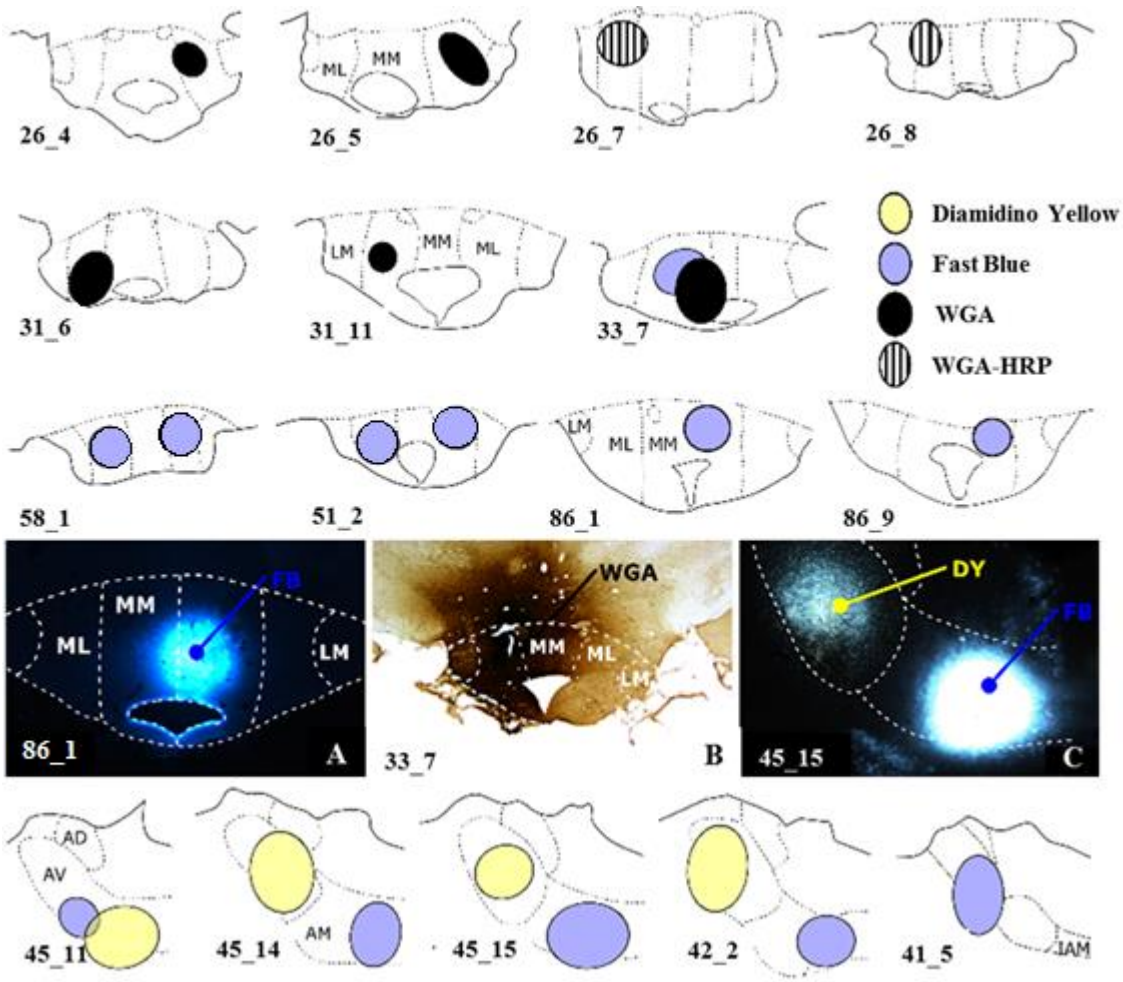

Figure 2.5 *Coronal sections depicting the location of each tracer injection in the rat mammillary bodies (top three rows and photomicrographs A and B) and anterior thalamus (bottom row and photomicrograph C). Mammillary body cases consisted of eight unilateral injections, four of which used wheat-germ agglutinin (WGA), two using WGA conjugated to horseradish peroxidase (WGA-HRP), and two using Fast Blue (FB). These two FB injections (86_1 and 86_9) specifically targeted pars medialis of the medial mammillary body (MM) (A), while the remaining cases were centred in pars lateralis of the medial mammillary body (ML) (B). Of three additional cases, two received bilateral injections of FB into pars lateralis, while case 33_7 received injections of WGA and FB in pars lateralis of the same hemisphere. In four anterior thalamic cases two different tracers [Diamidino Yellow (DY) and FB] were injected into either the anteroventral nucleus (AV) or the anteromedial nucleus (AM), and in the final case only FB was injected into AV. Scale bars = 250µm. Other abbreviations: AD = anterodorsal thalamic nucleus; IAM = interanteromedial nucleus; LM = lateral mammillary body.*

2.3.1.2 Subicular inputs to the mammillary bodies

The various retrograde tracer injections were centred in either pars lateralis (n = 9) or pars medialis (n = 2; FB, 86_1, 86_9) of the medial mammillary nucleus (Figure 2.5). These injections consistently led to retrogradely labelled cells across the proximal-distal

axis of the septal and adjacent intermediate subiculum (Figures 2.3 and 2.6A, B, 2.7A). The highest proportion of retrogradely labelled cells (relative to the NeuN counts) was, however, present on the proximal side of the central subiculum for all mammillary body injections in pars lateralis and pars medialis (i.e. R2; Figures 2.3 and 2.6A). A repeated measures ANOVA for all mammillary body cases revealed a significant main effect for region of interest along the proximal-distal plane (F (3, 33) = 33.20, $p < 0.001$). Follow-up simple effects tests found the lowest relative density of label was consistently in the distal most region (R4), which was significantly less than that in R1, R2 and R3 (R1: t (11) = -4.14, $p < 0.008$; R2: t (11) = -7.42, $p < 0.008$; and R3: t = (11) = -6.70, $p < 0.008$; Figure 2.6A). At the same time, labelled cell density typically increased going from the septal to the intermediate hippocampus according to a linear regression whereby cell counts in the mammillary body injection site group were significantly predicted by the anterior-posterior level of the section ($\beta = 1.47$, t (6) = 16.35, $p < 0.001$), which explained a significant proportion of the variance ($R^2 = 0.98$, F (1, 6) = 267.42, $p < 0.001$; Figure 2.7A).

Comparing separately the septal topographies of injections into pars lateralis and pars medialis of the medial mammillary nucleus (cases 86_1 and 86_9) it is apparent that the pars medialis injections resulted in less retrograde label in the distal-most portion of the subiculum, R4 (t (10) = 3.40, $p < 0.013$, Figure 2.6A), however, this was not the case for the other three more proximal regions of interest (all $p > 0.013$). In terms of their anterior to posterior topographies, pars lateralis and pars medialis both showed significant increases from septal to intermediate subiculum in separate regression analyses (pars lateralis: $\beta = 1.60$, t (6) = 11.34, $p < 0.001$, $R^2 = .96$, F (1, 6) = 128.56, $p < 0.001$; pars medialis: $\beta = 1.49$, t (6) = 4.38, $p < 0.001$, $R^2 = .76$, F (1, 6) = 19.21, $p < 0.01$; Figure 2.7A).

Considerable retrograde label was also present in the temporal (ventral) subiculum following tracer injections into pars lateralis or pars medialis of the medial mammillary nucleus (Figure 2.6B). Along the proximal-distal axis, there was an apparent increase from proximal to distal temporal subiculum for pars lateralis injections, but not for pars medialis injections (Figure 2.6B). A repeated measures ANOVA revealed a significant main effect of region of interest for the pars lateralis injections (F (3, 18) = 8.45, $p < 0.05$), but follow-up simple effects showed that no significant differences existed for pairwise comparisons between individual regions of interest (all $p < 0.008$). For pars medialis injection sites, no significant main effect along the proximal-distal axis was found (F (3, 3) = 0.34, $p = 0.67$). Analysis of the topography along the temporal-intermediate axis was only possible for all pars lateralis injections, as for one pars medialis case the label was not visible for all five sections, leaving only one case. A linear regression found that section level significantly predicted pars lateralis cell counts going posteriorly ($\beta = 2.15$, t (6) = 11.18, $p < 0.001$, $R^2 = .98$, F (1, 6) = 125.00, $p < 0.001$, Figure 2.7B).

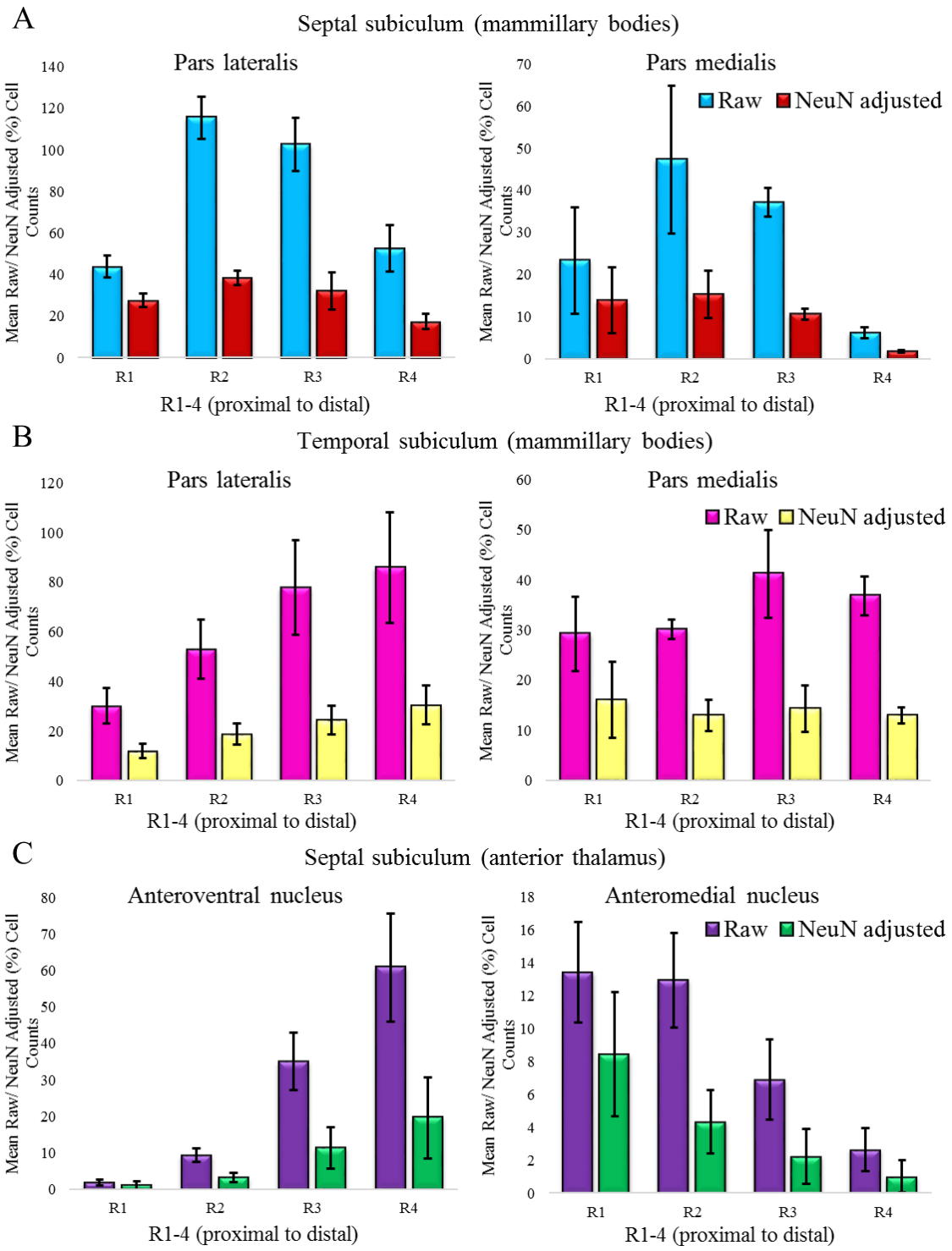

Figure 2.6 *Raw and NeuN adjusted mean cell counts in septal subiculum for pars lateralis (left) and pars medialis (right) injections (A); in temporal subiculum for pars lateralis (left) and pars medialis (right) injections (B); and in septal subiculum for the anteroventral nucleus (left) and anteromedial nucleus (right) injections (C), across the proximal-distal length of the subiculum. NB. Differing scales used to show pattern clearly.*

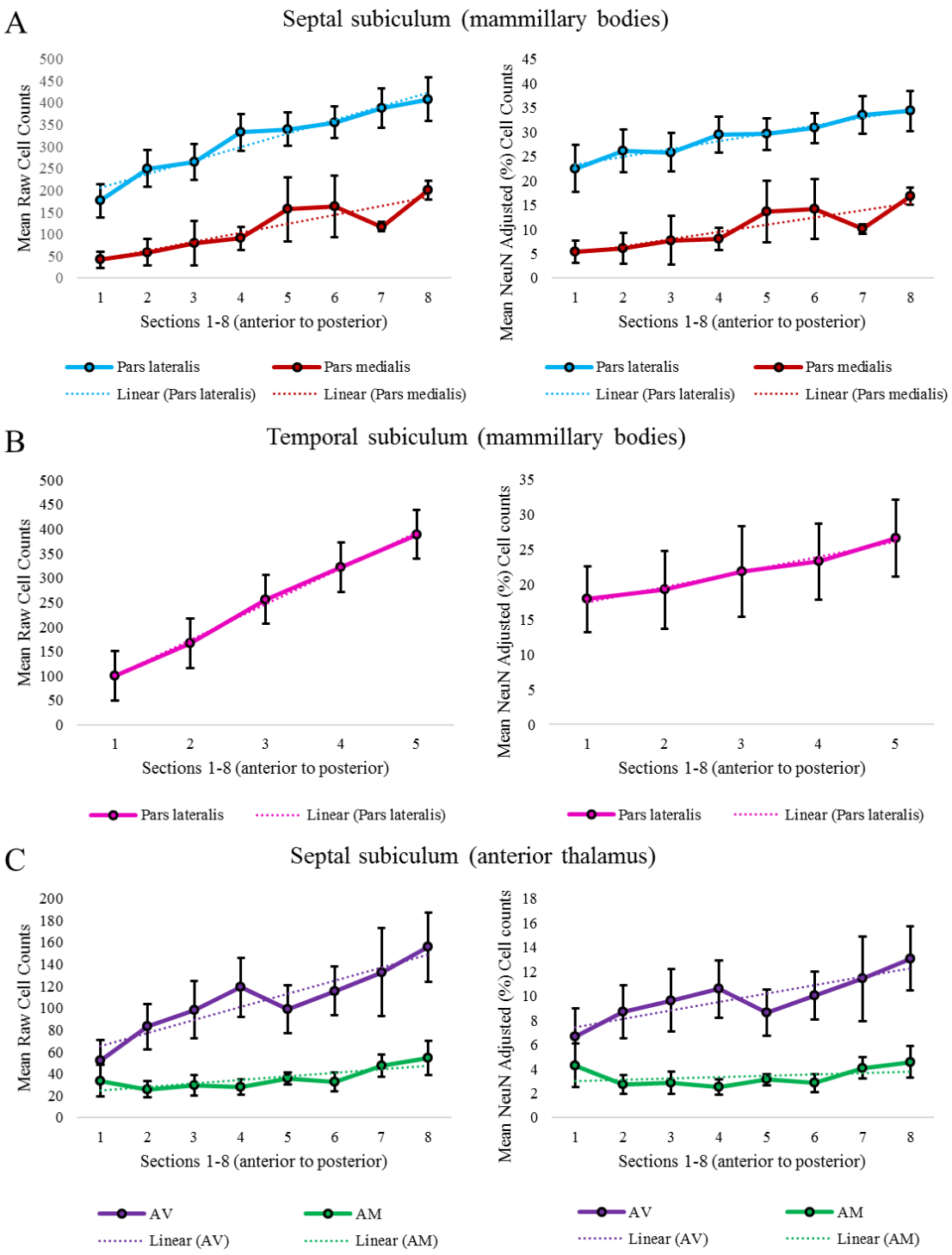

Figure 2.7 *Raw (left) and NeuN adjusted (right) cell counts for pars lateralis and pars medialis injections in septal subiculum (A); pars lateralis injections in temporal subiculum (B); and anteroventral nucleus and anteromedial nucleus injections in septal subiculum (C), across the anterior-posterior length of the subiculum. Abbreviations: AM = anteromedial nucleus; AV = anteroventral nucleus. NB. Differing scales used to show pattern clearly.*

2.3.1.3 Subicular inputs to the anteromedial thalamic nucleus

Anteromedial nucleus injections consistently resulted in most labelled cells being found in the proximal subiculum and the least in the distal subiculum (Figure 2.3 and right of 2.6C). Consequently, the highest proportion of labelled cells, relative to NeuN cell counts, was in the proximal subiculum, and a main effect was found across the regions of interest in this direction (F (3, 9) = 21.37, $p < 0.001$), although no pairwise comparisons were significant in this group once Bonferroni-adjustment had been applied (right of Figure 2.6C). There was no significant increase or decrease in the proportion of retrogradely labelled cells (NeuN-adjusted) from septal to intermediate hippocampus ($\beta = 0.11$, t (6) = 0.88, $p = 0.41$; $R^2 = .12$, F (1, 6) = 0.77, $p = 0.41$; right of Figure 2.7C). In no case did the anteromedial nucleus injection appear to cross the midline, although the injections typically spread medially to reach the edge of the interanteromedial nucleus. The lack of label in the temporal (ventral) subiculum meant that this region was not included in these analyses (also for the anteroventral nucleus).

2.3.1.4 Subicular inputs to the anteroventral thalamic nucleus

Anteroventral nucleus injections revealed an increasing gradient of inputs from proximal (lowest) to distal (highest) subiculum, which was supported by the repeated measures ANOVA revealing a main effect of proximal-distal region (F (3, 12) = 13.30, $p < 0.001$), albeit the only significant pairwise comparison was found between the most proximal region (R1) and the adjacent R2 (left of Figure 2.6C). Linear regression analysis of the anterior-posterior axis revealed a significant increase from septal to intermediate subiculum in anteroventral nucleus projections ($\beta = 0.69$, t (6) = 4.24, $p < 0.01$; $R^2 = .75$, F (1, 6) = 17.95, $p < 0.01$; right of Figure 2.7C).

2.3.2 Monkey

The three cases with HRP injections into the medial mammillary bodies displayed extensive label across the mid, i.e. pyramidal, cell layer of the subiculum. In contrast, all of the monkeys with thalamic tracer injections had label confined within the deepest subiculum layer. Along the four subdivisions in the proximal-distal plane, the mammillary bodies, the anteromedial nucleus, and anteroventral nucleus all showed very similar distributions in the source of their inputs. The distal half of the subiculum consistently had the highest cell counts. In fact, area R3 contained the highest number and highest proportion of labelled cells (relative to the total number of NeuN cells) in all cases, i.e. irrespective of whether the injection site was in the mammillary bodies or the anterior thalamus (Figure 2.4). These analyses are, however, largely descriptive due to the relatively small number of cases, the variety of the tracer types that were used, the way in which tracers were visualised, and the period of time from surgery.

2.3.2.1 Monkey injection sites

For the mammillary body injections, three cynomolgus monkeys (MB1, MB2, MB3) received WGA-HRP into the medial mammillary nucleus, the injection MB3 received was slightly more medial, while the most lateral injection was in MB2, and MB1 was somewhere in between (Figure 2.8). For case MB1 the injection was predominantly in the right medial mammillary nucleus, and for MB2 and MB3 it was mostly in the left medial mammillary nucleus. In all cases the injections appeared moderately large, such that reaction product extended laterally to reach the lateral mammillary nucleus and medially to the midline. The active injection site was almost certainly far smaller than the overall area of reaction product (see Saunders et al., 2012).

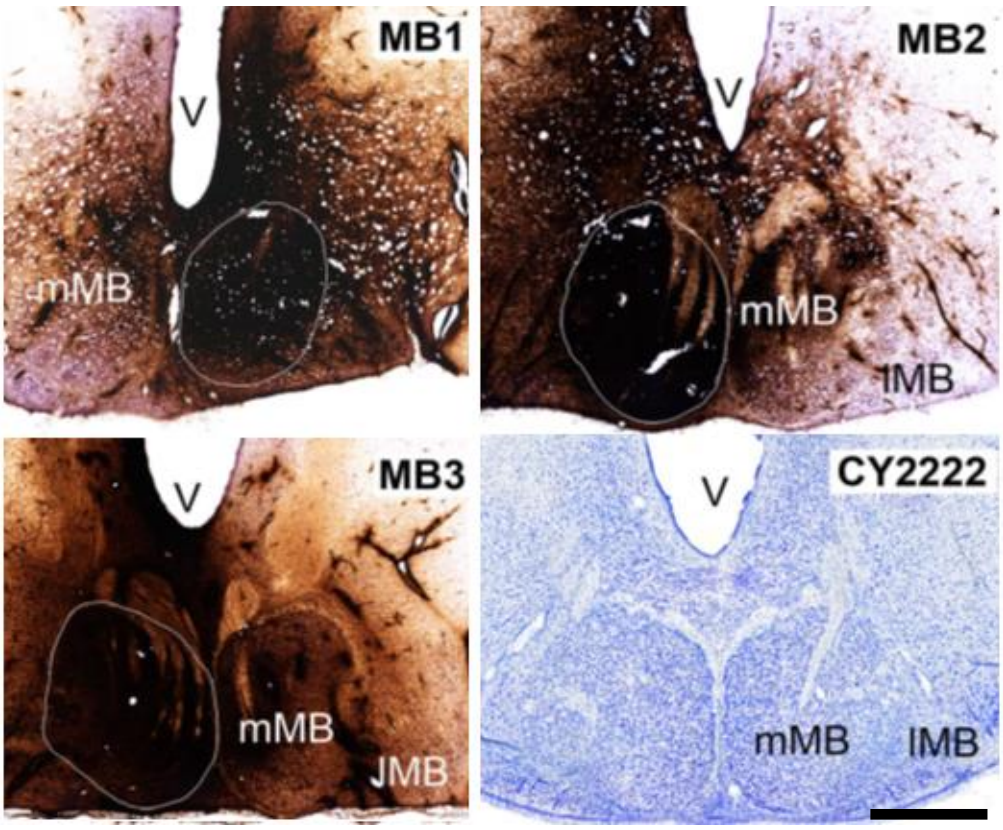

Figure 2.8 *Neuronal tracer injection sites in the macaque mammillary bodies. (A-C) In three cases (MB1, MB2 and MB3, respectively), unilateral injections of HRP were made into the medial mammillary body nucleus. (D) cresyl violet-stained coronal section through the mammillary bodies of a cynomolgus monkey. Abbreviations: lMB = lateral mammillary body; mMB = medial mammillary body; V = ventricle. Scale bar = 1mm.*

Five tracer injection cases primarily involved the anteromedial nucleus (Figure 2.9). Cases ACy1, ACy2, and ACy26 all had HRP injections centred in the midline of the anteromedial thalamic nucleus, with some spread into adjacent nuclei. In case ACy1, a large injection of HRP was centred in the anteromedial nucleus, but spread laterally to touch the border with the anteroventral nucleus, and caudally to touch the rostral mediodorsal nucleus. This injection also spread medial-ventrally, involving midline nuclei such as the nucleus reuniens, adjacent to the anteromedial nucleus. For case ACy2, the HRP injection was mostly contained within the anteromedial nucleus, reaching the midline (Figure 2.9). This case showed low levels of HRP transport throughout the brain. The HRP injection in case ACy26 involved the anteromedial

nucleus, but also extended ventrally to include the midline nuclei, seemingly reaching nucleus reuniens (Figure 2.9).

Case BRh3 received FB fluorescent retrograde tracer injections into the caudal anteromedial nucleus. In the left hemisphere of BRh3, FB was injected into the mid and caudal anteromedial nucleus (Figure 2.9). Only case BRh5 had a tracer injection (FB) into the left anteroventral nucleus. This injection was localised centrally in the more medial and caudal part of the nucleus (Figure 2.9).

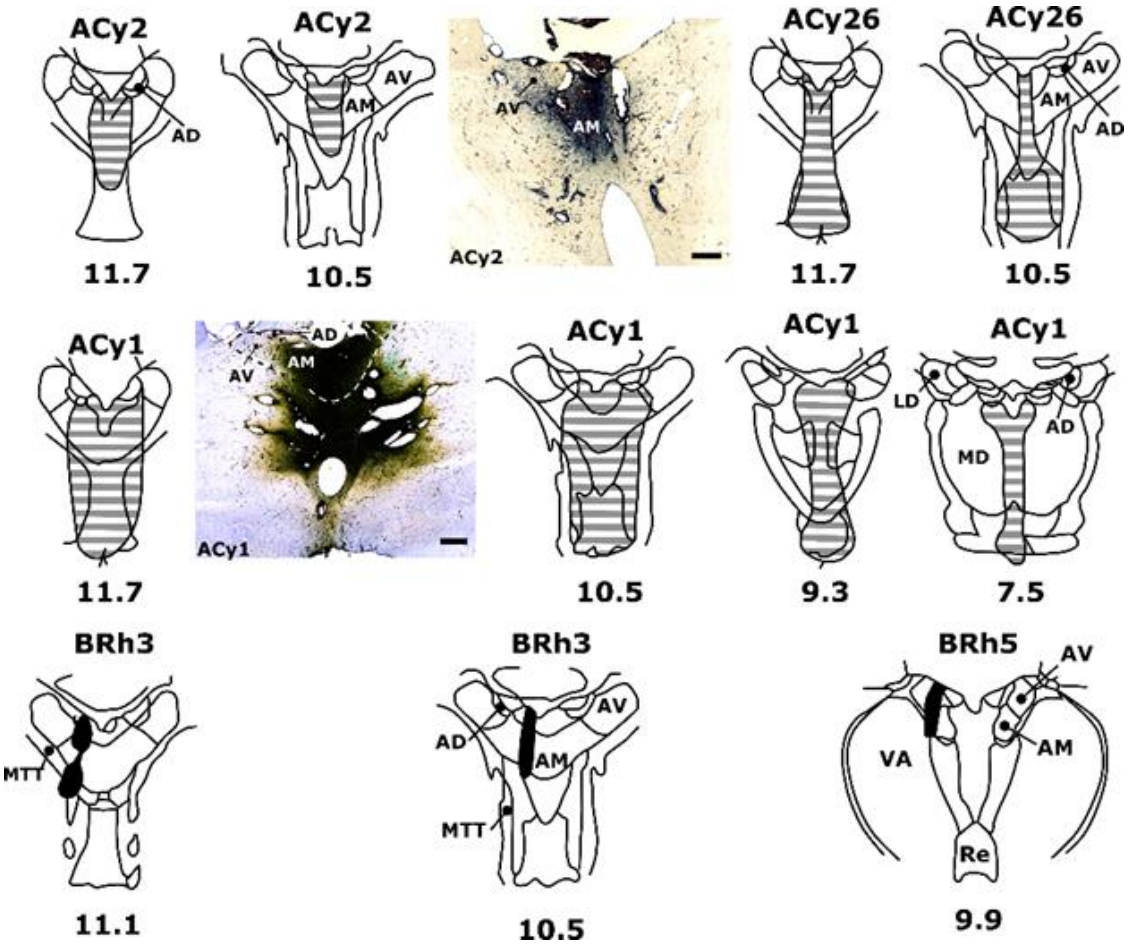

Figure 2.9 *Neuronal tracer injection sites in the anterior thalamus of macaque monkeys. In four cases, injections of either HRP (cases ACy1, ACy2 and ACy26) or Fast Blue (FB; case BRh3) were centred in the anteromedial nucleus. In one additional case an injection of FB was centred in the caudal anteroventral nucleus (case BRh5). Photomicrograph insets show tracer spread in coronal sections of the anterior thalamus for HRP cases ACy2 (top centre) and ACy1 (mid left). Numbers below each schematic diagram represent anterior-posterior levels, relative to bregma, according to Olszewski (1952). Abbreviations: AD = anterodorsal nucleus; AM = anteromedial nucleus; AV = anteroventral nucleus; LD = laterodorsal nucleus; MD = mediodorsal nucleus; MTT = mammillothalamic tract; Re = nucleus reuniens; VA = ventral anterior nucleus. Scale bar = 500lm. Image taken from Christiansen et al. (2016b).*

2.3.2.2 Subicular inputs to the mammillary bodies

For the three cases with medial mammillary body injections (MB1, MB2, and MB3), the patterns of retrograde label in the subiculum were, in many regards, very consistent. Label spanned the entire width of the subiculum, but the largest amount of normalised labelled cells was repeatedly found in the mid-region of the subiculum (R2 and R3), with a consistent small bias towards the second to most distal subdivision of this region (Figure 2.10). The most proximal portion of the subiculum (prosubiculum) contained

the least label. The subiculum label was confined to the pyramidal cell layer. In the anterior-posterior plane, all three monkeys showed an increase in number of labelled cells from anterior to posterior subiculum (Figure 2.11). This increase was least obvious in case MB3. A feature consistent in all cases was that the laminar location of the label shifted when going from proximal to distal subiculum (Figure 2.4). In the more proximal subiculum the cells projecting to the mammillary bodies were deep cells, i.e. just above the polymorphic layer, but they increasingly occupied a more superficial location when going more distally. A direct comparison of these contrasting patterns in the rat and monkey brain can be seen in Figure 6.2 on page 220.

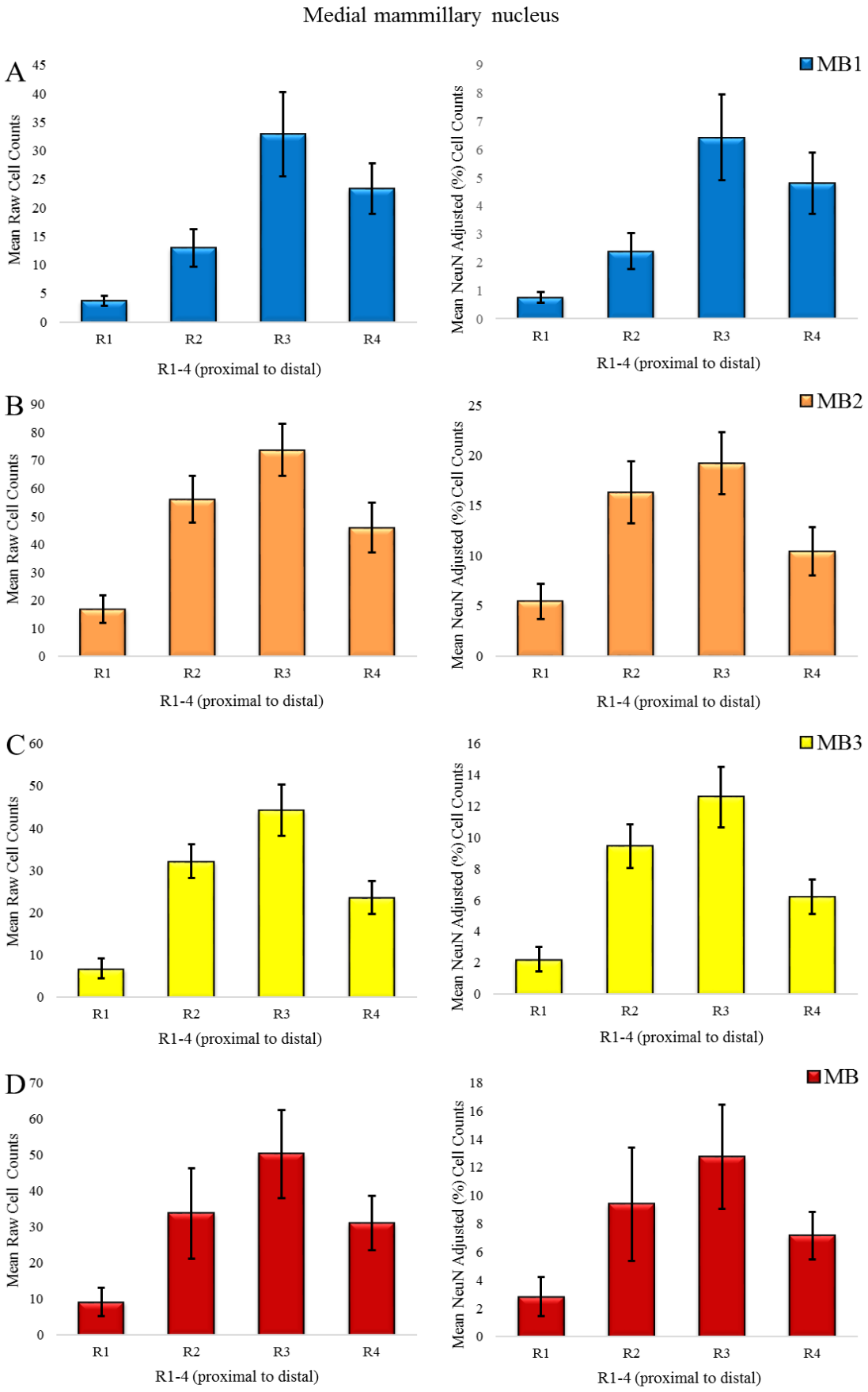

Figure 2.10 *Raw (left) and NeuN adjusted (right) cell counts for mammillary body cases MB1 (A), MB2 (B), MB3 (C) and the mean of all three cases (D) across the proximal-distal length of the subiculum. Abbreviation: MB = mammillary bodies. NB. Differing scales used to show pattern clearly.*

Medial mammillary nucleus

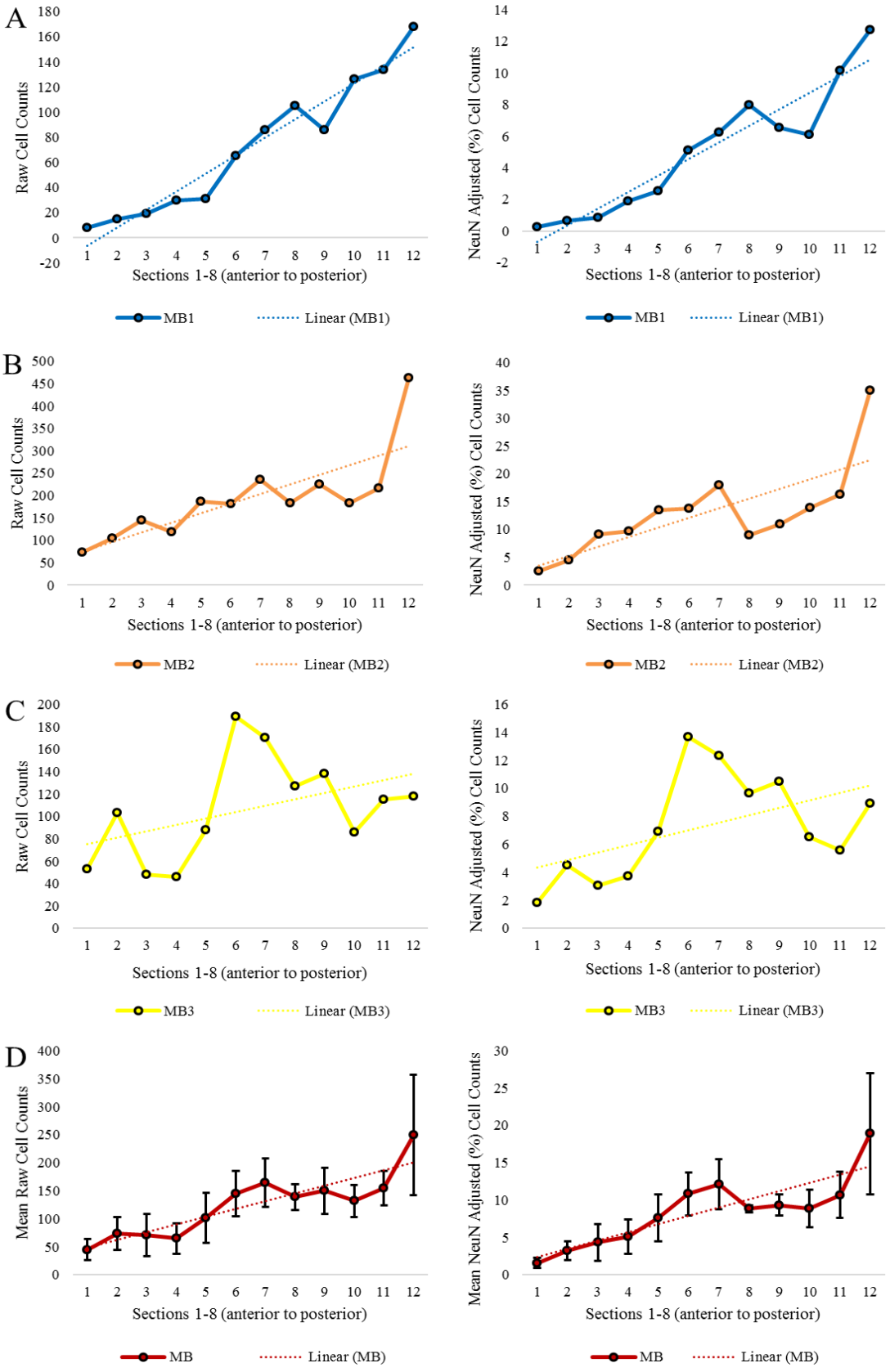

Figure 2.11 *Raw (left) and NeuN adjusted (right) cell counts for mammillary body cases MB1 (A), MB2 (B), MB3 (C) and the mean of all three cases (D) across the anterior-posterior length of the subiculum. Abbreviation: MB = mammillary bodies. NB. Differing scales used to show pattern clearly.*

2.3.2.3 Subicular inputs to the anteromedial nucleus

The three HRP injection cases (ACy1, ACy2, and ACy26) received only a single tracer injection into the anteromedial nucleus, with varying encroachment into adjacent nuclei. There was a lot of variation in the total numbers of labelled cells across the three HRP cases, however, there was a clear consistency in the distribution of label. Once again, the fewest labelled cells were found in the most proximal portion of the subiculum, i.e. the prosubiculum (R1), while the second most distal region (R3) again contained the largest number of labelled cells (Figure 2.12). This proximal-distal distribution was maintained along the entire rostral-caudal extent of the subiculum. From cases ACy1, ACy2 and ACy26 an anterior-posterior gradient also emerged, with the anterior subiculum possessing the greatest number of inputs to the anteromedial thalamic nucleus (Figure 2.13). Throughout, the labelled cells were confined to the deepest cell layer so that most label was found in polymorphic cells, though some were also found in pyramidal cells at the upper junction of this lamina of the subiculum.

The pattern of cell counts in case BRh3 (rhesus) matched those of the HRP cases. The prosubiculum (R1) again had the least label, and the more distal end of the subiculum consistently had the most label (R3). Although the most anterior three sections could not be counted, due to a localised infarct, the numbers of labelled cells mostly decreased going posterior, so that the most anterior sections (back of the uncus) contained the highest number of labelled subicular cells in BRh3 (~90 cells per section) while the most posterior sections contained about half that number. However, there was a peak in the middle of the anterior-posterior axis, so the decreasing gradient was not linear nor as clear-cut as for the HRP cases.

2.3.2.4 Subicular inputs to the anteroventral nucleus

There was only anteroventral nucleus injection data for one case, BRh5, but the pattern of labelled cells from this injection was in such stark contrast to that of the other injection sites that it warrants consideration. In a manner similar to the anteromedial injections, the least labelled cells were found in the most proximal subiculum (i.e. the prosubiculum, R1), with the two most distal sectors containing the largest numbers of cells projecting to the thalamus (R3 and R4). Cell counts along the anterior-posterior axis revealed a gradual, consistent increase in label density going towards the posterior hippocampus. This anterior-posterior profile bore a striking contrast to that seen for the anteromedial thalamus injections. The labelled cells were restricted to the deepest cell layer for both BRh3 and BRh5.

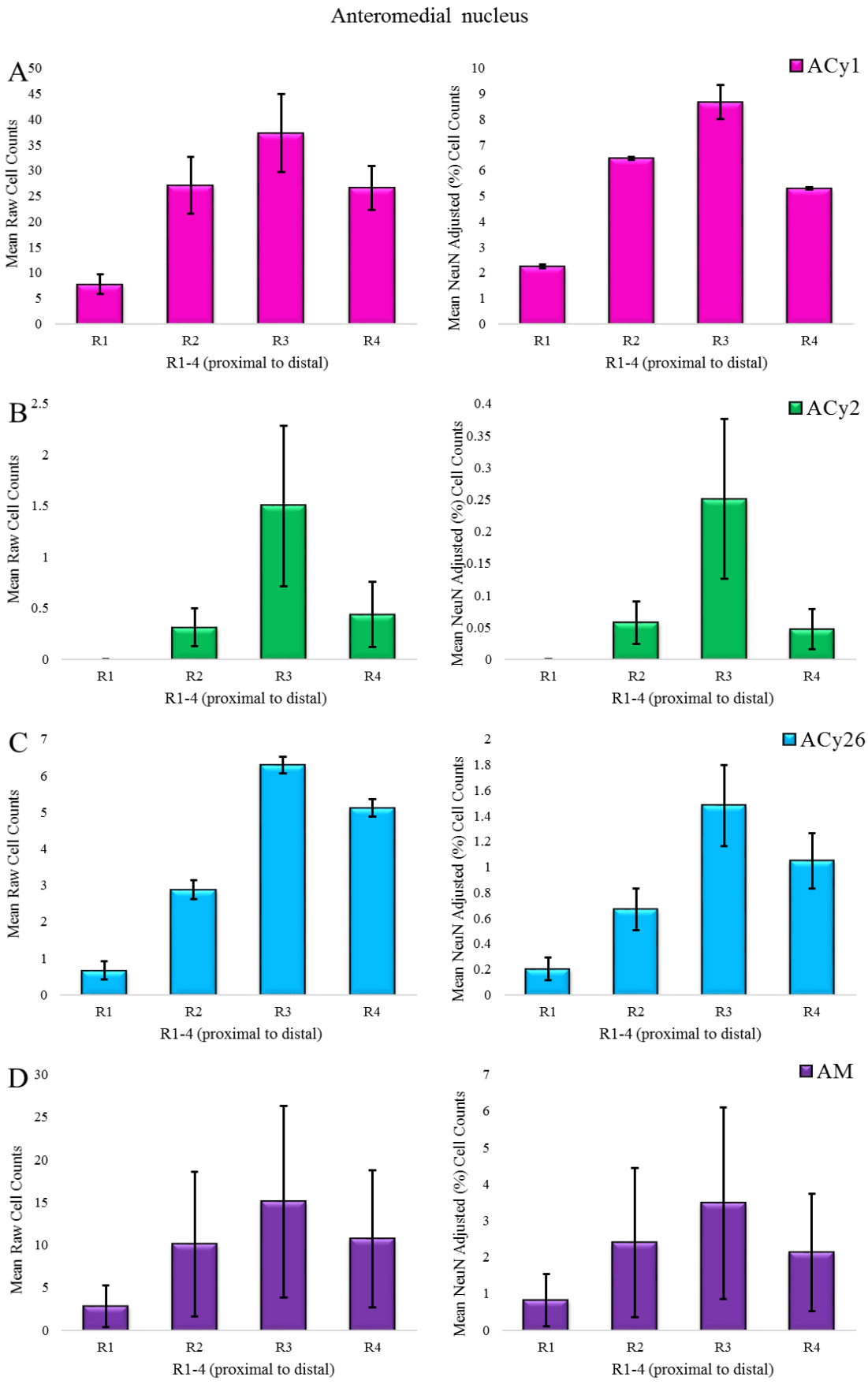

Figure 2.12 *Raw (left) and NeuN adjusted (right) cell counts for anteromedial nucleus cases ACy1 (A), ACy2 (B), ACy263 (C) and the mean of all three cases (D) across proximal-distal length of the subiculum. Abbreviation: AM = anteromedial nucleus. NB. Differing scales used to show pattern clearly.*

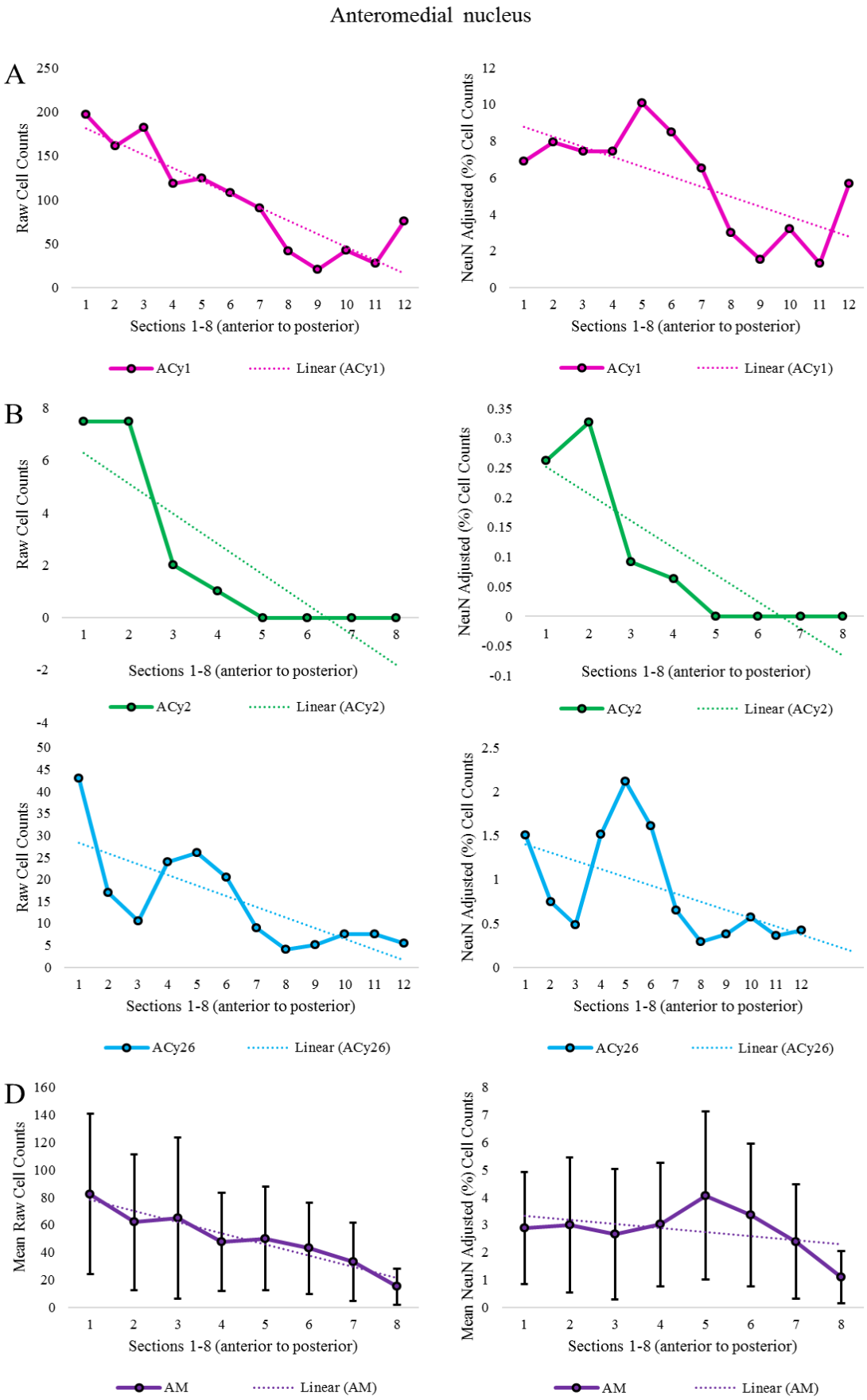

Figure 2.13 *Raw (left) and NeuN adjusted (right) cell counts for anteromedial nucleus cases ACy1 (A), ACy2 (B), ACy263 (C) and the mean of all three cases (D) across anterior-posterior length of the subiculum. Abbreviation: AM = anteromedial nucleus. NB. Differing scales used to show pattern clearly.*

2.4 Discussion

The principal aim of this study was to systematically investigate differences in the topographies of projections from the subiculum to the anteromedial and anteroventral thalamic nuclei and mammillary bodies in 1. the rodent and 2. the primate brain. This was achieved through the use of a number of different types of retrograde tracers injected into the sites of interest in these animals, and by quantifying cell counts along the proximal-distal and anterior-posterior axes of the subiculum. Despite previous studies having described hippocampal efferents to the diencephalon in both rats (Ishizuka, 2001; Meibach and Siegel, 1975, 1977a, b; Naber and Witter, 1998; Swanson and Cowan, 1977; Wright et al., 2010, 2013) and monkeys (Aggleton et al., 1986, 2005b; Krayniak et al., 1979; Xiao and Barbas, 2002b), the present study quantified and compared, where possible, the pattern of these connections both within and across species. The data from the monkey experiments were, however, limited by both the numbers of cases and variations in their methodology. Consequently, comparisons involving these cases are descriptive. A particular focus throughout the study concerned how the origins of these diencephalic projections respect different hippocampal planes.

2.4.1 Laminae of the subiculum

In line with previous studies (Aggleton et al., 1986, 2005b; Ishizuka, 2001; Kishi et al., 2000; Meibach and Siegel, 1975, 1977a, b; Naber and Witter, 1998; Sikes et al., 1977; Wright et al., 2010, 2013), this study found that the outputs to the thalamus and mammillary bodies were clearly segregated by their laminae of origin in both rats and monkeys (see also Aggleton et al., 2005b; Ishizuka, 2001). Cell laminae comparisons revealed how mammillary body inputs arose from intermediate layers while the thalamic inputs arose from the deepest subiculum cell layer. In the rat, these thalamic projections arose from modified pyramidal cells, while in the monkey much of this

input came from deep polymorphic cells (see also Aggleton et al., 1986, 2005b; Xiao and Barbas, 2002b). A similar laminar segregation is also seen in the squirrel monkey (Krayniak et al., 1979), implying that this is a very general feature of subiculum organisation. In the rat it has been possible to further confirm this laminar separation as individual subiculum cells do not project to both the mammillary bodies and the anterior thalamus (Wright et al., 2010). Based on their parahippocampal projections, it has been proposed that the deepest subiculum layer in the rat (thalamic inputs) is comparable to isocortical layer VI, while more superficial pyramidal cells (mammillary inputs) reflect isocortical layer V (Honda and Ishizuka, 2015).

2.4.2 Transverse (proximal-distal) axis of the subiculum

In the rat, the proximal–distal plane revealed opposing gradients of inputs to the rat anteroventral nucleus and anteromedial nucleus (Figures 2.3 and 2.6C), with inputs to the rat medial mammillary nucleus showing a third pattern. The majority of mammillary body projections from the septal hippocampus arose from the central subiculum while more distal inputs arose from the temporal subiculum (Figure 2.6A, B). Anteromedial thalamic projections in the rat originated predominantly from the proximal subiculum, along a steep gradient, whereas anteroventral projections originated mainly from distal subiculum, showing the reverse gradient. Mammillary body projections were positioned between the two - mostly in the second-most proximal region.

The more distal tendency of anteroventral nucleus projections from the subiculum was also found by Ishizuka (2001). The proximal-distal gradients found here also fit with other, previous findings of a proximal-distal divide for anterior thalamic nuclei projections in the rat (Meibach and Seigel, 1975, Wright et al., 2010). However, here the slope of the gradient within this structure has been quantified using four divisions,

revealing a steady increase from proximal to distal subiculum for anteromedial projections and vice versa for anteroventral projections. Moreover, although mammillary body efferents were found in more superficial layers and throughout the septal-temporal extent of the subiculum in previously outlined research in the rat (Meibach and Siegel, 1975; Witter et al., 1990; Wright et al., 2010), the graded proximal-distal nature of these projections has not previously been analysed. This gradient is of particular interest in this study as mammillary body outputs showed a high preference for the central two subdivisions of the subiculum, which was largely positioned between the anteromedial and anteroventral output sites.

In the rat, the proximal subiculum projections to the anteromedial nucleus overlap with the sources of inputs to the lateral entorhinal cortex, perirhinal cortex and prelimbic cortex (Aggleton, 2012; Ishizuka, 2001; Jay and Witter, 1991; Kloosterman et al., 2003; Naber and Witter, 1998; Naber et al., 2000; Witter et al., 2000a, b). Unlike the anteromedial thalamic connections, these hippocampal-cortical projections also originate from distal CA1. Based on these interactions, e.g. with the perirhinal cortex and lateral entorhinal cortex, the rat proximal subiculum might be expected to preferentially process object-based information (Ahn and Lee, 2015; Bussey and Saksida, 2007; Diana et al., 2007; Witter et al., 2000a, b). In contrast, the rat distal subiculum is more closely connected with the medial entorhinal cortex and postrhinal cortex, regions containing positional and navigational information (Burwell and Hafeman, 2003; Fyhn et al., 2004; Hafting et al., 2005).

The evidence for a functional proximal-distal gradient in the rat remains, at present, preliminary, with most support coming from electrophysiological studies. The two principal cell types in the rat subiculum are “bursting” and “spiking”, names that reflect

their electrophysiological properties (O'Mara, 2005). The distribution of bursting cells seems to remain positioned relative to the apical dendrites, whereas the axons of spiking cells have a more widespread dispersal in the transverse plane (Witter, 2006). A study from Kim and Spruston (2012) looked at the relationship between patterns of firing and target location in subicular neurons. Their results showed that, in line with previous observations, the distal subiculum projected predominantly to medial entorhinal cortex, retrosplenial cortex, and ventromedial hypothalamus, and consisted mainly of bursting neuronal cell types (~80%), while the opposite was true for proximal projections to lateral entorhinal cortex, nucleus accumbens, and orbitofrontal cortices, which consisted mainly of spiking neuronal cell types (~80%). Amidst these were projections to thalamic nuclei arising from intermediate subiculum, of which 50% were likely to be bursting neurons. The likelihood maps of bursting versus spiking neurons along the transverse plane projecting to their efferent targets are consistent with previous electrophysiological findings of these cell types.

Moreover, cells with spatial firing properties are found in the subiculum. Place firing by subiculum cells shows more coherence in the distal subiculum, associated with higher firing rates than the proximal subiculum (Sharp and Green, 1994). A complementary study from Kim et al. (2012) once more revealed a proximal-distal gradient in the subiculum in terms of sparse to dense firing rates, coding spatial representations. The proximal subiculum displayed sparse, canonical firing rates, but moving towards distal subiculum the firing rates became higher and more distributed. The authors inferred that the distributed spatial representation in the subiculum carries more information about spatial location and contextual cues than the sparse representations in CA1. More indirect evidence comes from the finding that proximal CA1 activity (most closely

interlinked with distal subiculum) has greater spatial resolution than distal CA1 (most closely interlinked with proximal subiculum; Henriksen et al., 2010).

Preliminary evidence for the complementary gradient (object-based processing in the proximal subiculum) comes from the differential activity of distal CA1 cells, as measured by Arc expression, for nonspatial learning (Nakamura et al., 2013; see also Hunsaker et al., 2008). Caution is, however, required as some electrophysiological studies of subicular spatial cells, e.g. boundary vector cells and place cells, have failed to find proximal-distal differences (Brotons-Mas et al., 2010; Lever et al., 2009).

In contrast to the rodent proximal-distal topography along the subiculum, the macaque subiculum showed similar profiles of label in the proximal-distal plane for all of the diencephalic targets examined. The greatest number of projections consistently arose from the more distal (R3) subiculum (Figures 2.4, 2.10 and 2.12). Support for this finding comes from a study that also placed retrograde tracers in the anteromedial nucleus of macaque monkeys (Xiao and Barbas, 2002b). Again, the distal subiculum was depicted as the major source of hippocampal inputs, with projections to the anteromedial nucleus present along the full anterior-posterior axis of the hippocampus. Intriguingly, that same study described some additional anteromedial thalamic inputs from CA3 (Xiao and Barbas, 2002b), something not observed in the present material.

Yet, anatomical proximal-distal topographies do exist in the monkey hippocampus for other connections. Examples already mentioned include how the proximal subiculum (and distal CA1) contain the majority of projections to prefrontal cortex, amygdala and nucleus accumbens, as well as connections with the perirhinal and rostral entorhinal cortices (Aggleton, 1986; Blatt and Rosene, 1998; Insausti and Munoz, 2001; Saunders

and Rosene, 1988; Suzuki and Amaral, 1990; Van Hoesen et al., 1979; Witter and Amaral, 1991). In contrast, the distal subiculum is preferentially interconnected with both caudal and lateral entorhinal cortex, as well as the parahippocampal areas TH and TF (Aggleton, 2012). These connections would again seem to provide a potential distinction between object based (proximal) and scene- or context-based (distal) connections within the monkey subiculum (Diana et al., 2007; Murray et al., 2007; Ritchey et al., 2015). Unlike rats, however, the majority of inputs to the medial diencephalon consistently arose from the distal half of the monkey subiculum, suggesting a bias towards scene- or context-based information.

2.4.3 Longitudinal (anterior-posterior/septal-temporal) axis of the subiculum

Research with rodents has repeatedly pointed to a greater specialisation in the septal (i.e. posterior) hippocampus for processing high resolution spatial information (Bannerman et al., 1999; Fanselow and Dong, 2010; Moser et al., 1995). An overarching conceptualisation, based initially on electrophysiological findings from rodent studies, is that the anterior hippocampus provides coarse, global representations while the more posterior hippocampus is required for fine-grained local representations (Collin et al., 2015; Poppenk et al., 2013). Other models also emphasise spatial information processing in the posterior hippocampus but with a transition to more emotion-related responses, including stress and anxiety, in the anterior hippocampus (Chase et al., 2015; O'Mara, 2005; Strange et al., 2014).

These functional models can readily be linked to the projections from the rat subiculum. The greater concentration of mammillary body and anterior thalamic inputs from the posterior half of the rat hippocampus, which is most marked for the anterior thalamic projections, fits with the considerable amount of evidence highlighting the importance

of these same diencephalic sites for spatial learning (Aggleton and Nelson, 2015; Beracochea and Jaffard,1987; Sutherland and Rodriguez, 1989; Vann, 2005, 2010; Vann and Aggleton, 2003). Furthermore, disconnection studies confirm that the rat anterior thalamic nuclei function conjointly with the hippocampus to support spatial learning (Henry et al., 2004; Warburton et al., 2001), with both the anteroventral nuclei and anteromedial nuclei involved (Aggleton et al., 1996; Aggleton and Nelson, 2015; Byatt and Dalrymple-Alford, 1996).

In the case of the rat mammillary bodies, hippocampal inputs also arise from the temporal ("anterior") subiculum, where there is a slight change in the proximal-distal profile of subiculum cells. These temporal subiculum projections terminate in the ventral mammillary bodies, while the septal (i.e. "posterior") subiculum preferentially terminates in the dorsal mammillary bodies (Kishi et al., 2000; Meibach and Siegel, 1975, 1977a), implying functional differences within the medial mammillary nucleus (see also Hopkins, 2005; Shibata, 1992). The presumption is that the rat mammillary bodies are involved in more than just spatial information.

There is growing evidence that human memory processes follow similar hippocampal gradients, such that increasingly refined contextual processing in the posterior hippocampus enhances the details of episodic memory (Collin et al., 2015; Poppenk et al., 2013; Poppenk and Moscovitch, 2011; Ranganath and Ritchey, 2012; Strange et al., 2014; Woollett et al., 2009). This functional gradient would appear to match the monkey medial mammillary body inputs, which show a gradual anterior-posterior shift, with most projections arising from the posterior hippocampus. As with rats, the macaque mammillary bodies are linked with scene and spatial learning (Aggleton and Mishkin, 1985; Parker and Gaffan, 1997a), consistent with human structural and

functional imaging findings that point to a relative posterior hippocampal specialisation for space and navigation (Poppenk et al., 2013; Strange et al., 2014; Woollett et al., 2009; see also Ranganath and Ritchey, 2012). There is also considerable clinical evidence highlighting the importance of the human mammillary bodies for episodic memory (Dusoir et al., 1990; Tsivilis et al., 2008; Vann, 2010; Vann and Aggleton, 2004; Vann and Nelson, 2015). It is, therefore, intriguing that the posterior hippocampus is more closely associated with accurate episodic memory (Collin et al., 2015; Poppenk et al., 2013; Poppenk and Moscovitch, 2011; Strange et al., 2014), thus matching these mammillary body gradients.

In the light of their shared roles in spatial navigation and episodic memory, it is also notable that the monkey retrosplenial cortex receives inputs from subicular cells that share the same topography in all three planes with the cells that project to the mammillary bodies (Aggleton, 2012; Kobayashi and Amaral, 2003). The potential significance of these shared features stems from the importance of the human retrosplenial cortex for aspects of episodic memory (Auger et al., 2012; Epstein, 2008; Maguire, 2001; Vann et al., 2009a), i.e. functions that seemingly overlap with those of the mammillary bodies.

The projections to the primate anteromedial nucleus predominantly arose from the anterior subiculum, a gradient shared with some other hippocampal efferents, e.g. those to the prefrontal cortex, perirhinal cortex, the amygdala and nucleus accumbens (Aggleton, 1986; Barbas and Blatt, 1995; Blatt and Rosene, 1998; Carmichael and Price, 1995; Friedman et al., 2002; Saunders and Rosene, 1988). The inclusion of prefrontal cortex is intriguing as it is the anteromedial nuclei, rather than the anteroventral nuclei, that are particularly interconnected with prefrontal cortex (Kievet

and Kuypers, 1977; Xiao and Barbas, 2002a, b). The implication is that the anteromedial nuclei provide an indirect route that interlinks the rostral subiculum with the prefrontal cortex, alongside the direct prefrontal connections from the subiculum (Aggleton et al., 2015; Carmichael and Price, 1995; Rosene and Van Hoesen, 1977; Xiao and Barbas, 2002b). A further prefrontal route is probably provided by nucleus reuniens, which also receives direct inputs from the subiculum (Aggleton et al., 1986). Indeed, two of the HRP injections (ACy1, ACy26; Figure 2.9) appeared to reach nucleus reuniens, although the distribution of subiculum label appeared no different from the two anteromedial nucleus injections cases in which this midline nucleus was not involved. This apparent lack of difference might reflect the lightness of the projections from the subiculum to nucleus reuniens in macaque monkeys (Aggleton et al., 1986).

The preliminary evidence (case BRh5) also suggests that some subicular-thalamic inputs in the primate brain (potentially to the anteroventral nuclei) have the opposite anterior-posterior gradient, i.e. they principally arise from the posterior hippocampus. This caudal hippocampal gradient, also shown by mammillary body outputs, is shared with connections to the retrosplenial cortex, caudolateral entorhinal cortices, anterior cingulate cortex (area 24) and area TE (Aggleton et al., 2005b; Insausti and Munoz, 2001; Kobayashi and Amaral, 2003; Suzuki and Amaral, 1994; Yukie, 2000). It has been suggested that the anteroventral nuclei in rodents provide a “return loop”, taking information back to the hippocampal formation, in contrast to the “feed-forward” prefrontal connections of the anteromedial nuclei (Aggleton et al., 2010; see also Xiao and Barbas, 2002a). Unfortunately, the return connections in the primate brain from the thalamus to the hippocampus are poorly understood. While it is known that all three anterior thalamic nuclei, as well as the laterodorsal nucleus, project directly to the

hippocampal formation of monkeys (Amaral and Cowan, 1980; DeVito, 1980), the density of these inputs, including the balance between the anteromedial and anteroventral nuclei, along with their sites of termination within the hippocampus, remain to be detailed. It is also known that the thalamus projects directly to the entorhinal cortex, though these inputs arise from midline nuclei rather than the anterior thalamic nuclei (Insausti et al., 1987). Clearly, there is a need to improve our understanding of thalamohippocampal inputs in the primate.

2.4.4 General implications and future directions

Much evidence supports the notion that the subiculum itself is highly involved in spatial memory encoding and retrieval. For example, IEG imaging in the form of Fos staining has indicated an increase in neuronal activation in the subiculum and other hippocampal subfields following performance of a radial arm maze (RAM) task in rats (Vann et al., 2000b). This Fos increase was found when contrasted with a control task in which the animal ran up and down one arm of a maze repeatedly. Other examples of increased subiculum Fos include when a rat is required to use novel spatial landmarks to perform an RAM task (Vann et al., 2000b). A further study by Jenkins et al. (2003) compared the distribution of c-*fos* activity in the hippocampal region during a Morris water maze task in which rats either had to learn a location within a session, taxing working memory, or find a submerged platform always directly related to the position of a landmark. The distribution of networks involved was compared using structural equation modelling, and revealed subicular involvement only in the landmark-based task, which requires the computation of a specific heading angle from the landmark.

Electrophysiological evidence has also shown location-related cell firing throughout the hippocampus in the freely-moving animal (e.g. O'Keefe, 1979, O'Mara, 1995),

however, the precision of the firing fields is not as apparent in subicular neurons as it is in CA1 place cells. While it is evident that the hippocampus is involved in a number of episodic memory processes in the primate brain, including spatial memory (Alvarado and Bachevalier, 2000), they have not been so distinctly separated in relation to anatomical substrates as they have been in the rat.

Based on the aforementioned research, another route this research could take in future is to look at graded differences in IEGs such as c-*fos* and *zif268* to see how their topographies of expression differ for different functional task differences. It seems logical that this should be the case as electrophysiological recording studies have already revealed differences in cell firing properties along the proximal-distal axis of other hippocampal substrates, namely CA1. For instance, Henriksen, et al. (2010) revealed spatial tuning within the entorhinal inputs to CA1; medial entorhinal cortex principally projects to proximal CA1 while lateral entorhinal cortex projects to distal CA1. Tetrode recordings were taken along the entirety of the proximal-distal plane in a 1-2m cylindrical box, which is able to produce firing data from multiple neurons at more than one location. Synchrony of medial entorhinal cortex theta oscillations was weaker in distal CA1 than proximal, which is plausible given the density of projections from this region in the proximal portion compared to distal CA1. Distal CA1 contained larger firing fields and firing was more wide-spread than that for proximal and to a lesser extent intermediate CA1. The amount of firing fields per cell increased along the proximal-distal axis; suggesting a role for distal CA1 in representing non-spatial information about objects and contexts. In relation to the subiculum, this suggests that distal subiculum should be more so involved in spatial memory, as it receives its inputs from proximal CA1, shown here to be involved in spatial memory, whereas proximal

subiculum receives inputs from distal CA1, suggestive of processing non-spatial information.

These studies look primarily at relationships between anatomical and electrophysiological cell properties. More detailed behavioural analyses have not yet been undertaken in this respect, making it fascinating to see if there are differential neuronal activations in these graded regions for different tasks that tax different aspects of episodic memory, such as object recognition or spatial memory, in accordance with their afferent and efferent projection sites. One would predict more activation in the subicular origins of the projections to the mammillary bodies, retrosplenial and anterior thalamic nuclei, as well as the proximal CA1, distal CA3, medial entorhinal cortex and postrhinal cortices, for spatial tasks (e.g. taxing allocentric strategies). Different activation patterns should emerge from non-spatial tasks, e.g. object recognition, which might rely on other inputs, such as distal CA1, proximal CA3, lateral entorhinal cortex, and perirhinal cortex. While many studies have confirmed the segregation of hippocampal inputs and outputs, this does not give us an understanding of how this breaks down into even more intricate topographies and why they are arranged in such a way. The implications of these findings are widespread, suggesting some functional segregation must be taking place in the memory system, else diencephalic projections would consist of intermixed neurons as their proximity to each other would not matter due to their performance of similar functions. As of yet, no studies have managed to selectively tax aspects of memory that rely predominantly on either the anteroventral or anteromedial thalamic nuclei, but their connectivity indicates that differences will emerge. Finally, research is needed to re-affirm the present findings in the rat using different tracer mechanisms, for example anterograde tracers such as Phaseolus vulgaris

(PHA-L) in each subicular region to confirm forward projections specifically to their targets.

2.4.5 Conclusions

The findings from the primate brain and rat brain are somewhat different, which may be expected in light of past results looking at subiculum topography. The proximal-distal organisation of anteroventral nucleus, anteromedial nucleus and mammillary body efferents in the rat was not replicated in the primate; rather, the primate subicular efferents to the anterior thalamic nuclei and mammillary bodies appeared to have a rostral-caudal gradient. Subicular origins were denser at the caudal end for the anteroventral thalamic nuclei and mammillary body projections, whereas anteromedial thalamic nuclei had denser origins at the rostral end of the subiculum.

One aim of the present study was to help determine whether the Papez circuit is organised so that it could potentially provide high-resolution, parallel information streams from the hippocampus to the medial diencephalon (Aggleton et al., 2010; Jankowski et al., 2015; Vann and Nelson, 2015). There is, for example, a potential distinction between object-based (proximal subiculum) and context-based (distal subiculum) information streams (Aggleton, 2012; Nakamura et al., 2013; Ritchey et al., 2015), seemingly reflected in the respective connections of the rat subiculum with the anteromedial and anteroventral thalamus. In contrast, the sources of the inputs to the rat mammillary bodies are more widely distributed across both the proximal-distal plane and the anterior-posterior plane of the hippocampus. Given that the mammillary bodies then project very densely, in a topographic manner, upon the anterior thalamic nuclei (Hopkins, 2005; Shibata, 1992), there remains the potential for object-based and context-based information to be relayed indirectly to different parts of the anterior

thalamic nuclei. A further segregation arises from the laminae separation of the subicular inputs to the mammillary bodies and the anterior thalamic nuclei, raising the question of whether the cell populations in this plane of the subiculum process different information types (Naber and Witter, 1998; Wright et al., 2013). For the monkey, a further challenge is to understand why the same proximal-distal zone (R3) contains the highest proportion of inputs to these various medial diencephalic targets. One intriguing clue comes from functional imaging evidence that the distal subiculum, along with presubiculum and parasubiculum, may be especially involved in the mental construction of scenes (Zeidman et al., 2015).

Chapter 3: A functional analysis of the rat subiculum using the immediate-early gene *zif268*

3.1 Introduction

The anatomical study reported in Chapter 2 revealed a clear topography along the proximal-distal axis of the subiculum, which reflected its different diencephalic targets. The anteroventral thalamic nuclei projections predominantly arise from distal subiculum while the projections to the anteromedial thalamic nuclei originate in proximal subiculum. In contrast, the mammillary body connections mainly arise from the middle region of the subiculum. There is also a proximal-distal organisation with other subicular connections. The proximal subiculum is primarily connected to distal CA1, lateral entorhinal cortex, perirhinal cortex and prelimbic cortex (Jay and Witter, 1991; Kosel et al., 1983; Naber et al., 1997, 1998, 2000, 2001a; Witter, 2006). On the other hand, the distal subiculum is primarily connected with proximal CA1, medial entorhinal cortex and postrhinal cortex (Amaral et al., 1991; Kloosterman et al., 2003; Naber et al., 2001a, b). It is, therefore, possible that differences in connectivity along the proximal-distal subiculum underpin functional differences along this axis.

Based on the connections with the lateral entorhinal cortex and perirhinal cortex, it might be predicted that the proximal subiculum preferentially processes object-based information. Electrophysiology, lesion and IEG studies have all highlighted the importance of the perirhinal cortex for object recognition (Albasser et al., 2010; Brown and Xiang, 1998; Desimone, 1996; Murray and Richmond, 2001; Ringo, 1996; Wan et al., 1999; Winters et al., 2008; Zhu et al., 1995a, b, 1996). Similarly, cells within the lateral entorhinal cortex have been found to fire in response to both novel and displaced objects (Deshmukh and Knierim, 2011). IEG studies have indicated a role for the lateral entorhinal cortex in processing object-related information (Wilson et al., 2013). Furthermore, the proximal CA3-distal CA1 projection shows a preferential involvement in non-spatial tasks (Nakamura et al., 2013), which in turn are connected more strongly

to the proximal subiculum. Distal CA1 has been shown in other studies to be sensitive to 3D object information, which alters its place field size, and also to odour-associations (Burke et al., 2011; Igarashi et al., 2014a, b), suggesting a non-spatial role for these cells.

In contrast to the proximal subiculum, the connectivity of the distal subiculum suggests a potential role in spatial processing. Findings from lesion and IEG studies are consistent with a role for the postrhinal cortex in spatial memory processes (Liu and Bilkey, 2002; Vann et al., 2000b). The medial entorhinal cortex is also strongly implicated in spatial memory, given the presence of grid cells, head direction cells and border cells in this region (Hafting et al., 2005; Sargolini et al., 2006; Solstad et al., 2008). Also, there is a spatial encoding gradient in CA1 in which the proximal part, which receives innervations from medial entorhinal cortex and distal CA3 and projects to distal subiculum, shows more spatial tuning and synchrony with medial entorhinal cortex theta oscillations than the distal part of CA1 (Henriksen et al., 2010). Furthermore, neurons activated during context learning were more likely to be re-activated at test phase for proximal CA1 than distal CA1, including for context fear conditioning and exposure to a novel environment (Nakazawa et al., 2016). This was also true for areas connected with proximal CA1 (medial entorhinal cortex, distal CA3), which also showed higher reactivation than those areas connected with distal CA1 (lateral entorhinal cortex, proximal CA3). Moreover, lesions to proximal but not distal CA1 resulted in impaired context memory retrieval. Hartzell et al. (2013) conducted a study in which rats explored either the same or two novel environments with the same object and examined, using Arc mRNA imaging, which parts of CA1 showed evidence of remapping for the separate environments. Again, proximal CA1 was found to show more evidence of remapping for the novel environments than distal CA1, suggesting

greater sensitivity to spatial context. These findings in combination suggest a microcircuit whereby the efferents to distal subiculum are selectively involved in spatial/context memory processes.

While the topography of subiculum connections with the parahippocampal cortex suggests a functional (object:spatial) division along the proximal-distal axis, the same division does not appear to be relayed on to the diencephalon. To date, no studies have found functional dissociations (object:spatial) between the anteromedial thalamic nuclei and anteroventral thalamic nuclei, despite their relative differences in electrophysiological properties and anatomical connections (Aggleton et al., 1996; Albo et al., 2003; Mitchell and Dalrymple-Alford, 2005, 2006; Tsanov et al. 2011; Vann et al., 2000a; Vann and Aggleton, 2004; Vertes et al., 2001, 2004; Wright et al., 2013). Both thalamic nuclei have been implicated in spatial memory but not object recognition (Aggleton et al., 1995, 1996; Aggleton and Nelson, 2015; Aggleton and Saghal, 1993; Dumont and Aggleton, 2013). Similar results have been found for the mammillary bodies, with lesion studies producing impairments on spatial memory tasks but not for object recognition tasks (Aggleton et al., 1995, 1996; Nelson and Vann, 2014; Santín et al., 2003; Vann and Aggleton, 2003). These results would seem to suggest a role for the entire proximal-distal extent of the subiculum in spatial memory but not object recognition memory.

The aim of the present study was to test two contrasting predictions concerning subiculum function. The first prediction is that a dissociation between object and spatial memory would be found along the proximal-distal axis of the subiculum, consistent with its known parahippocampal cortex connectivity, i.e. proximal subiculum would be selectively involved in object memory whereas distal subiculum would be preferentially

involved in spatial memory. The second prediction is that the entire proximal-distal extent of the subiculum is involved in spatial memory processes but not object-memory, as suggested by its diencephalic connectivity. The long-axis of the subiculum was also explored, as in the previous Chapter, to discern any potential differences in function from septal-intermediate dorsal subiculum, as the septal hippocampus shows more involvement in spatial learning in rodents, with a transition to emotional processes in the anterior hippocampus (Bannerman et al., 1999; Chase et al., 2015; Fanselow and Dong, 2010; Moser et al., 1995; O'Mara, 2005; Strange et al., 2014).

The expression of the IEG *zif268* was used as a marker of neuronal activity to assess the relative activation of the subiculum in rats that had performed spatial or object memory tasks. Four groups of animals were included in the study. Four groups performed either A. a working memory task in a radial-arm maze, B. an object recognition task in a radial-arm maze, C. a radial-arm maze behavioural control, matched for sensory-motor experience but without a mnemonic component, or D. no behavioural task but instead was a home-cage control group, to determine whether any of the behavioural conditions increased subiculum activity above baseline levels. The tissue from all animals was processed for expression of *zif268* and the number of Zif268-positive cells was quantified along the proximal-distal axis of the dorsal subiculum. The focus was on the dorsal subiculum as it is the principal source of hippocampal inputs to the anterior thalamic nuclei (Wright et al., 2013).

3.2 Methods

The behavioural training and immunohistochemistry for this experiment were carried out by Eman Amin, Anna Powell, and Liad Baruchin under the supervision of John Aggleton at Cardiff University.

3.2.1 Subjects

Forty-four male Lister Hooded rats (Harlan Bicester, UK) weighing 270-300g were used in the experiment. There were eleven rats in each of the four experimental conditions: Spatial Memory task, Object Recognition task, Behavioural Control, and the Home-Cage Control. Rats were housed in pairs under diurnal light conditions (14 hours light/10 hours dark). Behavioural testing was carried out during the light phase at the same time each day. Throughout the duration of the experiment, rats were maintained at, or above, 85% of their free-feeding body weight and water was available *ad libitum*. Prior to the start of the experiment, all rats were thoroughly habituated to handling. All aspects of the study adhered to the UK Animals (Scientific Procedures) Act, 1986, and had been approved by a local ethics committee.

3.2.2 Apparatus

An eight-arm radial maze was used for testing. The maze consisted of an octagonal central platform (diameter 34cm) with eight equally spaced radial arms (87cm long, 10cm wide), each ending in a recessed cylindrical food-well (diameter 2cm, 0.5cm deep). The base of the central platform and the arms were made of wood, and the walls of the arms were made of clear Perspex (24cm high). The central platform was placed on a pillar made of clear Perspex (diameter 34.5cm, 55cm high). A small container was placed in the centre of the maze, which acted as an additional food-well. A clear Perspex sliding door (12cm high) blocked the entrance to each arm, and thus controlled access to and from the central platform. A pulley system was used for each door so that the experimenter could control the arms from a distance. The maze was located in a rectangular room with salient visual cues such as geometric shapes and high contrast stimuli on the walls. Two standard ceiling lights were present throughout the

experiment, giving a mean light intensity of 671.0 lx, as measured in the centre of the central platform. To move the rats from their holding room to other test rooms they were placed in individual cages with an aluminium roof, floor and walls. This ensured that the rats could not see additional stimuli and they were being conveyed during the experiment.

3.2.3 Procedure

All animals in the three behavioural groups were tested in the radial-arm maze and underwent the same number of "arm runs" and received the same number of reward pellets. This was to match the experiences of the rats as closely as possible so that the principal difference across the three groups concerned the extent to which object or spatial memory were taxed. Animals in the three behavioural groups were placed in a dark, quiet room for 30 minutes prior to training and for 30 minutes after the test session. On the final test day all animals in the three behavioural test groups were placed in the dark room for 90 minutes after testing to minimise any unwanted disturbance before the animals were perfused. Animals in the Home-Cage Control group were also placed in the same dark room for the same amount of time but instead of undergoing behavioural training, they were returned to their holding room for the period corresponding to the test session and then returned to the quiet, dark room. This period was extended to 90 minutes on the final test day to match the other three groups.

3.2.3.1 Spatial Memory condition

Rats in this group were habituated to the radial-arm maze over three days, with all of the arms initially open for exploration. On each day the rats spent 15 minutes in the maze. On day 1, reward pellets (sucrose pellets in papers weighing 45 mg, Noyes Purified Rodent Diet, Sandown, U.K.) were scattered liberally around the maze (10g per rat). On

day 2, pellets were placed in and around the centre and arm wells (5g per rat), while on day 3, pellets were placed in the centre and arm wells only.

Animals in the Spatial Memory group were subsequently trained on the working memory version of the radial-arm maze task (Olton et al., 1978; see Figure 3.1 for an example of a correct and incorrect trial outcome) in which the optimal option for the animal is to visit each arm only once to collect the food reward. All eight arms were baited and an additional reward pellet was placed in the central platform, which was replaced after each arm entry. For each arm run, the rats were held for 30 seconds in the central platform before all doors were raised. Once the rat had selected an arm, the doors would be closed for 30 seconds, then the doors were raised again and the rat would return to the centre, which had been re-baited with a food pellet to match the other behavioural conditions. After the rat had made eight arm choices, irrespective of whether any of the same arms had been re-entered, the rats were held for 1 minute in the centre of the maze and all the arms were re-baited (signalling the start of a new test session). Each session consisted of 16 arm choices, i.e. 2 x eight choices. Errors were counted as re-entries into arms that had previously been explored within that session. Training took place until rats reached a criterion of 85% correct arm choices, which took approximately six days. Any rats that did not reach the criterion by this point were excluded from the analyses.

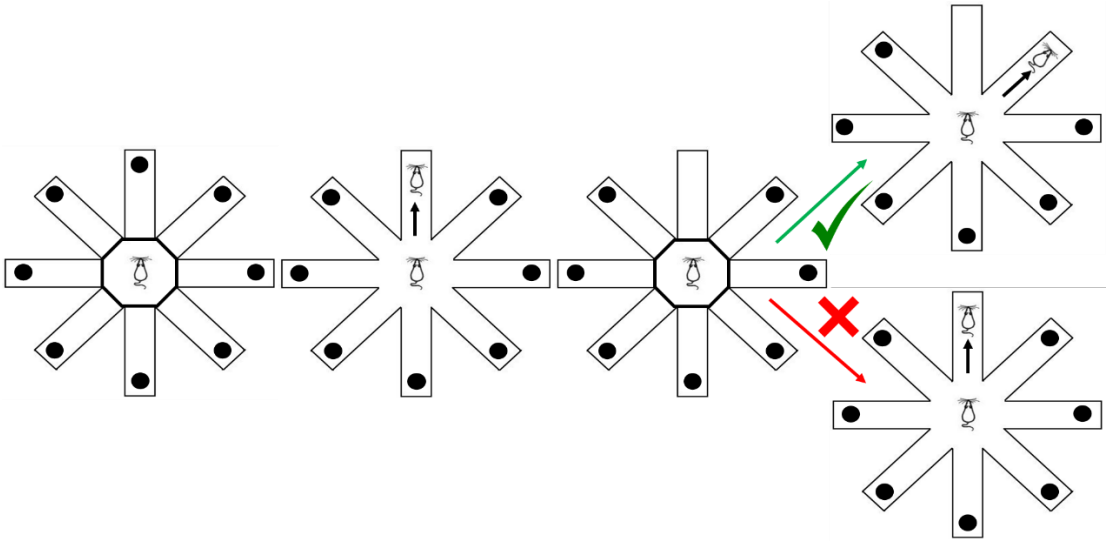

Figure 3.1 *Spatial Memory task: Example of a radial-arm maze training/test session trial, with the upper right outcome (green) being an example of a correct arm choice after the prior choice, i.e. selecting a previously unvisited arm. Meanwhile, the bottom right outcome (red) depicts an incorrect arm choice following the prior choice (visiting a previously visited arm).*

3.2.3.2 Object Memory condition

Animals in the Object Recognition group were given three days of habituation where they were allowed to explore the central platform and one of the arms of the maze (all other arms remained closed off by doors). Each habituation session lasted 15 minutes. On day 1, pellets were scattered liberally around the maze (10g per rat). On day 2, pellets (5g per rat), were placed in and around the centre and the well in the one arm. On day 3, pellets were only placed in the well of the one arm and the well in the centre of the maze.

Rats underwent approximately six days of training. The exact number was set individually for each rat based on the amount of time taken for their "matched" spatial memory task rat to reach the 85% criterion of correct trials in the spatial memory task. Each session involved 16 sets of 1 minute trials, whereby rats spent 30 seconds in the central area of the maze and 30 seconds in the open arm of the maze. Simple objects such as blocks and cups were placed at the centre of the maze and at the end of arm. The

reward pellet was placed in the food well and the sample object was placed on top of the food-well. A reward pellet was also placed between the two objects in the central platform.

Testing took place over one day, again to match the Spatial Memory group. A session consisted of 16 x 1 minute trials where rats spent 30 seconds in the central platform and 30 seconds in the arm of the maze. The well under the objects in the arm and the area between the two central objects was baited. Object A was presented first at the end of the arm, then object A was paired with a novel object B, in the centre of the maze. Next, object C was presented at the end of the arm and then paired with novel object D in the centre of the maze, and so on for 16 trials (see Figure 3.2 for the order and placement of the presentation of objects). Novel objects were counterbalanced in terms of whether they were placed on the left or right in the centre of the maze.

The test session was video-recorded and the exploratory behavior was timed. Object exploration was defined as directing the nose at a distance <1cm from the object with the vibrissae moving, and/or touching it with the nose or paws. Behavior that did not count as exploration included when rats sat on the object, if they used the object to rear upward with their nose pointing at the ceiling, or chewing the object.

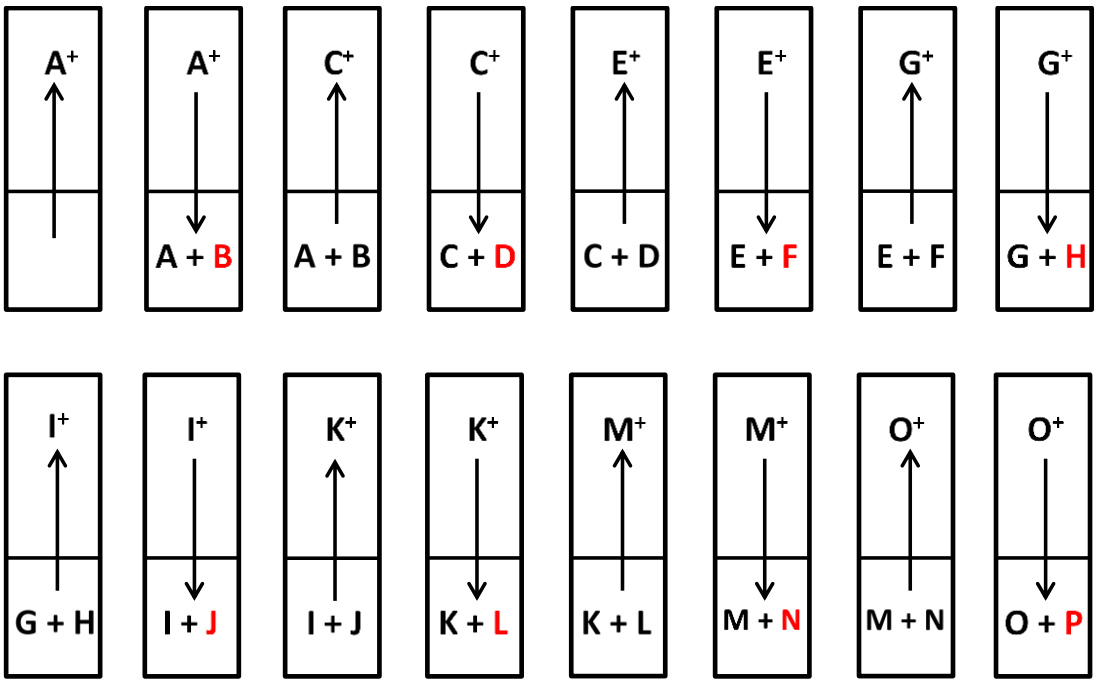

Figure 3.2 *Diagram of the order and layout of novel (in red) and familiar objects (in black) for the 16 test day trials. The sample object was located at the end of the arm and the test objects were located in the central platform of the radial-arm maze.*

3.2.3.3 Behavioural Control condition

The training and test sessions consisted of 16 trials, in which one arm and the centre of the radial-arm maze were baited. The animals were required to run up and down the single arm to obtain reward pellets. The arm used was the same as for the Novel Object condition. During each trial, the rat was contained for 30 seconds in the central area and 30 seconds in the arm by the doors at the start of each arm. Consequently, each trial lasted one minute. No objects were present in the maze.

3.2.3.4 Home-Cage Control condition

The Home-Cage Controls remained in their home cages. They were, however, yoked to the Spatial Memory group so that when that group were being trained and tested, this group was also transferred to the dark room 30 minutes before and after "testing" during the training phase, and for 30 minutes before testing and 90 minutes afterwards on the final test day, prior to perfusion. Otherwise these rats remained in their holding room.

3.2.4 zif268 immunostaining

Ninety minutes after completing the final test session, and after being held in a dark holding room to help reduce further neuronal activation, the rats were deeply anaesthetised with sodium pentobarbital (60mg/kg, Euthatal, Rhone Merieux, UK) and transcardially perfused with 0.1 M PBS followed by 4% paraformaldehyde in 0.1 M PBS (PFA). The brains were removed and post-fixed in PFA for 4 hours and then transferred to a 25% sucrose solution overnight at room temperature with gentle agitation. Four adjacent series of coronal sections (40μm) were cut on a freezing sliding microtome. Three series from each animal were collected in PBS. A standard protocol was then used for *zif268* immunohistochemistry (Albasser et al., 2007). The fourth series of sections was collected in 0.1 M PBST. Sections were then transferred to 0.3% hydrogen peroxide in PBST (peroxidase blocked) for 10 minutes in order to stop endogenous peroxidase, then washed several times in PBST.

The sections were then incubated in PBST containing *zif268* (also known as Egr-1／Krox-24／NGFI-A, antibody 1:3000; C-19, Santa Cruz Biotechnology, USA), for 48 hours at 4˚C and periodically rotated. A PBST wash was then carried out and sections were incubated for *zif268* in biotinylated goat anti-rabbit secondary antibody (diluted 1:200 in PBST; Vectastain, Vector Laboratories, Burlingame, USA) and 1.5% normal goat serum. Sections were washed again then processed using avidin-biotinylated horseradish peroxidase complex in PBST (Elite Kit, Vector Laboratories) for 1 hour at room temperature, and again constantly rotated. Sections were washed again in PBST and then in 0.05 M Tris buffer.

Diaminobenzidine (DAB Substrate Kit; Vector Laboratories) was used to visualize the reaction which was subsequently halted by washing the sections in cold PBS. Finally, the sections were mounted onto gelatine-coated slides, dehydrated through a gradually increasing concentration of alcohol solutions, and coverslipped. For all experiments, tissue from each of the behavioural groups was processed simultaneously in squads of four (i.e. one from each condition).

3.2.5 Image acquisition and analysis

Two to three images were combined from each coronal brain section to span the proximal-distal length of the septal (dorsal) subiculum for each hemisphere. These images were captured using AnalysSIS^D (Soft-Imaging Systems, Olympus, UK), with an Olympus DP70 camera attached to a Leica DMRB microscope, with bright-field microscopy (10xs magnification). These images were then montaged into composite images using Microsoft ICE, a freeware downloaded online.

Coronal sections were counted, each 160µm apart, starting from rostral dorsal subiculum (bregma = -5.04, Paxinos and Watson, 2004) to where the subiculum begins to descend inferiorly, i.e. at the intermediate subiculum (bregma = -6.36, Paxinos and Watson, 2004). This region corresponded to eight sections in total. ImageJ (Schneider, Rasband, and Eliceiri, 2012) was used to count the Zif268-positive cells in the rat dorsal subiculum, with the experimenter being blind to which group each case was assigned. Using the rat brain atlas of Paxinos and Watson (2004), the dorsal subiculum was identified and measured along its entire length, from the proximal border with CA1, to its distal border with retrosplenial cortex. The subiculum was then divided into four proximal-distal regions (Rs; Figure 3.3). These regions were saved and overlaid onto the image for counting. All cases were converted to 8-bit greyscale images and

thresholded manually so that only stained particles were included in the cell count. Cells were then automatically counted using ImageJ's Analyze Particles function from the Analyze menu, whilst consistently checking the thresholded image against the original, to ensure only normal neuronal cells were included, and not artefacts or glial cells. The particle size was defined as 20-150,00μm^2. All cell counts were carried out by an observer (K.C.) who was unaware of the group designations of the individual animals, i.e. they were "blind".

Only the septal and intermediate subiculum were counted as these are the regions that project to the anterior thalamic nuclei (Wright et al. 2010, 2013). The temporal (ventral) subiculum was not looked at as it does not share these same anterior thalamic nuclei connections, rather it has been shown to be more involved in stress, anxiety and reward, and is suggested to regulate the hypothalamic-pituitary-adrenal axis (O'Mara, 2005; O'Mara et al., 2009).

For the normalised data, the Zif268 cell counts for each subject were normalised according to the mean neuron counts for each region of interest (ROI), according to the three NeuN cases used to establish the numbers of neurons in each ROI (outlined in Chapter 2). The cell count procedure for these NeuN cases is described in Chapter 2. Consequently, normalisation involved dividing the raw Zif268-positive cell count by the NeuN cell count for that section and transverse regions of interest and multiplying this by 100 to give a percentage score.

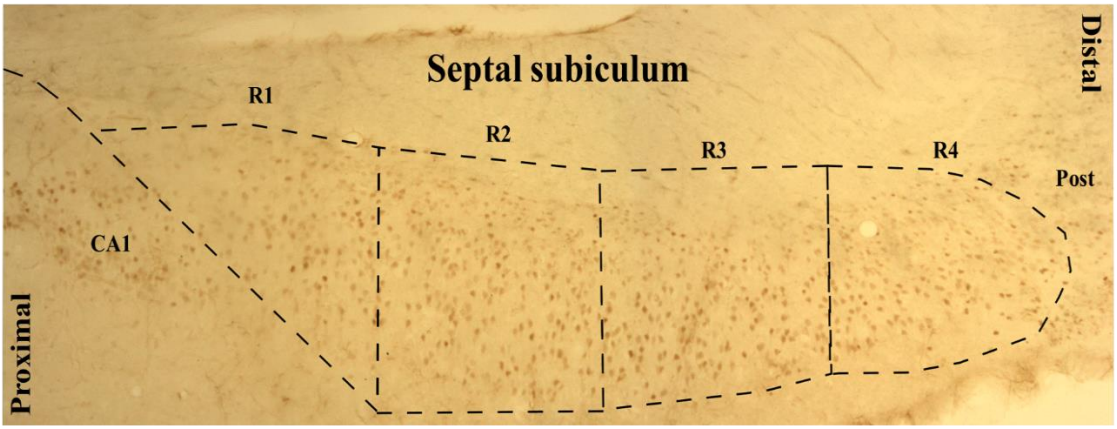

Figure 3.3 *A coronal section from the rat dorsal subiculum that has been stained for* Zif268*. The subiculum has been divided into the four regions of interest, R1-R4 from proximal (adjacent to CA1) to distal [adjacent to postsubiculum (Post)].*

3.2.6 Statistical analyses

Behaviour: For the novel Object Recognition group, the Index D1 (time spent exploring the novel object minus time spent exploring the familiar object) and Index D2 [D1 divided by total exploration time (i.e. novel + familiar object exploration time)] were calculated (Ennaceur and Delacour, 1988). The second measure, D2, takes into account differences in total exploration times as D1 is divided by the total amount of exploration given to both objects. Thus, the D2 ratio can fall between -1 and +1. If the ratio is positive, the rat exhibits a preference for novel objects. The D2 score was calculated using the cumulative data across the multiple trials. The mean D1 and D2 scores for each group were examined using a one-sample t-test to determine if these scores were significantly above chance level (i.e. scores of zero).

Cell counts: A mixed design ANOVA (group x region of interest, 4 x 4) was performed on the raw and normalized data using the statistical software SPSS (SPSS Inc., Chicago, IL). Statistical significance was set at a probability level of $p < 0.05$ for all tests. Where the assumption of sphericity is violated, Greenhouse-Geisser adjusted significance values are reported. Linear regression analyses were conducted between anterior-posterior level and average cell count for each section (8 sections running anterior to

posterior) for all groups separately, whereby section number (1-8) is the predictive independent variable, and the mean cell count for each section for each group was the dependent variable.

3.3 Results

3.3.1 Behavioural analysis

The mean percentage correct score and standard error of the Spatial Memory group in the radial-arm maze for the final session of training was 76.56% ± 4.42 (12.25 from 16 trials), i.e. a little below the preceding threshold criterion.

For the Object Recognition group, the mean overall D1 (3.66 ± 1.66) and the final updated D2 (0.40 ± 0.14) Index scores were significantly above chance (t (7) = 6.24, $p < 0.001$; and t (7) = 8.26, $p < 0.001$, respectively). These scores show that the rats were discriminating the novel from the familiar objects.

3.3.2 Raw Zif268-positive cell count data

The mean cell counts for each of the four proximal-distal regions of interest for the four test conditions are shown Figure 3.4. There was no overall, main effect of group (F (3, 28) = 1.51, $p > 0.05$). There was, however an overall effect of region (F (3, 84) = 33.26, $p < 0.001$). The results of the mixed design ANOVA revealed no significant group by region interaction (F (9, 84) = 1.20, $p > 0.05$). Thus, while R2 had the highest Zif268-positive counts and R4 (the most distal) had the lowest counts, there were no differences relating to test condition.

Regression analyses revealed significant linear relationships for all groups between Zif268-positive cell counts and section number going from anterior (lower) to posterior

(higher) (Figure 3.5). Anterior-posterior level significantly predicted cell count for the Spatial Memory group $\beta = 29.62$, t (6) = 12.62, $p < 0.001$, and explained a significant portion of the variance $R^2 = 0.92$, F (1, 6) = 72.31, $p < 0.001$, with the gradient in the number of cells increasing in the posterior direction. A similar effect of section level was also found for the Object Memory group ($\beta = 34.43$, t (6) = 15.46, $p < 0.001$ and $R^2 = 0.97$, F (1, 6) = 195.34, $p < 0.001$), Behaviour Control group ($\beta = 27.22$, t (6) = 7.09, $p < 0.001$ and $R^2 = 0.84$, F (1, 6) = 31.53, $p < 0.001$), and Home-Cage Control group ($\beta = 29.28$, t (6) = 8.18, $p < 0.001$ and $R^2 = 0.90$, F (1, 6) = 53.31, $p < 0.001$).

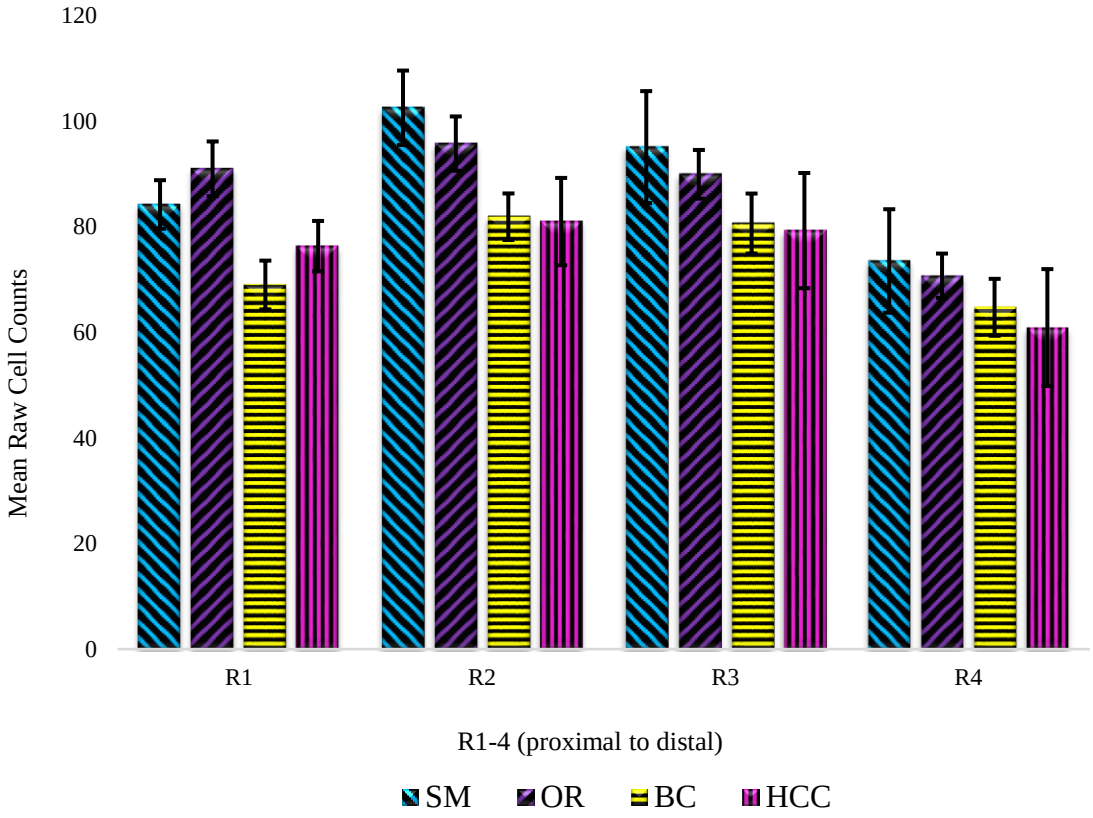

Figure 3.4 *Mean raw cell counts of Zif268-positive cells for R1-4 (proximal to distal subiculum) for the Spatial Memory (SM), Object Recognition (OR), Behavioural Control (BC) and Home-Cage Control (HCC) conditions. The data depicted are the mean averaged across all coronal sections counted. The bars show the standard error of the means.*

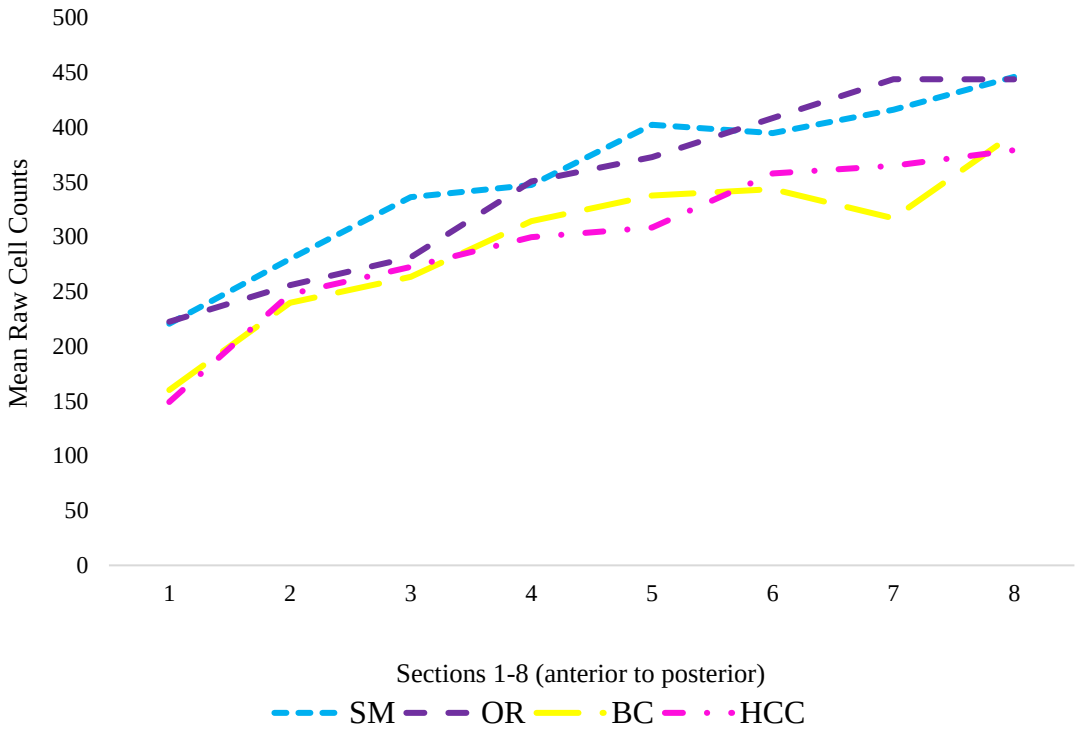

Figure 3.5 *Mean raw cell counts for Zif268-positive cell counts for the Spatial Memory (SM), Object Recognition (OR), Behavioural Control (BC) and Home-Cage Control (HCC) conditions. The graph shows the mean counts from coronal sections 1-8 (i.e. from most septal to intermediate subiculum).*

3.3.3 Normalised Zif268-positive cell count data

A limitation with the raw Zif268 counts is that the four subiculum ROIs contain different numbers of neurons (see Chapter 2). To compensate, the Zif268 cell counts were normalised (see 3.2 Methods). Figure 3.6 shows the differences between mean normalised regional cell counts for each group. While no main effect of group was found (F (3, 28) = 1.86, $p > 0.05$), there was a significant main effect of region (F (3, 84) = 351.43, $p < 0.001$). On inspection, it can be seen that the proximal subiculum (R1) had the highest proportion of Zif268-positive cells. There was, in addition, a significant interaction between group and region (F (9, 84) = 3.10, $p < 0.05$).

Closer analysis of the cell counts across regions within each group (Figure 3.6) found significant regional differences for the Spatial Memory group (F (3, 21) = 55.14, $p < 0.001$), the Object Recognition group (F (3, 21) = 144.30, $p < 0.001$), the Behaviour

Control group (F (3, 21) = 44.51, $p < 0.001$), and the Home-Cage Control group (F (3, 21) = 288.01, $p < 0.001$). Simple effects tests for these differences showed the differences to lie between R1 and regions R2, R3 and R4; between R2 and R4; and R3 and R4 in the Spatial Memory group; all region combinations in the Object Recognition group; between R1 and regions R2, R3 and R4 in the Behaviour Control group; and between R1 and regions R2, R3 and R4; between R2 and R4; and between R3 and R4 in the Home-Cage Control group.

Follow-up simple effects tests between groups for each region revealed no differences between Rs 2, 3 and 4 (F (3, 28) = 2.75, $p > 0.05$; F (3, 28) = 0.78, $p > 0.05$; and F (3, 28) = 0.59, $p > 0.05$ respectively). However, a significant difference was found for R1 (F (3, 28) = 4.09, $p < 0.05$). Pairwise comparisons found this difference to lie between only the Object Recognition group (highest cell counts) and the Behaviour Control group (lowest counts) [F (1, 14) = 10.14, $p < 0.008$ (Bonferroni adjusted p value)].

The normalised cell count was significantly predicted by section number going anterior to posterior for all groups, based on linear regression analyses (Figure 3.7). This gradient again increased along the posterior direction. Cell counts in the Spatial Memory group were significantly predicted by anterior-posterior section ($\beta = 1.28$, t (6) = 6.87, $p < 0.001$), and explained a significant proportion of the variance ($R^2 = 0.89$, F (1, 6) = 47.25, $p < 0.001$), this also held true for the Object Memory group ($\beta = 1.73$, t (6) = 7.13, $p < 0.001$ and $R^2 = 0.89$, F (1, 6) = 50.80, $p < 0.001$), Behaviour Control group ($\beta = 1.36$, t (6) = 4.51, $p < 0.001$ and $R^2 = 0.77$, F (1, 6) = 20.34, $p < 0.005$), and Home-Cage Control group ($\beta = 1.56$, t (6) = 5.36, $p < 0.001$ and $R^2 = 0.83$, F (1, 6) = 28.73, $p < 0.005$).

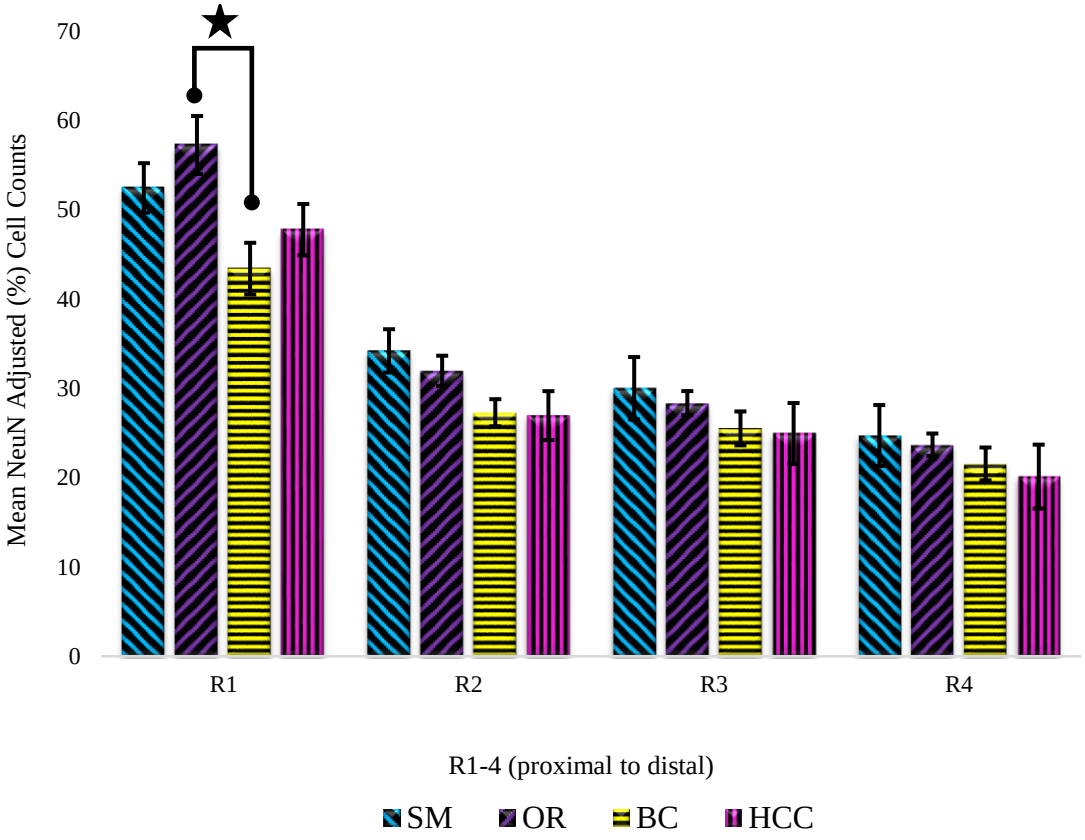

Figure 3.6 *Mean normalised cell counts of Zif268-positive cells for R1 - 4 (proximal to distal subiculum) for the Spatial Memory (SM), Object Recognition (OR), Behavioural Control (BC) and Home-Cage Control (HCC) conditions. The data depicted are the mean averaged across all coronal sections counted. The bars show the standard error of the means.* ★ *= significant interaction.*

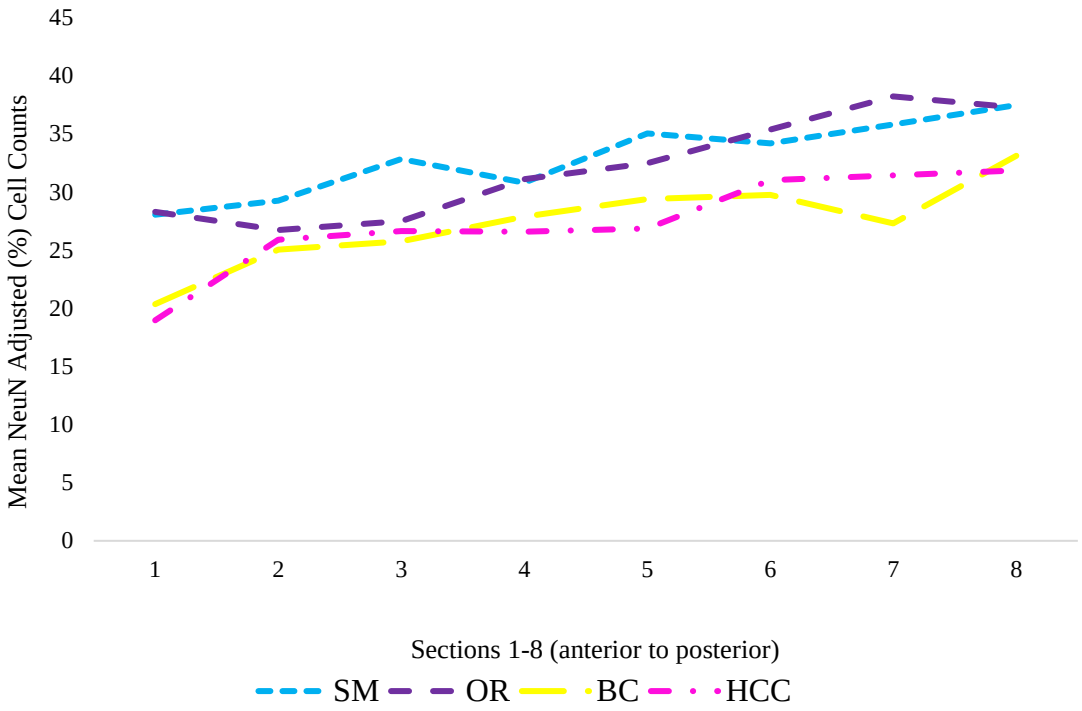

Figure 3.7 *Mean normalised cell counts for Zif268-positive cell counts for the Spatial Memory (SM), Object Recognition (OR), Behavioural Control (BC) and Home-Cage Control (HCC) conditions. The graph shows the counts from coronal sections 1-8 (i.e. from most septal to intermediate subiculum).*

3.4 Discussion

The aim of this study was to determine if there are any differences along the proximal-distal axis of the dorsal subiculum in terms of *zif268* activation following a spatial memory task, an object memory task, a behavioural control task, and home-cage control (baseline) task. It was predicted, based on prior research, that the proximal subiculum would show most object memory activation while the distal subiculum would show most spatial memory activation, with respect to *zif268*. Contrary to these predictions, no significant interaction was found in the raw cell count data between group and region. There was, however, an increase in Zif268-positive cell counts going from the most septal to the intermediate hippocampus, but this anterior-posterior effect was found for all groups, suggesting a generally higher level of *zif268* activity in the intermediate subiculum, irrespective of task demands.

3.4.1 Proximal subiculum and object recognition memory

It could be argued that the normalised data are more informative as they relate to the proportion of cells within a given region that is Zif268-positive. In contrast to the raw counts, R1 (the most proximal) had the highest levels of Zif268. There was also a significant group by region interaction (Figure 3.6) that largely arose from the difference between the Object Recognition group and the Behavioural Control group. This condition difference, which was supported by the simple effects, was consistent with the prediction that the Object Recognition group should show disproportionately more activation in the proximal end of the subiculum. Support came from the behavioural data, which showed that this group showed a clear preference for the novel objects, as revealed by both the D1 and D2 scores. This support was tempered, however, by two findings. First, there was no region of interest interaction between the Spatial Memory and Object Memory groups, despite the starting rationale that they should show opposite gradients of *zif268* activity along the proximal-distal axis. Second, *zif268* activity was not significantly higher in R1 when the Object Recognition group were compared with the Home-Cage controls. It should, however, be remembered that the Home-Cage controls did not remain in their holding room prior to perfusion, rather they were moved to the same quiet, dark room as the other three groups for the same durations.

3.4.2 Subiculum involvement in navigation

One possibility is that object stimuli do enhance activity in the proximal subiculum but this subtle effect is largely overshadowed by how the entire subiculum is activated by context or by navigation processes in general. It is presumed that the subiculum is involved in navigation (O'Mara, 2009), and 45% of its spatial pyramidal cells fire in light and in darkness, suggesting a role for the subiculum in path integration not

requiring visual input (Brotons-Mas et al., 2010). Thus, increased subicular activation could follow any navigational episode, even when spatial memory or information processing is not required. Additional activation could come from boundary vector cells (Lever et al., 2009). At first sight, this does not explain the activation in the Home-Cage control group, who were only moved back and forth between rooms and received no additional experimental procedures. It is, however, possible that these "baseline" rats were passively navigating the move from the dark room to the holding room and back again, which could be possible given the subiculum's suggested role in path integration even in darkness (Brotons-Mas et al., 2010). The cage moving would also promote activity in the home-cage and exploration of the dark room by senses other than vision. From looking at other studies in which the baseline controls were just taken from the home-cage, with no other manipulation involved, it would appear that the room moving component of the baseline condition raised *zif268* expression (i.e. Jenkins et al., 2006; Toscano et al., 2006).

The apparent lack of a differential response to the spatial memory task seems surprising given how other IEG imaging studies have shown that the subiculum can increase activity following a spatial test. For example, Vann et al., 2000b found increases in dorsal subiculum c-*fos* activity in an eight-arm radial maze task compared to travelling up and down one arm (baseline condition) in one experiment, and in a second experiment c-*fos* activity increased when performing the eight-arm radial maze task in a room novel to that in which they were trained. The present Spatial Memory condition was based on the radial-arm maze task from the first experiment of Vann et al. (2000b), as well as adopting a similar maze control condition (Behaviour Control). Nevertheless, no significant Spatial Memory: Behaviour Control difference was found in the present study. One obvious difference is that the present study examined *zif268* rather than c-*fos*

(Vann et al., 2000b). It has been suggested that *zif268* is less functionally sensitive than c-*fos*, so this might be why no differences were found in the present study (Barry et al., 2015). However, *zif268* activity increases have been found in other studies looking at spatial memory (Hall et al., 2001; Toscano et al., 2006). In one of these studies, early and late hippocampal activity during learning of a radial-arm maze task was associated not in changes in absolute levels of Zif268 between experimental and control groups but in changes to the activity correlations with different hippocampal subregions (Poirier et al., 2008).

Other evidence that subicular IEG activity is related to spatial processing comes from a study by Wan et al., (1999). That study found no difference in subicular activation for viewing novel as opposed to familiar picture stimuli, when presented in a paired-viewing task. Likewise, Albasser et al., (2010) found no significant differences in subicular activity for novel versus familiar objects in the bow-tie maze. In contrast, Wan et al. (1999) did find significant changes (decreases) in subicular activation after viewing novel as opposed to familiar spatial arrangements of items using the same paired-viewing procedure. These results again suggest a diminished role for the subiculum for object recognition when compared with spatial memory.

In a further study, Jenkins et al., (2004) looked at c-*fos* activation following a radial-arm maze task in which salient visual external cues for guidance were spatially rearranged at test. Fos increases were only found within the postsubiculum of the subicular region in response to visual cue rearrangement. This result again indicates that the subicular cortices are involved in spatial memory, consistent with it inputs. The subiculum itself did not, however, appear to show any significant changes in that study (Jenkins et al., 2004), even though it also used a similar radial-maze procedure with cue rearrangement,

rather than novel room, as in Vann et al. (2000b). A further IEG study failed to find the subiculum to be involved in processing novel temporal configurations of external spatial stimuli in a radial-arm maze task (Amin et al., 2006). These findings, in conclusion, suggest that the subiculum has a very specific spatial involvement in active spatial working memory and contextual learning (Vann et al., 2000a, b; Wan et al., 1999), but not in the spatial rearrangement of familiar cues (Jenkins et al, 2004) or their temporal rearrangement (Amin et al., 2006).

3.4.3 zif268 as a marker for memory-related activity

While it is thought that *zif268* is sometime a less sensitive IEG marker than c-*fos*, as mentioned above and suggested by the lack of significant functional findings here, there is a reason this particular IEG was chosen for this study. *zif268* is presumed to be involved in synaptic plasticity and learning (Guzowski, 2002; Tischmeyer and Grimm, 1999), including the consolidation and reconsolidation of several types of long-term memory (Besnard et al., 2013; Davis et al., 2003; Jones et al., 2001; Maroteaux et al., 2014; Veyrac et al., 2014). The same stimulation conditions that induce *zif268* expression are highly correlated with those that induce long-term potentiation (long-lasting increased connectivity strength between neurons) of the perforant path granule cell synapse, which suggests that *zif268* plays a role in long term hippocampal synaptic plasticity (Cole et al., 1989). Induction of long term potentiation (LTP) in the dentate gyrus can in fact result in increased expression of *zif268* (Wisden et al., 1990). In addition, *zif268* appears to be involved more specifically in spatial memory in rodents (Penke et al., 2013), making it especially useful for observing hippocampal involvement in spatial learning (Fordyce et al., 1994; Hall et al., 2001; Toscano et al., 2006). However, *zif268* has higher resting levels generally and also results in more continuous expression once regulation is increased (Kerr et al., 1996; Zangenehpour and

Chaudhuri, 2002) which can make it harder to measure the effect of external events on fluctuations in activity levels.

3.4.4 Electrophysiological activity of subiculum

Electrophysiological studies have tended to reveal inconsistent findings regarding the role of the subiculum in object processing. Anderson and O'Mara (2003, 2004) found subiculum cells that fire according to the running speed and location of an environment, but no correlation between cell firing and object novelty or familiarity. However, there has been more recent research suggesting otherwise. Chang and Huerta (2012) looked into dorsal subicular cell firing in response to object recognition and found theta power to be significantly higher in the dorsal subiculum when mice explored novel objects as opposed to familiar objects. The authors also found a subset of dorsal subiculum units that were selectively responsive to novel object exploration, suggesting some neurons were tuned specifically to novelty during novel object exploration. Perhaps the sparsity of object-firing neurons explains why functional IEG differences for object recognition tasks have often not been observed.

The subiculum's electrophysiological involvement in spatial processing, however, is widely demonstrated. One example concerns boundary vector cells (Lever et al., 2009), which are found in the subiculum and fire in response to a rat's distance from a boundary as well as to the boundary itself. Furthermore, there are changes along the proximal-distal axis of the subiculum in terms of cell firing properties; the proximal portion contains more regular spiking cells, whereas the distal subiculum contains more bursting cells, and this gradient in cell type matches their outputs (Kim and Spruston, 2012). Moreover, distal subiculum cells show slightly higher spatial resolution and greater ability to carry spatial information, in line with the hypothesis (Sharp and Green,

1994; but see Brotons-Mas et al., 2010; Kim et al., 2012). Again, these findings accord with the inputs from proximal CA1, which show greater spatial modulation than distal CA1 (Henriksen et al, 2010). Despite these electrophysiological results, the present study found only small differences in subiculum activity with respect to task.

3.4.5 Results of subicular lesions

Other relevant evidence comes from lesion studies, though selective subicular lesions are very difficult to produce. Typically, it is the intermediate subiculum that is targeted while the dorsal subiculum is spared, making such studies difficult to interpret (Aggleton, 2012). One study (Potvin et al., 2010) has, however, demonstrated that, as with many studies of entire hippocampus lesions, subiculum only lesions can spare object recognition but do affect spatial location recognition (Brown et al., 2010; Mumby, 2001). Morris et al. (1990) also investigated the effects of subiculum and hippocampus lesions separately and combined on the Morris water maze task and found that subicular lesions alone impaired spatial learning, comparably to hippocampus proper lesions, although in a matching-to-place task subicular lesions did not affect place learning to the same extent as hippocampal lesions. Combined lesions of the two sites always resulted in larger spatial learning deficits. Morris et al. (1990) also noticed rats' use of qualitatively different paths to find a hidden platform following subicular versus hippocampal damage. Subicular lesions have also been shown to be similar to hippocampus proper lesions in working memory tasks such as matching-to-place, however, dissimilarly leaving reference memory unaffected (Galani et al., 1997, 1998a, b). One possible explanation is that the subiculum is specifically important for long-term spatial memory, as often deficits found following lesions to this area can be restored with retraining in this group, but this recovery is not seen in those with entire hippocampal lesions (Bolhuis et al., 1994; Morris et al., 1990).

Although the subiculum appears to be involved in spatial memory, as noted, subicular lesions tend to have additive effects to hippocampus proper lesions, often exacerbating effects when both are combined (Morris et al., 1990; Potvin et al., 2007). In some experiments, selective hippocampal lesions only show any effect once the subiculum is included in the surgery, for example in nonmatching-to-place in a T-maze (Potvin et al., 2007). At the same time, this combination is not required for impairments on the radial-arm maze (e.g. Potvin et al., 2006). Another study by Potvin et al. (2009) found that dorsal hippocampal lesions resulted in impairments on radial-arm maze trials involving both overlapping external cues (requiring pattern separation) and distinct spatial cues (no pattern separation needed). In contrast, dorsal subicular lesions only impaired the pattern separation abilities. These findings suggest that the subiculum plays a complementary, but individual role, in supporting pattern separation by the hippocampus.

3.4.6 Results of lesions to subicular efferents

In turn, damage to subicular outputs seems to result in similar outcomes in terms of differences between object and spatial memory. For instance, lesions in the rat mammillary bodies and mammillothalamic tract appear to have no effect on object/non-spatial recognition memory or delayed non-matching to sample (Aggleton et al., 1990, 1995; Nelson and Vann, 2014). However, mammillothalamic tract lesions do disrupt object-in-place memory (Nelson and Vann, 2014), and mammillary body lesions result in abnormal visual scene processing involving the integration of objects (Vann, 2004). It therefore appears that the effective use of spatial/scene information relies on this diencephalic structure. Likewise, the anterior thalamic nuclei also do not appear to be directly involved in object recognition memory (Dumont and Aggleton, 2013), but

again play a key role in object-location association memory (Sziklas and Petrides, 1999). Both lesions of the anteroventral and anteromedial thalamic nuclei result in similar spatial memory deficits, as assessed by the radial-arm maze (Aggleton et al., 1986; Byatt and Dalrymple-Alford, 1996). Furthermore, unilateral anterior thalamic nuclei lesions result in widespread ipsilateral hippocampal hypoactivity as measured by IEG expression, including within the subiculum (Jenkins et al., 2002a, b).

However, as shown in Chapter 2, the proximal and distal subiculum preferentially project to the anteromedial and anteroventral thalamic nucleus, respectively, and one might predict that based on their inputs from the hippocampus they would be differentially involved in object and spatial information. It is, however, difficult to separate the contributions of the individual anterior thalamic nuclei, as is demonstrated by Aggleton et al. (1996). The authors made cytotoxic lesions in rats centred in either the anteromedial thalamic nucleus, the anteroventral and anterodorsal thalamic nuclei, or all thee nuclei combined, and found that while lesions to anteromedial thalamic nuclei or anteroventral/anterodorsal thalamic nuclei produced initial learning deficits, only combined anterior thalamic lesions produced enduring impairments on a T maze alternation task. Both individual lesion and sham groups were able to use allocentric cues in a cross maze task, however, the combined lesion group were not. The implication is that all anterior thalamic nuclei contribute to spatial memory tasks (see also Byatt and Dalrymple-Alford, 1996), so that a proximal-distal subiculum separation based on “space” alone might prove too crude a distinction.

3.4.7 Conclusions

In conclusion, while this study did not find significant differences along the proximal-distal subicular axis for object recognition versus spatial memory activation, this null effect could be due to a number of factors. It is possible that the subiculum has similar activation patterns for spatial and object information, although this is not in line with previous studies which have found higher activation in the subiculum for spatial memory tasks compared to controls (Vann et al., 2000a, b; Wan et al., 1999). At the same time, the normalised data partially supported the hypotheses that the proximal subiculum should show higher object recognition involvement, although this difference was only significant with the Behavioral Control group. It is, however, naïve to imagine that the Object Recognition condition was truly nonspatial. It is known from object-in-place tasks that rats spontaneously link object identity with spatial location (Dix and Aggleton, 1999), learning that depends on the hippocampus. In the present study, rats ran up and down the arm of a radial-arm maze with distal room cues visible and objects present in different places and at different times. The complexity of this task may, therefore, help explain why it showed the best discrimination between regions of interest and between some of the test conditions. Consequently, this condition might have been better run in a maze with high, opaque walls, although that would have created additional task differences.

Future studies are needed to investigate how best to separate and compare the different planes of the subiculum (transverse, longitudinal and laminar). At the same time, it would be most helpful to understand more about the different functions of the various diencephalic targets of the subiculum, at the level of individual nuclei. One example of how this might prove informative concerns how the temporal (ventral) subiculum has only sparse projections to the anterior thalamic nuclei projections while it provides

dense projections to the mammillary bodies (Christiansen et al., 2016b; Meibach and Siegel, 1975, 1977a). It could be valuable, therefore, to scrutinise sites of origin within the temporal subiculum that give rise to projections to the mammillary bodies and, presumably, further contribute to spatial memory, yet scarcely project to the anterior thalamic nuclei (Neave et al., 1997; Vann and Aggleton, 2003, 2004).

Chapter 4: The status of the precommissural and postcommissural fornix and their roles in executive functioning and episodic memory in normal ageing and amnestic Mild Cognitive Impairment: a diffusion MRI tractography study

4.1 Introduction

The fornix is a central white matter tract within a network of structures known as the Papez Circuit (Papez, 1937). The fornix is the principal efferent and afferent system for those areas outside of the medial temporal lobe that are connected with the hippocampus. The network of structures within Papez Circuit are now known to be important for spatial and episodic memory (Delay and Brion, 1969; Markowitsch, 1997). Evidence, such as that from damage to the tract in patients and from diffusion MRI tractography studies in healthy populations, reveals a key involvement in memory (Aggleton et al., 2000; Hodges and Carpenter, 1991; McMackin et al., 1995; Metzler-Baddeley et al., 2011; Rudebeck et al., 2009; Vann et al., 2008). In diffusion MRI studies, for example, indices of fornix microstructure correlate with episodic memory performance (Metzler-Baddeley et al., 2011; Rudebeck et al., 2009). The fornix is also particularly involved in spatial memory in monkeys and rodents (Aggleton and Brown, 2002; Aggleton et al., 1995; Gaffan, 1992, 1994; Gaffan and Harrison, 1989a; Gaffan et al., 2001; Wible et al., 1992). Unsurprisingly, aMCI, which disproportionately affects episodic memory (Albert et al., 2011), appears to consistently compromise the fornix according to diffusion tensor MRI tractography (Metzler-Baddeley et al., 2012a; Oishi et al., 2012; Zhuang et al., 2012).

However, nearly all fornix studies treat this white matter tract as a unitary structure, despite it splitting into two distinct pathways at the level of the anterior commissure: the precommissural fornix and postcommissural fornix (Poletti and Creswell, 1977; Figure 4.1). These two different pathways connect the hippocampus to different structures. The precommissural fornix connects the hippocampus to the basal forebrain (including septum), ventral striatum and the prefrontal cortex, and contains return projections from the septum to the hippocampus. On the other hand, the postcommissural fornix connects

the hippocampus to the anterior thalamic nuclei and mammillary bodies, which are located within the medial diencephalon (Aggleton, 2012; Aggleton et al., 1987; Barbas and Blatt, 1995; Carmichael and Price, 1995; Poletti and Creswell, 1977; Shah et al., 2012).

Given these different patterns of connectivity, it is possible that the precommissural and postcommissural fornix support different cognitive functions. The medial diencephalic sites (e.g. the mammillary bodies and anterior thalamic nuclei) are important for episodic memory and recollective memory in particular (Aggleton and Brown, 1999; Aggleton et al., 2010; Graff-Radford et al., 1990; Tanaka et al., 1997; Van der Werf et al., 2000; Vann et al., 2009b, see also Chapter 2). It might, therefore, be predicted that the postcommissural fornix particularly supports these functions. Meanwhile, the basal forebrain and prefrontal cortex are important for a variety of cognitive tasks, including motor control, attention, motivation, reward anticipation, reinforced learning and executive functioning, which might be more dependent on the connections of the precommissural fornix (Abler et al., 2006; Baxter and Chiba, 1999; Braver et al., 2009; Crutcher and DeLong, 1984; Francois et al., 2014; Kimura, 1986; Knight et al., 1995; Knutson et al., 2000, 2001, 2008; Konishi et al., 1998; Kouneiher et al., 2009; Mian et al., 2014; Mink et al., 1983; Momennejad and Haynes, 2013; Moore et al., 2009; Muranishi et al., 2011; Oberhuber et al., 2013; Powell et al., 2012; Ramnani et al., 2004; Reverberi et al., 2012; Risbrough et al., 2002; Roitman and Loriaux, 2014; Rolls and Wilson, 1990; Seghier and Price 2010; Stern and Passingham, 1995; Voytko et al., 1994; Waltz et al., 1999; Wymbs et al., 2012; Yamada et al., 2004; Yu et al., 2013).

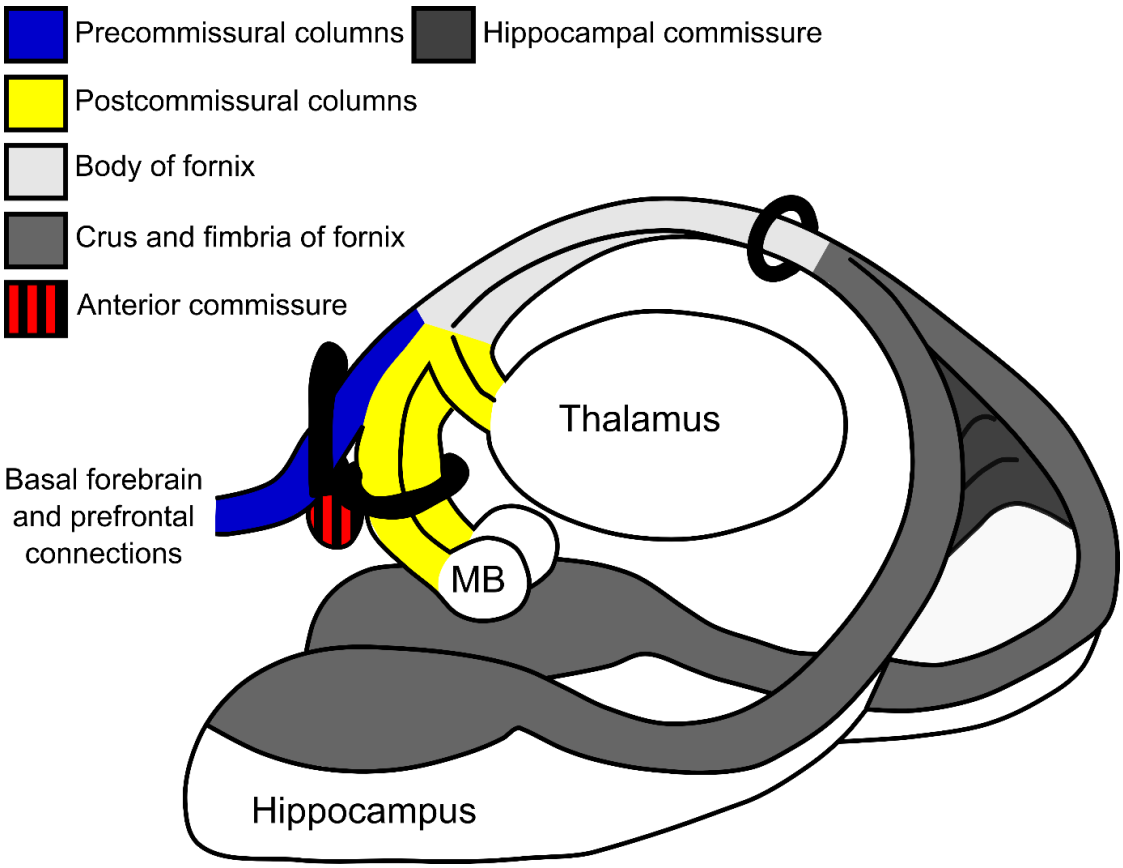

Figure 4.1 *Schematic of the principal components of the fornix and the main areas to which it connects. The black rings represent the placement of the various "AND" and "NOT" gates used for the tract reconstructions, as well as the seed ring around the body of the fornix. Abbreviation: MB = mammillary bodies.*

To date, there are only a few studies that have looked at separate lesions of the precommissural and postcommissural fornix and these studies have only been carried out in rats. The earliest study reported impairments on a spatial alternation task following both precommissural and postcommissural fornix lesions (Henderson and Greene, 1977). A subsequent study found no behavioural impairments following postcommissural fornix lesions whereas precommissural fornix lesions resulted in initial impairments on a spatial alternation task (Thomas, 1978). More recent studies have found postcommissural fornix lesions to result in either mild or no impairments on spatial memory tasks (Vann, 2013; Vann et al., 2011). From these limited rat studies, it is not yet clear how the precommissural and postcommissural fornices contribute to memory.

Therefore, the first goal of this study was to develop an anatomically guided protocol for the *in vivo* reconstruction of precommissural and postcommissural fornix fibres in humans. Separating the reconstructions of precommissural and postcommissural fornix fibres should provide a useful tool for investigating any functional dissociations between these different hippocampal networks, as well as for studying age and disease related effects on these distinct systems. By reconstructing precommissural and postcommissural fibres, it also becomes possible to examine whether these different fibre populations intermingle within the body of the fornix or whether they retain distinct topographies.

To date, only two studies have investigated the precommissural and postcommissural fornix using MRI. The first study (Yeo et al., 2013) used probabilistic tractography to reconstruct the precommissural and postcommissural fornices. They reported larger levels of fractional anisotropy (FA), an index of white matter coherence and diffusion directionality, and reduced levels of mean diffusivity (MD) (average diffusion in all directions) in the postcommissural compared to the precommissural fornix. The second study (Chen et al., 2015) investigated the effects of ageing on six sub-components of the fornix, including the column, body, crus, fimbria, and precommissural and postcommisural columns, and found age-related changes in radial diffusivity (RD), i.e. the diffusion perpendicular to the fibres, and axial diffusivity (AD), i.e. the diffusion along the fibres, in all subregions (Chen et al., 2015).

The present study extended these previous findings by investigating the effects of both ageing and neurodegeneration on precommissural and postcommissural white matter microstructure in the fornix of healthy older adults (53-93 years of age) and a group of individuals with aMCI. The study used deterministic tractography based on the

modified damped Richardson-Lucy (dRL) algorithm for spherical deconvolution that allows, in contrast to conventional diffusion tensor imaging (DTI), tracking through areas of complex fibre architecture (for example crossing and kissing fibres, found in the voxels at the level of the anterior commissure which contain both anterior commissural fibres, and precommissural and postcommissural fibres) and regions affected by isotropic partial volume (Dell'Acqua et al., 2010). It is important to control for CSF based partial volume artefacts in the fornix since this tract is surrounded by the third ventricle, and volume artefacts may be accentuated by age- and disease-related atrophy (Metzler-Baddeley et al., 2012b).

Fibres of the crus and the fimbria of the fornix from the precommissural and postcommissural fornix reconstructions were excluded in this study. This omission was because of the fibre crossing and intermingling that occurs between the columns of the fornix and the crus and fimbria of the fornix (Saunders and Aggleton, 2007), given the aim to minimise any partial volume effects between the two fibre populations.

To isolate the two divisions of the fornix, it was necessary to seed different groups of fibres as they descend close to the anterior commissure in the columns of the fornix. At this level, the precommissural and postcommissural divisions contain roughly similar numbers of fibres (Daitz, 1953; Powell et al., 1957). It can be anticipated that the postcommissural reconstructions predominantly involved the connections of the hippocampus with the hypothalamus, including the mammillary bodies (Aggleton et al., 2005b; Poletti and Creswell, 1977, Figure 4.1). Although the postcommissural fornix also contains many hippocampal projections to the anterior thalamic nuclei (Aggleton et al., 1986), these fibres were largely excluded from the present study as they turn

caudally into the rostral thalamus, just as the columns of the fornix begin to descend (Poletti and Creswell, 1977; Figure 4.1).

White matter microstructure in the precommissural and postcommissural fornix segments was investigated with the diffusion-weighted imaging-based indices of FA, MD, RD and AD (Pierpaoli and Basser, 1996). All diffusion-based indices were corrected for CSF-based, partial volume artefacts with the Free Water Elimination (FWE) method (Pasternak et al., 2009). The FWE method also generates a measure of tissue volume fraction (*f*), an index that reflects the volume remaining in each voxel attributable to tissue after the elimination of free water (Metzler-Baddeley et al., 2012b; Pasternak et al., 2009).

There were four aims: 1. to demonstrate whether it was possible to separate the precommissural fornix from the postcommissural fornix, 2. to investigate correlations between the microstructural indices for the two fornix segmentations in a group of healthy older adults, allowing further investigations of age-related effects on microstructure, 3. to study potential aMCI related effects on white matter microstructure in the two fornical segments, and 4. to study whether individual differences in the microstructure of the postcommissural and precommissural fornix fibres were related to differences in episodic memory and executive function, respectively.

4.2 Methods

The MRI and cognitive data comprise part of a project into healthy and pathological ageing (aMCI) (see Metzler-Baddeley et al., 2011, 2012a). As such, participant recruitment, scanning and neuropsychological testing were all carried out by other investigators: John Evans, Derek Jones, Claudia Metzler-Baddeley, and Mike

O'Sullivan. John Evans and Derek Jones oversaw the diffusion MRI image protocols and acquisition, while Claudia Metzler-Baddeley and Mike O'Sullivan were in charge of participant recruitment, testing, and analysis of data. Mike O'Sullivan was the principal investigator and supervisor of the study.

4.2.1 Participants

4.2.1.1 Healthy Ageing Cohort

A total of forty-four healthy control participants was recruited through advertisements in the local community, GP waiting rooms, newsletters, mail, and via the School of Psychology Community Panel of healthy research volunteers at Cardiff University (Metzler-Baddeley et al., 2011). Participants were between 53 and 93 years of age (mean age 67.7, standard deviation 8.6; 22 female). Participants were excluded if they had any of the following: history of neurological or mental disorder (as depicted in the Diagnostic and Statistical Manual of Mental Disorders) such as moderate to severe head injury, substance or alcohol abuse, stroke/cerebral haemorrhage, symptomatic memory or other cognitive decline, vascular disease elsewhere (peripheral vascular disease, carotid or vertebral artery stenosis or previous coronary intervention), structural heart disease or failure, and MRI contra-indications. Three participants were later excluded due to ill health, motion artefacts or white matter hyper-intensities. A further two participants had missing or incomplete scan data. Therefore, 39 participants were included in the final analyses.

4.2.1.2 aMCI group and their Matched Control group

Patients in the aMCI group were recruited through the Cardiff Memory Clinic, as described in Metzler-Baddeley et al. (2012a). A neurologist recruited and assessed willing and suitable patients. Inclusion criteria were based on a standard memory clinic

assessment which included clinical history, vascular risk factors, full neurological examination, basic haematology and biochemistry investigations, previous neuroimaging with computed tomography (CT) or MRI, and cognitive screening with the Addenbrooke's Cognitive Examination (ACE) (Mioshi et al., 2006). Objective memory impairment was confirmed by a score more than 1.5 standard deviations (S.D.) below age-matched controls on either the ACE verbal memory sub-score (Mioshi et al., 2006) or the visual memory test from the Repeatable Battery for the Assessment of Neurological Status (RBANS) (Randolph et al., 1998). All of the participants scored ≥ 24 on the Mini-Mental State Examination (MMSE) (mean = 26, S.D. = 1.7) and had a Clinical Dementia Rating of 0.5 (Morris, 1993). The aMCI diagnoses relied on current criteria (Albert et al., 2011).

Depression was also screened using the 15-item Geriatric Depression Scale (Sheikh and Yesavage, 1986). Patients were not included if they possessed any of the same exclusion criteria as that for the Healthy Ageing Cohort. Additionally, none of the patients possessed characteristic cognitive/behavioural indications nor met diagnostic criteria suggestive of other degenerative disorders such as frontotemporal lobar degeneration, corticobasal degeneration, or dementia with Lewy bodies.

All aMCI patients demonstrated episodic memory impairments as assessed with the Free and Cued Selective Reminding Test (FCSRT; Grober et al., 1997) and the Doors and People Test (Baddeley et al., 1994). Additional executive dysfunction was evident in several patients, whereas the others possessed purely amnestic MCI (Metzler-Baddeley et al., 2012a). Measures of executive function came from subtests from the Wechsler Adult Intelligence Scale - Third UK Edition (WAIS-III UK; Wechsler, 1997), the Stroop test (Trenerry et al., 1989), the Tower of London Test from the Delis and

Kaplan Executive Function System battery (as detailed in D-KEFS; Delis et al., 2001) and verbal fluency (FAS test, see Metzler-Baddeley et al., 2012a). The final 24 aMCI participants (11 females) ranged from 58 to 90 years of age with a mean age of 76.7 (S.D. 7.5).

A subgroup of 20 control participants (10 females) was selected from the Healthy Ageing Cohort based on demographic variables and verbal intelligence, in order to provide an age and verbal-IQ Matched Control group for the aMCI patients. These Matched Controls were all between 66 and 93 years of age (mean age 74, S.D. 6.5) and had verbal IQ scores no higher than two standard deviations above the average patient in the National Adult Reading Test (NART; Nelson and Willison, 1991).

4.2.2 Diffusion-weighted MRI and T_1-weighted MRI scanning protocols

The diffusion-weighted MRI data were acquired at the Cardiff University Brain Research and Imaging Centre (CUBRIC) with the in-house scanner, a 3T GE HDx MRI system (General Electric Healthcare). Whole oblique axial brain coverage (parallel to the inter-commissural plane) was acquired with a twice-refocused spin-echo echo-planar imaging (EPI) sequence. Data acquisition was peripherally gated to the cardiac cycle. The data comprised 60 slices of 2.4mm thickness, with a field of view of 23cm and a 96 × 96 acquisition matrix, with an echo delay time (TE) of 87ms and parallel imaging with an ASSET factor of two. The b-value was 1200s/mm2. Diffusion information was encoded along 30 isotropically distributed directions with three additional non-diffusion-weighted scans according to an optimised gradient vector scheme (Jones et al., 1999). The total acquisition time was ~13 minutes per participant. Alongside this scan, anatomical data were acquired with a T_1-weighted 3D fast spoiled gradient echo (FSPGR) scan using an oblique-axial acquisition plane with 1mm

isotropic resolution. The matrix size was 256 × 192 × 176mm (zero-padded to 256 × 256 × 176mm). In addition, the repetition time (TR) was 7.9ms, the TE was 3.0ms, the inversion time (TI) was 450ms, and the flip angle was 200˚. The acquisition time for the T_1 scan was ~7 minutes. The diffusion-weighted data were corrected for distortions induced by the diffusion-weighted gradients, artefacts due to head motion, and EPI-induced geometrical distortions by registering each image volume to their T_1-weighted anatomical images, which were down-sampled to a resolution of 1.5 × 1.5 × 1.5mm in order to speed up processing time (Irfanoglu et al., 2012; Pierpaoli, 2011), with appropriate reorientation of the encoding vectors (Leemans and Jones, 2009) in ExploreDTI (Version 4.8.3) (Leemans et al., 2009). A two compartment model using the FWE approach (Pasternak et al., 2009) was then fitted to derive maps of FA, MD, RD and AD (Pierpaoli and Basser, 1996), together with a map of the *f* in each voxel (Metzler-Baddeley et al., 2012b).

4.2.3 Tractography and tract-specific measures

Fornix fibres were reconstructed using ExploreDTI version 4.8.3 (Leemans et al., 2009). In-house modifications were utilised to support the modified dRL spherical deconvolution method for whole brain tractography (Dell'Acqua et al., 2010). Spherical deconvolution based tracking algorithms permit extraction of multiple peaks in the fibre orientation density function (fODF) in voxels with complex fibre architecture and make it possible to track through crossing and kissing fibres within the same voxel. The dRL method also reduces isotropic partial volume effects that can degrade spherical deconvolution results. Fibre tracts were reconstructed by producing estimates of dRL fODFs at the centre of each image voxel and then positioning seed points at the vertices of a 2 × 2 × 2mm grid superimposed over the image. The tracking then interpolated local fODF estimates at each seed point and propagated 0.5mm along orientations

indicated by up to four supra 0.05 fODF magnitude threshold peaks (ignoring one per axially symmetric pair), allowing four potential streamlines to emanate from each seed point. Individual streamlines were then propagated by interpolating the fODF at their new location and propagating 0.5mm along the minimally subtending fODF peak, repeating this process until the minimally subtending peak magnitude fell below 0.05 or the change of direction between successive 0.5mm steps exceeded 45°. This procedure was then repeated by tracking in the opposite direction from the initial seed point. Streamlines outside a minimum of 10mm and maximum of 500mm length were discarded. At each 0.5mm step local estimates of FA, RD, MD, AD and *f* were acquired through interpolation of associated parameter maps.

4.2.4 Regions of interest

Three-dimensional fibre reconstructions of the precommissural and postcommissural fornix segments were obtained by applying way-point Boolean logic region of interest (ROI) gates ("AND", "SEED" and "NOT" gates) to segregate specific tracts from the whole brain tractography data produced by the dRL algorithm. ROIs were drawn manually whilst blind to the group membership of each dataset on direction-encoded colour maps in participant's native space. The ROIs were placed according to a series of anatomical landmark protocols. Firstly, the anterior body of the fornix was reconstructed (abFornix; Figure 4.2A), which included fibres from both the precommissural and postcommissural fornices, and fibres running to the anterior thalamus. This initial reconstruction was achieved by marking the location of six slices posterior to the anterior commissure on the mid-sagittal plane, and placing a "SEED" gate encapsulating the body of the fornix on the coronal plane. Fibres that were inconsistent with known fornix anatomy were excluded from the reconstructions by placing "NOT" gates on: i. coronal slices immediately anterior to the genu of the corpus

callosum and immediately posterior to the splenium of the corpus callosum, ii. axial slices at the level of the lower limit of the body of the corpus callosum and at the level of the upper limit of the pons, and iii. sagittal slices lateral to the fornix at the edge of the medial temporal lobe for each hemisphere.

The precommissural fornix and its component fibres were then distinguished by adding an "AND" ROI just in front of the anterior commissure on a coronal plane around the visible columns, thus selecting the tracts that extend in front of the anterior commissure (Figure 4.2B). A "NOT" ROI was also used, this time on an axial plane, as it offered the easiest delineation of the columns, posterior to the anterior commissure, to ensure no overlap occurred between the two tract divisions.

The postcommissural fornix reconstructions followed the exact same protocol as the precommissural fornix reconstructions, except the "AND" and "NOT" ROIs were reversed so that only tracts running behind the anterior commissure were included (Figure 4.2C).

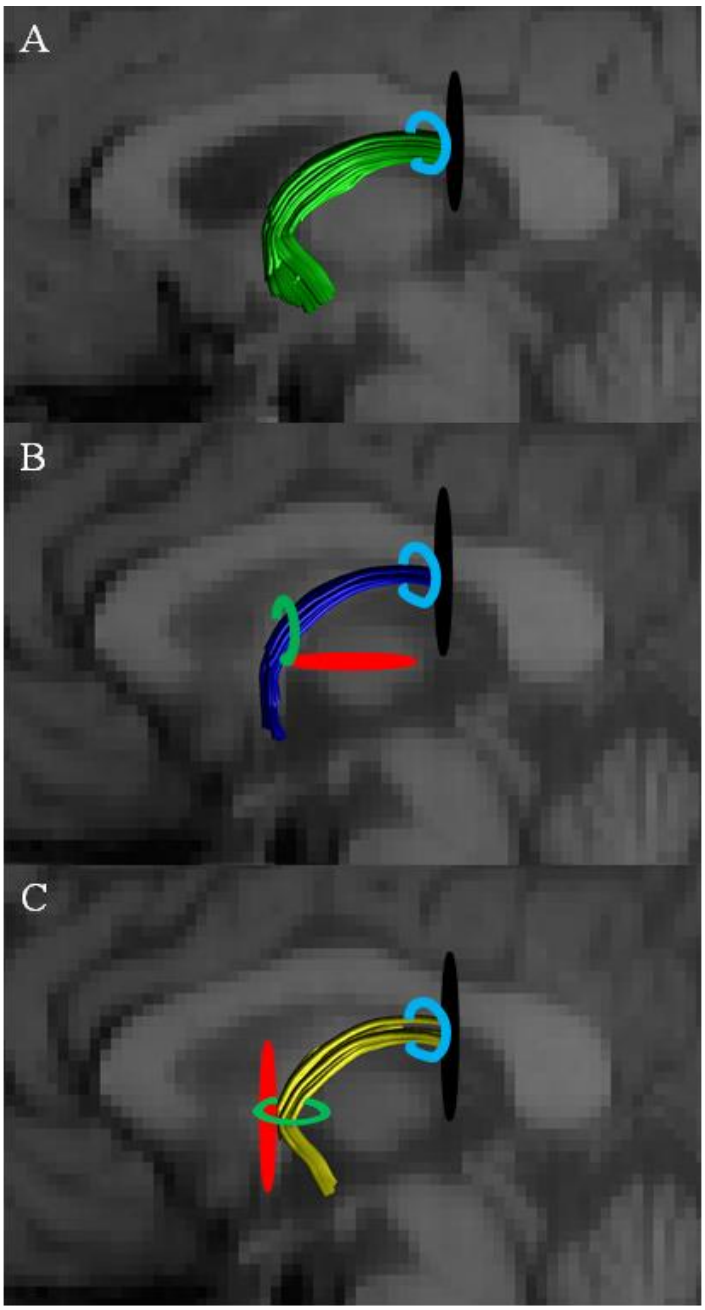

Figure 4.2 *Depictions of the region of interest (ROI) placements on midsagittal slices to obtain: (A) the anterior body of the fornix (abFornix, green), (B) the precommissural fornix and associated fibres (dark blue), and the (C) postcommissural fornix and associated fibres (yellow). Splitter tool placement is indicated in black, "NOT" gates are in red, "SEED" gates are in light blue and "AND" gates are in light green.*

The delineation took advantage of how the precommissural and postcommissural fibres separate at the anterior columns of the fornix. To minimise overlap, reconstructions of the precommissural and postcommissural division only included fibres up to the crus of

the fornix (Figure 4.1), i.e. fibres bending downwards towards the medial temporal lobes and hippocampus were excluded using tract segmentation tools (the "splitter" tool) within ExploreDTI_4.8.3. This procedure was also chosen to avoid tract "jumping" in areas where tracts pass close or across each other, whereby one tract voxel "jumps" onto a neighbouring tract voxel due to the angle/FA threshold being very similar to the neighbouring voxel (Jones and Cercignani, 2010). This was to ensure more precise diffusion derived measures representing the different tracts, and also to make across group comparisons more reliable, due to the fornix reconstructions in some of the aMCI participants not extending beyond the crus of the fornix (example shown in Figure 4.3).

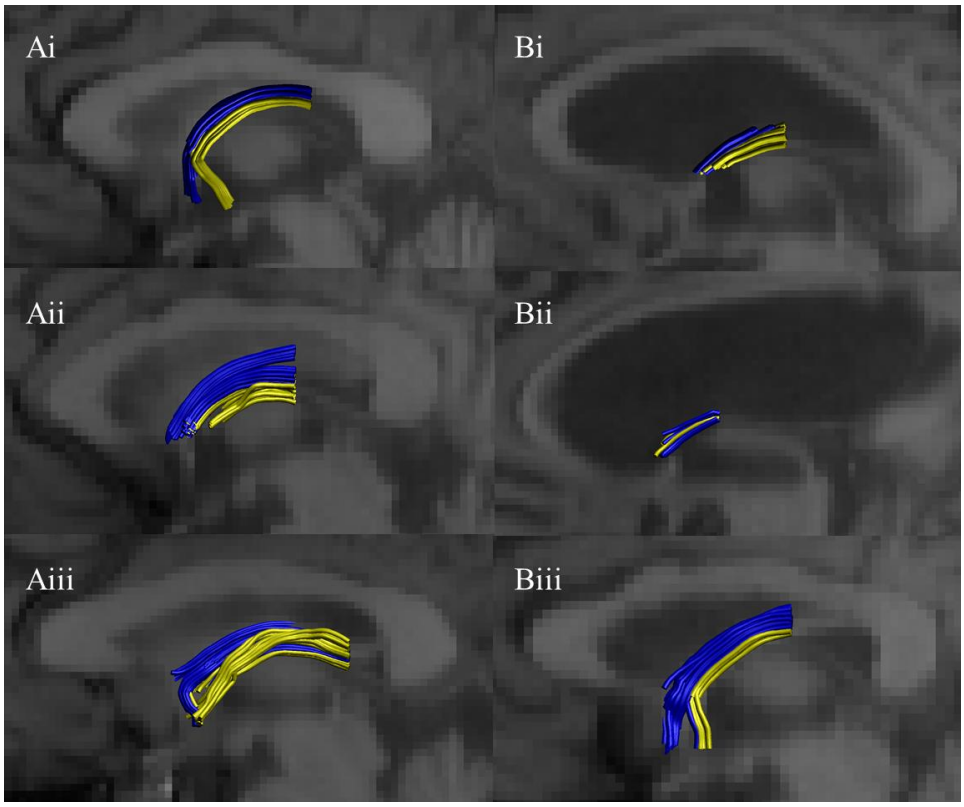

Figure 4.3 *Three examples of tract reconstructions on midsagittal slices from: (Ai-iii) the Healthy ageing group, and (Bi-iii) the Mild Cognitive Impairment group. The precommissural fornix is blue and the postcommissural fornix is yellow.*

4.2.5 Cognitive testing

Participants underwent two 1.5 hour testing sessions in order to assess memory and executive function.

4.2.5.1 Executive function

Executive function was measured via a number of means. The Stroop test (Trenerry et al., 1989) was administered to test for ability to supress/inhibit incongruent responses. In this test participants must read aloud the colour of a word rather than the word itself, which is also a colour, e.g. RED. Suppression score (correct responses controlled for by speed), base time (average speed for correct response), and total errors were the outcome measures. The Tower of London test from Delis and Kaplan Executive Function System battery (as detailed in D-KEFS; Delis et al., 2001) was used to assess for problem solving skills. Participants are given an initial position consisting of three differently coloured balls on three pegs and must rearrange these into a given goal position in as few moves as possible. The dependent variables for this task were the total achievement score (based on how many towers were completed in the allotted time and how many moves it took to complete them), the move accuracy ratio (ratio of number of moves used divided by number of moves necessary for completion), and the first move ratio (the amount of time taken to complete the first move after accuracy is accounted for).

The Digit Span forwards task from the Wechsler Adult Intelligence Scale - Third UK Edition (WAIS-III UK; Wechsler, 1997) was used to assess verbal working memory span. For this task, a participant must recall as many digits in the correct order as possible, with the outcome measure being the maximum they can correctly recall. The

Digit Symbol Substitution test from WAIS-III was also used to assess response speed and focused attention, this involves a number of digit-symbol pairs (e.g. 1/-, 2/⊥, 3/Λ etc.). Afterwards the subject is presented with a list of the digits and must note down the corresponding symbol as fast as possible. The number of correct symbols within the specified time frame is measured.

Verbal fluency was also measured via tests from D-KEFS for verbal generation and fluency, which consisted of letter fluency using letters F, A and S, and category fluency using animals and boys' names. A paper and pen version of the verbal trails test provided a measure of attention switching abilities. In this version of the task, participants had to connect canonical sequences of randomly positioned numbers or letters as a baseline condition and then alternate between letters and numbers (e.g. A, 2, C, 4 etc.). The dependent variables were based upon baseline time and total switch errors (Baddeley, 1996).

4.2.5.2 Episodic memory

Recall and recognition memory were assessed both immediately following learning and after a delay in the visual and verbal domain, using a difficulty matched task known as the Doors and People Test (Baddeley et al., 1994). As an example, participants must remember and recall names of people or recognise a previously presented door out of four very similar doors. Total scores were obtained for each domain, e.g. immediate and delayed verbal and visual recall, and verbal and visual recognition. Free and cued verbal recall abilities were assessed by the Free and Cued Selective Reminding Test (FCSRT; Grober et al., 1997). The measures were as follows: free recall immediately after learning (immediate recall), free recall following a brief distraction (free recall), total recall following a brief distraction (total recall; free and cued words not previously

recalled), and free and total recall following a delay period (delayed free recall and delayed total recall). Association memory for object-location pairings was also tested (Blackwell et al., 2004) using a paper and pencil Paired Associate Learning task (PAL) where participants had to memorise locations of up to eight visual symbols. Performance was assessed by three measures: maximum number of consecutive pairings recalled, errors, and error to success ratio.

4.2.6 Statistical analyses

All statistical analyses used SPSS v. 20 (IBM Corp, 2011) and Q-Value for large-scale analyses (Storey, 2003). All microstructural data for each tract were inspected for outliers defined as > 3 times the absolute Z scores from the mean. Based on this criterion, one value for abFornix, precommissural and postcommissural fornix MD; two values for abFornix, precommissural and postcommissural fornix A; one value for abFornix FA in the aMCI group; and two values for postcommissural fornix *f* (one in the aMCI cohort and one in their control cohort) were excluded from the data analyses. Table 4.1 shows the number of participants for all cognitive tests once outliers and missing values (due to participant no-show/testing problems) were removed. Greenhouse-Geisser corrected values are reported when the data violate the assumption of sphericity.

4.2.6.1 Assessment of cognitive decline in aMCI group compared to Matched Control group

Independent t-tests between the cognitive measures of the Matched Control and aMCI groups helped to establish the existence of cognitive and memory deficits in the patient group. Significance was determined using Bonferroni-adjusted alpha levels.

Executive Function Frequency	Healthy Ageing Cohort (n)	aMCI (n)	Matched Control group (n)
Stroop			
Suppression score	38	22	19
Base time	38	23	19
Errors	38	21	19
Tower of London			
Achievement	38	22	19
Tower move accuracy	37	21	18
First move ratio	37	22	19
Digit Span Forwards	39	24	20
Digit Symbol Score	38	22	19
Verbal Fluency			
Letter fluency total	39	22	20
Category fluency total	39	22	20
Category fluency errors	38	22	19
Verbal Trails			
Base time	37	22	19
Switch errors	37	22	19
Episodic memory			
Doors and People			
Immediate verbal recall	39	24	20
Immediate visual recall	38	23	19
Delayed verbal recall	38	23	20
Delayed visual recall	38	23	19
Verbal recognition	39	23	20
Visual recognition	38	24	19
FCSRT			
Immediate recall	38	22	19
Free recall	39	22	20
Total recall	38	22	19
Delayed free recall	39	22	20
Delayed total recall	37	22	18
Paired Associative Learning			
Learning level	38	22	19
Errors	38	22	19

Table 4.1 *The number of participants with values for all cognitive measures, once outliers (above 3 z scores from the mean) and missing values due to incomplete data were removed. Abbreviation: aMCI = amnestic Mild Cognitive Impairment; FCSRT = Free and Cued Selective Reminding Test.*

4.2.6.2 Assessment of overlap between the precommissural and postcommissural fornix tracts

The overlap between the precommissural and postcommissural fornices was assessed by means of Dice coefficients computed for each individual (Dice, 1945). The Dice coefficient is essentially a measure of similarity between two samples and was calculated with the following formula (where x is the Dice coefficient, A and B are two separate samples and C is the overlap between them): $x = 2C/ (A + B)$. Dice coefficients vary between 0 and 1, the higher the coefficient the higher the level of overlap between the samples.

Visual comparisons were also made of the two tract locations in the Healthy Ageing Cohort. For this, all participants' T_1 scans and subsequently their precommissural and postcommissural tract nifti volumes were transformed into the Montreal Neurological Institute (MNI) standard T_1 1 x 1 x 1mm template space using initial linear and then non-linear warping (Andersson et al., 2010; Jenkinson et al., 2012; Jenkinson and Smith, 2001). Voxel thresholding was set at 70%, meaning that only those voxels in which 70% of the participants possessed a reconstructed tract in that location remained visible (Jones et al., 2013).

4.2.6.3 Assessment of white matter microstructure in the precommissural and postcommissural fornix tracts: effects of age and aMCI

Pearson's r correlation coefficients were calculated between the MRI diffusion indices (FA, RD, MD, AD and *f*) derived for the abFornix, precommissural fornix, and postcommissural fornix to determine their degree of co-linearity for the Healthy Ageing Cohort, and for the aMCI group and their Matched Control group. For the Healthy Ageing Cohort (n = 39) correlations were also calculated with age. It is appreciated that

the measures derived from the abFornix are not independent from those of the precommissural or postcommissural fornix, indeed the abFornix is largely comprised of these two components. Nevertheless, these correlations indicate the extent to which the two divisions of the fornix provide proxy measures for more complete tract reconstructions. Family-wise significance levels were 0.0017 for each separate correlational analysis consisting of 30 correlations (Healthy Ageing Cohort plus age, and aMCI and Matched Controls), based on Bonferroni corrections.

To investigate whether white matter microstructure in the fornix was differentially affected by aMCI, independent t-tests were first conducted between the aMCI and Matched Control groups for FA, RD, MD, AD and *f* in the abFornix. The Bonferroni corrected alpha level was 0.01. Subsequent analyses of variance (ANOVA) involved the between-factor of group (controls and aMCI) and the within-factor of tract (precommissural and postcommissural fornix) for each microstructural measure (FA, RD, MD, AD and *f*) separately. (The abFornix was not included in these ANOVAs as it contains both precommissural and postcommissural fibres and, hence, is not independent.) Significant interactions ($p \leq 0.05$) were followed up with simple effects tests.

4.2.6.4 Assessment of correlations between cognitive function measures and white matter microstructure: Healthy Ageing Cohort (n = 39), aMCI group (n = 24), and Matched Control group (n = 20)

Pearson's r zero-order and age-partialled correlational analyses were conducted between measures of executive function and episodic memory described previously and abFornix, precommissural fornix, and postcommissural fornix diffusion indices (FA, RD, MD, AD and *f*) for each group separately.

The above large-scale analyses were subjected to a false discovery rate analysis using Q-value (Storey, 2003). False discovery rates were applied separately for p values from each type of correlational analysis, for each group and cognitive function separately, e.g. all p values from the zero-order correlations between executive function and all diffusion derived measures for all tracts in the Healthy Ageing Cohort (Table 4.8). Q-values, which are derived from false discovery rates, assign significance to multiple tests performed simultaneously. The false discovery rate is the expected proportion of all significant tests that are false positives, i.e. of all the tests found to be significant, 5% of them will be false discoveries. The Q-value software provides the user with the proportion of their significant results that are true discoveries (Storey, 2003). This analysis can only be performed on a large number of p values and so was only performed for these analyses. Q-values were used rather than correcting using the Bonferroni method as with large-scale comparisons this method is less likely to produce a Type II error.

4.3 Results

4.3.1 Comparisons between aMCI group (n = 24) and Matched Control group (n = 20) for cognitive measures

4.3.1.1 Executive function

Four of the thirteen measures of executive function were significantly lower in the aMCI group compared to the control group (Table 4.2).

Executive Function	Matched Control group		aMCI group			
	Mean	S.D. ±	Mean	S.D. ±	t statistic	p value
Stroop						
Suppression score	93.42	59.09	27.72	19.07	4.67	**5.E-05**
Base time	66.42	74.48	20.83	15.08	-1.45	0.17
Errors	0.68	1.86	2.82	1.92	-1.55	0.13
Tower of London						
Achievement	18.00	13.32	4.17	3.92	3.71	**7.E-04**
Tower move accuracy	1.31	1.29	0.42	0.22	0.18	0.85
First move ratio	4.56	2.63	2.07	3.36	2.18	0.04
Digit Span Forwards	10.35	9.46	2.02	1.84	1.53	0.14
Digit Symbol Score	35.68	11.43	56.47	18.63	4.23	**2.E-04**
Verbal Fluency						
Letter fluency total	43.15	35.36	11.28	14.07	1.97	0.05
Category fluency total	39.50	25.50	8.08	10.92	4.69	**3.E-05**
Category fluency errors	0.53	1.23	1.45	0.77	-1.97	0.06
Verbal Trails						
Base time	23.79	27.93	5.68	4.29	-2.65	0.01
Switch errors	1.16	1.05	1.29	1.57	0.25	0.80

Table 4.2 *Means and Standard Deviations for executive function measures in the aMCI group and Matched Control group, accompanied by t-test statistics and associated p values showing group differences, those in bold highlight p values passing Bonferroni adjustment ($p < 0.004$). Abbreviation: aMCI = amnestic Mild Cognitive Impairment.*

4.3.1.2 Episodic memory

The aMCI group was significantly worse than the Matched Control group on all episodic measures with the exception of the PAL error measure (Table 4.3).

Episodic Memory	Matched Control group		aMCI group			
	Mean	S.D. ±	Mean	S.D. ±	t statistic	p value
Doors and People						
Immediate verbal recall	26.05	5.85	10.29	7.01	8.12	**6.E-10**
Immediate visual recall	32.16	5.10	15.70	8.81	7.56	**6.E-09**
Delayed verbal recall	10.30	2.11	1.87	2.20	12.82	**7.E-16**
Delayed visual recall	11.53	1.07	4.96	3.62	8.27	**8.E-09**
Verbal recognition	15.85	2.91	12.00	4.88	3.19	**4.E-03**
Visual recognition	18.95	3.32	12.46	4.36	5.53	**3.E-06**
FCSRT						
Immediate recall	15.47	0.61	12.45	1.92	6.98	**2.E-07**
Free recall	29.30	8.36	11.68	9.15	6.52	**1.E-07**
Total recall	46.05	3.17	28.82	12.32	6.32	**2.E-06**
Delayed free recall	11.05	3.44	3.32	3.52	7.19	**1.E-08**
Delayed total recall	15.56	0.92	8.91	5.49	5.58	**1.E-05**
Paired Associative Learning						
Learning level	4.05	1.08	1.64	1.22	6.74	**6.E-08**
Errors	6.21	2.53	4.73	1.88	2.10	**0.04**

Table 4.3 *Means and Standard Deviations for the episodic memory measures in the aMCI group and Matched Control group, accompanied by t-test statistics and associated p values showing group differences, those in bold highlight p values passing Bonferroni adjustment ($p < 0.004$). Abbreviations: aMCI = amnestic Mild Cognitive Impairment; FCSRT = Free and Cued Selective Reminding Test.*

4.3.2 Tract reconstructions

Reconstructions of the precommissural and postcommissural fornices were achieved for all participants in both the Healthy Ageing Cohort and the aMCI patients (Figure 4.3). However, visual inspection of the reconstructions revealed much variability in tract trajectories in both groups. While many reconstructions involved the columns of the fornix, with clear evidence of an anterior-posterior split, some reconstructions stopped at the beginning of the columns or were less clearly divided by the anterior commissure (Figure 4.3). Evidence that aMCI affects these tracts came from comparisons based on the length of the white matter reconstructions. For all three tract reconstructions, the mean length of the fibres was lower in the aMCI group than the Matched Controls

(abFornix, t (42) = 2.20, p = 0.033; precommissural fornix, t (42) = 3.37, p = 0.002; postcommissural fornix, t (42) = 3.85, p = 0.0003).

4.3.3 Overlap of precommissural and postcommissural fornix: Healthy Ageing Cohort (n = 39)

The mean Dice coefficient between the precommissural and postcommissural fornix was 0.28 (S.D. = 0.19), with a range from 0 to 0.64 (where a score of 1 would reflect complete overlap). The median coefficient score was 0.24. Figure 4.4 shows the mean overlap between the two tracts once thresholded so that only the voxels in which 70% of participants possess a tract waypoint remain. Only three voxels in the healthy older adults showed overlap when using this criterion. This same 70% threshold revealed that the separation between these two tracts begins before the fornix divides around the anterior commissure; the precommissural fornix fibres are located in the dorsal part of the body of the fornix (Figure 4.4) while the postcommissural fibres comprise more ventral parts of the body of the fornix (Figure 4.4).

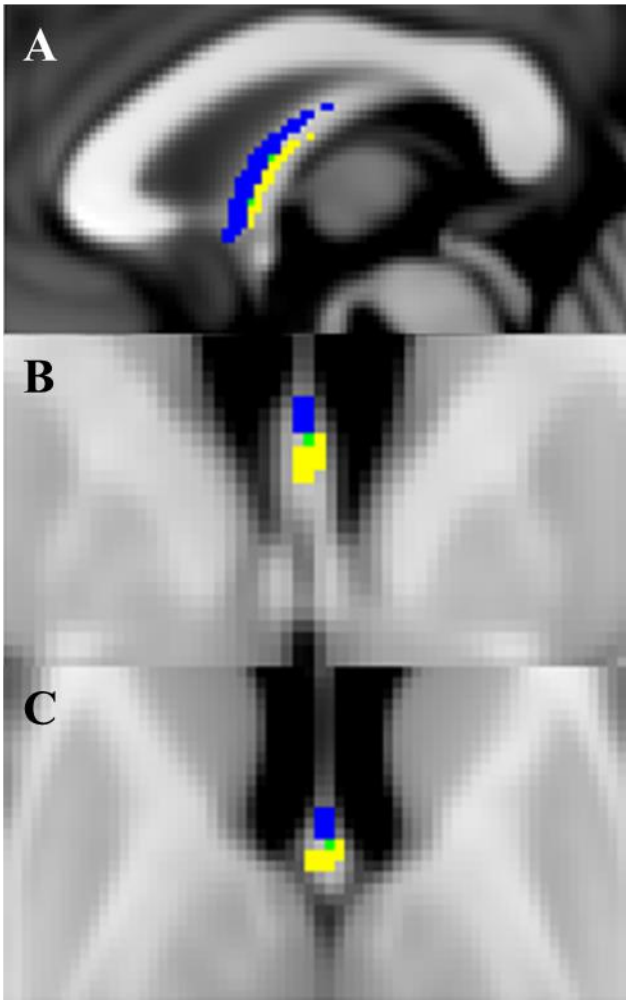

Figure 4.4 *Thresholded visualisation maps for the Healthy Ageing Cohort (n = 39) presented in standard MNI space. The precommissural fornix is in blue and the postcommissural fornix in yellow, with overlap shown in green. The images are presented in MNI space from sagittal (A), coronal (B) and axial (C) perspectives. MNI co-ordinates: X = 90; Y = 127; Z = 81.*

4.3.4 Correlations between precommissural and postcommissural fornix diffusion MRI measures: Healthy Ageing Cohort (n = 39)

In the Healthy Ageing Cohort, all of the abFornix indices correlated significantly with their precommissural and postcommissural counterparts. In contrast, for those correlations between the precommissural and postcommissural divisions, only the RD, MD, and AD values correlated significantly (Table 4.4). Furthermore, age correlated with RD, MD, and AD, but not with FA or *f*, for the abFornix and postcommissural fornix. For the precommissural fornix, trends (significant at uncorrected level) were observed for correlations between age and RD, MD and AD (Table 4.5). Fisher's r to z tests revealed that the correlations in the postcommissural fornix RD, MD and AD

measures with age were not significantly different to those of the precommissural fornix (RD: $z = 1.48$, p = 0.069 1-tailed; MD: $z = 1.35$, p = 0.087 1-tailed; AD: $z = 0.90$, p = 0.183 1-tailed).

Healthy Ageing Cohort (n = 39)										
	Precommissural Fornix					**Postcommissural Fornix**				
abFornix	FA	RD	MD	AD	*f*	FA	RD	MD	AD	*f*
FA	**0.60**					**0.63**				
RD		**0.91**					**0.88**			
MD			**0.91**					**0.86**		
AD				**0.87**					**0.79**	
f					**0.74**					**0.71**
Postcommissural Fornix										
FA	0.24									
RD		**0.75**								
MD			**0.71**							
AD				**0.57**						
f					0.35					

Table 4.4 *Pearson r correlation coefficients between all microstructural indices in the Healthy Ageing Cohort. Those in bold are significant at the Bonferroni-adjusted alpha level of $p \leq 0.0017$. The term abFornix refers to the anterior part of the body of the fornix. Abbreviations: abFornix = anterior body of the fornix; AD = axial diffusivity; f = tissue volume fraction; FA = fractional anisotropy; MD = mean diffusivity; RD = radial diffusivity.*

Healthy Ageing Cohort (n = 39)

	abFornix					Precommissural Fornix					Postcommissural Fornix				
	FA	RD	MD	AD	*f*	FA	RD	MD	AD	*f*	FA	RD	MD	AD	*f*
M	0.34	1.06	1.33	1.87	0.60	0.37	1.02	1.31	1.90	0.61	0.34	1.06	1.34	1.88	0.61
S.D.	0.02	0.11	0.13	0.18	0.04	0.03	0.10	0.12	0.17	0.05	0.04	0.12	0.14	0.21	0.04
Age (r)	-0.13	**0.60**	**0.60**	**0.58**	-0.16	-0.25	0.48	0.46	0.40	-0.09	-0.16	**0.62**	**0.60**	**0.52**	-0.31

Table 4.5 *The upper row gives the mean and standard deviation of the three diffusion derived indices of white matter for each of the three portions of the fornix in the Healthy Ageing Cohort. The lower row gives the Pearson r correlation coefficients between the three tract diffusion derived measures and age. Those in bold are significant at the Bonferroni-adjusted alpha level of $p \leq 0.0017$. Abbreviations: abFornix = anterior body of the fornix; AD = axial diffusivity; f = tissue volume fraction; FA = fractional anisotropy; M = mean; MD = mean diffusivity; RD = radial diffusivity; S.D. = standard deviation. Units for RD, MD, and AD are given as $x10^3$ mm^2 s^{-1}.*

4.3.5 Correlations between the anterior body of the fornix (abFornix), precommissural fornix, and postcommissural fornix diffusion MRI measures: aMCI group (n=24) and Matched Control group (n = 20)

In the aMCI group, all of the abFornix diffusion measures, except for AD, correlated with their counterpart measures taken from just the precommissural fornix (Table 4.6). All but the *f* measure also correlated between the postcommissural and abFornix for the aMCI patients (Table 4.6). Correlations between the precommissural and postcommissural fornices of the aMCI group were significant for FA, RD, and MD.

In the Matched Control group, all of the abFornix diffusion measures correlated with their corresponding postcommissural fornix diffusion measures except for FA (Table 4.6). For the corresponding comparisons between the abFornix and precommissural fornix, RD, MD and AD were significantly correlated (Table 4.6). Between the precommissural and postcommissural fornix, RD and MD were significantly correlated but no significant correlations were observed for FA, AD, or *f* (Table 4.6).

aMCI group (n = 24)										
	Precommissural Fornix					**Postcommissural Fornix**				
abFornix	FA	RD	MD	AD	*f*	FA	RD	MD	AD	*f*
FA	**0.74**					**0.69**				
RD		**0.86**					**0.86**			
MD			**0.75**					**0.85**		
AD				0.55					**0.76**	
f					**0.63**					0.44
Postcommissural Fornix										
FA	**0.72**									
RD		**0.80**								
MD			**0.81**							
AD				0.60						
f					0.38					
Matched Control group (n = 20)										
	Precommissural Fornix					**Postcommissural Fornix**				
abFornix	FA	RD	MD	AD	*f*	FA	RD	MD	AD	*f*
FA	0.52					0.59				
RD		**0.92**					**0.89**			
MD			**0.94**					**0.86**		
AD				**0.91**					**0.79**	
f					0.50					**0.70**
Postcommissural Fornix										
FA	0.22									
RD		**0.75**								
MD			**0.74**							
AD				0.65						
f					0.01					

Table 4.6 *Pearson r correlations for all tract diffusion derived measures in the aMCI group and their Matched Control group. Those in bold are significant at the Bonferroni-adjusted alpha level of $p \leq 0.0017$. The term abFornix refers to the anterior part of the body of the fornix. Abbreviations: abFornix = anterior body of the fornix; AD = axial diffusivity; f, tissue volume fraction; FA = fractional anisotropy; MD = mean diffusivity; RD = radial diffusivity.*

4.3.6 Comparisons between aMCI group (n=24) and Matched Control group (n = 20) for tract measures

When considering just the abFornix, the Matched Controls showed larger FA scores than the aMCI cases [t (41) = 2.43, p = 0.02] (Table 4.7). In contrast, no significant group effects were observed for RD, MD, AD, or f in the abFornix [RD, t (42) = 0.97, p = 0.83; MD, t (42) = 1.20, p = 0.24; AD, t (42) = 1.35, p = 0.18; and f, t (42) = 1.30, p = 0.10].

For the two tract divisions, there was a significant group by tract interaction for FA [F (1, 42) = 6.23, p <0.05]. Inspection of the data (Table 4.7), suggests a relative decrease in FA scores for the precommissural fornix for the aMCI cases, with a relative increase for the postcommissural fornix. However, follow up simple effects tests were not significant. For RD, there was no interaction [(F (1, 42) = 1.48, p = 0.23] and also no group effect [F (1, 42) = 0.05, p = 0.83]. There were no main effects of group or group by tract interactions for MD or AD [F (1, 41) = 0.03, p = 0.87 and F (1, 41) = 0.26, p = 0.62 for MD; and F (1, 40) = 1.12, p = 0.30, and F (1, 40) = 2.03, p = 0.32 for AD]. While there was also no interaction for f (F < 1), there was a main effect of group [F (1, 40) = 8.70, p b 0.01], reflecting lower f scores in the aMCI patients.

	aMCI group (n =24)	Matched Control group (n = 20)
abFornix		
FA	0.32 (0.04)	0.34 (0.02)
RD	1.06 (0.13) $x10^3$	1.09 (0.12) $x10^3$
MD	1.32 (0.15) $x10^3$	1.37 (0.15) $x10^3$
AD	1.84 (0.21) $x10^3$	1.93 (0.21) $x10^3$
f	0.58 (0.05)	0.59 (0.03)
Precommissural Fornix		
FA	0.33 (0.07)	0.36 (0.03)
RD	1.08 (0.12) $x10^3$	1.05 (0.11) $x10^3$
MD	1.37 (0.13) $x10^3$	1.34 (0.14) $x10^3$
AD	1.95 (0.15) $x10^3$	1.92 (0.21) $x10^3$
f	0.59 (0.05)	0.61 (0.04)
Postcommissural Fornix		
FA	0.35 (0.07)	0.34 (0.04)
RD	1.08 (0.19) $x10^3$	1.09 (0.14) $x10^3$
MD	1.40 (0.21) $x10^3$	1.38 (0.16) $x10^3$
AD	2.03 (0.26) $x10^3$	1.94 (0.22) $x10^3$
f	0.57 (0.05)	0.60 (0.04)

Table 4.7 *Means and standard deviations for the anterior body of the fornix (abFornix), precommissural fornix, and postcommissural fornix for each diffusion derived index for the amnesic Mild Cognitive Impairment (aMCI) and Matched Control groups. Abbreviations: abFornix = anterior body of the fornix; AD = axial diffusivity; f = tissue volume fraction; FA, fractional anisotropy; MD = medial diffusivity; RD, radial diffusivity. Units for RD, MD, and AD are given as* $x10^3$ mm^2 s^{-1}.

4.3.7 Correlations between abFornix, precommissural fornix, and postcommissural fornix diffusion MRI indices and executive function and episodic memory measures: Healthy Ageing Cohort (n = 39)

No significant correlations existed between any of the executive function measures and any of the diffusion derived measures for the three tracts, irrespective of whether age was partialled out of the correlation (Tables 4.8 and 4.9). However, with regards to the episodic memory measures, a number of Pearson's r correlations remained significant proceeding false discovery rate analysis, particularly for the RD, MD and AD measures (Table 4.10).

abFornix: RD, MD, AD and *f* correlated with immediate and delayed visual recall, and visual and verbal recognition from the Doors and People test, along with free recall from the FCSRT. The measures RD, MD and AD also correlated with total recall, delayed free recall, and delayed total recall from the FCSRT. The RD scores correlated with learning level from the PAL task.

Precommissural fornix: For the Doors and People test, RD, MD and AD correlated with immediate visual recall and visual and verbal recognition, *f* correlated with verbal recognition and AD correlated with delayed visual recall. The FCSRT free recall and delayed total recall measures correlated with RD and MD.

Postcommissural fornix: For the Doors and People test, FA, RD and *f* correlated with visual recognition and FA and RD correlated with immediate visual recall. Delayed visual recall correlated with RD and MD, and verbal recognition correlated with RD, MD, AD and *f*. Finally, FCSRT free recall, total recall, delayed free recall, and delayed total recall correlated with RD, MD, and AD, while delayed total recall also correlated with *f*.

However, none of the correlations for any of the tracts remained significant once age had been partialled out (Table 4.11).

4.3.8 Correlations between abFornix, precommissural fornix, and postcommissural fornix diffusion MRI indices and executive function and episodic memory measures: aMCI group (n = 24) and Matched Control group (n = 20)

None of the Pearson's r correlations for the aMCI or Matched Control groups were significant once false discovery rate was applied, irrespective of whether age was partialled out (Tables 4.12-4.19).

Healthy Ageing Cohort (n = 39)

Executive function	abFornix					Precommissural Fornix					Postcommissural Fornix				
	FA	RD	MD	AD	*f*	FA	RD	MD	AD	*f*	FA	RD	MD	AD	*f*
Stroop															
Suppression score	0.25	-0.22	-0.17	-0.11	0.30	0.26	-0.24	-0.18	-0.09	0.29	0.35	-0.20	-0.11	0.00	0.13
Base time	-0.29	0.22	0.17	0.11	-0.21	-0.21	0.29	0.26	0.20	0.03	-0.27	0.25	0.18	0.08	-0.30
Errors	0.00	-0.11	-0.10	-0.09	-0.18	-0.17	-0.13	-0.17	-0.20	-0.08	0.14	-0.10	-0.05	0.01	-0.27
Tower of London															
Achievement	0.01	0.23	0.24	0.23	-0.05	0.10	0.20	0.24	0.26	0.01	0.09	0.10	0.13	0.16	-0.11
Tower move accuracy	-0.04	-0.15	-0.16	-0.18	-0.03	-0.20	0.02	-0.04	-0.11	-0.13	-0.02	-0.08	-0.09	-0.10	-0.04
First move ratio	-0.18	-0.13	-0.16	-0.19	0.09	-0.02	-0.15	-0.15	-0.14	0.01	-0.07	-0.10	-0.12	-0.13	0.02
Digit Span Forwards	0.43	-0.20	-0.13	-0.03	0.25	0.34	-0.26	-0.18	-0.07	0.28	0.36	-0.16	-0.06	0.05	0.11
Digit Symbol Score	0.33	-0.41	-0.36	-0.28	0.31	0.25	-0.33	-0.29	-0.21	0.12	0.37	-0.44	-0.34	-0.19	0.39
Verbal Fluency															
Language fluency total	0.10	-0.33	-0.32	-0.30	0.25	0.27	-0.34	-0.29	-0.21	0.10	0.05	-0.33	-0.35	-0.32	0.23
Category fluency total	0.35	-0.42	-0.37	-0.29	0.34	0.45	-0.45	-0.36	-0.22	0.25	0.31	-0.41	-0.33	-0.22	0.30
Category fluency errors	0.14	0.01	0.04	0.08	0.07	0.10	-0.05	-0.01	0.03	0.11	-0.04	0.01	0.00	-0.02	0.00
Verbal Trails															
Base time	-0.28	0.13	0.08	0.01	-0.01	-0.10	0.25	0.24	0.21	0.08	-0.20	0.07	0.01	-0.06	-0.08
Switch errors	-0.24	0.23	0.18	0.12	-0.28	-0.41	0.32	0.22	0.08	-0.31	-0.08	0.37	0.37	0.33	-0.35

Table 4.8 *Zero-order Pearson's r correlations between executive function measures and white matter microstructure in the Healthy Ageing Cohort (n = 39) for precommissural and postcommissural fornices. Abbreviations: abFornix = anterior body of the fornix; AD = axial diffusivity; f = tissue volume fraction; FCSRT = Free and Cued Selective Reminding Test; FA = fractional anisotropy; MD = mean diffusivity; RD = radial diffusivity. None of the correlations passed false discovery rate analysis.*

Healthy Ageing Cohort (n = 39)															
Executive function	abFornix					Precommissural Fornix					Postcommissural Fornix				
	FA	RD	MD	AD	*f*	FA	RD	MD	AD	*f*	FA	RD	MD	AD	*f*
Stroop															
Suppression score	0.24	-0.20	-0.26	-0.17	0.29	0.25	-0.22	-0.15	-0.05	0.28	0.34	-0.18	-0.06	0.06	0.11
Base time	-0.27	0.16	0.15	0.05	-0.19	-0.18	0.25	0.22	0.16	0.04	-0.25	0.20	0.11	0.00	-0.27
Errors	0.00	-0.14	-0.04	-0.01	-0.18	-0.17	-0.15	-0.20	-0.22	-0.08	0.14	-0.13	-0.07	0.00	-0.28
Tower of London															
Achievement	0.02	0.24	0.23	0.22	-0.04	0.12	0.20	0.24	0.26	0.02	0.10	0.07	0.12	0.15	-0.10
Tower move accuracy	-0.10	0.16	-0.11	-0.16	-0.11	-0.36	0.29	0.20	0.07	-0.19	-0.10	0.27	0.24	0.17	-0.20
First move ratio	-0.15	-0.45	-0.40	-0.44	0.15	0.07	-0.38	-0.38	-0.33	0.05	-0.01	-0.43	-0.45	-0.39	0.15
Digit Span Forwards	0.43	-0.23	-0.21	-0.08	0.25	0.34	-0.27	-0.18	-0.06	0.28	0.36	-0.18	-0.05	0.08	0.10
Digit Symbol Score	0.30	-0.29	-0.24	-0.12	0.27	0.18	-0.22	-0.17	-0.10	0.10	0.34	-0.33	-0.19	-0.03	0.32
Verbal Fluency															
Language fluency total	0.06	-0.21	-0.16	-0.15	0.22	0.21	-0.25	-0.19	-0.11	0.08	0.01	-0.21	-0.23	-0.22	0.16
Category fluency total	0.32	-0.26	-0.19	-0.12	0.31	0.39	-0.33	-0.23	-0.08	0.23	0.27	-0.23	-0.14	-0.02	0.21
Category fluency errors	0.12	0.15	0.26	0.30	0.04	0.06	0.04	0.08	0.12	0.10	-0.07	0.16	0.13	0.09	-0.06
Verbal Trails															
Base time	-0.29	0.21	0.14	0.05	-0.02	-0.11	0.31	0.30	0.25	0.07	-0.21	0.13	0.05	-0.04	-0.10
Switch errors	-0.24	0.25	0.15	0.09	-0.28	-0.41	0.34	0.23	0.07	-0.31	-0.07	0.44	0.43	0.35	-0.36

Table 4.9 *Age-partialled Pearson's r correlations between executive function measures and white matter microstructure in the Healthy Ageing Cohort (n = 39) for precommissural and postcommissural fornices. Abbreviations: abFornix = anterior body of the fornix; AD = axial diffusivity; f = tissue volume fraction; FA = fractional anisotropy; FCSRT = Free and Cued Selective Reminding Test; MD = mean diffusivity; RD = radial diffusivity. None of the correlations passed false discovery rate analysis.*

Healthy Ageing Cohort (n = 39)															
Episodic memory	abFornix					Precommissural Fornix					Postcommissural Fornix				
	FA	RD	MD	AD	*f*	FA	RD	MD	AD	*f*	FA	RD	MD	AD	*f*
Doors and People															
Immediate verbal recall	0.18	-0.20	-0.17	-0.12	0.21	0.29	-0.25	-0.19	-0.09	0.18	0.11	-0.20	-0.18	-0.14	0.08
Immediate visual recall	0.12	**-0.46**	**-0.46**	**-0.42**	**0.38**	0.00	**-0.35**	**-0.38**	**-0.39**	0.23	**0.41**	**-0.43**	-0.30	-0.14	0.19
Delayed verbal recall	0.13	-0.16	-0.15	-0.12	0.28	0.21	-0.12	-0.08	-0.02	0.25	0.18	-0.23	-0.18	-0.10	0.14
Delayed visual recall	-0.13	**-0.33**	**-0.37**	**-0.40**	**0.31**	-0.23	-0.21	-0.30	**-0.37**	0.18	0.22	**-0.43**	**-0.36**	-0.25	0.31
Verbal recognition	0.07	**-0.43**	**-0.45**	**-0.45**	**0.47**	0.09	**-0.32**	**-0.35**	**-0.34**	**0.35**	-0.06	**-0.45**	**-0.50**	**-0.50**	**0.36**
Visual recognition	0.08	**-0.46**	**-0.46**	**-0.42**	**0.43**	-0.14	**-0.37**	**-0.45**	**-0.48**	0.21	**0.37**	**-0.41**	-0.30	-0.15	**0.32**
FCSRT															
Immediate recall	-0.03	-0.10	-0.12	-0.14	-0.02	-0.25	0.01	-0.07	-0.16	-0.08	0.02	-0.10	-0.10	-0.10	-0.08
Free recall	0.15	**-0.44**	**-0.44**	**-0.42**	**0.39**	0.28	**-0.35**	**-0.32**	-0.26	0.25	0.14	**-0.46**	**-0.44**	**-0.38**	0.27
Total recall	0.12	**-0.35**	**-0.34**	**-0.32**	0.12	0.21	-0.30	-0.28	-0.23	-0.03	0.09	**-0.42**	**-0.40**	**-0.34**	0.21
Delayed free recall	0.08	**-0.42**	**-0.43**	**-0.42**	0.26	0.07	-0.29	-0.31	-0.30	0.04	0.15	**-0.50**	**-0.48**	**-0.41**	0.24
Delayed total recall	0.15	**-0.47**	**-0.46**	**-0.43**	0.19	0.31	**-0.42**	**-0.38**	-0.29	0.15	0.16	**-0.55**	**-0.52**	**-0.42**	**0.34**
Paired Associative Learning															
Learning level	0.11	**-0.32**	-0.30	-0.27	0.20	-0.05	-0.27	-0.30	-0.31	-0.01	0.11	-0.30	-0.28	-0.22	0.22
Errors	-0.01	-0.03	-0.04	-0.06	-0.09	-0.27	0.13	0.04	-0.06	0.01	0.01	-0.23	-0.22	-0.19	0.26

Table 4.10 *Zero order Pearson's r correlations between episodic memory and white matter microstructure in the Healthy Ageing Cohort (n = 39) for precommissural and postcommissural fornices. Abbreviations: abFornix = anterior body of the fornix; AD = axial diffusivity; f = tissue volume fraction; FA = fractional anisotropy; FCSRT = Free and Cued Selective Reminding Test; MD = mean diffusivity; RD = radial diffusivity. Text in bold highlights those correlations that passed false discovery rate analysis.*

Healthy Ageing Cohort (n = 39)

Episodic memory	abFornix					Precommissural Fornix					Postcommissural Fornix				
	FA	RD	MD	AD	*f*	FA	RD	MD	AD	*f*	FA	RD	MD	AD	*f*
Doors and People															
Immediate verbal recall	0.17	-0.13	-0.09	-0.03	0.18	0.26	-0.20	-0.13	-0.02	0.17	0.09	-0.13	-0.10	-0.06	0.04
Immediate visual recall	0.07	-0.30	-0.29	-0.25	0.35	-0.12	-0.19	-0.24	-0.27	0.21	0.38	-0.25	-0.09	0.09	0.08
Delayed verbal recall	0.10	0.02	0.04	0.06	0.25	0.15	0.02	0.06	0.11	0.23	0.14	-0.07	-0.01	0.06	0.06
Delayed visual recall	-0.18	-0.18	-0.23	-0.27	0.28	-0.35	-0.06	-0.17	-0.28	0.16	0.18	-0.30	-0.21	-0.10	0.23
Verbal recognition	0.02	-0.28	-0.31	-0.31	0.45	0.00	-0.18	-0.21	-0.23	0.34	-0.13	-0.30	-0.37	-0.39	0.28
Visual recognition	0.04	-0.33	-0.32	-0.28	0.40	-0.26	-0.25	-0.34	-0.40	0.19	0.34	-0.25	-0.11	0.05	0.24
FCSRT															
Immediate recall	-0.07	0.07	0.05	0.02	-0.06	-0.34	0.16	0.06	-0.06	-0.11	-0.02	0.09	0.07	0.05	-0.18
Free recall	0.09	-0.17	-0.17	-0.15	0.36	0.17	-0.13	-0.10	-0.05	0.24	0.07	-0.18	-0.17	-0.14	0.13
Total recall	0.07	-0.14	-0.14	-0.12	0.07	0.12	-0.14	-0.12	-0.08	-0.07	0.02	-0.23	-0.22	-0.16	0.10
Delayed free recall	0.02	-0.19	-0.20	-0.19	0.21	-0.06	-0.08	-0.11	-0.13	0.00	0.08	-0.30	-0.27	-0.21	0.12
Delayed total recall	0.09	-0.16	-0.15	-0.12	0.12	0.20	-0.18	-0.13	-0.07	0.12	0.08	-0.27	-0.23	-0.15	0.20
Paired Associative Learning															
Learning level	0.08	-0.20	-0.18	-0.15	0.17	-0.13	-0.17	-0.21	-0.23	-0.04	0.07	-0.18	-0.15	-0.10	0.15
Errors	0.00	-0.08	-0.10	-0.11	-0.08	-0.27	0.12	0.02	-0.09	-0.23	0.02	-0.34	-0.32	-0.25	0.29

Table 4.11 *Age-partialled Pearson's r correlations between episodic memory and white matter microstructure in the Healthy Ageing Cohort (n = 39) for precommissural and postcommissural fornices. Abbreviations: abFornix = anterior body of the fornix; AD = axial diffusivity; f = tissue volume fraction; FA = fractional anisotropy; FCSRT = Free and Cued Selective Reminding Test; MD = mean diffusivity; RD = radial diffusivity. None of the correlations passed false discovery rate analysis.*

aMCI group (n = 24)

Executive function	abFornix					Precommissural Fornix					Postcommissural Fornix				
	FA	RD	MD	AD	*f*	FA	RD	MD	AD	*f*	FA	RD	MD	AD	*f*
Stroop															
Suppression score	0.18	-0.05	-0.08	-0.09	0.07	0.20	-0.07	-0.13	-0.20	-0.19	-0.01	0.07	-0.03	-0.17	-0.02
Base time	0.01	-0.05	0.12	0.20	-0.25	-0.11	-0.22	-0.07	-0.02	-0.08	-0.16	-0.13	-0.04	-0.03	-0.09
Errors	-0.28	-0.40	-0.25	-0.31	-0.05	0.10	-0.37	-0.11	-0.14	-0.09	-0.14	-0.25	-0.15	-0.29	0.01
Tower of London															
Achievement	0.10	0.06	-0.08	-0.02	0.10	-0.03	0.16	-0.02	0.04	0.34	0.14	0.12	0.05	0.21	0.20
Tower move accuracy	-0.15	0.18	0.12	0.02	-0.07	-0.02	0.08	0.02	-0.12	-0.02	-0.29	0.25	0.12	-0.11	0.17
First move ratio	0.27	0.09	-0.01	-0.03	0.17	0.27	0.19	0.07	0.04	0.04	0.30	0.11	0.02	0.00	0.49
Digit Span Forwards	0.28	0.07	0.00	0.13	0.32	0.16	-0.03	-0.07	0.21	0.18	0.10	0.00	-0.05	0.12	-0.13
Digit Symbol Score	0.06	0.03	-0.18	-0.24	0.36	0.24	0.15	0.02	0.09	0.22	0.11	0.11	-0.04	-0.08	0.22
Verbal Fluency															
Language fluency total	0.46	0.13	0.11	0.14	-0.13	0.44	-0.02	-0.05	0.01	0.00	0.10	0.34	0.23	0.08	0.18
Category fluency total	0.13	-0.07	-0.09	-0.04	0.16	0.06	-0.10	-0.12	-0.04	0.10	-0.12	0.04	-0.04	-0.09	0.51
Category fluency errors	-0.16	-0.48	-0.20	-0.21	0.03	0.08	-0.47	-0.07	-0.04	0.09	-0.08	-0.32	-0.09	-0.19	0.40
Verbal Trails															
Base time	0.11	0.22	0.12	0.17	-0.13	-0.04	0.08	-0.11	-0.10	-0.10	-0.24	0.25	0.08	0.03	0.03
Switch errors	-0.44	-0.37	-0.33	-0.49	-0.25	0.04	-0.19	-0.04	-0.19	-0.24	-0.09	-0.34	-0.30	-0.50	-0.24

Table 4.12 *Zero order Pearson's r correlations between executive function and white matter microstructure in the aMCI group (n = 24) for precommissural and postcommissural fornices. Abbreviations: abFornix = anterior body of the fornix; aMCI = amnestic Mild Cognitive Impairment; AD = axial diffusivity; f = tissue volume fraction; FA = fractional anisotropy; MD = mean diffusivity; RD = radial diffusivity. None of the correlations passed false discovery rate analysis.*

aMCI group (n = 24)															
Executive function	abFornix					Precommissural Fornix					Postcommissural Fornix				
	FA	RD	MD	AD	*f*	FA	RD	MD	AD	*f*	FA	RD	MD	AD	*f*
Stroop															
Suppression score	0.39	0.18	0.03	-0.01	0.02	0.37	0.21	0.01	-0.08	-0.28	0.19	0.29	0.09	-0.05	-0.21
Base time	-0.06	-0.14	0.08	0.17	-0.23	-0.17	-0.38	-0.13	-0.08	-0.06	-0.25	-0.22	-0.09	-0.09	-0.02
Errors	-0.28	-0.41	-0.24	-0.31	-0.06	0.13	-0.40	-0.10	-0.12	-0.11	-0.12	-0.24	-0.13	-0.29	-0.02
Tower of London															
Achievement	0.06	0.01	-0.11	-0.04	0.11	-0.07	0.12	-0.06	0.00	0.36	0.10	0.08	0.02	0.18	0.26
Tower move accuracy	-0.10	0.28	0.17	0.05	-0.09	0.03	0.20	0.07	-0.08	-0.04	-0.25	0.34	0.16	-0.08	0.12
First move ratio	0.43	0.27	0.07	0.03	0.14	0.39	0.44	0.19	0.14	0.00	0.48	0.25	0.11	0.09	0.43
Digit Span Forwards	0.30	0.09	0.01	0.14	0.32	0.17	-0.02	-0.07	0.23	0.18	0.11	0.01	-0.05	0.13	-0.15
Digit Symbol Score	0.18	0.18	-0.12	-0.19	0.34	0.35	0.38	0.12	0.20	0.19	0.24	0.25	0.03	0.01	0.13
Verbal Fluency															
Language fluency total	0.47	0.12	0.10	0.13	-0.12	0.44	-0.06	-0.08	-0.01	0.01	0.08	0.35	0.22	0.07	0.22
Category fluency total	0.25	0.05	-0.02	0.01	0.13	0.15	0.04	-0.04	0.04	0.07	-0.03	0.15	0.03	-0.02	0.46
Category fluency errors	-0.03	-0.38	-0.12	-0.15	-0.01	0.20	-0.35	0.05	0.08	0.04	0.06	-0.21	0.00	-0.10	0.30
Verbal Trails															
Base time	0.14	0.28	0.13	0.18	-0.14	-0.03	0.13	-0.10	-0.09	-0.11	-0.24	0.29	0.09	0.05	0.01
Switch errors	-0.41	-0.33	-0.30	-0.47	-0.28	0.10	-0.11	0.02	-0.15	-0.27	-0.02	-0.30	-0.27	-0.48	-0.34

Table 4.13 *Age-partialled Pearson's r correlations between executive function and white matter microstructure in the aMCI group (n = 24) for precommissural and postcommissural fornices. Abbreviations: abFornix = anterior body of the fornix; aMCI = amnestic Mild Cognitive Impairment; AD = axial diffusivity; f = tissue volume fraction; FA = fractional anisotropy; MD = mean diffusivity; RD = radial diffusivity. None of the correlations passed false discovery rate analysis.*

Matched Control group (n = 20)

Executive function	abFornix					Precommissural Fornix					Postcommissural Fornix				
	FA	RD	MD	AD	*f*	FA	RD	MD	AD	*f*	FA	RD	MD	AD	*f*
Stroop															
Suppression score	0.32	-0.30	-0.25	-0.18	0.32	0.23	-0.31	-0.23	-0.13	0.22	0.50	-0.19	-0.07	0.07	0.02
Base time	0.10	0.17	0.20	0.23	-0.56	0.08	0.26	0.29	0.30	0.02	-0.14	0.19	0.17	0.14	-0.49
Errors	-0.07	-0.24	-0.24	-0.24	0.04	-0.22	-0.24	-0.27	-0.29	0.18	0.22	-0.25	-0.20	-0.12	-0.21
Tower of London															
Achievement	0.06	0.27	0.27	0.26	-0.16	0.20	0.36	0.39	0.38	-0.03	-0.09	0.10	0.09	0.07	-0.22
Tower move accuracy	0.30	-0.06	-0.01	0.05	0.09	-0.08	-0.02	-0.03	-0.05	0.07	0.21	0.07	0.13	0.19	-0.08
First move ratio	-0.26	-0.26	-0.30	-0.34	0.16	-0.01	-0.33	-0.32	-0.28	0.08	-0.08	-0.25	-0.29	-0.31	0.19
Digit Span Forwards	0.57	-0.12	-0.03	0.08	0.16	0.31	-0.13	-0.04	0.05	0.34	0.47	0.00	0.11	0.25	-0.03
Digit Symbol Score	0.38	-0.44	-0.39	-0.32	0.41	0.10	-0.31	-0.28	-0.23	0.16	0.57	-0.42	-0.29	-0.11	0.45
Verbal Fluency															
Language fluency total	0.20	-0.26	-0.24	-0.20	0.14	0.18	-0.34	-0.30	-0.22	0.11	0.34	-0.24	-0.19	-0.10	0.15
Category fluency total	0.55	-0.40	-0.32	-0.23	0.28	0.42	-0.40	-0.30	-0.17	0.18	0.56	-0.40	-0.29	-0.13	0.25
Category fluency errors	0.15	0.20	0.25	0.29	-0.30	0.29	0.02	0.12	0.22	0.01	0.19	0.14	0.21	0.28	-0.24
Verbal Trails															
Base time	-0.16	0.03	0.01	-0.01	-0.10	0.21	0.01	0.08	0.14	0.30	-0.09	0.02	0.00	-0.03	-0.30
Switch errors	-0.27	0.23	0.19	0.13	-0.11	-0.33	0.30	0.20	0.08	-0.24	-0.15	0.37	0.36	0.31	-0.12

Table 4.14 *Zero order Pearson's r correlations between executive function and white matter microstructure in the Matched Control group (n = 20) for precommissural and postcommissural fornices. Abbreviations: abFornix = anterior body of the fornix; AD = axial diffusivity; f = tissue volume fraction; FA = fractional anisotropy; MD = mean diffusivity; RD = radial diffusivity. None of the correlations passed false discovery rate analysis.*

Matched Control group (n = 20)															
Executive function	abFornix					Precommissural Fornix					Postcommissural Fornix				
	FA	RD	MD	AD	*f*	FA	RD	MD	AD	*f*	FA	RD	MD	AD	*f*
Stroop															
Suppression score	0.29	-0.13	-0.06	0.02	0.22	0.19	-0.15	-0.06	0.02	0.14	0.44	0.05	0.20	0.33	-0.12
Base time	0.11	0.17	0.21	0.25	-0.58	0.09	0.28	0.31	0.30	0.04	-0.13	0.20	0.18	0.13	-0.50
Errors	-0.09	-0.23	-0.24	-0.23	0.01	-0.23	-0.23	-0.27	-0.28	0.17	0.20	-0.25	-0.18	-0.09	-0.26
Tower of London															
Achievement	0.04	0.44	0.43	0.41	-0.22	0.18	0.51	0.53	0.49	-0.07	-0.13	0.25	0.22	0.16	-0.28
Tower move accuracy	0.32	-0.14	-0.07	0.00	0.12	-0.08	-0.07	-0.08	-0.09	0.10	0.25	0.03	0.11	0.18	-0.06
First move ratio	-0.24	-0.44	-0.49	-0.52	0.22	0.01	-0.48	-0.46	-0.39	0.12	-0.04	-0.47	-0.49	-0.46	0.26
Digit Span Forwards	0.58	-0.13	-0.02	0.11	0.16	0.31	-0.13	-0.04	0.07	0.34	0.48	0.02	0.17	0.32	-0.04
Digit Symbol Score	0.35	-0.28	-0.21	-0.13	0.31	0.06	-0.13	-0.11	-0.07	0.06	0.52	-0.24	-0.06	0.14	0.36
Verbal Fluency															
Language fluency total	0.17	-0.11	-0.08	-0.04	0.04	0.15	-0.24	-0.18	-0.11	0.03	0.28	-0.07	-0.01	0.07	0.05
Category fluency total	0.57	-0.06	0.05	0.18	0.09	0.42	-0.13	0.00	0.13	0.03	0.50	-0.01	0.14	0.28	0.05
Category fluency errors	0.12	0.42	0.47	0.51	-0.41	0.27	0.16	0.26	0.34	-0.05	0.14	0.37	0.44	0.47	-0.34
Verbal Trails															
Base time	-0.21	0.24	0.21	0.17	-0.21	0.19	0.19	0.26	0.29	0.25	-0.17	0.27	0.22	0.14	-0.43
Switch errors	-0.25	0.17	0.12	0.04	-0.05	-0.32	0.26	0.14	0.00	-0.20	-0.11	0.36	0.33	0.26	-0.06

Table 4.15 *Age-partialled Pearson's r correlations between executive function and white matter microstructure in the Matched Control group (n = 20) for precommissural and postcommissural fornices. Abbreviations: abFornix = anterior body of the fornix; AD = axial diffusivity; f = tissue volume fraction; FA = fractional anisotropy; MD = mean diffusivity; RD = radial diffusivity. None of the correlations passed false discovery rate analysis.*

aMCI group (n = 24)

Episodic memory	abFornix					Precommissural Fornix					Postcommissural Fornix				
	FA	RD	MD	AD	*f*	FA	RD	MD	AD	*f*	FA	RD	MD	AD	*f*
Doors and People															
Immediate verbal recall	-0.07	0.12	0.04	-0.09	0.23	0.12	0.07	-0.01	-0.19	0.27	0.01	0.14	0.05	-0.13	0.40
Immediate visual recall	0.15	-0.09	0.03	0.08	0.19	0.22	-0.26	-0.10	0.04	0.19	-0.07	-0.01	0.03	-0.03	0.52
Delayed verbal recall	0.06	-0.07	-0.02	-0.04	0.26	0.14	-0.28	-0.23	-0.24	0.27	-0.08	-0.06	-0.09	-0.22	0.25
Delayed visual recall	0.12	0.09	0.20	0.21	0.21	0.20	-0.06	0.12	0.19	0.19	-0.06	0.14	0.18	0.10	0.61
Verbal recognition	0.22	0.26	0.25	0.17	0.05	0.42	0.22	0.28	0.26	-0.02	0.15	0.30	0.24	0.05	0.00
Visual recognition	0.07	-0.05	0.12	0.14	0.41	0.11	-0.13	0.09	0.14	0.23	-0.03	-0.10	-0.02	-0.11	0.36
FCSRT															
Immediate recall	0.27	0.24	0.11	0.09	0.03	0.13	0.12	-0.11	-0.23	-0.05	0.11	0.17	0.02	-0.07	0.55
Free recall	0.01	-0.10	-0.06	-0.11	0.10	0.12	-0.25	-0.24	-0.33	-0.03	-0.23	0.05	-0.04	-0.28	0.52
Total recall	-0.09	0.08	-0.01	-0.15	-0.02	0.06	0.07	-0.04	-0.25	-0.09	-0.12	0.13	0.00	-0.24	0.34
Delayed free recall	-0.17	0.11	0.05	-0.04	0.12	-0.06	-0.02	-0.09	-0.20	0.04	-0.37	0.14	-0.01	-0.24	0.50
Delayed total recall	-0.09	0.26	0.16	0.04	0.01	-0.02	0.20	0.08	-0.10	-0.05	-0.13	0.17	0.04	-0.15	0.30
Paired Associative Learning															
Learning level	0.28	0.09	-0.03	0.26	0.45	-0.20	0.03	-0.16	0.20	0.47	-0.21	-0.01	-0.16	0.10	0.45
Errors	0.16	-0.03	-0.22	0.12	0.46	-0.31	-0.03	-0.26	0.29	0.44	-0.24	-0.20	-0.34	0.06	-0.19

Table 4.16 *Zero order Pearson's r correlations between episodic memory and white matter microstructure in the aMCI group (n = 24) for precommissural and postcommissural fornices. Abbreviations: abFornix = anterior body of the fornix; aMCI = amnestic Mild Cognitive Impairment; AD = axial diffusivity; f = tissue volume fraction; FA = fractional anisotropy; FCSRT = Free and Cued Selective Reminding Test; MD = mean diffusivity; RD = radial diffusivity. None of the correlations passed false discovery rate analysis.*

aMCI group (n = 24)

Episodic memory	abFornix					Precommissural Fornix					Postcommissural Fornix				
	FA	RD	MD	AD	*f*	FA	RD	MD	AD	*f*	FA	RD	MD	AD	*f*
Doors and People															
Immediate verbal recall	0.02	0.26	0.11	-0.05	0.20	0.21	0.25	0.08	-0.12	0.24	0.11	0.26	0.12	-0.06	0.35
Immediate visual recall	0.35	0.12	0.15	0.18	0.16	0.39	-0.06	0.04	0.19	0.15	0.10	0.18	0.15	0.10	0.43
Delayed verbal recall	0.11	-0.01	0.01	-0.01	0.25	0.19	-0.25	-0.20	-0.21	0.25	-0.03	-0.01	-0.06	-0.19	0.22
Delayed visual recall	0.27	0.28	0.31	0.30	0.18	0.33	0.16	0.25	0.33	0.15	0.08	0.31	0.29	0.22	0.56
Verbal recognition	0.34	0.42	0.33	0.23	0.02	0.53	0.43	0.39	0.36	-0.06	0.27	0.44	0.31	0.13	-0.10
Visual recognition	0.24	0.16	0.25	0.24	0.40	0.25	0.12	0.25	0.30	0.19	0.14	0.06	0.09	0.00	0.25
FCSRT															
Immediate recall	0.20	0.15	0.06	0.04	0.06	0.07	-0.02	-0.20	-0.33	-0.01	0.02	0.09	-0.04	-0.15	0.72
Free recall	0.16	0.08	0.03	-0.04	0.06	0.26	-0.07	-0.14	-0.24	-0.10	-0.11	0.22	0.06	-0.20	0.45
Total recall	-0.06	0.14	0.01	-0.13	-0.03	0.10	0.15	-0.01	-0.23	-0.11	-0.09	0.19	0.02	-0.22	0.33
Delayed free recall	-0.10	0.24	0.11	0.00	0.10	0.00	0.12	-0.02	-0.14	0.01	-0.32	0.25	0.05	-0.19	0.47
Delayed total recall	-0.10	0.29	0.17	0.04	0.01	-0.02	0.25	0.09	-0.11	-0.05	-0.14	0.19	0.04	-0.15	0.33
Paired Associative Learning															
Learning level	0.50	0.34	0.08	0.38	0.43	-0.09	0.33	-0.03	0.37	0.45	-0.06	0.18	-0.06	0.25	0.35
Errors	0.15	-0.08	-0.25	0.11	0.48	-0.35	-0.09	-0.30	0.28	0.45	-0.29	-0.25	-0.38	0.04	-0.18

Table 4.17 *Age-partialled Pearson's r correlations between episodic memory and white matter microstructure in the aMCI group (n = 24) for precommissural and postcommissural fornices. Abbreviations: abFornix = anterior body of the fornix; aMCI = amnestic Mild Cognitive Impairment; AD = axial diffusivity; f = tissue volume fraction; FA = fractional anisotropy; FCSRT = Free and Cued Selective Reminding Test; MD = mean diffusivity; RD = radial diffusivity. None of the correlations passed false discovery rate analysis.*

Matched Control group (n = 20)

Episodic memory	abFornix					Precommissural Fornix					Postcommissural Fornix				
	FA	RD	MD	AD	*f*	FA	RD	MD	AD	*f*	FA	RD	MD	AD	*f*
Doors and People															
Immediate verbal recall	0.65	-0.16	-0.07	0.05	-0.02	0.38	-0.24	-0.14	-0.02	0.09	0.52	-0.17	-0.06	0.09	-0.12
Immediate visual recall	0.15	-0.50	-0.48	-0.44	0.40	-0.14	-0.38	-0.41	-0.41	0.24	0.59	-0.48	-0.34	-0.15	0.24
Delayed verbal recall	0.22	-0.03	0.00	0.03	0.01	0.15	-0.01	0.03	0.07	0.07	0.28	-0.16	-0.08	0.02	0.02
Delayed visual recall	-0.06	-0.38	-0.40	-0.41	0.45	-0.28	-0.28	-0.36	-0.40	0.17	0.36	-0.51	-0.43	-0.30	0.43
Verbal recognition	0.21	-0.34	-0.33	-0.30	0.23	-0.28	-0.12	-0.21	-0.28	0.03	0.04	-0.34	-0.37	-0.37	0.18
Visual recognition	0.27	-0.47	-0.43	-0.36	0.51	-0.32	-0.38	-0.46	-0.49	0.21	0.61	-0.40	-0.25	-0.06	0.31
FCSRT															
Immediate recall	0.01	-0.11	-0.12	-0.13	0.23	-0.40	0.01	-0.12	-0.22	-0.10	0.15	-0.26	-0.24	-0.19	0.18
Free recall	0.16	-0.35	-0.34	-0.32	0.49	0.02	-0.25	-0.26	-0.25	0.25	0.35	-0.42	-0.36	-0.27	0.27
Total recall	0.09	-0.27	-0.27	-0.26	0.22	0.10	-0.23	-0.21	-0.19	0.03	0.14	-0.43	-0.41	-0.36	0.29
Delayed free recall	0.18	-0.42	-0.41	-0.38	0.34	-0.12	-0.29	-0.33	-0.35	0.00	0.32	-0.55	-0.50	-0.41	0.29
Delayed total recall	0.15	-0.48	-0.48	-0.46	0.34	0.25	-0.45	-0.40	-0.33	0.24	0.22	-0.62	-0.59	-0.51	0.45
Paired Associative Learning															
Learning level	0.53	-0.52	-0.44	-0.33	0.31	-0.05	-0.48	-0.48	-0.44	0.07	0.43	-0.38	-0.29	-0.16	0.34
Errors	-0.08	-0.23	-0.25	-0.28	-0.05	-0.36	-0.06	-0.17	-0.25	-0.37	-0.10	-0.40	-0.44	-0.45	0.39

Table 4.18 *Zero order Pearson's r correlations between episodic memory and white matter microstructure in the Matched Control group (n = 20) for precommissural and postcommissural fornices. Abbreviations: abFornix = anterior body of the fornix; AD = axial diffusivity; f = tissue volume fraction; FA = fractional anisotropy; FCSRT = Free and Cued Selective Reminding Test; MD = mean diffusivity; RD = radial diffusivity. None of the correlations passed false discovery rate analysis.*

Matched Control group (n = 20)

Episodic memory	abFornix					Precommissural Fornix					Postcommissural Fornix				
	FA	RD	MD	AD	*f*	FA	RD	MD	AD	*f*	FA	RD	MD	AD	*f*
Doors and People															
Immediate verbal recall	0.64	0.07	0.20	0.34	-0.17	0.36	-0.06	0.05	0.16	0.00	0.47	0.09	0.23	0.36	-0.28
Immediate visual recall	0.06	-0.04	-0.01	0.02	0.21	-0.39	0.08	-0.02	-0.11	0.06	0.61	0.09	0.32	0.53	-0.06
Delayed verbal recall	0.18	0.27	0.31	0.34	-0.14	0.11	0.25	0.28	0.28	-0.03	0.20	0.14	0.22	0.29	-0.13
Delayed visual recall	-0.25	0.13	0.09	0.04	0.29	-0.56	0.19	0.04	-0.12	-0.04	0.22	-0.02	0.09	0.19	0.26
Verbal recognition	0.18	-0.25	-0.23	-0.20	0.15	-0.33	0.02	-0.09	-0.19	-0.05	-0.04	-0.24	-0.28	-0.29	0.10
Visual recognition	0.23	-0.30	-0.24	-0.16	0.42	-0.42	-0.21	-0.31	-0.38	0.11	0.57	-0.17	0.03	0.23	0.18
FCSRT															
Immediate recall	-0.06	0.23	0.22	0.18	0.08	-0.52	0.33	0.15	-0.03	-0.26	0.03	0.07	0.08	0.08	0.03
Free recall	0.09	0.02	0.03	0.03	0.36	-0.07	0.10	0.06	0.02	0.11	0.23	-0.03	0.03	0.09	0.09
Total recall	0.03	-0.02	-0.03	-0.03	0.08	0.05	0.00	0.00	0.00	-0.10	0.02	-0.22	-0.21	-0.17	0.17
Delayed free recall	0.12	-0.06	-0.05	-0.03	0.15	-0.26	0.07	-0.02	-0.11	-0.22	0.18	-0.23	-0.17	-0.10	0.10
Delayed total recall	0.04	0.06	0.06	0.07	0.08	0.25	-0.01	0.05	0.09	0.02	-0.02	-0.14	-0.14	-0.11	0.29
Paired Associative Learning															
Learning level	0.52	-0.51	-0.40	-0.26	0.26	-0.08	-0.45	-0.44	-0.40	0.01	0.40	-0.34	-0.21	-0.06	0.29
Errors	-0.09	-0.26	-0.29	-0.31	-0.07	-0.37	-0.05	-0.17	-0.26	-0.39	-0.11	-0.51	-0.54	-0.51	0.41

Table 4.19 *Age-partialled Pearson's r correlations between episodic memory and white matter microstructure in the Matched Control group (n = 20) for precommissural and postcommissural fornices. Abbreviations: abFornix = anterior body of the fornix; AD = axial diffusivity; f = tissue volume fraction; FA = fractional anisotropy; FCSRT = Free and Cued Selective Reminding Test; MD = mean diffusivity; RD = radial diffusivity. None of the correlations passed false discovery rate analysis.*

4.4 Discussion

The fornix is of considerable interest as it provides the principal route for projections from the hippocampal formation to the prefrontal cortex, ventral striatum, basal forebrain, hypothalamus, and thalamus, along with return inputs to the hippocampus from the hypothalamus, basal forebrain, and midbrain (Poletti and Creswell, 1977; Saunders and Aggleton, 2007; Swanson et al., 1987). These hippocampal connections differentially involve the precommissural fornix and postcommissural fornix (Figure 4.1), which may, therefore, support different cognitive functions given that anatomical tracing studies in animals show how individual hippocampal neurons rarely contribute axons to both the precommissural and postcommissural fornix (Donovan and Wyss, 1983; Naber and Witter, 1998).

The principal aim of the present study was to develop and evaluate a reliable anatomical protocol to reconstruct the two major subdivisions of the fornix, the precommissural and postcommissural tracts. In contrast to previous studies using probabilistic techniques (Chen et al., 2015; Yeo et al., 2013) this study employed deterministic tractography based on the dRL spherical deconvolution algorithm, whilst focusing the reconstructions on the precommissural and postcommissural columns and the body of the fornix to reduce partial volume between the two segments (Yeo et al., 2013). It was possible to reliably reconstruct the precommissural and postcommissural pathways, not only in healthy older adults but also in patients with aMCI, a patient population known to display significant degeneration in the fornix and connected regions (Metzler-Baddeley et al., 2012a; Oishi et al., 2012). Additional aims of the study were to investigate the effects of ageing and neurodegeneration on the microstructure of these two fornical divisions, following on from the findings by Chen et al. (2015) and Metzler-Baddeley et al. (2012a). The final aim of this study was to investigate

relationships between executive function and episodic memory and precommissural and postcommissural fornix microstructure.

4.4.1 Tractography of precommissural and postcommissural fornix subdivisions

The first step was to separate the precommissural fornix from the postcommissural fornix. This goal was achieved in all cases, even in those with presumed degenerative pathology (aMCI). The two fornix subdivisions were then compared with each other and with a more complete reconstruction of the anterior body of the fornix, the "abFornix". As noted, the abFornix was not simply the sum of the precommissural and postcommissural reconstructions as it would additionally include the hippocampal projections to the anterior thalamus, which were excluded from the postcommissural fornix reconstructions (Figure 4.1).

As can be seen from the 70% thresholded voxel visualisation in Figure 4.4, the present reconstructions show a clear separation between the precommissural and postcommissural fibres, not only after they have separated at the level of the anterior commissure, but also in the anterior body of the fornix. Whilst there was some overlap (as depicted by the three green voxels) the two segments were clearly separable. This tract separation was further supported by the low Dice coefficient between the two fornix divisions.

Despite clear evidence of a separation of fibres within the body of fornix (fibres for the precommissural fornix were located dorsally, while fibres for the postcommissural fornix were located ventrally, see Figures 4.3 and 4.4), little has been previously reported about the topography of fibres within the primate fornix. One study of macaque monkeys by Saunders and Aggleton (2007) found that fibres from the more

anterior hippocampus preferentially occupy the lateral fornix whereas posterior hippocampal fibres preferentially occupy the medial fornix. As neurons from the entire anterior-posterior length of the hippocampus contribute to the precommissural and postcommissural fornices (Aggleton, 2012; Aggleton et al., 2005b; Barbas and Blatt, 1995; Carmichael and Price, 1995; Friedman et al., 2002), there is the clear implication that hippocampal projections realign along the body of the fornix in the dorsal-ventral plane, prior to reaching the columns of the fornix. This same topographic separation may equally occur in those projections to the hippocampal formation via the fornix. For the precommissural fornix, return projections to the hippocampus predominantly arise from the septum (Saunders and Aggleton, 2007; Swanson et al., 1987). Consistent with the above prediction, it has been observed that the septal (precommissural) connections of the primate hippocampus are most dense in the medial portion of the fornix, immediately under the corpus callosum (Poletti and Creswell, 1977), i.e. in a dorsal location, consistent with this topography.

4.4.2 Microstructural properties of precommissural and postcommissural fornix subdivisions

In addition to investigating the topographical layout of the precommissural and postcommissural fornix, their microstructure was investigated using DTI-based indices of FA, MD, RD, AD and *f*.

In the Healthy Ageing Cohort, all five indices for the abFornix correlated with the corresponding index scores from both the precommissural and postcommissural pathways (Table 4.4). Similar patterns of correlations between abFornix and the two tract subdivisions were observed for the Matched Control and the aMCI groups, although some correlations were no longer significant when corrected for multiple

comparisons. This is may be due to the reduced sample size in these two groups (Table 4.6).

The consistent correlations in the Healthy Ageing Cohort between abFornix, precommissural fornix and postcommissural fornix were expected as the abFornix reconstructions consist of these two subdivisions, alongside anterior thalamic nuclei projections. Of more interest, therefore, was the finding that only the RD, MD and AD measures from the precommissural and postcommissural pathways correlated with each other whilst no significant correlations were observed for FA and *f* (Table 4.4). This suggests that overall diffusivity is more similar between these tracts than the partial volume within the voxels or the relative anisotropy. Similar correlations between abFornix, precommissural fornix and postcommissural fornix were found within the aMCI and Matched Control groups, except AD did not significantly correlate between the two subdivisions in the Matched Controls whereas FA also correlated between the two fornix subdivisions in the aMCI group.

As mentioned, significant positive correlations were observed between MD, AD and RD between the two tracts in the Healthy Ageing Cohort. Of these indices, MD measures the average diffusion in all directions, AD the diffusion along the principal axis, i.e. longitudinal diffusivity and RD the diffusion perpendicular to the principal axis. The positive correlations between the diffusivity indices suggest that diffusion properties in all directions were shared between the two fornical subdivisions. Diffusivity indices provide non-specific but sensitive markers of changes in diffusion due to the averaging of many possible variations in white matter properties, including changes in axonal myelin, membrane density and diameter, as well as fibre geometry and dispersion (Pierpaoli and Basser, 1996). Furthermore, although free water

correction was applied, it cannot be ruled out that some CSF based partial volume effects may remain and be shared by diffusivity indices from both subdivisions (Metzler-Baddeley et al., 2012b). Hence, the pattern of results suggests that the two tracts differ in microstructural properties of fibre tissue volume density and relative anisotropy but that more general diffusivity properties, for instance, due to atrophy based partial volume effects, may be shared. There is a clear need for future studies combining diffusion MRI and histology to validate the biological basis of these imaging markers and to investigate potential microstructural differences between the different fornix fibre populations.

The DTI-based indices from the present study can also be compared with those from the two earlier studies. Yeo et al. (2013) separated the precommissural and postcommissural fornix in young, healthy participants using probabilistic tractography. Despite using a younger population and a different tractography method, there was no statistical difference in FA estimates for the postcommissural fornix across the two studies (Yeo et al., 2013). In contrast, the precommissural FA estimates were significantly higher for the present study, presumably reflecting the different methods and different population groups.

4.4.3 Age-related effects on the microstructure of precommissural and postcommissural fornix subdivisions

Previous studies using diffusion MRI tractography have shown fornix fibres to be affected by both normal and pathological ageing. Fornix microstructure has been shown to correlate with age and to change in MCI and Alzheimer's disease (Metzler-Baddeley et al., 2011, 2012a; Oishi et al., 2012; Zhuang et al., 2012). However, these previous studies considered the fornix as a unitary structure whilst the present research explored

the effects of ageing and MCI on different fibre populations within the fornix (see also Cheng et al., 2015). For healthy older adults, positive correlations were found between age and MD, AD, and RD for the postcommissural fornix and abFornix, whilst no correlations were observed for FA and *f*. Similar trends were found for the precommissural fornix, but the correlations did not survive Bonferroni corrections. However, according to Fisher's r to z difference tests, there was no difference between the precommissural and postcommissural correlations with age. These results suggest that ageing has comparable effects on all fibres within the fornix.

In contrast, Chen et al. (2015) observed age-related changes in RD for the body of the fornix but not for the precommissural and postcommissural columns. This apparent dissociation may reflect differential sensitivities between the larger fibre populations in the body relative to the smaller and thinner fornix columns. Since the reconstructions in the present study included both columns and body it cannot be inferred whether the observed correlation between age and RD in the postcommissural fornix was primarily driven by fibres in the body or the columns.

The effects of age were comparable across both the precommissural and postcommissural fornices but the age-related changes were not found across all microstructural indices. Whilst ageing was associated with microstructural changes that affect the overall magnitude of diffusivity in various directions, no age-related effects were observed for FA and *f*. The lack of relationships between age and FA or *f* in the abFornix is in contrast to an earlier study, using the same participants, which did find such a relationship (Metzler-Baddeley et al., 2011). This discrepancy presumably arose from the differences in tract reconstruction, e.g. the abFornix reconstruction did not include fibres posterior to the crus. Another methodological difference concerns the

adoption of EPI-distortion corrections in the present analyses (Pierpaoli, 2011). Previous studies have reported systematic differences between tract reconstructions before and after EPI reconstruction (Andersson et al., 2004; Lee et al., 2004) with fibres appearing more symmetrical and more consistent with known anatomy after the correction. Thus, EPI correction may result in more precise tract reconstructions and, hence, enhanced sensitivity to RD and AD and reduced variation in FA. Indeed, it has been observed that diffusivity indices are more sensitive markers of age- and disease-related changes than FA (Acosta-Cabronero et al., 2010), and that FA and MD can be independent (Wieshmann et al., 1999).

4.4.4 aMCI related changes in microstructure of the precommissural and postcommissural fornix subdivisions

A clear disease-related dissociation between precommissural and postcommissural fornix fibres was not observed in this study. Although aMCI was associated with lower FA indices for the abFornix and there was a group by tract (precommissural and postcommissural fornix) interaction for this measure, no significant differences were present between patients and Matched Controls in the precommissural and postcommissural segmentations. These results suggest that aMCI is associated with pathological processes that affect both fibre populations, in which the postcommissural fornix (increase) and precommissural fornix (decrease) have FA alterations. That both fornix subdivisions are affected is consistent with evidence for hippocampal, basal forebrain and thalamic atrophy in this patient group (e.g. Aggleton et al., 2016; Grothe et al., 2010, 2012, 2013; Mufson et al., 2012).

The trends for lower FA in the abFornix and lower *f* across both precommissural and postcommissural tracts for aMCI patients compared to their Matched Controls were

consistent with previous reports of impaired fornix microstructure in aMCI and early Alzheimer's disease (Fletcher et al., 2013; Kantarci, 2014; Metzler-Baddeley et al., 2012a; Zhuang et al., 2012). Further studies are required to find out if there is a potential link between patterns of pathological change across the two fornix pathways with clinical profiles of symptomatology, rate of disease progression, and treatment response. One proposal would be to compare the status of the fornix tract divisions in pure amnestic MCI versus MCI patients with additional executive deficits (multi-domain MCI).

4.4.5 Correlations between microstructure in the three tracts and executive functioning and episodic memory

The final aim of this study was to investigate the relationship between the precommissural and postcommissural fornices and various cognitive functions. It was hypothesised that the precommissural fornix would show a stronger relationship with the executive functioning tasks, whereas the postcommissural fornix would show more of a relationship with the episodic memory tasks.

In terms of executive function, no relationships were found for abFornix, precommissural fornix or postcommissural fornix. Previous research has often found frontal executive/intellectual functioning (as measured by the WAIS-R III sub-scores, general arithmetic, trail making, verbal fluency and Wisconsin card sorting task, for example) to be relatively unimpaired following fornix transection (Hodges and Carpenter, 1991, damage to fornical columns; Poreh et al., 2006, lesions to the fornical columns; Vann et al., 2008, complete severance of left precommissural fornix with some right sparing, and postcommissural fornix damage with some partial bilateral sparing). In a diffusion MRI study, older adults without dementia (cognitively normal or

MCI) possessed a link between executive function/attention and FA measures of the posterior and anterior cingulum, but no such link to fornix FA (Kantarci et al., 2011).

However, Nestor et al. (2007) found correlations between fornix integrity and executive function in schizophrenic patients. Lee et al. (2012) also found a link between executive function and fornix FA in Alzheimer's disease. Although this same link was found with episodic memory, fornix FA was no longer a predictor of episodic memory once hippocampal volume was included in the multiple regression, while executive functioning remained a significant predictor. Another study found problem solving to be related to fornix FA and Alzheimer's disease, however, this relationship did not remain when age was entered into the regression analyses before DTI indices (Zahr et al., 2009). All in all, this research suggests that damage to the fornix alone (particularly the columns) is not sufficient to result in an executive functioning impairment. However, DTI indices, which represent the structural integrity of the entire tract and the neuronal network it connects, could prove more useful for investigating such relationships, particularly in diseased populations where such integrity breaks down (Lee et al., 2012; Nestor et al., 2007). This latter reason may be why such a dissociation was not found in this study, which looked at the prodromal phase of Alzheimer's (which can remain stable and be recovered from), and may prove to be more evident in fully developed Alzheimer's disease.

The present study did find a number of significant correlations between both precommissural fornix and postcommissural fornix and episodic memory; these included both recognition and recall tasks (Table 4.10). However, once age had been controlled for, none of these correlations remained significant. In the study by Metzler-Baddeley et al. (2011), which used the same cohort of participants as the present study,

fornix FA correlated with immediate free recall and total recall FCSRT measures, along with immediate visual recall from the Doors and People Test, but again, once age had been controlled for, none of the correlations remained significant. This suggests that these relationships were more strongly driven by age rather than demonstrating a specific role for these tracts in supporting mnemonic functions.

The lack of correlations between the fornix and episodic memory is surprising, given earlier studies. This may reflect the use of EPI-correction as well as truncating the fornix. Sample size may have contributed to the lack of a significant effect in the aMCI group. However, a previous study with the same groups of participants found that the Matched Control group exhibited a significant positive correlation between verbal free recall and tissue volume fraction for the fornix tract as a whole whilst such a correlation was absent in the aMCI group (Metzler-Baddeley et al., 2012a). Instead, recognition memory correlated with individual differences in tissue volume fraction of the parahippocampal cingulum in the aMCI but not the control group (Metzler-Baddeley et al., 2012a). Furthermore, the extent of this "shift" from the fornix to the parahippocampal cingulum was positively correlated with larger volumes of the basal forebrain and better memory performance in the patient group (Ray et al., 2015). Based on this pattern, it is possible that in the presence of a breakdown of fornix functionality in aMCI, other structures of the extended medial temporal and basal forebrain system may compensate for that loss. Thus, the lack of any significant correlations may be a result of already-reduced fornix functionality in aMCI.

A further consideration is that the postcommissural fornix reconstructions excluded the hippocampal projections to the anterior thalamic nuclei. It could be that this tract component plays the key role in episodic memory given the importance of the anterior

thalamic nuclei for memory (Harding et al., 2000; Tanaka et al., 2012; Van der Werf et al., 2003). This account does not, however, explain the lack of correlations with the abFornix as this tract reconstruction should include the projections to the anterior thalamic nuclei. Nevertheless, it would be useful in future studies to carry out postcommissural fornix reconstructions whereby hippocampal-anterior thalamic projections could be specifically assessed.

The separate reconstruction of precommissural and postcommissural fornix fibres will allow future research to investigate more closely the memory functions associated with these fibre segments. For instance, it could be the case that postcommissural fornix fibres are vital for encoding episodic memory whilst precommissural fibre connections with the prefrontal cortex and basal forebrain may play a more specific role in strategic aspects of encoding and retrieval. Therefore, a study could be performed directed at comparing this strategic element, for example a word list learning task where words can be categorised semantically thus allowing for strategy to aid encoding, versus a word list learning task where words are unrelated (Baxter and Chiba, 1999, Browning et al., 2005; Easton et al., 2012; Fletcher and Henson, 2001; Ray et al., 2015; Simons and Spiers, 2003).

4.4.6 Conclusions

Using deterministic tractography, it is possible to reconstruct the precommissural and postcommissural fornix in both healthy participants and those with aMCI. The fibres that form the precommissural and postcommissural fornices are also clearly distinguishable in the body of the fornix, i.e. before the tracts separate, showing there is a clear topography of projections within the fornix. While the fornix is affected in aMCI, the precommissural and postcommissural fornices do not appear to be

differentially affected by this disease. Episodic memory correlated with precommissural and postcommissural fornix measures only in the Healthy Ageing group, however only when age is not factored in, whereas executive functioning showed no relationship with or without the involvement of age. Future studies should examine these tracts and associated cognition in the fully developed Alzheimer's disease population, as it is likely that once aMCI has progressed to this stage the structural decline in these tracts will become more apparent, and it is possible that the postcommisural fornix will be more affected in those patients whose executive functioning remains relatively spared.

Chapter 5: Segregation and topography of the fornix based on its anterior and posterior hippocampal connections

5.1 Introduction

The fornix is often treated as a unitary structure even though it contains projections to distinct brain regions that could support different cognitive functions. The focus of Chapter 4 was to reconstruct the fornix by looking at precommissural and postcommissural components, i.e. separating the fornix on the basis of its target regions. An alternative approach is to reconstruct the fornix on the basis of where in the hippocampus the fornical fibres originate. Focusing on the anterior-posterior axis is the obvious first step given what is known about the fornix topography in the non-human primate (Saunders and Aggleton, 2007) and the growing evidence of functional differences along the longitudinal axis of the hippocampus (Collin et al., 2015; Colombo et al., 1998; Fanselow and Dong, 2010; Poppenk, 2013; Strange et al., 2014).

Despite the significance of the fornix for cognition, surprisingly little is understood about the organisation of the fibres within the human fornix. In macaque monkeys, the projections from the anterior hippocampus mainly occupy the lateral fornix, whereas the more medial fornix contains fibres from the posterior hippocampus (Saunders and Aggleton, 2007). A similar organisation exists in the rat, whereby fibres from the temporal hippocampus (equivalent to the primate anterior hippocampus) are located more laterally within the fornix, whereas fibres from the more septal hippocampus (equivalent to the posterior hippocampus) are found more medially (Swanson and Cowan, 1977; Wyss, et al., 1980). It is not yet known if the human fornix has a similar topography, even though such information could provide a useful means to compare the respective functions of anterior and posterior hippocampal networks (Aggleton, 2012; Strange, et al., 2014).

Numerous studies have investigated functional differences along the anterior-posterior

axis. In humans, the anterior hippocampus variously appears to be important for emotional and episodic memory, motivation and reward value, high level category representations, vestibular memory, navigation, way-finding, memory encoding, relational memory as measured by associative recognition, and pattern completion (Adcock et al., 2006; Dolcos et al., 2004; Furl et al., 2007; Giovanello et al, 2004; Hartley et al., 2003; Murty et al., 2010; Poppenk et al., 2013). In rodents, the anterior hippocampus (i.e. the ventral/temporal hippocampus) is more important for fear expression and anxiety, along with larger scale representations of space (Bannerman et al., 2002, 2004; Fanselow and Dong, 2010; Kjelstrup et al., 2002). On the other hand, the posterior hippocampus (dorsal/septal hippocampus in rodents) is thought to be more involved in spatial navigation, fine-grained visual memory, memory retrieval, and pattern separation (Maguire et al., 1998, 2000; Poppenk et al., 2013; Suthana et al., 2009). It has also been suggested that the posterior hippocampal two thirds exclusively support episodic memory (Greicius et al., 2003).

Consistent with these functional dissociations along the longitudinal axis, the anterior and posterior hippocampus are differentially connected to other brain regions. The anterior hippocampus (ventral/temporal hippocampus in rodents) preferentially projects to the amygdala, nucleus accumbens, and hypothalamus (apart from the mammillary bodies), as well as being indirectly connected with the ventral tegmental area (Catenoix et al., 2011; Kier et al., 2004; Poppenk et al., 2013; Smith et al., 2009). The primate anterior hippocampus also preferentially projects to the orbital and medial prefrontal cortex, and also shares reciprocal connections with the perirhinal cortex, some via the rostral medial band of the entorhinal cortex (Aggleton, 2012). The inputs to the anteromedial thalamic nucleus also preferentially arise from the anterior hippocampus (see Chapter 2). In rats, there are corresponding, preferential cortical connections

involving the anterior hippocampus with the medial frontal cortex, lateral entorhinal cortex, and perirhinal cortex (Dolorfo and Amaral, 1998; Fanselow and Dong, 2010; Jones and Witter, 2007; Libby et al., 2012; Schultz et al., 2012; Strange et al., 2014; Witter et al., 2000a, b). The direct hippocampal projections to the prefrontal cortex and nucleus accumbens pass through the fornix (Aggleton, 2012).

Meanwhile, the posterior hippocampus (dorsal/septal hippocampus in rodents), is preferentially connected with the posterior cingulate cortex (including retrosplenial cortex), the posterior parahippocampal cortex, and the caudal lateral band of the entorhinal cortex (the medial entorhinal cortex in rats) (Aggleton, 2012; Aggleton et al., 2012b; Strange et al., 2014). Other projections that predominantly arise from the posterior hippocampus include its dense inputs to the mammillary bodies (see Chapter 2). Of these connections, the projections to the mammillary bodies rely on the fornix.

These patterns of connectivity are consistent with the proposed functional distinctions, as the areas with which the anterior hippocampus predominantly connects are also more involved with motivational and emotional processes e.g. the amygdala, hypothalamus, nucleus accumbens, and orbital prefrontal cortex (Cardinal et al., 2002; Ikemoto and Panksepp, 1999; Kouneiher et al., 2009; Phelps and LeDoux, 2005; Rolls, 1990; Salamone, 1994; Sergerie et al., 2008), while the posterior hippocampus is linked with areas more involved in spatial memory processes e.g. retrosplenial cortex and mammillary bodies (Aggleton et al., 1995; Czajkowski et al., 2014; Vann and Aggleton, 2004; Vann et al., 2009a).

Given the nature of this study, the focus will be on areas connected to the anterior and posterior hippocampus by the fornix. Of these, the nucleus accumbens shows strong

involvement in decision making, reward probability, anticipation and prediction errors (Abler et al., 2006; Knutson et al., 2001; Matthews et al., 2004; Salamone et al., 2007), while the orbitomedial prefrontal cortex is thought to encode the valence of external rewards, as well as emotional stimuli (Shenhav et al., 2013; Winecoff et al., 2013). The orbitomedial prefrontal cortex may even play a role in moral value judgements (Hutcherson et al., 2015). Based on these connections, there may be a role in reward probability and the salience of stimuli for the anterior hippocampus and its fornical fibres. At the same time, the posterior hippocampus preferentially projects to the mammillary bodies and some of the anterior thalamic nuclei, via the fornix. The anterior thalamus and mammillary bodies are important for episodic memory in humans (Carlesimo et al., 2011; Tsivilis et al., 2008; Van der Werf et al., 2003) and spatial memory in rodents (Aggleton et al., 1996; Aggleton and Nelson, 2015; Vann and Aggleton, 2003, 2004). These diencephalic inputs suggest a more important role for context memory by the posterior hippocampus and its fornical connections.

Based on these differences in the longitudinal connectional topography of the hippocampus, this study aimed to evaluate whether there is a topography within the fornix when one divides the fornix according to its anterior hippocampal and posterior hippocampal connections. The present study, therefore, employed the dRL algorithm (Dell'Acqua, et al., 2010) for deterministic tractography on high angular resolution diffusion imaging data (HARDI) (Tuch, et al., 2002). The extent of overlap between the respective reconstructions for the anterior and posterior hippocampus was then determined quantitatively. In addition, a number of measures of white matter microstructure were derived for these two subpopulations of fornical fibres, namely, FA, RD (Basser, et al., 1994), MD, AD, and *f* (Pasternak, et al., 2009). Volumetric measurements were also acquired for the anterior and posterior hippocampi. These

measurements were then correlated with the diffusion metrics derived for the two fornix subdivisions.

5.2 Methods

The data used in this study formed part of a larger study carried out by Derek Jones, Karen Caeyenberghs, Sonya Foley and Claudia Metzler-Baddeley (derived works published in Caeyenberghs et al., 2016; Metzler-Baddeley et al., 2016). The diffusion and structural MRI scans used were part of the baseline assessment.

5.2.1 Participants

Forty-eight healthy volunteers were recruited from Cardiff University volunteer databases and from the local community via posters. Participants were eligible to take part if they had normal or corrected vision, no history of neurological or psychiatric illness, drug/alcohol abuse or MRI contraindications, and had a good command of English. Eight subjects were excluded from the present study due to dropping out of the study or being withdrawn. A total of 40 participants were included in the final participant dataset (mean age = 26.60; standard deviation = 6.46; 21 females, 1 left-handed).

5.2.2 Diffusion-weighted MRI and T1-weighted MRI scanning protocols

5.2.2.1 MRI acquisition

MRI data were acquired on a 3T General Electric HDx MRI system (GE Medical Systems, Milwaukee) using an eight channel receiver only head RF coil at the Cardiff University Brain Research Imaging Centre (CUBRIC). The MRI protocol was comprised of the following imaging sequences: a high resolution T_1 weighted anatomical scan (FSPGR) (256 x 256 acquisition matrix, TR = 7.8ms, TE = 2.9ms, flip

angle = 20, 172 slices, 1mm slice thickness, FOV = 23cm). Diffusion data were acquired employing a spin-echo echo-planar HARDI (Tuch et al., 2002) sequence with diffusion encoded along 60 isotropically distributed orientations alongside six non-diffusion weighted scans, according to an optimised gradient vector scheme (Jones et al., 1999) (96 x 96 acquisition matrix, TR/TE = 87ms, b-value = 1200s/mm2, 60 slices, 2.4mm slice thickness, spatial resolution 1.8 x 1.8 x 2.4mm). Data acquisition was peripherally gated to the cardiac cycle with a total acquisition time of ~30min depending on the heart rate.

5.2.2.2 MRI data processing

The diffusion-weighted HARDI data were corrected for distortions induced by the diffusion-weighted gradients, artefacts due to head motion and due to EPI-induced geometrical distortions by registering each image volume to the high-resolution T_1-weighted anatomical images (Irfanoglu et al., 2012), with appropriate reorientation of the encoding vectors (Leemans and Jones, 2009) in ExploreDTI (Version 4.8.3) (Leemans et al., 2009). A two compartment model using the Free Water Elimination (FWE) approach (Pasternak et al., 2009) was then fitted to derive maps of FA, RD, MD, and AD (Pierpaoli and Basser, 1996), together with a map of the *f* in each voxel (Metzler-Baddeley et al., 2012b).

5.2.2.3 Deterministic tractography

Whole brain tractography was performed for each participant in the participant's native space using the dRL algorithm (Dell'Acqua et al., 2010), which (in contrast to diffusion tensor MRI) allows the recovery of multiple fibre orientations within each voxel, including those affected by partial volume. The tracking algorithm estimated peaks in the fODF at the centre of each image voxel, and seed points that were positioned at the

vertices of a 2 x 2 x 2mm grid superimposed over the image. Up to four individual streamlines were then generated in 0.5mm steps along these axes, re-estimating the fODF peaks at each new location (Jeurissen, et al., 2011). Tracts were terminated if the fODF threshold fell below 0.05 or the direction of pathways changed through an angle greater than 45° between successive 0.5mm steps. This procedure was then repeated by tracking in the opposite direction from the initial seed-point. Streamlines outside a minimum of 10mm and maximum of 500mm length were discarded. At each 0.5mm step, local estimates of FA, RD, MD, AD, and *f* were acquired through interpolation of associated parameter maps. Mean scores were calculated for the various microstructure measures from the two hemispheres of each participant.

5.2.3 Reconstruction of anterior/posterior hippocampal fornices

Original reconstructions of the fornix were based on an anterior/posterior split of the hippocampus using each participant's T_1-weighted scan. ROIs were defined following Boolean logic by placing "SEED" (either/or), "AND" (inclusive) or "NOT" (exclusive) waypoint gates.

Anterior hippocampal fornix: For the segment of the fornix associated with the anterior portion of the hippocampus, a "SEED" ROI was placed around the body of the fornix, 6mm posterior to the anterior commissure, as defined by that participant's T_1-weighted scan (Figure 5.1Ai). An "AND" ROI was placed halfway along the length of the left hippocampus on the coronal plane as shown in Figure 5.1Bi. Consequently, the tract reconstructions reflected those signals that reach or extend anterior to this "AND" ROI. For consistency, the same coronal section provided the "AND" ROI for the two hemispheres. Microstructural indices (FA, RD, MD, AD, and *f*), were derived from both

hemispheres, which were then averaged to give a single overall mean value for each participant for each measure.

Posterior hippocampal fornix: For the posterior hippocampal fornix, the procedure was identical to that described above except that a "NOT" gate, instead of an "AND" ROI, was placed at the mid-hippocampal level (Figure 5.1Bii). This "NOT" gate should exclude those fibres continuing anteriorly to this point, i.e. only fibres reaching the posterior portion of the hippocampus were included. Microstructural indices were obtained by averaging across the two hemispheres for each participant.

For both the anterior and posterior hippocampal fornix fibre reconstructions, "NOT" ROIs were applied to exclude any extraneous fibres not consistent with known fornix anatomy. These "NOT" ROIs were placed as follows using the midline sagittal plane for reference: i, on the coronal slices immediately anterior to the genu of the corpus callosum and immediately posterior to the splenium of the corpus callosum; ii, on the axial slices at the level of the lower limit of the body of the corpus callosum and at the level of the upper limit of the pons; and iii, on the sagittal slices lateral to the fornix at the edge of the medial temporal lobe for each hemisphere.

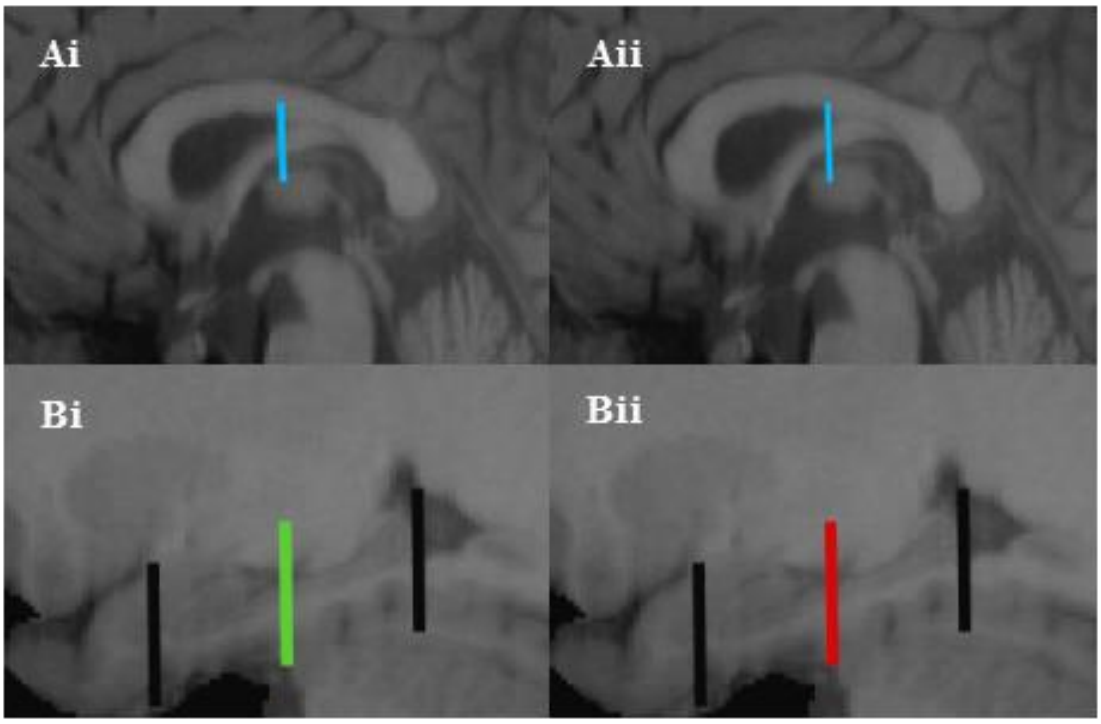

Figure 5.1 *Shared landmarks used for reconstructing the anterior (Ai, Bi) and posterior (Aii, Bii) hippocampal fornix. The same "SEED" gate is first placed around the body of the fornix (sagittal plane, blue bar Ai, ii). Midway between the head of the uncus and the tail of the hippocampus (both marked), a bar was placed as either an "AND" gate (Bi, green, anterior hippocampus) or a "NOT" gate (Bii, red, posterior hippocampus), using the lateral-most sagittal plane point where the uncus is still visible.*

To provide an initial overview of the findings, all of the FA diffusion maps, and subsequent anterior and posterior hippocampal fornix reconstructions (40 participants) were converted into nifti files and warped into the Montreal Neurological Institute (MNI) standard 2mm FA template for diffusion weighted scans using the same linear and non-linear warp methods outlined in the previous chapter. All nifti images were combined into one composite image across participants for each tract and the mean of this composite image was computed using FSL FMRIB software. In order to provide a visualisation of the overlap, all nifti images of each separate tract were merged then thresholded at 70% and binarised to show only voxels in which 70% of participants possessed either of the tracts in that location, and those in which overlap occurred (Figure 5.2).

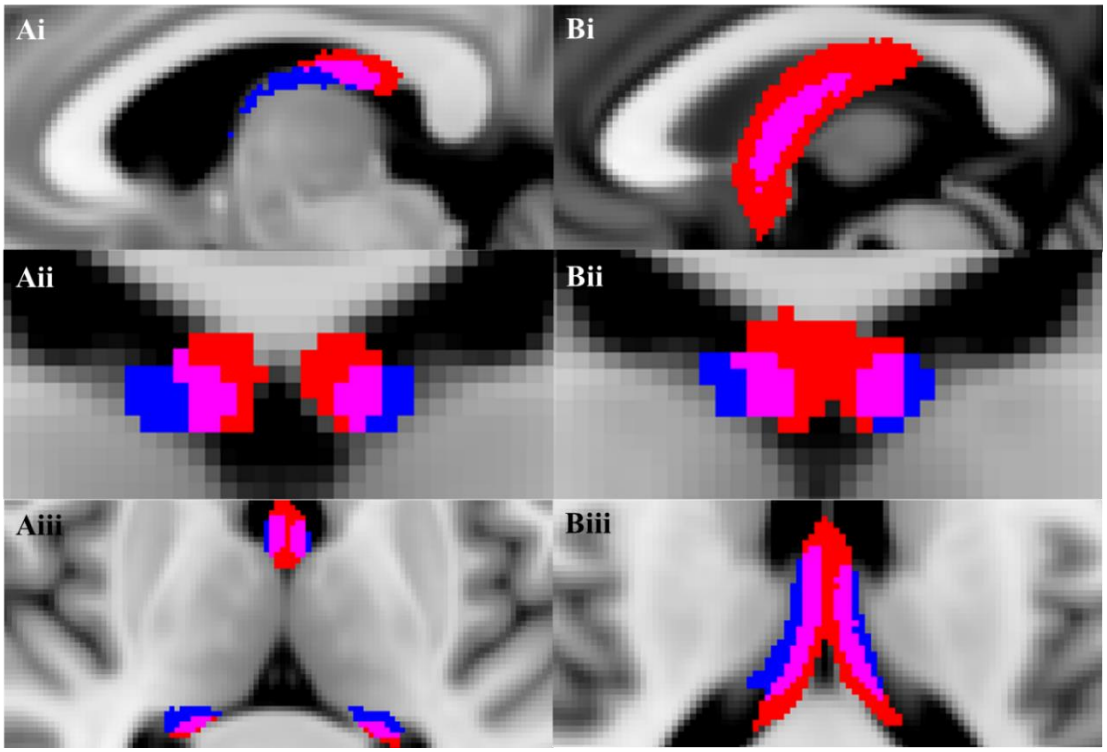

Figure 5.2 *Thresholded visualisation maps for anterior (blue) and posterior (red) hippocampal fornix, with overlap shown in pink, from a sagittal perspective (A/Bi), coronal perspective (A/Bii) and axial perspective (A/Biii). MNI co-ordinates (Ai-iii): X = 85; Y = 104; Z = 81 (Bi-iii): X = 89; Y = 108; Z = 89.*

5.2.4 Hippocampal volumes

Left and right hippocampal volumes were initially acquired for all participant's T_1 scans using FSL FIRST tools (Patenaude et al., 2011). These were then segmented into anterior and posterior portions by splitting the hippocampi along the posterior boundary of the uncus, defined on the mid-sagittal slice of each of the hippocampi in FSLView, and creating hand-drawn nifti masks of each segment for each hemisphere separately (Smith et al., 2004). The volume for these segments was then calculated with the fslstats command of the FSLUTILS package, which retrieves the total number of 1 x 1 x 1mm voxels in the structure (Smith et al., 2004). Hippocampal measurements were scaled according to a brain tissue volume estimate, normalised for subject head size, derived from SIENAX (Smith et al., 2001, 2002), part of FSL (Smith et al., 2004).

5.2.5 Statistical analyses

All statistical and graphical analyses employed SPSS v. 20 (IBM Corp, 2011). All microstructural and macrostructural data for each tract were inspected for outliers defined as values larger than three times the absolute z-score from the mean. Based on this criterion one value for anterior hippocampal fornix RD (n = 39), two values for posterior hippocampal fornix *f* (n = 38), one value for posterior hippocampal fornix MD (n = 39) and AD (n = 39), and one value for right anterior hippocampal volume (n = 39) were excluded from the analyses.

5.2.5.1 Assessment of overlap between fornix subdivisions

Quantitative assessments of overlap between the anterior and posterior hippocampal-derived fornices were also made (Dice, 1945). A Dice similarity coefficient was calculated for each individual using the following formula (where x is the Dice coefficient, A and B are two separate tract masks and C is the overlap between them): x = 2C/(A+B). Dice coefficients vary between 0 and 1, the higher the coefficient the greater the level of overlap between the samples. Dice coefficients were also inspected for outliers over three times the z-score from the mean in order to be removed, but none between anterior and posterior hippocampal fornix segments reached this criterion.

5.2.5.2 Relationship of microstructural indices from the two fornix subdivisions

Before comparing the microstructural indices for the anterior and posterior hippocampal reconstructions, the anterior hippocampal fornix streams were truncated at the posterior hippocampus, so that they began at the same coronal level as the posterior streams (Figure 5.3). This procedure excluded the additional part of the anterior hippocampal fornix (along the length of the hippocampus) that might otherwise confound the

comparisons by increasing the variance of the microstructural scores in the anterior hippocampal fornix fibres by having more voxels to extract the mean from.

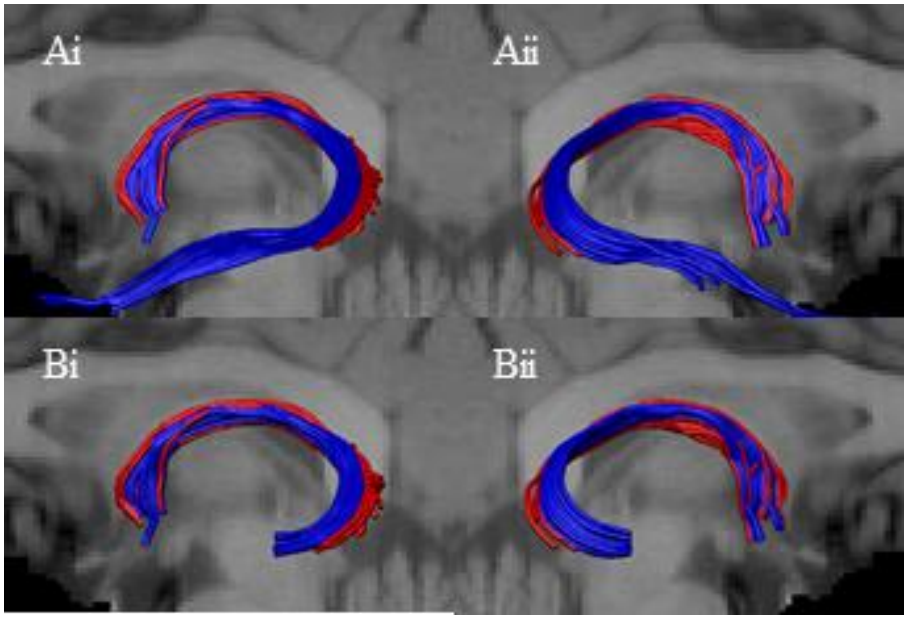

Figure 5.3. *A. Examples of fornix fibre streams for the anterior (blue) and posterior (red) hippocampus from a left sagittal (A/Bi) and right sagittal (A/Bii) view. B. Examples of the "truncated" anterior fornix fibre streams (blue) accompanied by the full posterior hippocampal streams (red). (Anterior hippocampal fornices were cut at the "AND"/ "NOT" gate levels depicted in Figure 5.1Ai, Aii).*

The microstructural indices (FA, RD, MD, AD, and *f*) for the anterior and the posterior hippocampal fornix subdivisions were separately compared using paired sample t-tests (two-tailed) and correlational analyses (Pearson's r correlations). For all analyses, a Bonferroni adjusted alpha level of 0.01 (i.e. 0.05 alpha level divided by five comparisons) helped to determine significance.

5.2.5.3 Relationships of microstructural indices from the two fornix subdivisions with anterior and posterior, left and right hippocampal volumes

Pearson's r bivariate correlations were used to assess the degree of collinearity between anterior and posterior hippocampal fornix measures and anterior and posterior portion volumes of the left and right hippocampi. This was performed for each fornical

subdivision separately, adopting a family-wise alpha level of (0.05/ (5 x 4)) 0.0025 to reach significance.

5.3 Results

5.3.1 Reconstructions

Both fornix subdivisions could be reconstructed in all 40 participants for both hemispheres. For all participants, the anterior hippocampal fibre streams occupied a lateral position within the body of the fornix, while the posterior hippocampal fibre streams were located in the medial portion of the fornix (Figures 5.3 and 5.4).

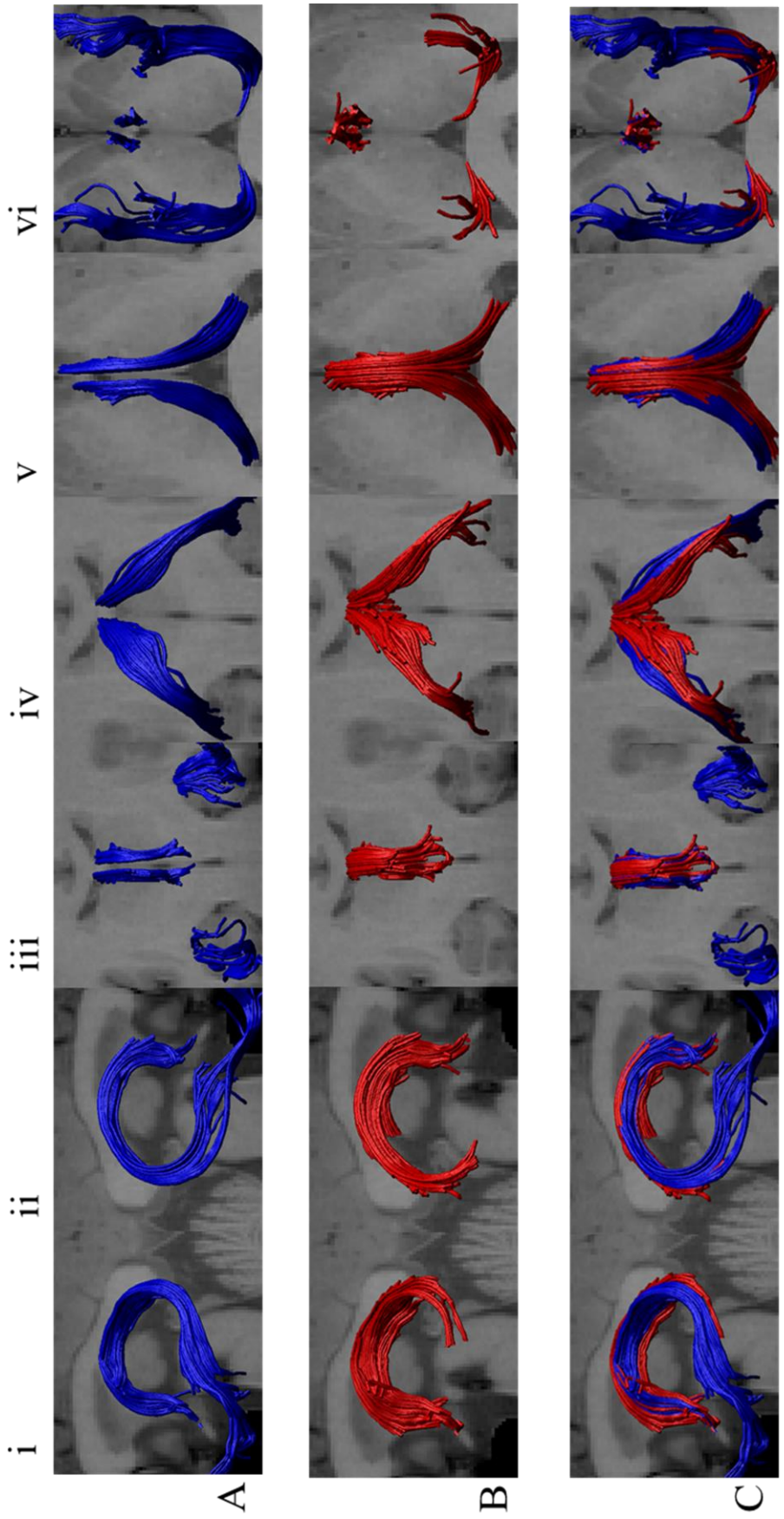

Figure 5.4 *The anterior (row A) and posterior (row B) hippocampal fornices, and both combined (row C) for one participant from the left sagittal (i); right sagittal (ii;) front coronal (iii); back coronal (iv); above axial (v); and below axial (vi) perspectives*

5.3.2 Dice coefficients and overlap

The median Dice coefficient for the anterior and posterior hippocampal fornix was 0.23 (lower quartile, 0.16; upper quartile, 0.30). Likewise, the mean Dice coefficient was similarly low (0.23; S.D. 0.09), again reflecting the low voxel overlap between the subdivisions (Cabezas, et al., 2011; Van Leemput, et al., 2009). Figure 5.5 reveals the interquartile range of Dice coefficients with outliers > 1.5 x this range removed.

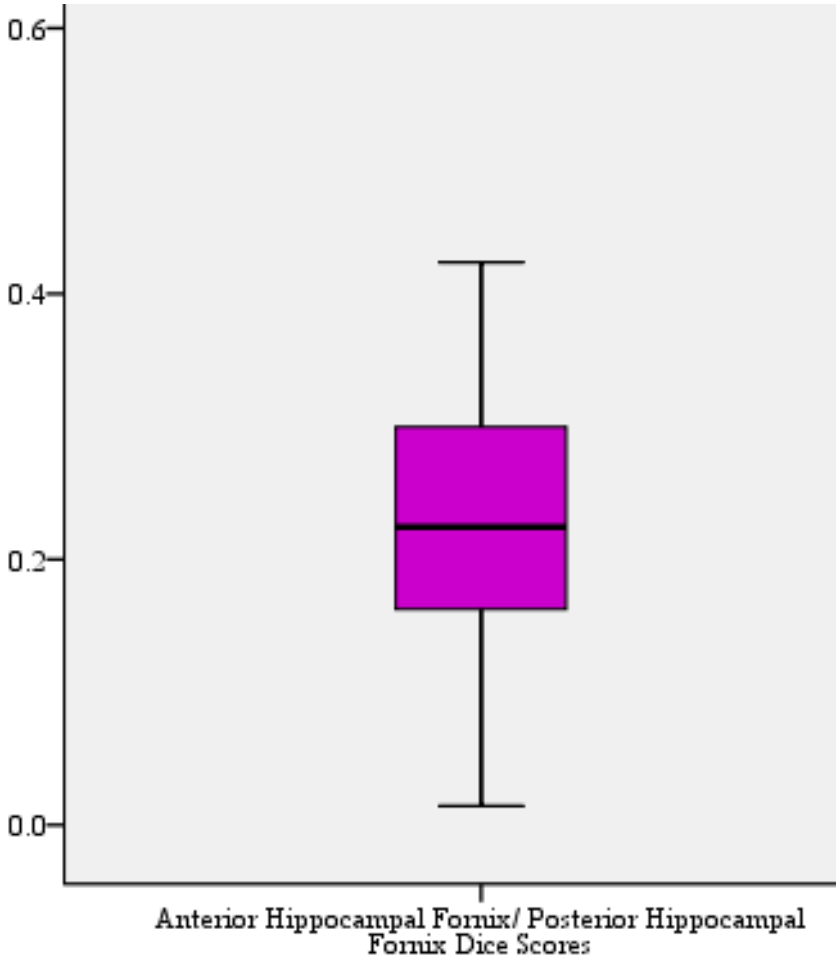

Figure 5.5 *Box and whisker plot graphs showing the median, interquartile range and minimum and maximum values for Dice coefficients between the anterior hippocampal fornix and posterior hippocampal fornix, and between the medial and lateral fornix, with outliers over 1.5 x the interquartile range removed.*

5.3.3 Correlations and t-tests between fornical subdivisions based on diffusion measures

Significant positive correlations (all $p < 0.01$ Bonferroni corrected) were found between the anterior and posterior hippocampal fornices for each of the five microstructural measures (Table 5.1). Despite these correlations, within-subject t-tests revealed differences for these same measures (all $p < 0.001$) between the anterior (truncated) hippocampal fornix and the posterior hippocampus (Table 5.2).

		Anterior (truncated) hippocampal fornix				
		FA	RD	MD	AD	*f*
Posterior hippocampal fornix	FA	**0.62**				
	RD		**0.75**			
	MD			**0.78**		
	AD				**0.70**	
	f					**0.68**

Table 5.1 *Correlations between anterior and posterior hippocampal fornix microstructural indices, for FA, RD, MD, AD, and f. All correlations were significant after Bonferroni correction (p < 0.001). Abbreviations: AD = axial diffusivity; f = tissue volume fraction; FA = fractional anisotropy; MD = medial diffusivity; RD = radial diffusivity. Those highlighted in bold reach Bonferroni-adjusted significance.*

	Anterior (truncated) hippocampal fornix	***Posterior hippocampal fornix***	***T-test p value***
FA (df 39)	0.37 (0.03)	0.38 (0.02)	**< 0.001**
RD (df 38)	0.86 (0.06) $x10^3$	0.91 (0.11) $x10^3$	**<0.001**
MD (df 38)	1.10 (0.08) x 10^3	1.20 (0.12) x 10^3	**<0.001**
AD (df 38)	1.58 (0.10) x 10^3	1.76 (0.15) x 10^3	**<0.001**
f (df 37)	0.70 (0.03)	0.66 (0.03)	**<0.001**

Table 5.2 *Means and (standard deviations) for anterior and posterior hippocampal fornices, and lateral and medial fornices, with paired samples t-test p values between the corresponding tracts. Abbreviations: AD = axial diffusivity; df = degrees of freedom; f = tissue volume fraction; FA = fractional anisotropy; MD = medial diffusivity; RD = radial diffusivity. Those highlighted in bold reach Bonferroni-adjusted significance.*

5.3.4 Correlations between fornical subdivision diffusion measures associated with the anterior and posterior hippocampus, with left and right hippocampal volumes

No significant correlations were found between either the anterior hippocampal fornix or the posterior hippocampal fornix with any of the hippocampal volume measures once the Bonferroni-adjusted alpha level was used (all $p > 0.0025$, Table 5.3). There were, however, trends (at uncorrected level) for negative relationships between RD, MD and AD for both fornix subdivisions and left anterior hippocampal volume, and a positive trend between posterior hippocampal *f* and left anterior hippocampal volume. There was also a trend towards a negative relationship between posterior hippocampal fornix FA and right anterior hippocampal volume (Table 5.3).

	Anterior (truncated) hippocampal fornix					***Posterior hippocampal fornix***				
	FA	RD	MD	AD	*f*	FA	RD	MD	AD	*f*
Left aHPC	0.19	-0.42	-0.38	-0.35	0.33	0.12	-0.21	-0.35	-0.35	0.33
Left pHPC	0.06	-0.06	-0.20	-0.20	-0.16	-0.04	-0.09	-0.11	-0.14	-0.01
Right aHPC	-0.08	-0.19	-0.17	-0.22	0.15	-0.35	0.05	-0.10	-0.21	-0.03
Right pHPC	0.17	0.16	0.10	0.18	-0.28	0.02	0.20	0.17	0.21	-0.16

Table 5.3 *Correlations between all fornix reconstruction diffusion measures and anterior and posterior hippocampal volumes for each hemisphere. Abbreviations: AD = axial diffusivity; aHPC = anterior hippocampal fornix; f = tissue volume fraction; FA = fractional anisotropy; MD = medial diffusivity; pHPC = posterior hippocampal fornix; RD = radial diffusivity. Those highlighted in bold reach Bonferroni-adjusted significance.*

5.4 Discussion

The fornix is the principal white matter tract associated with the hippocampal formation. However, despite its status, relatively little is known about the organisation of fibres within this tract in humans. In both non-human primates and rats, a topography exists along the medial-lateral axis of the fornix that relates to the long-axis of the hippocampus (Meibach and Siegel, 1977a; Saunders and Aggleton, 2007). To determine whether a similar topography exists in the human fornix, deterministic tractography was

used to reconstruct fornix fibres associated with either the anterior or posterior hippocampus. A clear distinction was found as fibres associated with the anterior hippocampus were located laterally within the body of the fornix whereas fibres associated with the posterior hippocampus were found medially. Thus, this study found the same topographical organisation as had been reported previously in non-human primates and rats (Meibach and Siegel, 1977a; Saunders and Aggleton, 2007). Formal analyses of the two fibre populations showed there to be little overlap between the pathways associated with the anterior and posterior hippocampus. It can be assumed that these two pathways not only reflect connections of the hippocampus proper (dentate gyrus, CA1-CA3), but also those of the subiculum, presubiculum, and parasubiculum (Chase, et al., 2015; Saunders and Aggleton, 2007).

Current diffusion-based MRI methods are unable to determine the direction of any particular connection, i.e. they cannot distinguish hippocampal efferents from afferents within the fornix. Nevertheless, it is most likely that the MRI signals principally reflected the topography of hippocampal efferents as the corresponding afferent fibres are far less numerous within the tract (Saunders and Aggleton, 2007). For this reason, it can be inferred that the more lateral fornix fibres preferentially innervate targets like the prefrontal cortex, nucleus accumbens, and the anteromedial thalamic nucleus, as in every instance the anterior hippocampus provides the most numerous inputs to these sites (Aggleton, et al., 2015; Barbas and Blatt, 1995; Chase, et al., 2015; Christiansen, et al., 2016b). In contrast, more posterior hippocampal projections in the fornix include the dense inputs to the mammillary bodies (Christiansen, et al., 2016b). It should, however, be emphasised that in the macaque brain these distinctions are relative, i.e. there is a gradient in the anterior-posterior inputs from the subiculum and CA1 rather than a sharp division between the anterior and posterior hippocampus (Aggleton, 2012; see also

Strange et al., 2014).

Studies with monkeys have also shown that some hippocampal afferents are organised topographically within the fornix (Saunders and Aggleton, 2007). Injections of a retrograde tracer directly into the fornix demonstrated how the basal forebrain projections to the hippocampus have a medial-lateral organisation within the tract. The most medial and more dorsal parts of the medial septum were found to project within the medial fornix (Saunders and Aggleton, 2007), possibly suggesting greater termination in the posterior hippocampus. Fibres located in the middle of the coronal plane of the fornix, i.e. in the intermediate part of the fornix, arose from more lateral cell populations in the medial septum and from the diagonal band of Broca. Interestingly, such a septal-hippocampal topography has been reported in both the rat and the cat, where the most medial part of the medial septum and the ventromedial part of the diagonal band innervate the septal hippocampus, i.e. the posterior hippocampus (Siegel, et al., 1974; Witter, 1986). In contrast, more lateral parts of the medial septum and the dorsomedial part of the diagonal band project upon the temporal (i.e. anterior) hippocampus.

5.4.1 Comparisons between microstructural indices of the anterior and posterior hippocampal fornix

Five white matter microstructural indices (FA, RD, MD, AD, and *f*) were acquired for the two fornix subpopulations. Perhaps unsurprisingly, given the close anatomical proximity of the two subpopulations, all microstructural measures significantly correlated across the two fornix reconstructions. However, clear differences arose when comparing absolute microstructural indices across the subpopulation of tracts, suggesting differences in the axonal organisation of the two subpopulations. Anterior

hippocampal/lateral fornix fibres exhibited significantly lower FA as well as RD, MD and AD but higher *f*, than posterior hippocampal/medial fornix fibres. The pattern of larger FA, RD, MD and AD measures suggests a more coherently aligned and more densely packed axon population in medial portions compared to lateral portions of the fornix. As can be seen in Figure 5.4, however, the anterior hippocampal/lateral fornix reconstructions contained a larger proportion of fanning out fibres as they passed across the anterior hippocampus, but the microstructural indices were not extracted from these. Anterior hippocampal/lateral fornix fibres, however, showed higher *f*, i.e. a higher fraction of the signal attributable to tissue after the free water correction, than posterior hippocampal/medial fibres.

5.4.2 Fornix anterior-posterior hippocampal topography and function

An implication of the tract reconstructions is that there are topographic distinctions within the medial-lateral dimension of the fornix that are likely to reflect corresponding differences of function along the long-axis of the hippocampus. Of the two areas, the anterior hippocampus has been more linked to stress, anxiety and emotional processing (Bannerman, et al., 1999; Chase, et al., 2015; O'Mara, 2005). Meanwhile, the posterior hippocampus is more typically linked to fine-grain spatial processing (Poppenk, et al., 2013; Strange, et al., 2014). One interpretation is that the anterior hippocampus is important for forming large-scale representations of the environment, whereas the posterior hippocampus provides more detailed representations (Poppenk, et al., 2013; Strange, et al., 2014). As a consequence, it has been proposed that relative differences along this axis include memory encoding, scene construction and imagining events (anterior hippocampus), along with memory retrieval and navigation (posterior hippocampus) (Poppenk, et al., 2013; Zeidman and Maguire, 2016). The current tractography protocol now allows future investigations to examine the relationships

between these different aspects of cognition, alongside the respective sets of white matter connections.

5.4.3 Other fornical topographies

The fornix can also be separated into precommissural and postcommissural fibres (Poletti and Creswell, 1977; see also Chapter 4). This distinction can also be captured using diffusion tractography, as shown in the previous chapter (Christiansen, et al., 2016a). The precommissural fornix contains hippocampal connections with the basal forebrain, ventral striatum, and prefrontal cortex, whereas the postcommissural fornix connections reach the medial thalamus and hypothalamus (Poletti and Creswell, 1977). Using diffusion imaging, the precommissural and postcommissural fibres were found to occupy different locations within the body of the fornix: the postcommissural fornix fibres were located dorsally whereas the precommissural fibres were located ventrally (Christiansen, et al., 2016a). Together with the present results, these findings suggest that there is a topography along the two planes of the fornix, i.e. within both the dorsal-ventral and medial-lateral axes of the tract, with both topographies reflecting different sets of hippocampal connections. Consequently, hippocampal efferents to prefrontal cortex should first predominantly occupy the lateral fornix and then the dorsal fornix, going anteriorly along the body of the fornix.

5.4.4 Correlations between microstructural indices of anterior and posterior hippocampal fornix and anterior and posterior hippocampal volumes

No significant correlations were found between either anterior hippocampal or posterior hippocampal fornix diffusion measures and hippocampal volumes. This is perhaps not surprising given there is likely to be limited variation in a young, healthy population. It would, therefore, be of interest to see if any correlations were found in an older

population. Another potential reason for the lack of correlations between volumetric and diffusion measures is that the fornix measures were combined across hemispheres; comparing measures within hemispheres might be a better approach.

5.4.5 Conclusions

The present study demonstrated a clear separation of human fornical fibres depending on whether they were associated with the anterior or posterior hippocampus. Fibres associated with the anterior hippocampus were located laterally within the body of the fornix whereas fibres associated with the posterior hippocampus were located medially. These findings pave the way for future work to determine whether these fornical subpopulations contribute to different cognitive functions and whether they are differentially affected by pathological conditions such as MCI and Alzheimer's disease, both known to be associated with microstructural changes in the fornix (Fletcher, et al., 2013; Sexton, et al., 2010; Chapter 4). The present findings offer a means to help determine whether there are differential rates of disruption in the white matter associated with the anterior and posterior hippocampus in these diseases.

Chapter 6: General Discussion

6.1 Summary and limitations

The extended hippocampal system has been repeatedly implicated in memory, however there is still very little known about how the structures within the extended hippocampal system support these cognitive functions. A better understanding of how these regions are connected is a critical first step in potentially understanding their function. Therefore, the principle aim of this thesis was to systematically investigate the connectivity within the extended hippocampal system across species. Where possible, the function of these different pathways was assessed. This was achieved using a variety of different methods across species, such as retrograde tracer injections and IEG imaging in the rodent, retrograde tracer injections in the primate, and diffusion and structural MRI techniques in humans. The following sections will discuss the findings and broader implications of the experimental chapters.

It is well-established that the subiculum projects to both the anterior thalamic nuclei and mammillary bodies (Figure 6.1) and it has been recently shown that these projections arise from different laminae within the subiculum (Aggleton et al., 1986; Ishizuka, 2001; Krayniak et al., 1979; Meibach and Siegel, 1975; Sikes et al., 1977; Wright et al., 2010). The aim of Chapter 2 was to extend these findings by looking at how these diencephalic projections are organised along the proximal-distal (columnar) and anterior-posterior axes of the subiculum. The pattern of projections from the subiculum is summarised in Figure 6.2. In brief, in the rat, the projections to the mammillary bodies mainly arise from the central subiculum at the septal pole of the hippocampus and from distal subiculum at the temporal pole of the hippocampus. The projections in the rat to the anterior thalamic nuclei are found in the septal and intermediate hippocampus and the anteromedial and anteroventral nuclei show complementary topographies: proximal subiculum projects to the anteromedial nucleus and distal

subiculum projects to the anteroventral nucleus. In the macaque, the diencephalic projections were dissociated along the anterior-posterior plane.

Given these different, parallel connections between the subiculum and the medial diencephalon, the question is whether these different pathways support different cognitive functions in the rat. When considering what roles these pathways may support it may be helpful to consider the inputs to the different parts of the subiculum. The proximal subiculum is preferentially associated with an object-based stream given its associations with the perirhinal cortex and lateral entorhinal cortex (Albasser et al., 2010; Brown and Xiang, 1998; Deshmukh and Knierim, 2011; Desimone, 1996; Murray and Richmond, 2001; Ringo, 1996; Wan et al., 1999; Wilson et al., 2013; Winters et al., 2008; Zhu et al., 1995a, b, 1996). The distal subiculum is preferentially associated with a spatial-based stream given its associations with medial entorhinal and postrhinal cortices. It might, therefore, be predicted that the hippocampal-anteromedial projections support object-based memory and the hippocampal-anteroventral projections support spatial memory. To investigate these potential dissociations, an IEG study was carried out comparing the relative involvement of the different subiculum regions for object recognition and a spatial working memory task (Chapter 3).

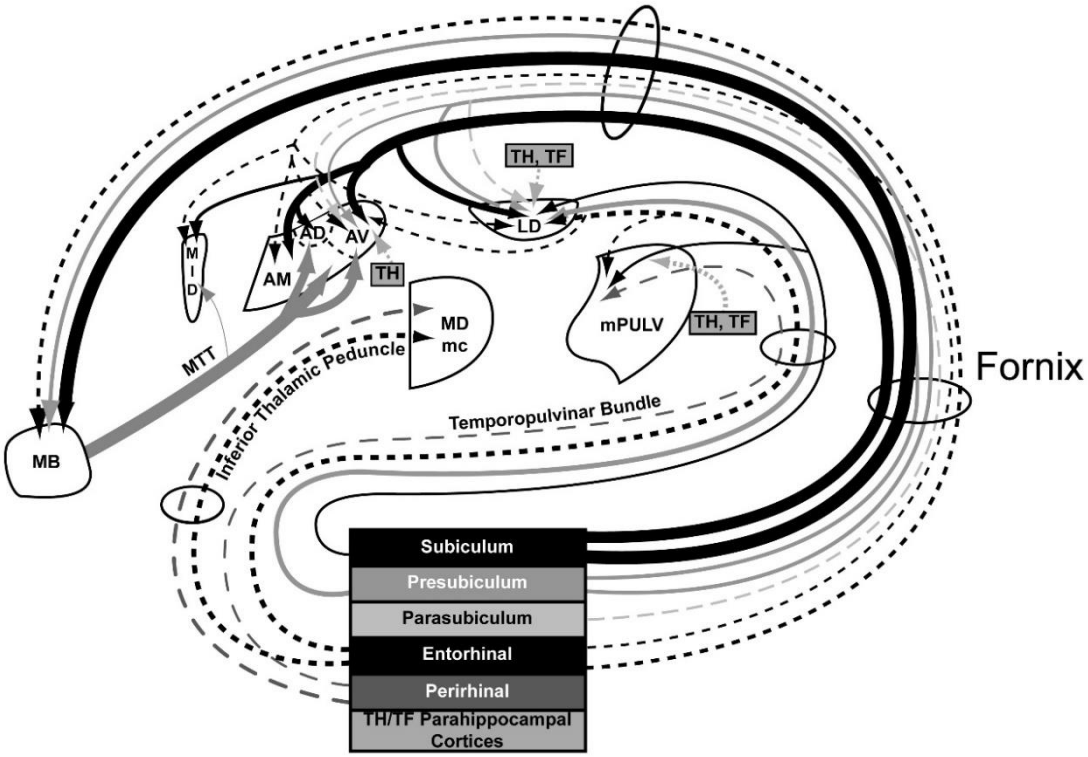

Figure 6.1 *Summary diagram showing the routes by which the hippocampus and parahippocampal region project to the thalamus. The thickness of the lines reflects the density of the projection while the ovals group together the connections within a particular tract. The figure includes previously published data concerning the efferents from the subiculum (Aggleton et al., 1986) and the parahippocampal region (Yeterian and Pandya, 1988). The perirhinal cortex has been separated into areas 35 and 36. Routes are not provided for the parahippocampal cortex as they have not yet been determined. Abbreviations: AD = anterior dorsal nucleus; AM = anteromedial nucleus; AV = anteroventral nucleus; LD = nucleus lateralis dorsalis; MB = mammillary bodies, MD = medial dorsal nucleus, including pars magnocellular (mc); mPULV = medial pulvinar nucleus; MTT = mammillothalamic tract; TF, TH = parahippocampal cortex. (From Aggleton, 2008).*

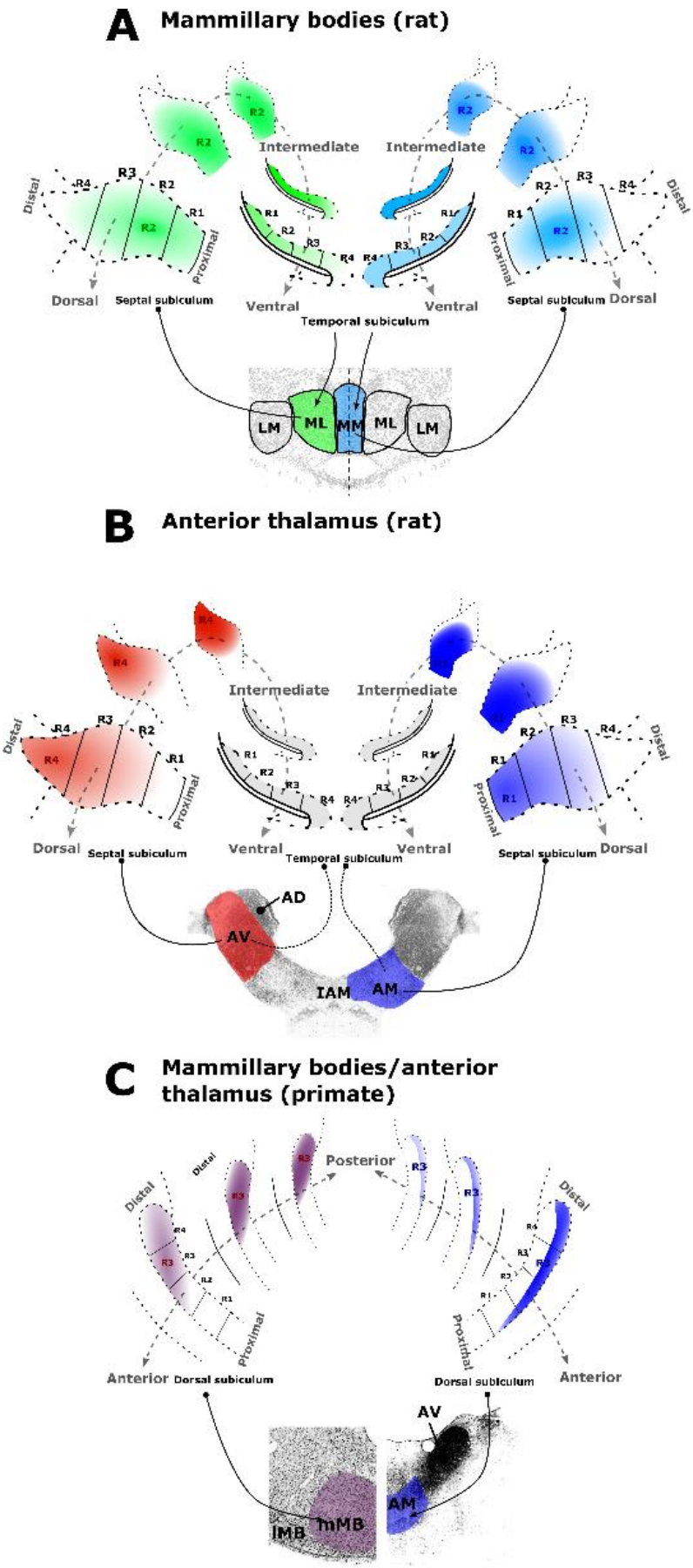

Figure 6.2
Schematic summaries of the topographic sources of the subicular inputs to the rat medial mammillary bodies (A), the rat anterior thalamic nuclei (B), and to the macaque (C) medial mammillary bodies (C left) and anteromedial thalamic nucleus (C right). Denser sources of subicular label correspond to denser colours. Abbreviations: AD = anterodorsal nucleus; AM = anteromedial nucleus; AV = anteroventral nucleus; IAM = interanteromedial nucleus; mMB = medial mammillary body; MM = medial mammillary nucleus of the medial mammillary body; ML = lateral mammillary nucleus of the medial mammillary body; LM/lMB = lateral mammillary body. Taken from Christiansen et al., 2016b; image courtesy of Chris Dillingham.

Expression of the IEG *zif268*, was compared across four groups: Spatial Memory, Object Memory, Behavioural Control, and Home-Cage Control groups. While there were no group differences using the raw Zif268-positive cells counts, when the data were normalised against total cell numbers (as estimated using NeuN), a difference did emerge; there were significantly greater levels of *zif268* expression in the most proximal part of the subiculum in the Object Memory group, compared to the Behavioural Control Group. This pattern is consistent with a greater involvement for the proximal subiculum for object-based memory. The present findings do not, however, show a clear-cut dissociation between object and spatial memory within the subiculum.

The results from Chapter 2 demonstrate the complementary, parallel pathways from the subiculum to the medial diencephalon, and the findings from Chapter 3 suggest that the projections from the proximal subiculum to the anteroventral anterior thalamic nucleus might contribute to aspects of object-based memory. Further studies are needed to determine whether these separate hippocampal-diencephalic pathways are *necessary* for memory and, if so, whether they support different processes. It would be technically very difficult to selectively lesion the proximal/distal subregions within the subiculum, however, there are a number of more recent techniques that would make it possible to selectively "turn on" and "turn off" the cells that project to the anteromedial thalamic nucleus, the anteroventral thalamic nucleus and the mammillary bodies. These include chemogenetic and optogenetic approaches (Deisseroth, 2011; Sternson and Roth, 2014). Combining these techniques with behavioural testing would enable one to test whether these pathways are required for different aspects of memory and whether they provide unique or redundant information.

The attempt to functionally dissociate the different subicular pathways in the present thesis did not provide clear-cut findings. This may be because the Zif268-positive counts may include cells in addition to those that project to the medial diencephalon. An alternative approach would be to combine retrograde tracing with IEG imaging. This would make it possible to look at behavioural-induced activity specifically across the different hippocampal-medial diencephalic pathways.

The first two experimental chapters investigated the extended-hippocampal system using animal models while the second two experimental chapters investigated hippocampal connections in humans using MRI. The focus of Chapters 4 and 5 was the fornix, the principle white matter tract associated with the hippocampus. The fornix has repeatedly been shown to be important for memory across different species (Aggleton and Brown, 2002; Aggleton et al., 1995, 2000; Gaffan, 1992, 1994; Gaffan and Harrison, 1989a; Gaffan et al., 2001; Hodges and Carpenter, 1991; McMackin et al., 1995; Metzler-Baddeley et al., 2011; Rudebeck et al., 2009; Vann et al., 2008) however it is typically treated as a unitary tract. In fact, the fornix carries fibres to and from quite distinct brain regions and to and from different parts of the hippocampus. It is, therefore, possible that the different fibres within the fornix support different functions.

In Chapter 4, deterministic tractography was used to reconstruct the precommissural and postcommissural subcomponents of the fornix. The precommissural fornix carries fibres to the prefrontal cortex and to and from the basal forebrain whereas the postcommissural fornix innervates the anterior thalamic nuclei, mammillary bodies and hypothalamus. The precommissural and postcommissural fibres were clearly separable even at the level of the body of the fornix: the precommissural fibres were located

dorsally and the postcommissural fibres were located ventrally. Given the different regions connected by the precommissural and postcommissural fornices, a further aim was to see whether they were associated with different cognitive functions. There were no clear dissociations between the precommissural and postcommissural fornix in terms of correlations with episodic memory measures. Furthermore, neither tract seemed to be differentially affected by age or a disease state (aMCI). As mentioned in Chapter 4, the cognitive measures used were part of a larger study and thus not specifically chosen to look at precommissural and postcommissural fornix function. As previous studies implicate the prefrontal cortex (precommissural) in strategic encoding of various information types and the mammillary bodies (postcommissural) in recollection (Lepage et al., 2000; Mian et al., 2014; Momennejad and Haynes, 2013; Tsivilis et al., 2008), a future study focusing on these two tracts could investigate strategic encoding abilities. This approach might help to dissociate the contributions of these two components of the fornix. It also would be wise, according to recent research, to consider gender differences when investigating structures involved in ageing and ageing-related disease (Martínez-Pinilla et al., 2016).

Diffusion tractography is a rapidly progressing field and there are continual advances in terms of data acquisition and processing. The study described in Chapter 4 made use of a diffusion data set acquired with 30 directions, however, more recent studies acquire HARDI data with a minimum of 45 directions to allow more precise intra-voxel estimates of fibre orientation distributions in areas of complex fibre orientation, e.g. crossing fibres (Tournier et al., 2007; Tournier et al., 2004; Tournier et al., 2013, Tuch et al., 2002). It would therefore be desirable to replicate the reported tractography findings in HARDI data acquired with more diffusion directions.

With regards to the interpretation of differences in the diffusion tensor based metrics of fractional anisotropy and mean, axial and radial diffusivity it is important to recognise that they are sensitive to differences in axon calibre and myelination, but also to fibre organisation and orientational complexity and, hence, are not specific to any one biological property of white matter (Beaulieu and Allen, 1994a, b; De Santis et al., 2014). Novel multi-compartment models of diffusion, such as the composite hindered and restricted model of diffusion (CHARMED) (Assaf and Basser, 2005) or the AxCaliber model (Assaf et al., 2008), may provide more specific indices of white matter properties such as axon diameter or density. In addition, more fibre specific indices have been developed such as hindrance modulated orientational anisotropy (HMOA), which may provide more unique information about the anisotropic properties of the fibres of interest (Dell'Acqua et al., 2013) and about the impact of disease on white matter tracts (Christiansen et al., 2016a; Froudist-Walsh et al., 2015). It is possible that these different methodologies might have produced clearer dissociations between the precommissural and postcommissural fornices than those observed in the current study.

The aim of Chapter 5 was also to look at the organisation of fibres within the fornix but with a focus on the longitudinal axis of the hippocampus. The primary goals of this experimental chapter were to reliably reconstruct fornical fibres arising from either the anterior portion of the hippocampus (up to the posterior limit of the uncus) or the posterior hippocampus (from the posterior limit of the uncus onwards, i.e. the "tail") in a healthy population. Related goals were to assess their topography and degree of overlap, and to compare their similarities in terms of white matter structural properties. These data were derived from the baseline assessments of a working memory training study in healthy young participants by Metzler-Baddeley et al. (2016).

The goals of this study were achieved using diffusion MRI tractography, as in Chapter 4. This time, however, the diffusion data consisted of 60 direction HARDI data and the participants were younger and, thus, should have minimal tract degeneration. A standardised protocol for extracting the different fornical subcomponents was created and the same diffusion measures as those in Chapter 4 were retrieved for comparisons between tracts.

The subsequent reconstructions demonstrated a very distinct topography, whereby anterior hippocampal fibres occupy the more lateral fornix while posterior hippocampal fibres occupy a more medial fornix location, albeit with some overlap in the intermediate medial-lateral area, which constituted roughly a third of the total fornix volume visually. This finding fits with research in monkeys, which shows there to be a medial, intermediate, and lateral division of the fornix (Saunders and Aggleton, 2007). The implication is that an additional study targeting mid-hippocampal levels might have revealed a concentration of fibres in the human intermediate fornix. This possibility is supported by the different connectional profiles with the subiculum and CA3 of the medial, intermediate and lateral fornix fibres (Saunders and Aggleton, 2007). Furthermore, this anterior/posterior hippocampal topography is different from that found when separating the fornical fibres according to the precommissural and postcommissural fornix columns as in Chapter 4, which found a dorsal and ventral topography for each tract respectively.

While the microstructural indices correlated, there were significant differences across the tracts for all measures, whereby the anterior hippocampal fornix exhibited lower FA, MD, RD and AD but had higher *f* than the posterior hippocampal fornix, thus making

these potentially useful measures to uncover differences in these tracts in diseased states such as MCI and Alzheimer's disease, or to explore differential effects of these tracts on different cognitive functions as suggested above. No relationships were found with hippocampal volumes, but this is likely due to the fact that the population was young and healthy, and so no detriments in hippocampal volume or fornix fibres would be expected, resulting in the absence of the necessary variation to detect such a relationship.

This study paves the way for future studies into potential functional dissociations of different fornical fibre networks. One potential limitation of the study in Chapter 5 is that the signal indices from the tracts from both hemispheres were combined. It might have been more informative to look at each tract separately for each hemisphere, especially given the functional and morphological differences that have been reported across the two hemispheres (Abrahams et al., 1997; Bohbot et al, 1998; Burgess et al., 2002; Maguire et al., 1997; de Toledo-Morrell et al., 2000; Shipton et al., 2014; Smith and Milner, 1981). It was decided to combine the data as although the anterior hippocampal fornix segments are lateralised, making it easy to separate by hemisphere, the posterior/medial fornix sits immediately by the midline. Consequently, it would be difficult to separate these signals due to the intermingling and crossing fibres in the body of the fornix (Saunders and Aggleton, 2007). In hindsight, it would have been better to use a different ROI placement to deal with this issue. Future studies should take into account these precommissural/postcommissural, left/right, and anterior/posterior hippocampal differences in fornix function, and see whether, for instance, the anterior hippocampal fornix fibres are associated with emotional memory and motivation, and the posterior hippocampal fornix fibres with spatial and episodic memory.

6.2 Broader implications

What is immediately apparent across the body of work in this thesis is the difference in anatomical resolution that can be achieved in animal studies compared to human studies. However, resolution for MRI and fMRI is constantly improving. For example, it is now possible to obtain measurements of the hippocampal subfields including the CA areas, the dentate gyrus, presubiculum and subiculum, using an automated protocol for structural MRI at 3T, which can be used to look at these structures in pathological ageing (Lee et al., 2012; Mueller et al., 2007; Van Leemput et al., 2009). This has also been achieved with functional MRI at 3 and 7T (Copara et al., 2014; Garrett et al., 2015; Suthana et al., 2009, 2015). It is therefore likely that in the future the proximal-distal axis of the subiculum may be investigated in the human brain *in vivo*. The functions of the anterior and posterior portions of the subiculum and CA areas could already certainly be investigated and compared with that found in monkeys, however, the resolution required for this was unfortunately beyond the scope of this thesis.

The resolution of diffusion MRI has scope for improvement, and while in the mouse brain it is possible to reach 0.125mm isotropic resolutions (Wu et al., 2013) this is not yet achievable in humans. This difference is due to the limitations of building the higher Tesla scanners needed (11.7T for the aforementioned resolution in mice), powerful gradient coils large enough for whole-brain studies, and obtaining clinically feasible scanning times on a 3T scanner. Higher resolutions can be achieved using post-mortem fixed tissue using 3T scanners, but with very lengthy scanning times (from ~6 to 37 hours for different techniques, McNab et al., 2009; Miller et al., 2011). Ideally research would look at the connections of the human hippocampal system down to the level of individual axons, which may never be achievable. Instead, it might be more appropriate

to focus on bundles of axons that are distinguished by their intricate and distinct intra-plane (i.e. laminar, transverse and longitudinal) topographies.

Another important implication to be drawn from Chapters 4 and 5 relates to work currently being done with the hope of curing/preventing Alzheimer's disease. As the fornix is a key white matter tract involved, a clinical trial has now been conducted looking at the safety and outcome of deep brain stimulation (DBS) of this structure (Laxton et al., 2010; Lozano et al., 2016). While glucose metabolism increased and there was some suggestion of cognitive improvement/slowing of decline in phase I of this primary outcome data (n = 6), an overall cognitive benefit was not found for the group as a whole in phase II (n = 42). However, some indication of clinical outcome and glucose metabolism benefit was found in participants over 65 years of age (n = 30).

In DBS studies focused on relieving the cognitive decline in Alzheimer's disease, it would be prudent to consider the detailed anatomy of the fornix underlying the various cognitive functions impaired, and thus the work outlined in this thesis could prove informative in such research. For instance, if a patient suffered more severely from spatial memory/retrieval deficits, the postcommissural fornix or posterior hippocampal fornix (ventral/medial in location) could be a better target site for electrode implantation, due to the connections with other structures which show higher involvement in these processes.

6.3 Concluding remarks

The experimental studies reported in this thesis have begun to highlight the complexity of the connections of the hippocampal formation. There are multiple, parallel pathways by which the hippocampus can communicate with the medial diencephalon. For this reason, previous functional models are presumably oversimplified. Likewise, it is clear that there are multiple, parallel pathways within the fornix and again treating the fornix as a unitary structure may be counterproductive when trying to understand what cognitive functions it supports. Together, the work in this thesis provides a useful framework for advancing our understanding of the functions of the extended hippocampal system.

References

Abler, B., Walter, H., Erk, S., Kammerer, H. & Spitzer, M. (2006). Prediction error as a linear function of reward probability is coded in human nucleus accumbens. *NeuroImage, 31,* pp 790-795.

Abrahams, S., Pickering, A., Polkey, C. E. & Morris, R. G. (1997). Spatial memory deficits in patients with unilateral damage to the right hippocampal formation. *Neuropsychologia, 35,* pp 11-24.

Acosta-Cabronero, J., Williams, G. B., Pengas, G. & Nestor, P. J. (2010). Absolute diffusivities define the landscape of white matter degeneration in Alzheimer's disease. *Brain, 133,* pp 529-539.

Adcock, R. A., Thangavel, A., Whitfield-Gabrieli, S., Knutson, B. & Gabrieli J. D. (2006). Reward-motivated learning: mesolimbic activation precedes memory formation. A critical role for the anterior hippocampus in relational memory: Evidence from an fMRI study comparing associative and item recognition. *Neuron, 50,* pp 507–517.

Aggleton, J. P. & Brown, M. W. (1999). Episodic memory, amnesia, and the hippocampal-anterior thalamic axis. *The Behavioral and Brain Sciences, 22,* pp 425-444.

Aggleton, J. P. & Brown, M. W. (2002). Integrating systems for event memory: testing the contribution of the fornix. In Squire, L. R. & Schacter, D. (Eds.), *Neuropsychology of Memory* (3rd edition) (pp 377-394). New York, US: Guilford.

Aggleton, J. P. & Christiansen, K. (2015). The subiculum: the heart of the extended hippocampal system. *Progress in Brain Research, 219,* pp 65-82.

Aggleton, J. P. & Mishkin, M. (1985). Mamillary-body lesions and visual recognition in monkeys. *Experimental Brain Research, 58,* pp 190-197.

Aggleton, J. P. & Nelson, A. (2015). Why do lesions in the anterior thalamic nuclei cause such severe spatial deficits? *Neuroscience and Biobehavioural Reviews, 54,* pp 131-144.

Aggleton, J. P. & Sahgal, A. (1993). The contribution of the anterior thalamic nuclei to anterograde amnesia. *Neuropsychologia, 31,* pp 1001-1019.

Aggleton, J. P. (1985). X-ray localization of limbic structures in the cynomolgus monkey (Macaca fascicularis). *Journal of Neuroscience Methods, 14,* pp 101-108.

Aggleton, J. P. (1986). A description of the amygdalo-hippocampal interconnections in the macaque monkey. *Experimental Brain Research, 64,* pp 515-526.

Aggleton, J. P. (2008). Understanding anterograde amnesia: disconnections and hidden lesions. *The Quarterly Journal of Experimental Psychology, 61,* pp 1441-1471.

Aggleton, J. P. (2012). Multiple anatomical systems embedded within the primate medial temporal lobe: implications for hippocampal function. *Neuroscience and Biobehavioural Reviews, 36,* pp 1579-1596.

Aggleton, J. P. (2013). Looking back: understanding amnesia – Is it time to forget HM? *The Psychologist, 26,* pp 612-615.

Aggleton, J. P., Brown, M. W. & Albasser, M. M. (2012a). Contrasting brain activity patterns for item recognition memory and associative recognition memory: insights from immediate-early gene functional imaging. *Neuropsychologia, 50,* pp 3141-3155.

Aggleton, J. P., Desimone, R. & Mishkin, M. (1986). The origin, course, and terminaion of the hippocampothalamic projections in the macaque. *The Journal of Comparative Neurology, 243,* pp 409-421.

Aggleton, J. P., Friedman, D. P. & Mishkin, M. (1987). A comparison between the connections of the amygdala and hippocampus with the basal forebrain in the macaque. *Experimental Brain Research, 67,* pp 556-568.

Aggleton, J. P., Hunt, P. R. & Shaw, C. (1990). The effects of mammillary body and combined amygdalar-fornix lesions on tests of delayed non-matching-to-sample in the rat. *Behavioural Brain Research, 40,* pp 145-157.

Aggleton, J. P., Hunt, P. R., Nagle, S. & Neave, N. (1996). The effects of selective lesions within the anterior thalamic nuclei on spatial memory in the rat. *Behavioural Brain Research, 81*, pp 189-198.

Aggleton, J. P., Keith, A. B., Rawlins, J. N., Hunt, P. R. & Sahgal, A. (1992). Removal of the hippocampus and transection of the fornix produce comparable deficits on delayed non-matching to position by rats. *Behavioural Brain Research, 52,* pp 61-71.

Aggleton, J. P., McMackin, D., Carpenter, K., Hornak, J., Kapur, N., Halpin, S., Wiles, C. M., Kamel, H., Brennan, P., Carton, S., & Gaffan, D. (2000). Differential cognitive effects of colloid cysts in the third ventricle that spare or compromise the fornix. *Brain, 123,* pp 800-815.

Aggleton, J. P., Neave, N., Nagle, S. & Hunt, P. R. (1995). A comparison of the effects of anterior thalamic, mammillary body, and fornix lesions on reinforced spatial alternation. *Behavioural Brain Research, 68,* pp 91-101.

Aggleton, J. P., O'Mara, S. M., Vann, S. D., Wright, N. F., Tsanov, M. & Erichsen, J. T. (2010). Hippocampal-anterior thalamic pathways for memory: uncovering a network of direct and indirect actions. *The European Journal of Neuroscience, 31*, pp 2292-2307.

Aggleton, J. P., Pralus, A., Nelson, A. J. D. & Hornberger, M. (2016). Thalamic pathology and memory loss in early Alzheimer's disease: moving the focus from the medial temporal lobe to Papez circuit. *Brain, 139,* pp 1877-1890.

Aggleton, J. P., Saunders, R. C., Wright, N. F. & Vann, S. D. (2014). The origin of projections from the posterior cingulate and retrosplenial cortices to the anterior, medial dorsal and laterodorsal thalamic nuclei of macaque monkeys. *The European Journal of Neuroscience, 39,* pp 107-123.

Aggleton, J. P., Vann, S. D., Denby, C., Dix, S., Mayes, A. R., Roberts, N. & Yonelinas, A. P. (2005a). Sparing of the familiarity component of recognition memory in a patient with hippocampal pathology. *Neuropsychologia, 43,* pp 1810-1823.

Aggleton, J. P., Vann, S. D. & Saunders, R. C. (2005b). Projections from the hippocampal region to the mammillary bodies in macaque monkeys. *The European Journal of Neuroscience, 22,* pp 2519-2530.

Aggleton, J. P., Wright, N. F., Rosene, D. L. & Saunders, R. C. (2015). Complementary patterns of direct amygdala and hippocampal projections to the macaque prefrontal cortex. *Cerebral Cortex, 25,* pp 4351-4373.

Aggleton, J. P., Wright, N. F., Vann, S. D. & Saunders, R. C. (2012b). Medial temporal lobe projections to the retrosplenial cortex of the macaque monkey. *Hippocampus, 22,* pp 1883-1900.

Agster, K. L. & Burwell, R. D. (2013). Hippocampal and subicular efferents and afferents of the perirhinal, postrhinal, and entorhinal cortices of the rat. *Behavioural Brain Research, 254,* pp 50-64.

Agster, K. L., Fortin, N. J. & Eichenbaum, H. B. (2002). The hippocampus and disambiguation of overlapping sequences. *The Journal of Neuroscience, 22,* pp 5760-5768.

Ahn, J.-R. & Lee, I. (2015). Neural correlates of object associated choice behavior in the perirhinal cortex of rats. *The Journal of Neuroscience, 35,* pp 1692-1705.

Aizenstein, H. J. & Klunk, W. E. (2015). Where is hippocampal activity in the cascade of Alzheimer's disease biomarkers? *Brain, 138,* pp 831-833.

Akintunde, A. & Buxton, D. F. (1992). Origins and collateralization of corticospinal, corticopontine, corticorubral and corticostriatal tracts: a multiple retrograde fluorescent tracing study. *Brain Research, 586,* pp 208-218.

Albasser, M. M., Amin, E., Lin, T. C., Iordanova, M. D. & Aggleton, J. P. (2012). Evidence that the rat hippocampus has contrasting roles in object recognition memory and object recency memory. *Behavioral Neuroscience, 126,* pp 659-669.

Albasser, M. M., Poirier, G. L. & Aggleton, J. P. (2010). Qualitatively different modes of perirhinal-hippocampal engagement when rats explore novel vs. familiar objects as revealed by c-Fos imaging. *The European Journal of Neuroscience, 31,* pp 134-147.

Albasser, M. M., Poirier, G., Warburton, E. C. & Aggleton, J. P. (2007). Hippocampal lesions halve immediate–early gene protein counts in retrosplenial cortex: distal dysfunctions in a spatial memory system. *The European Journal of Neuroscience, 26,* pp 1254-1266.

Albert, M. S., DeKosky, S. T., Dickson, D., Dubios, B., Feldman, H. H., Fox, N. C., Gamst, A., Holtzman, D. M., Jagust, W. J., Petersen, R. C., Snyder, P. J., Carillo, M. C., Thies, B. & Phelps, C. H. (2011). The diagnosis of mild cognitive impairment due to Alzheimer's disease: recommendations from the National Institute on Aging-Alzheimer's Association workgroups on diagnostic guidelines for Alzheimer's disease. *Alzheimer's & Dementia, 7*, pp 270-279.

Albo, Z., Viana Di Prisco, G. & Vertes, R. P. (2003). Anterior thalamic unit discharge profiles and coherence with hippocampal theta rhythm. *Thalamus & Related Systems, 2*, pp 133-144.

Allen, G. V. & Hopkins, D. A. (1988). Mamillary body in the rat: a cytoarchitectonic, Golgi, and ultrastructural analysis. *The Journal of Comparative Neurology, 275*, pp 39-64.

Alvarado, M. C. & Bachevalier, J. (2000). Revisiting the maturation of medial temporal lobe memory functions in primates. *Learning & Memory, 7*, pp 244-256.

Alvarez, P., Zola-Morgan, S. & Squire, L. R. (1995). Damage limited to the hippocampal region produces long-lasting memory impairment in monkeys. *The Journal of Neuroscience, 15*, pp 3796-3807.

Amaral, D. G. & Cowan, W. M. (1980). Subcortical afferents to the hippocampal formation in the monkey. *The Journal of Comparative Neurology, 189*, pp 573-591.

Amaral, D. G., Dolorfo, C. & Alvarez-Royo, P. (1991). Organization of CAl projections to the subiculum: a PHA-L analysis in the rat. *Hippocampus, 1,* pp 415-436.

Amin, E., Pearce, J. M., Brown, M. W., & Aggleton, J. P. (2006). Novel temporal configurations of stimuli produce discrete changes in immediate-early gene expression in the rat hippocampus. *The European Journal of Neuroscience, 24,* pp 2611-2621.

Anderson, M. & O'Mara, S. M. (2004). Activity of subicular units on a spatial and non-spatial version of an open-field object exploration task. *Experimental Brain Research, 159,* pp 519-529.

Anderson, M. I. & O'Mara, S. M. (2003). Analysis of recordings of single-unit firing and population activity in the dorsal subiculum of unrestrained, freely moving rats. *Journal of Neurophysiology, 90,* pp 655-665.

Andersson, J. L. R., Jenkinson, M. & Smith, S. (2010). Non-linear registration, aka spatial normalisation. *FMRIB technical report TR07JA2.*

Andersson, J. L., Richter, M., Richter, W., Skare, S., Nunes, R. G., Robson, M. D., Behrens, T. E. (2004). Effects of susceptibility distortions on tractography. *Proceedings of the International Society for Magnetic Resonance in Medicine, 11,* p 87.

Assaf, Y. & Basser, P. J. (2005). Composite hindered and restricted model of diffusion (CHARMED) MR imaging of the human brain. *NeuroImage, 27,* pp 48-58.

Assaf, Y., Blumenfeld-Katzir, T., Yovel, Y. & Basser, P. J. (2008). AxCaliber: a method for measuring axon diameter distribution from diffusion MRI. *Magnetic Resonance in Medicine, 59,* pp 1347-1354.

Astur, R. S., Taylor, L. B., Mamelak, A. N., Philpott, L. & Sutherland, R. J. (2002). Humans with hippocampus damage display severe spatial memory impairments in a virtual Morris water task. *Behavioural Brain Research, 132,* pp 77-84.

Auger, S. D., Mullally, S. L. & Maguire, E. A. (2012). Retrosplenial cortex codes for permanent landmarks. *Public Library of Science One, 7,* doi:10.1371/journal.pone.0043620.

Bachevalier, J., Parkinson, J. K. & Mishkin, M. (1985a). Visual recognition in monkeys: effects of separate vs. combined transection of fornix and amygdalofugal pathways. *Experimental Brain Research, 57,* pp 554-561.

Bachevalier, J., Saunders, R. C. & Mishkin, M. (1985b). Visual recognition in monkeys: effects of transection of fornix. *Experimental Brain Research, 57,* pp 547-553.

Baddeley, A. D. (1996). Exploring the central executive. *Quarterly Journal of Experimental Psychology, 49A,* pp 5-28.

Baddeley, A. D., Emslie, H. & Nimmo-Smith, I. (1994). *Doors and People test.* Bury St Edmunds, UK: Thames Valley Test Company.

Bannerman, D. M., Deacon, R. M, Offen, S, Friswell, J., Grubb, M & Rawlins, J. N. (2002). Double dissociation of function within the hippocampus: spatial memory and hyponeophagia. *Behavioral Neuroscience, 111,* pp 884-901.

Bannerman, D. M., Rawlins, J. N., McHugh, S. B., Deacon, R. M., Yee, B. K., Bast, T., Zhang, W. N., Pothuizen, H. H. & Feldon, J. (2004). Regional dissociations within the hippocampus--memory and anxiety. *Neuroscience and Biobehavioral Reviews, 28,* pp 273-283.

Bannerman, D. M., Yee, B. K., Good, M. A., Heupel, M. J., Iversen, S. D. & Rawlins, J. N. (1999). Double dissociation of function within the hippocampus: a comparison of dorsal, ventral, and complete hippocampal cytotoxic lesions. *Behavioral Neuroscience, 113,* pp 1170-1188.

Barbas, H. & Blatt, G.J. (1995). Topographically specific hippocampal projections target functionally distinct prefrontal areas in the rhesus monkey. *Hippocampus, 5*, pp 511–533.

Barbizet, J. (1963). Defect of memorizing of hippocampal-mammillary origin: a review. *Journal of Neurology, Neurosurgery, and Psychiatry, 26,* pp 127-135.

Barry, D. N. & Commins, S. (2011). Imaging spatial learning in the brain using immediate early genes: insights, opportunities and limitations. *Reviews in the Neurosciences, 22,* pp 131-142.

Barry, D. N., Coogan, A. N., & Commins, S. (2015). The time course of systems consolidation of spatial memory from recent to remote retention: a comparison of the Immediate Early Genes Zif268, c-Fos and Arc. *Neurobiology of Learning Memory, 128,* pp 46-55.

Basser, P.J. (1995). Inferring microstructural features and the physiological state of tissues from diffusion-weighted images. *NMR in Biomedicine, 8,* pp 333–344.

Basser, P. J., Mattiello, J. & LeBihan, D. (1994). MR diffusion tensor spectroscopy and imaging. *Biophysical Journal, 66,* pp 259-267.

Bast, T. (2007). Toward an integrated perspective on hippocampal function: from a rapid encoding of experience to adaptive behaviour. *Reviews in the Neurosciences, 18,* pp 253-281.

Baxter, M. G. & Chiba, A. A. (1999). Cognitive functions of the basal forebrain. *Current Opinion in Neurobiology, 9,* pp 178-183.

Beason-Held, L. L., Rosene, D. L., Killiany, R. J. & Moss, M. B. (1999). Hippocampal formation lesions produce memory impairment in the rhesus monkey. *Hippocampus, 9,* pp 562-574.

Beaulieu, C. & Allen, P. S. (1994a). Determinants of anisotropic water diffusion in nerves. *Magnetic Resonance in Medicine, 31,* pp 394-400.

Beaulieu, C. & Allen, P. S. (1994b). Water diffusion in the giant axon of the squid: implications for diffusion-weighted MRI of the nervous system. *Magnetic Resonance in Medicine, 32,* pp 579-583.

Bechterew, W. (1900). Demonstration eines Gehirns mit Zerstörung der vorderen und inneren Teile der Hirnrinde beider Schläfenlappen. *Neurologisches Zentralblatt, 19,* pp 990-991.

Behrens, T. E. J., Woolrich, M. W., Jenkinson, M., Johansen-Berg, H., Nunes, R. G., Clare, S., Matthews, P. M., Brady, J. M. & Smith, S. M. (2003). Characterization and propagation of uncertainty in diffusion-weighted MR imaging. *Magnetic Resonance in Medicine, 50,* pp 1077-1088.

Benedek, L. & Juba, A. (1940). Weitere Beitrage zur Frage des anatomischen Substrates des Korsakowchen symptomen komplexes. *Archiv für Psychiatrie und Nervenkrankheiten, 111*, pp 505-516.

Benedek, L. & Juba, A. (1941). Uber das anomische sub-strat des Korsakowschen Syndromes. *Schweizerisches Archiv far Psychiatrie und Nervenkrankheiten, 46,* pp 174-184.

Beracochea, D. J. & Jaffard, R. (1987). Impairment of spontaneous alternation behavior in sequential test procedures following mammillary body lesions in mice: evidence for time-dependent interference-related memory deficits. *Behavioural Neuroscience, 101*, pp 187-197.

Besnard, A., Caboche, J. & Laroche, S. (2013). Recall and reconsolidation of contextual fear memory: differential control by ERK and Zif268 expression dosage. *Plos One, 8,* doi:10.1371/journal.pone.0072006.

Blackwell, A. D., Sahakian, B. J., Vesey, R., Semple, J. M., Robbins, T. W. & Hodges, J. R. (2004). Detecting dementia: novel neuropsychological markers of preclinical Alzheimer's disease. *Dementia and Geriatric Cognitive Disorders, 17,* pp 42-48.

Blatt, G. J. & Rosene, D. L. (1998). Organization of direct hippocampal efferent projections to the cerebral cortex of the rhesus monkey: projections from CA1, prosubiculum, and subiculum to the temporal lobe. *The Journal of Comparative Neurology, 392,* pp 92–114.

Bohbot, V. D., Kalina, M., Stepankova, K., Spackova, N., Petrides, M. & Nadel, L. (1998). Spatial memory deficits in patients with lesions to the right hippocampus and to the right parahippocampal cortex. *Neuropsychologia, 36,* pp 1217-1238.

Bolhuis, J. J., Stewart, C. A. & Forrest, E. M. (1994). Retrograde amnesia and memory reactivation in rats with ibotenate lesions to the hippocampus or subiculum. *The Quarterly Journal of Experimental Psychology B, Comparative and Physiological Psychology, 47,* pp 129-150.

Brasted, P. J., Bussey, T. J., Murray, E. A. & Wise, A. S. P. (2002). Fornix transection impairs conditional visuomotor learning in tasks involving nonspatially differentiated responses. *Journal of Neurophysiology, 87*, pp 631-633.

Braver, T. S., Paxton, J. L., Locke, H. S. & Barch, D. M. (2009). Flexible neural mechanisms of cognitive control within human prefrontal cortex. *Proceedings of the National Academy of Sciences of the United States of America, 106,* pp 7351-7356.

Bray, N. (2014). The hippocampus encodes objects in time. *Nature Reviews Neuroscience, 15,* p 281.

Brotons-Mas, J. R., Montejo, N., O'Mara, S. M. & Sanchez-Vives, M. V. (2010). Stability of subicular place fields across multiple light and dark transitions. *The European Journal of Neuroscience, 32,* pp 648-658.

Brown, M. W. & Aggleton, J. P. (2001). Recognition memory: what are the roles of the perirhinal cortex and hippocampus? *Nature Reviews Neuroscience, 2,* pp 51-61.

Brown, M. W. & Xiang, J. Z. (1998). Recognition memory: neuronal substrates of the judgement of prior occurrence. *Progress in Neurobiology, 55,* pp 149-189.

Brown M. W., Warburton E. C. & Aggleton J. P. (2010). Recognition memory: material, processes, and substrates. *Hippocampus, 20,* pp 1228-1244.

Brown, M. W., Wilson, F. A. W. & Riches, I. P. (1987). Neuronal evidence that inferomedial temporal cortex is more important than hippocampus in certain processes underlying recognition memory. *Brain Research, 409,* pp 158-162.

Browning, P. G. F., Easton, A., Buckley, M. J. & Gaffan, D. (2005). The role of prefrontal cortex in object-in-place learning in monkeys. *The European Journal of Neuroscience, 22,* pp 3281-3291.

Bubb, E., Kinnavane, L., & Aggleton J. P. (submitted). Papez circuit, emotion and memory: time for a change of direction. *Brain and Neuroscience Advances.*

Buckley, M. J., Charles, D. P., Browning, P. G. F. & Gaffan, D. (2004). Learning and retrieval of concurrently presented spatial discrimination tasks: role of the fornix. *Behavioural Neuroscience, 118*, pp 138-149.

Buckley, M. J., Wilson, C. R. E. & Gaffan, D. (2008). Fornix transection impairs visuospatial memory acquisition more than retrieval. *Behavioural Neuroscience, 122*, pp 44-53.

Burgess, N., Maguire, E. A. & O'Keefe, J. (2002). The human hippocampus and spatial and episodic memory. *Neuron, 35,* pp 625-641.

Burke, S. N., Maurer, A. P., Nematollahi, S., Uprety, A. R., Wallace, J. L. & Barnes C. A. (2011). The influence of objects on place field expression and size in distal hippocampal CA1. *Hippocampus, 21,* pp 783-801.

Burwell, R. D. & Hafeman, D. M. (2003). Positional firing properties of postrhinal cortex neurons. *Neuroscience, 119,* pp 577-588.

Bussey, T. J. & Saksida, L. M. (2007). Memory, perception, and the ventral visual-perirhinal-hippocampal stream: thinking outside of the boxes. *Hippocampus, 17,* pp 898-908.

Bussey, T. J., Warburton, E. C., Aggleton, J. P. & Muir, J. L. (1998). Fornix lesions can facilitate acquisition of the transverse patterning task: a challenge for 'configural' theories of hippocampal function. *The Journal of Neuroscience, 18,* pp 1622-1631.

Byatt, G. & Dalrymple-Alford, J. C. (1996). Both anteromedial and anteroventral thalamic lesions impair radial-maze learning in rats. *Behavioral Neuroscience, 110,* pp 1335-1348.

Cabezas, M., Oliver, A., Llado, X., Freixenet, J. & Cuadra, M. B. (2011). A review of atlas-based segmentation for magnetic resonance brain images. *Computer Methods and Programs in Biomedicine, 104*, pp 158-177.

Caeyenberghs, K., Metzler-Baddeley, C., Foley, S. & Jones, D. (2016). Dynamics of the human structural connectome underlying working memory training. *The Journal of Neuroscience, 36,* pp 4056-4066.

Carlesimo, G. A., Lombardi, M. G. & Caltagirone, C. (2011). Vascular thalamic amnesia: a reappraisal. *Neuropsychologia, 49,* pp 777-789.

Carmichael, S. T. & Price, J. L. (1995). Limbic connections of the orbital and medial prefrontal cortex in macaque monkeys. *The Journal of Comparative Neurology, 363,* pp 615-641.

Cassel, J. C., Cassel, S., Galani, R., Kelche, C., Will, B. & Jarrard, L. (1998). Fimbria-fornix vs selective hippocampal lesions in rats: effects on locomotor activity and spatial learning and memory. *Neurobiology of Learning and Memory, 69,* pp 22-45.

Catani, M. & Thiebaut de Schotten, M. (2008). A diffusion tensor imaging tractography atlas for virtual in vivo dissections. *Cortex, 44,* pp 1105-1132.

Catenoix, H., Magnin, M., Mauguière, F. & Ryylin, P. (2011). Evoked potential study of hippocampal efferent projections in the human brain. *Clinical Neurophysiology: Official Journal of the International Federation of Clinical Neurophysiology, 122,* pp 2488-2497.

Cardinal, R. N., Parkinson, J. A., Hall, J. & Everitt, B. J. (2002). Emotion and motivation: the role of the amygdala, ventral striatum, and prefrontal cortex. *Neuroscience and Biobehavioral Reviews, 26,* pp 321-352.

Chang, E. H. & Huerta, P. T. (2012). Neurophysiological correlates of object recognition in the dorsal subiculum. *Frontiers in Behavioral Neuroscience, 6,* doi:10.3389/fnbeh.2012.00046.

Chase, H. W., Clos, M., Dibble, S., Fox, P., Grace, A. A., Phillips, M. L. & Eickhoff, S. B. (2015). Evidence for an anterior-posterior differentiation in the human hippocampal formation revealed by meta-analytic parcellation of fMRI coordinate maps: focus on the subiculum. *NeuroImage, 113,* pp 44-60.

Chaudhuri, A. (1997). Neural activity mapping with inducible transcription factors. *Neuroreport, 8,* pp 3-7.

Chen, D. Q., Strauss, I., Hayes, D. J., Davis, K. D., & Hodaie, M. (2015). Age-related changes in diffusion tensor imaging metrics of fornix subregions in healthy humans. *Stereotactic and Functional Neurosurgery, 93,* pp 151-159.

Chinnakkaruppan, A. 1. Wintzer, M. E., McHugh, T. J. & Rosenblum, K. (2014). Differential contribution of hippocampal subfields to components of associative taste learning. *The Journal of Neuroscience, 34,* pp 11007-11015.

Christiansen, K., Aggleton, J. P., Parker, G. D., O'Sullivan, M. J., Vann, S. D., & Metzler-Baddeley, C. (2016a). The status of the precommissural and postcommissural fornix in normal ageing and mild cognitive impairment: An MRI tractography study. *NeuroImage, 130,* pp 35-47.

Christiansen, K., Dillingham, C. M., Wright, N. F., Saunders, R. C., Vann, S. D., & Aggleton J. P. (2016b). Complementary subicular pathways to the anterior thalamic nuclei and mammillary bodies in the rat and macaque monkey brain. *The European Journal of Neuroscience, 43,* pp 1044-1061.

Chrobak, J. J. & Amaral, D. G. (2007). Entorhinal cortex of the monkey: VII. intrinsic connections. *The Journal of Comparative Neurology, 500,* pp 612-633.

Ciccarelli, O., Catani, M., Johansen-Berg, H., Clark, C. & Thompson, A. (2008). Diffusion-based tractography in neurological disorders: concepts, applications, and future developments. *The Lancet Neurology, 7,* pp 715-727.

Cole, A. J., Saffen, D. W., Baraban, J. M. & Worley, P. F. (1989). Rapid increase of an immediate early gene messenger RNA in hippocampal neurons by synaptic NMDA receptor activation. *Nature, 340,* pp 474-476.

Collin, S. H. P., Milivojevic, B. & Doeller, C. F. (2015). Memory hierarchies map onto the hippocampal long axis in humans. *Nature Neuroscience, 18,* pp 1562-1564.

Colombo, M., Fernandez, T., Nakamura, K. & Gross, C. G. (1998). Functional differentiation along the anterior-posterior axis of the hippocampus in monkeys. *Journal of Neurophysiology, 80,* pp 1002-1005.

Copara, M. S., Hassan, A. S., Kyle, C. T., Libby, L. A., Ranganath, C. & Ekstrom, A. D. (2014). Complementary roles of human hippocampal subregions during retrieval of spatiotemporal context. *The Journal of Neuroscience, 34,* pp 6834-6842.

Corkin, S. (2002). What's new with the amnesic patient H.M.? *Nature Reviews Neuroscience, 3,* pp 153-160.

Crutcher, M. D. & DeLong, M. R. (1984). Single cell studies of the primate putamen. *Experimental Brain Research, 53,* pp 244-258.

Czajkowski, R., Jayaprakash, B., Wiltgen, B., Rogerson, T., Guzman-Karlsson, M. C., Barth, A. L., Trachtenberg, J. T. & Silva, A. J. (2014). Encoding and storage of spatial information in the retrosplenial cortex. *Proceedings of the National Academy of Sciences of the United States of America, 111,* pp 8661-8666.

Daitz, H. (1953). Note on the fibre content of the fornix system. *Brain, 76,* pp 509-512.

Davis, A., Bozon, B. & Laroche, S. (2003). How necessary is the activation of the immediate early gene zif268 in synaptic plasticity and learning? *Behavioural Brain Research, 142,* pp 17-30.

Deisseroth, K. (2011). Optogenetics. *Nature Methods, 8,* pp 26-29.

Delay, J. & Brion, S. (1969). *Le Syndrome de Korsakoff.* Paris, France: Masson.

Delis, D. C., Kaplan, E. & Kramer, J. H. (2001). *Delis–Kaplan Executive Function System (D-KEFS).* Oxford, UK: Pearson Assessment.

Dell'Acqua, F., Scifo, P., Rizzo, G., Catani, M., Simmons, A., Scotti, G. & Fazio, F. (2010). A modified damped Richardson-Lucy algorithm to reduce isotropic background effects in spherical deconvolution. *NeuroImage, 49,* pp 1446-1458.

Dell'Acqua, F., Simmons, A., Williams, S. C. & Catani, M. (2013). Can spherical deconvolution provide more information than fibre orientations? Hindrance modulated orientational anisotropy, a true-tract specific index to characterize white matter diffusion. *Human Brain Mapping, 34,* pp 2464-2483.

De Santis, S., Drakesmith, M., Bells, S., Assaf, Y. & Jones, D. K. (2014). Why diffusion tensor MRI does well only some of the time: variance and covariance of white matter tissue microstructure attributes in the living human brain. *NeuroImage, 89,* pp 35-44.

Deshmukh, S. S. & Knierim, J. J. (2011). Representation of non-spatial and spatial information in the lateral entorhinal cortex. *Frontiers of Behavioural Neuroscience, 5,* pp 1-33.

Desimone, R. (1996). Neural mechanisms for visual memory and their role in attention. *Proceedings of the National Academy of Sciences of the United States of America, 93,* pp 13494-13499.

DeVito, J. L. (1980). Subcortical projections to the hippocampal formation in squirrel monkey (Saimiri sciureus). *Brain Research Bulletin, 5,* pp 285-289.

Diana, R. A., Yonelinas, A. P. & Ranganath, C. (2007). Imaging recollection and familiarity in the medial temporal lobe: a three-component model. *Trends in Cognitive Sciences, 11,* pp 380-386.

Dice, L. R. (1945). Measures of the amount of ecologic association between species. *Ecology, 26,* pp 297-302.

Dickerson, B. C., Salat, D. H., Greve, D. N., Chua, E. F., Rand-Giovannetti, E., Rentz, D. M., Bertram, L., Mullin, K., Tanzi, R. E., Blacker, D., Albert, M. S. & Sperling, R. A. (2005). Increased hippocampal activation in mild cognitive impairment compared to normal aging and AD. *Neurology, 65,* pp 404-411.

Dillingham, C. M., Erichsen, J. T., O'Mara, S. M., Aggleton, J. P. & Vann, S. D. (2015). Fornical and nonfornical projections from the rat hippocampal formation to the anterior thalamic nuclei. *Hippocampus, 25,* pp 977-992.

Dix, S. L. & Aggleton, J. P. (1999). Extending the spontaneous preference test of recognition: evidence of object-location and object-context recognition. *Behavioural Brain Research, 99,* pp 191-200.

Dolcos, G., LaBar, K. S. & Cabeza, R. (2004). Interaction between the amygdala and the medial temporal lobe memory system predicts better memory for emotional events. *Neuron, 42,* pp 855-863.

Dolorfo, C. A. & Amaral, D. G. (1998). Entorhinal cortex of the rat: topographic organization of the cells of origin of the perforant path projection to the dentate gyrus. *The Journal of Comparative Neurology, 398,* pp 25-48.

Domesick, V. B. (1970). The fasculus cinguli in the rat. *Brain Research, 20,* pp 19-32.

Donovan, M. K. & Wyss, J. M. (1983). Evidence for some collateralisation between the cortical and diencephalic efferent axons of the rat subicular cortex. *Brain Research, 259,* pp 181-192.

Dumont, J. R. & Aggleton, J. P. (2013). Dissociation of recognition and recency memory judgments after anterior thalamic nuclei lesions in rats. *Behavioral Neuroscience, 127,* pp 415-431.

Dumont, J. R., Amin, E., Poirier, G. L., Albasser, M. M. & Aggleton, J. P. (2012). Anterior thalamic nuclei lesions in rats disrupt markers of neural plasticity in distal limbic brain regions. *Neuroscience, 224,* pp 81-101.

Dumont, J. R., Amin, E., Wright, N. F., Dillingham, C. M., & Aggleton, J. P. (2015). The impact of fornix lesions in rats on spatial learning tasks sensitive to anterior thalamic and hippocampal damage. *Behavioural Brain Research, 278,* pp 360-374.

Dumont, J., Petrides, M. & Sziklas, V. (2007). Functional dissociation between fornix and hippocampus in spatial conditional learning. *Hippocampus, 17,* pp 1170-1179.

Dusoir, H., Kapur, N., Byrnes, D. P., McKinstry, S. & Hoare, R. D. (1990). The role of diencephalic pathology in human memory disorder: evidence from a penetrating paranasal brain injury. *Brain, 113,* pp 1695-1706.

Easton, A., Douchamps, V., Eacott, M. & Lever, C. (2012). A specific role for septohippocampal acetylcholine in memory? *Neuropsychologia, 50,* pp 3156-3168.

Easton, A., Zinkivskay, A. & Eacott, M. J. (2009). Recollection is impaired, but familiarity remains intact in rats with lesions of the fornix. *Hippocampus, 19,* pp 837-843.

Eichenbaum, H. (2000). Cortical–hippocampal networks for declarative memory. *Nature Reviews Neuroscience, 1,* pp 41-50.

Ennaceur, A. & Delacour, J. (1988). A new one-trial test for neurobiological studies of memory in rats. 1: Behavioral data. *Behavioural Brain Research, 31,* pp 47-59.

Epstein, R. A. (2008). Parahippocampal and retrosplenial contributions to human spatial navigation. *Trends in Cognitive Sciences, 12,* pp 388-396.

Ezzyat, Y. & Davachi, L. (2014). Similarity breeds proximity: pattern similarity within and across contexts is related to later mnemonic judgments of temporal proximity. *Neuron, 81,* pp 1179-1189.

Fanselow, M. S. & Dong, H. W. (2010). Are the dorsal and ventral hippocampus functionally distinct structures? *Neuron, 65,* pp 7-19.

Faraji, J., Lehmann, H., Metz, G. A. & Sutherland, R. J. (2008). Rats with hippocampal lesion show impaired learning and memory in the ziggurat task: a new task to evaluate spatial behavior. *Behavioural Brain Research, 189,* pp 17-31.

Farquharson, S., Tournier, J. D., Calamante, F., Fabinyi, G., Schneider-Kolsky, M., Jackson, G. D. & Connelly, A. (2013). White matter fibre tractography: why we need to move beyond DTI. *Journal of Neurosurgery, 118*, pp 1367-1377.

Fletcher, E., Raman, M., Huebner, P., Liu, A., Mungas, D., Carmichael, O. & DeCarli, C. (2013). Loss of fornix white matter volume as a predictor of cognitive impairment in cognitively normal elderly individuals. *JAMA Neurology, 70*, pp 1389-1395.

Fletcher, P.C. & Henson, R. (2001). Frontal lobes and humanmemory: insights from functional neuroimaging. *Brain, 124*, pp 849-881.

Fordyce, D. E., Bhat, R. V., Baraban, J. M. & Wehner, J. M. (1994). Genetic and activity-dependent regulation of zif268 expression: association with spatial learning. *Hippocampus, 4*, pp 559-568.

Fortin, N. J., Agster, K. L. & Eichenbaum, H. B. (2002). Critical role of the hippocampus in memory for sequences of events. *Nature Neuroscience, 5*, pp 458-462.

Francois, J., Huxter, J., Conway, M. W., Lowry, J. P., Tricklebank, M. D. & Gilmour, G. (2014). Differential contributions of infralimbic prefrontal cortex and nucleus accumbens during reward-based learning and extinction. *The Journal of Neuroscience, 34*, pp 596-607.

Friedman, D. P., Aggleton, J. P. & Saunders, R. C. (2002). A comparison of hippocampal, amygdala, and perirhinal projections to the nucleus accumbens: a combined anterograde and retrograde tracing study in the macaque brain. *The Journal of Comparative Neurology, 450,* pp 345-365.

Froudist-Walsh, S., Karolis, V., Caldinelli, C., Brittain, P. J., Kroll, J., Rodríguez-Toscano, E., Tesse, M., Colquhoun, M., Howes, O., Dell'Acqua, F., Thiebaut de Schotten, M., Murray, R. M., Williams, S. C. & Nosarti, C. (2015). Very early brain damage leads to remodeling of the working memory system in adulthood: a combined fMRI/tractography study. *The Journal of Neuroscience, 35,* pp 15787-15799.

Furl, N., van Rijsbergen, N. J., Treves, A. & Dolan, R. J. (2007). Face adaptation aftereffects reveal anterior medial temporal cortex role in high level category representation. *NeuroImage, 37,* pp 300-310.

Fuster, J. (2008). *The prefrontal cortex.* Massachusetts, US: Academic Press.

Fyhn, M., Molden, S., Witter, M. P., Moser, E. & Moser, M. (2004). Spatial representation in the entorhinal cortex. *Science, 305,* pp 1258-1264.

Gaffan, D. & Harrison, S. (1989a). A comparison of the effects of fornix transection and sulcus principalis ablation upon spatial learning by monkeys. *Behavioural Brain Research, 31,* pp 207-220.

Gaffan, D. & Harrison, S. (1989b). Place memory and scene memory: effects of fornix transection in the monkey. *Experimental Brain Research, 74,* pp 202-212.

Gaffan, D. & Gaffan, E. A. (1991). Amnesia in man following transection of the fornix. A review. *Brain, 114,* pp 2611-2618.

Gaffan, D. (1992). Amnesia for complex naturalistic scenes and for objects following fornix transection in the rhesus monkey. *The European Journal of Neuroscience, 4*, pp 381-388.

Gaffan, D. (1993). Normal forgetting, impaired acquisition in memory for complex naturalistic scenes by fornix transected monkeys. *Neuropsychologia, 31*, pp 403-406.

Gaffan, D. (1994). Scene-specific memory for objects: a model of episodic memory impairment in monkeys with fornix transection. *Journal of Cognitive Neuroscience, 6,* pp 305-320.

Gaffan, D., Gaffan, E. A. & Harrison, S. (1984a). Effects of fornix transection on spontaneous and trained non-matching by monkeys. *The Quarterly Journal of Experimental Psychology. B, Comparative and Physiological Psychology, 36,* pp 285-303.

Gaffan, D., Parker, A. & Easton, A. (2001). Dense amnesia in the monkey after transection of fornix, amygdala and anterior temporal stem. *Neuropsychologia, 39*, pp 51-70.

Gaffan, D., Saunders, R. C., Gaffan, E. A., Harrison, S., Shields, C. & Owen, M. J. (1984b). Effects of fornix transection upon associative memory in monkeys: role of the hippocampus in learned action. *The Quarterly Journal of Experimental Psychology. B, Comparative and Physiological Psychology, 36,* pp 173-221.

Galani, R., Coutureau, E., & Kelche, C. (1998a). Effects of enriched postoperative housing conditions on spatial memory deficits in rats with selective lesions of either the hippocampus, subiculum or entorhinal cortex. *Restorative Neurology and Neuroscience, 13,* pp 173-184.

Galani, R., Jarrard, L. E., Will, B. E., & Kelche, C. (1997). Effects of postoperative housing conditions on functional recovery in rats with lesions of the hippocampus, subiculum, or entorhinal cortex. *Neurobiology of Learning and Memory, 67,* pp 43-56.

Galani, R., Obis, S., Coutureau, E., Jarrard, L. & Cassel, J. C. (2002). A comparison of the effects of fimbria-fornix, hippocampal, or entorhinal cortex lesions on spatial reference and working memory in rats: short versus long postsurgical recovery period. *Neurobiology of Learning and Memory, 77,* pp 1-16.

Galani, R., Weiss, I., Cassel, J. C., & Kelche, C. (1998b). Spatial memory, habituation, and reactions to spatial and nonspatial changes in rats with selective lesions of the hippocampus, the entorhinal cortex or the subiculum. *Behavioural Brain Research, 96,* pp 1-12.

Garcia-Bengochea, F. & Friedman, W. A. (1987). Persistent memory loss following section of the anterior fornix in humans: a historical review. *Surgical Neurology, 27*, pp 361-364.

Garrett, A., Gupta, S., Reiss, A. L., Waring, J., Sudheimer, K., Anker, L., Sosa, N., Hallmayer, J. F. & O'Hara, R. (2015). Impact of 5-HTTLPR on hippocampal subregional activation in older adults. *Translational Psychiatry, 5,* doi:10.1038/tp.2015.131.

Gaykema, R. P., Gaál, G., Traber, J., Hersh, L. B. & Luiten, P. G. (1991). The basal forebrain cholinergic system: efferent and afferent connectivity and long-term effects of lesions. *Acta Psychiatrica Scandinavica Supplementum, 366,* pp 14-26.

Georges-François, P., Rolls, E. T. & Robertson, R. G. (1999). Spatial view cells in the primate hippocampus: allocentric view not head direction or eye position or place. *Cerebral Cortex, 9,* pp 197-212.

Giovanello, K. S., Schnyer, D. M. & Verfaellie, M. (2004). A critical role for the anterior hippocampus in relational memory: evidence from an fMRI study comparing associative and item recognition. *Hippocampus. 14,* pp 5-8.

Gold, A. E. & Kesner, R. P. (2005). The role of the CA3 subregion of the dorsal hippocampus in spatial pattern completion in the rat. *Hippocampus, 15,* pp 808-814.

Goldman-Rakic, P. S., Selemon, L. D. & Schwartz, M. L. (1984). Dual pathways connecting the dorsolateral prefrontal cortex with the hippocampal formation and parahippocampal cortex in the rhesus monkey. *Neuroscience, 12*, pp 719-743.

Good, M. (2002). Spatial memory and hippocampal function: where are we now? *Psicológica, 23,* pp 109-138.

Graff-Radford, N. R., Tranel, D., Van Hoesen, G. R. & Brandt, J. P. (1990). Diencephalic amnesia. *Brain, 113*, pp 1-25.

Greicius, M. D., Krasnow, B., Boyett-Anderson, J. M., Eliez, S., Schatzberg, A. F., Reiss, A. L. & Menon, V. (2003). Regional analysis of hippocampal activation during memory encoding and retrieval: fMRI study. *Hippocampus, 13*, pp 167-174.

Grober, E., Merling, A., Heimlich, T. & Lipton, R. B. (1997). Comparison of selective reminding and free and cued selective reminding in the elderly. *Journal of Clinical and Experimental Neuropsychology, 19,* pp 643-654.

van Groen, T. & Wyss, J. M. (1990a). The connections of the presubiculum and parasubiculum in the rat. *Brain Research, 518,* pp 227-243.

van Groen, T. & Wyss, J. M. (1990b). The postsubicular cortex in the rat: characterization of the fourth region of the subicular cortex and its connections. *Brain Research, 529*, pp 165-177.

Grothe, M., Heinsen, H. & Teipel, S. J. (2012). Atrophy of the cholinergic basal forebrain over the adult age range and in early stages of Alzheimer's disease. *Biological Psychiatry, 71,* pp 805-813.

Grothe, M., Heinsen, H. & Teipel, S. J. (2013). Longitudinal measures of cholinergic forebrain atrophy in the transition from healthy aging to Alzheimer's disease. *Neurobiology of Aging, 34,* pp 1210-1220.

Grothe, M., Zaborszky, L., Atienza, M., Gil-Neciga, E., Rodriguez-Romero, R., Teipel, S. J., Amunts, K., Suarez-Gonzalez, A. & Cantero, J. L. (2010). Reduction of basal forebrain cholinergic system parallels cognitive impairment in patients at high risk of developing Alzheimer's disease. *Cerebral Cortex, 20,* pp 1685-1695.

Guzowski, J. F. (2002). Insights into immediate-early gene function in hippocampal memory consolidation using antisense oligonucleotide and fluorescent imaging approaches. *Hippocampus, 12,* pp 86-104.

Guzowski, J. F., Setlow, B., Wagner, E. K. & McGaugh, J. L. (2001). Experience-dependent gene expression in the rat hippocampus after spatial learning: a comparison of the immediate-early genes Arc, c-fos, and zif268. *The Journal of Neuroscience, 21,* pp 5089-5098.

Hafting, T., Fyhn, M., Molden, S., Moser, B. & Moser., E. (2005). Microstructure of a spatial map in the entorhinal cortex. *Nature, 436,* pp 801-806.

Hall, J., Thomas, K. L., Everitt, B. J. (2001). Cellular imaging of zif268 expression in the hippocampus and amygdala during contextual and cued fear memory retrieval: selective activation of hippocampal CA1 neurons during the recall of contextual memories. *The Journal of Neuroscience, 21,* pp 2186-2193.

Hanker, J. S., Yates, P. E., Metz, C. B. & Rustioni, A. (1977). A new specific, sensitive and non-carcinogenic reagent for the demonstration of horeseradish-peroxidase. *The Histochemical Journal, 9,* pp 789-792.

Harding, A., Halliday, G., Caine, D. & Kril, J. (2000). Degeneration of anterior thalamic nuclei differentiates alcoholics with amnesia. *Brain, 123,* pp 141-154.

Hardy, H. & Heimer, L. (1977). A safer and more sensitive substitute for diamino-benzidine in the light microscopic demonstration of retrograde and anterograde axonal transport of HRP. *Neuroscience Letters, 5,* pp 235-240.

Hartley, T., Maguire, E. A., Spiers, H. J. & Burgess, N. (2003). The well-worn route and the path less traveled: distinct neural bases of route following and wayfinding in humans. *Neuron, 37,* 877-888.

Hartzell, A. L., Burke, S. N., Hoang, L. T., Lister, J. P., Rodriguez, C. N. & Barnes, C. A. (2013). Transcription of the immediate-early gene Arc in CA1 of the hippocampus reveals activity differences along the proximodistal axis that are attenuated by advanced age. *The Journal of Neuroscience, 33,* pp 3424-3433.

Heckers, S., Rauch, S., Goff, D., Savage, C., Schacter, D., Fischman, A. & Alpert, N. (1998). Impaired recruitment of the hippocampus during conscious recollection in schizophrenia. *Nature Neuroscience, 1,* pp 318-323.

Heilbronner, S. R. & Haber, S. N. (2014). Frontal cortical and subcortical projections provide a basis for segmenting the cingulum bundle: implications for neuroimaging and psychiatric disorders. *The Journal of Neuroscience, 34,* pp 10041-10054.

Henderson, J. & Greene, E. (1977). Behavioral effects of lesions of precommissural and postcommissural fornix. *Brain Research Bulletin, 2*, pp 123-129.

Henriksen, E. J., Colgin, L. L., Barnes, C. A., Witter, M. P., Moser, M. & Moser, E. I. (2010). Spatial representation along the proximodistal axis of CA1. *Neuron, 68,* pp 127-137.

Henry, J., Petrides, M., St-Laurent, M. & Sziklas, V. (2004). Spatial conditional associative learning: effects of thalamo-hippocampal disconnection in rats. *Neuroreport, 15, pp* 2427-2431.

Heuer, E. & Bachevalier, J. (2011). Effects of selective neonatal hippocampal lesions on tests of object and spatial recognition memory in monkeys. *Behavioral Neuroscience, 125,* pp 137-149.

Hitti, F. L. & Siegelbaum, S. A. (2014). The hippocampal CA2 region is essential for social memory. *Nature, 508,* pp 88-92.

Hoang, L. T. & Kesner, R. P. (2008). Dorsal hippocampus, CA3, and CA1 lesions disrupt temporal sequence completion. *Behavioral Neuroscience, 122,* pp 9-15.

Hodges, J. R. & Carpenter, K. (1991). Anterograde amnesia with fornix damage following removal of IIIrd ventricle colloid cyst. *Journal of Neurology, Neurosurgery, and Psychiatry, 5,* pp 633–638.

Hofstetter, S., Tavor, I., Moryosef, S. T. & Assaf, Y. (2013). Short-term learning induces white matter plasticity in the fornix. *The Journal of Neuroscience, 33*, pp 12844-12850.

Hoge, J. & Kesner, R. (2007). Role of CA3 and CA1 subregions of the dorsal hippocampus on temporal processing of objects. *Neurobiology of Learning and Memory, 88,* pp 225-231.

Honda, Y. & Ishizuka, N. (2015). Topographic distribution of cortical projection cells in the rat subiculum. *Neuroscience Research, 92,* pp 1-20.

Hopkins, D. A. (2005). Neuroanatomy of head direction cell circuits. In Wiener, S. I. & Taube, J. S. (Eds.), *Head Direction Cells and the Neural Mechanisms of Spatial Orientation* (pp 17-44). Cambridge, MA: MIT Press.

Hsieh, L. T., Gruber, M. J., Jenkins, L. J. & Ranganath, C. (2014). Hippocampal activity patterns carry information about objects in temporal context. *Neuron, 81,* pp 1165–1178.

Hunsaker, M. R., Rosenberg, J. S. & Kesner, R. P. (2008). The role of the dentate gyrus, CA3a, b, and CA3c for detecting spatial and environmental novelty. *Hippocampus, 18,* pp 1064-1073.

Hutcherson, C. A., Montaser-Kouhsari, L., Woodward, J. & Rangel, A. (2015). Emotional and utilitarian appraisals of moral dilemmas are encoded in separate areas and integrated in ventromedial prefrontal cortex. *The Journal of Neuroscience, 35,* pp 12593-12605.

Igarashi, K. M., Ito, H. T., Moser, E. I. & Moser, M. B. (2014a). Functional diversity along the transverse axis of hippocampal area CA1. *FEBS Letters, 588,* pp 2470-2476.

Igarashi, K. M., Lu, L., Colgin, L. L., Moser, M. B. & Moser, E. I. (2014b). Coordination of entorhinal-hippocampal ensemble activity during associative learning. *Nature, 510,* pp 143-147.

Ikemoto, S. & Panksepp, J. (1999). The role of nucleus accumbens dopamine in motivated behavior: a unifying interpretation with special reference to reward-seeking. *Brain Research Reviews, 31,* 6-41.

Insausti, R., Amaral, D. G. & Cowan, W. M. (1987). The entorhinal cortex of the monkey: III subcortical afferents. *The Journal of Comparative Neurology, 264,* pp 396-408.

Insausti, R. & Muñoz, M. (2001). Cortical projections of the non-entorhinal hippocampal formation in the cynomolgus monkey (Macaca fascicularis). *The European Journal of Neuroscience, 14,* pp 435-451.

Irfanoglu, M. O., Walker, L., Sarlls, J., Marenco, S. & Pierpaoli, C. (2012). Effects of image distortions originating from susceptibility variations and concomitant fields on diffusion MRI tractography results. *NeuroImage, 61,* pp 275-288.

Ishizuka, N. (2001). Laminar organization of the pyramidal cell layer of the subiculum in the rat. *The Journal of Comparative Neurology, 435,* pp 89-110.

Jang, S. H., Choi, B. Y., Kim, S. H., Chang, C. H., Jung, Y. J. & Kwon, H. G. (2014). Injury of the mammillothalamic tract in patients with subarachnoid haemorrhage: a retrospective diffusion tensor imaging study. *BMJ Open, 4,* doi:10.1136/bmjopen-2014-005613.

Jankowski, M. M., Passecker, J., Nurul Islam, M. D., Vann, S. D., Erichsen, J., Aggleton, J. P. & O'Mara, S. M. (2015). Evidence for spatially-responsive neurons in the rostral thalamus. *Frontiers in Behavioral Neuroscience, 9,* p 256.

Jarrard, L. E. (1993). On the role of the hippocampus in learning and memory in the rat. *Behavioral and Neural Biology, 60,* pp 9-26.

Jay, T. M. & Witter, M. P. (1991). Distribution of hippocampal CA1 and subicular efferents in the prefrontal cortex of the rat studied by means of anterograde transport of Phaseolus vulgaris-leucoagglutinin. *The Journal of Comparative Neurology, 313,* pp 574-586.

Jeneson, A., Kirwan, C. B., Hopkins, R. O., Wixted, J. T. & Squire, L. R. (2010). Recognition memory and the hippocampus: A test of the hippocampal contribution to recollection and familiarity. *Learning & Memory, 17,* pp 63-70.

Jenkins, T. A., Amin, E., Brown, M. W. & Aggleton, J. P. (2006). Changes in immediate early gene expression in the rat brain after unilateral lesions of the hippocampus. *Neuroscience, 137,* pp 747-759.

Jenkins, T. A., Amin, E., Harold, G. T., Pearce, J. M. & Aggleton, J. P. (2003). Distinct patterns of hippocampal formation activity associated with different spatial tasks: a Fos imaging study in rats. *Experimental Brain Research, 151,* pp 514-523.

Jenkins, T. A., Amin, E., Pearce, J. M., Brown, M. W. & Aggleton, J. P. (2004). Novel spatial arrangements of familiar visual stimuli promote activity in the rat hippocampal formation but not the parahippocampal cortices: a c-fos expression study. *Neuroscience, 124,* pp 43-52.

Jenkins, T. A., Dias, R., Amin, E., & Aggleton, J. P. (2002a). Changes in Fos expression in the rat brain after unilateral lesions of the anterior thalamic nuclei. *The European Journal of Neuroscience, 16,* pp 1425-1432.

Jenkins, T. A., Dias, R., Amin, E., Brown, M. W. & Aggleton, J. P. (2002b). Fos imaging reveals that lesions of the anterior thalamic nuclei produce widespread limbic hypoactivity in rats. *The Journal of Neuroscience, 22,* pp 5230-5238.

Jenkinson, M., Beckmann, C. F., Behrens, T. E., Woolrich, M. W. & Smith, S. M. (2012). FSL. *NeuroImage, 62,* 782-790.

Jenkinson, M. & Smith, S. M. (2001). A global optimisation method for robust affine registration of brain images. *Medical Image Analysis, 5,* pp 143-156.

Jessen, F., Scheef, F. L., Germeshausen, L., Tawo, Y., Kockler, M., Kuhn, K. U., Maier, W., Schild, H. H. & Heun, R. (2003). Reduced hippocampal activation during encoding and recognition of words in schizophrenia patients. *The American Journal of Psychiatry, 160,* pp 1305-1312.

Jones, B. F. & Witter, M. P. (2007). Cingulate cortex projections to the parahippocampal region and hippocampal formation in the rat. *Hippocampus, 17,* pp 957–976.

Jones, D. K. & Cercignani, M. (2010). Twenty-five pitfalls in the analysis of diffusion MRI data. *NMR in Biomedicine,* 23, pp 803-820.

Jones, D. K., Christiansen, K. F., Chapman, R. C. & Aggleton, J. P. (2013). Distinct components of the cingulum bundle revealed by diffusion MRI fibre tracking: implications for neuropsychological investigations. *Neuropsychologia, 51,* pp 67-78.

Jones, D. K., Horsfield, M. A. & Simmons, A. (1999). Optimal strategies for measuring diffusion in anisotropic systems by magnetic resonance imaging. *Magnetic Resonance in Medicine,* 42, pp 515–525.

Jones, M. W., Errington, M. L., French, P. J., Fine, A., Bliss, T. V., Garel, S., Charnay, P., Bozon, B., Laroche, S. & Davis, S. (2001). A requirement for the immediate early gene Zif268 in the expression of late LTP and long-term memories. *Nature Neuroscience*, *4,* pp 289-296.

Jongen-Rêlo, A. L. & Feldon, J. (2002). Specific neuronal protein: a new tool for histological evaluation of excitotoxic lesions. *Physiology & Behavior, 76,* pp 449-456.

Kantarci, K., (2014). Fractional anisotropy of the fornix and hippocampal atrophy in Alzheimer's disease. *Frontiers in Aging Neuroscience*, *6,* p 316.

Kantarci, K., Senjem, M. L., Avula, R., Zhang, B., Samikoglu, A. R., Weigand, S. D., Przybelski, S. A., Edmonson, H. A., Vemuri, P., Knopman, D. S., Boeve, B. F., Ivnik, R. J., Smith, G. E., Petersen, R. C., & Jack, C. R. Jr. (2011). Diffusion tensor imaging and cognitive function in older adults with no dementia. *Neurology, 77,* pp 26-34.

Kerr, J. E., Beck, S. G., & Handa, R. J. (1996). Androgens selectively modulate C-fos messenger RNA induction in the rat hippocampus following novelty. *Neuroscience, 74,* pp 757-766.

Kesner, R. P. & Hopkins, R. O. (2006). Mnemonic functions of the hippocampus: A comparison between animals and humans. *Biological Psychology, 73,* pp 3-18.

Kesner, R. P. & Warthen, D. K. (2010). Implications of CA3 NMDA and opiate receptors for spatial pattern completion in rats. *Hippocampus, 20,* pp 550-557.

Kesner, R. P. (2007a). Behavioral functions of the CA3 subregion of the hippocampus. *Learning & Memory, 14,* pp 771-781.

Kesner, R. P (2007b). A behavioral analysis of dentate gyrus function. *Progress in Brain Research, 163,* pp 567-576.

Kesner, R. P. (2013). Role of the hippocampus in mediating interference as measured by pattern separation processes. *Behavioural Processes, 93,* pp 148-154.

Kesner, R. P., Gilbert, P. E. & Barua, L. A. (2002). The role of the hippocampus in memory for the temporal order of a sequence of odors. *Behavioral Neuroscience, 116,* pp 286-290.

Kier, E. L., Staib, L. H., Davis, L. M. & Bronen, R. A. (2004). MR imaging of the temporal stem: anatomic dissection tractography of the uncinate fasciculus, inferior occipitofrontal fasciculus, and Meyer's loop of the optic radiation. *American Journal of Neuroradiology, 37,* pp 300-310.

Kievet, J. & Kuypers, H. G. J. M. (1977). Organization of the thalamo-cortical connexions to the frontal lobe in the rhesus monkey. *Experimental Brain Research, 29,* pp 299-322.

Kim, S. M., Ganguli, S. & Frank, L., M. (2012). Spatial information outflow from the hippocampal circuit: distributed spatial coding and phase precession in the subiculum. *The Journal of Neurology, 32,* pp 11539-11558.

Kim, Y. & Sprutson, N. (2012). Target-specific output patterns are predicted by the distribution of regular-spiking and bursting pyramidal neurons in the subiculum. *Hippocampus, 22,* pp 693-706.

Kimura, M. (1986). The role of primate putamen neurons in the association of sensory stimuli with movement. *Neuroscience Research, 3,* pp 436-443.

Kishi, T., Tsumori, T., Ono, K., Yokota, S., Ishino, H. & Yasui, Y. (2000). Topographical organization of projections from the subiculum to the hypothalamus in the rat. *The Journal of Comparative Neurology, 419,* p 205-222.

Kitt, C. A., Mitchell, S. J., DeLong, M. R., Wainer, B. H. & Price, D. L. (1987). Fibre pathways of basal forebrain cholinergic neurons in monkeys. *Brain Research, 406,* pp 192–206.

Kjelstrup, K. G., Tuvnes, F. A., Steffenach, H-A., Murison, R., Moser, E. I. & Moser, M-B. (2002). Reduced fear expression after lesions of the ventral hippocampus.

Proceedings of the National Academy of Sciences of the United States of America, 99, pp 10825-10830.

Kloosterman, F., Witter, P. & van Haeften, T. (2003). Topographical and laminar organization of subicular projections to the parahippocampal region of the rat. *The Journal of Comparative Neurology, 455,* pp 156-71.

Knight, R. T., Grabowecky, M. F. & Scabini, D. (1995). Role of human prefrontal cortex in attention control. *Advances in Neurology, 66,* pp 21-34.

Knutson, B., Adams, C. M., Fong, G. W. & Hommer, D. (2001). Anticipation of increasing monetary reward selectively recruits nucleus accumbens. *The Journal of Neuroscience, 21,* pp 1-5.

Knutson, B., Westdorp, A., Kaiser, E. & Hommer, D. (2000). fMRI visualization of brain activity during a monetary incentive delay task. *NeuroImage, 12,* pp 20-27.

Knutson, B., Wimmer, G. E., Kuhnen, C. M. & Winkielman, P. (2008). Nucleus accumbens activation mediates the influence of reward cues on financial risk taking. *Neuroreport, 15,* pp 509-513.

Kobayashi Y. & Amaral, D. C. (2003). Macaque monkey retrosplenial cortex: II. Cortical afferents. *The Journal of Comparative Neurology, 466,* pp 48-79.

Koliatsos, V. E., Martin, L. J., Walker, L. C., Richardson, R. T., DeLong, M. R. & Price, D. L. (1988). Topographic, non-collateralized basal forebrain projections to the amygdala, hippocampus, and anterior cingulate cortex in the rhesus monkey. *Brain Research, 463,* pp 133-139.

Konishi, S., Nakajima, K., Uchida, I., Kameyama, M., Nakahara, K., Sekihara, K. & Miyashita, Y. (1998). Transient activation of inferior prefrontal cortex during cognitive set shifting. *Nature Neuroscience, 1*, pp 80-84.

Kosel, K. C., Van Hoesen, G. W. & Rosene, D. L. (1983). A direct projection from the perirhinal cortex (area 35) to the subiculum in the rat. *Brain Research, 269,* pp 347-351.

Kouneiher, F., Charron, S. & Koechlin, E. (2009). Motivation and cognitive control in the human prefrontal cortex. *Nature Neuroscience, 12*, pp 939-945.

Krayniak, P. F., Siegel, A., Meibach, R. C., Fruchtman, D. & Scrimenti, M. (1979). Origin of the fornix system in the squirrel monkey. *Brain Research, 160,* pp 401-411.

Kristensson, K. & Olsson, Y. (1971). Uptake and retrograde axonal transport of peroxidase in hypoglossal neurones. *Acta Neuropathologica, 19,* pp 1-9.

Kubik, S., Miyashita, T. & Guzowski, J. F. (2007). Using immediate-early genes to map hippocampal subregional functions. *Learning & Memory, 14,* pp 758-770.

Kwok, S. C. & Buckley, M. J. (2009). Fornix transected macaques make fewer perseverative errors than controls during the early stages of learning conditional visuospatial discriminations. *Behavioural Brain Research, 205*, pp 207-213.

Kwon, H. G., Hong, J. H. & Jang S. H. (2010). Mammillothalamic tract in human brain: diffusion tensor tractography study. *Neuroscience Letters, 481,* pp 51-53.

Kwon, H. G., Lee, H. D. & Jang, S. H. (2014). Injury of the mammillothalamic tract in patients with thalamic hemorrhage. *Frontiers in Human Neuroscience, 8,* p 259.

Lanciego, J. L. & Wouterlood, F. G. (2011). A half century of experimental neuroanatomical tracing. *Journal of Chemical Neuroanatomy, 42,* pp 157-183.

Lavenex, P. B., Amaral, D. G. & Lavenex, P. (2006). Hippocampal lesion prevents spatial relational learning in adult macaque monkeys. *The Journal of Neuroscience, 26,* pp 4546-4558.

Laxton, A. W., Tang-Wai, D. F., McAndrews, M. P., Zumsteg, D., Wennberg, R., Keren, R., Wherrett, J., Naglie, G., Hamani, C., Smith, G. S. & Lozano, A. M. (2010). A phase I trial of deep brain stimulation of memory circuits in Alzheimer's disease. *Annals of Neurology, 68,* pp 521-534.

Lee, D. Y., Fletcher, E., Carmichael, O. T., Singh, B., Mungas, D., Reed, B., Martinez, O., Buonocore, M. H., Persianinova, M. & Decarli, C. (2012). Sub-regional hippocampal injury is associated with fornix degeneration in Alzheimer’s disease. *Frontiers in Aging Neuroscience, 4,* pp 1-10.

Lee, H., Wang, C., Deshmukh, S. S. & Knierim, J. J. (2015). Neural population evidence of functional heterogeneity along the CA3 transverse axis: pattern completion versus pattern separation. *Neuron, 87*, pp 1093-1104.

Lee, I., Hunsaker, M. R. & Kesner, R. P. (2005). The role of hippocampal subregions in detecting spatial novelty. *Behavioral Neuroscience, 119*, pp 145-153.

Lee, J., Laza, M., Holden, J., Griley, E. & Alexander, A. L. (2004). Correction of B0 EPI distortions in diffusion tensor imaging and white matter tractography. *Proceedings of the International Society for Magnetic Resonance Imaging, 11*, p 2172.

Leemans, A. & Jones, D. K. (2009). The B-matrix must be rotated when correcting for subject motion in DTI data. *Magnetic Resonance in Medicine, 61*, pp 1336 –1349.

Leemans, A., Jeurissen, B., Siibers, J., Jones, D. K. (2009). ExploreDTI: a graphical tool box for processing, analyzing, and visualizing diffusion MR data. *Proceedings of the International Society for Magnetic Resonance Imaging, 17*, p 3537.

Lehmann, H., Rourke, B. K., Booker, A. & Glenn, M. J. (2013). Single session contextual fear conditioning remains dependent on the hippocampus despite an increase in the number of context-shock pairings during learning. *Neurobiology of Learning and Memory, 106*, pp 294-299.

Lepage, M., Ghaffar, O., Nyberg, L. & Tulving, E. (2000). Prefrontal cortex and episodic memory retrieval mode. *Proceedings of the National Academy of Sciences of the United States of America, 97,* pp 506-511.

Lepage, M., Habib, R. & Tulving, E. (1998). Hippocampal PET activations of memory encoding and retrieval: the HI PER model. *Hippocampus, 8, pp* 313–322.

Leutgeb, J. K., Leutgeb, S., Moser, M. B. & Moser, E. I. (2007). Pattern separation in the dentate gyrus and CA3 of the hippocampus. *Science, 315,* pp 961-966.

Lever, C., Burton, S., Jeewajee, A., O'Keefe, J. & Burgess, N. (2009). Boundary vector cells in the subiculum of the hippocampal formation. *The Journal of Neuroscience, 29,* pp 9771-9777.

Libby, L. A., Ekstrom, A. D., Ragland, J D. & Ranganath, C. (2012) Differential connectivity of perirhinal and parahippocampal cortices within human hippocampal subregions revealed by high-resolution functional imaging. *The Journal of Neuroscience, 32,* pp 6550-6560.

Liu, P. & Bilkey, D K. (2002). The effects of NMDA lesions centered on the postrhinal cortex on spatial memory tasks in the rat. *Behavioral Neuroscience, 116,* pp 860-873.

Lorente De Nó, R. (1934). Studies on the structure of the cerebral cortex. II. Continuation of the study of the ammonic system. *Journal für Psychologie und Neurologie, 46,* pp 113–177.

Lozano, A. M., Fosdick, L., Chakravarty, M. M., Leoutsakos, J. M., Munro, C., Oh, E., Drake, K. E., Lyman, C. H., Rosenberg, P. B., Anderson, W. S., Tang-Wai, D. F., Pendergrass, J. C., Salloway, S., Asaad, W. F., Ponce, F. A., Burke, A., Sabbagh, M., Wolk, D. A., Baltuch, G., Okun, M. S., Foote, K. D., McAndrews, M. P., Giacobbe, P., Targum, S. D., Lyketsos, C. G. & Smith, G. S. (2016). A phase II study of fornix deep brain stimulation in mild Alzheimer's disease. *Journal of Alzheimer's Disease, 54,* pp 777-787.

MacDonald, C. J., Lepage, K. Q., Eden, U. T. & Eichenbaum, H. (2011). Hippocampal "time cells" bridge the gap in memory for discontiguous events. *Neuron, 71,* pp 737-749.

Maguire, E. A. (2001). The retrosplenial contribution to human navigation: a review of lesion and neuroimaging findings. *Scandinavian Journal of Psychology, 42,* pp 225-238.

Maguire, E. A., Burgess, N., Donnett, J.G., Frackowiak, R. S., Frith, C. D. & O'Keefe, J. (1998). Knowing where and getting there: a human navigation network. *Science, 280,* pp 921-924.

Maguire, E. A., Frackowiak, R. S. & Frith, C. D. (1997). Recalling routes around London: activation of the right hippocampus in taxi drivers. *The Journal of Neuroscience, 17,* pp 7103-7110.

Maguire, E. A., Gadian, D. G., Johnsrude, I. S., Good, C. D., Ashburner, J., Frackowiak, R. S. J. & Frith, C. D. (2000). Navigation-related structural change in the hippocampi of taxi drivers. *Proceedings of the National Academy of Sciences, 97*, pp 4398-4403.

Maguire, E. A., Vargha-Khadem, F. & Mishkin, M. (2001). The effects of bilateral hippocampal damage on fMRI regional activations and interactions during memory retrieval. *Brain, 124,* pp 1156-1170.

Maren, S. & Fanselow, M. S. (1997). Electrolytic lesions of the fimbria/fornix, dorsal hippocampus, or entorhinal cortex produce anterograde deficits in contextual fear conditioning in rats. *Neurobiology of Learning and Memory, 67,* pp 142-149.

Marfurt, C. F., Turner, D. F. & Adams, C. E. (1988). Stabilization of tetramethylbenzidine (TMB) reaction product at the electron microscopic level by ammonium molybdate. *Journal of Neuroscience Methods, 25*, pp 215-223.

Markowitsch, H. J. (1997). Varieties of memory: systems, structures, mechanisms of disturbance. *Neurology, Psychiatry and Brain Research, 5*, pp 37-56.

Maroteaux, M., Valjent, E., Longueville, S., Topilko, P., Girault, J. A. & Hervé, D. (2014). Role of the plasticity-associated transcription factor zif268 in the early phase of instrumental learning. *PloS One, 9,* doi:10.1371/journal.pone.0081868.

Martínez-Pinilla, E., Ordóñez, C., del Valle, E., Navarro, A. & Tolivia, J. (2016). Neuronal density in brain during aging and in Alzheimer's disease. *Frontiers in Aging Neuroscience, 8,* doi:10.3389/fnagi.2016.00213.

Matthews, S. C., Simmons, A. N., Lane, S. D. & Paulus, M. P. (2004). Selective activation of the nucleus accumbens during risk-taking decision making. *Neuroreport, 15*, pp 2123-2127.

McDonald, R. J., Murphy, R. A., Guarraci, F. A., Gortler, J. R., White, N. M. & Baker, A. G. (1997). Systematic comparison of the effects of hippocampal and fornix-fimbria lesions on acquisition of three configural discriminations. *Hippocampus, 7*, pp 371–388.

McNab, J. A., Jbabdi, S., Deoni, S. C., Douaud, G., Behrens, T. E. & Miller, K. L. (2009). High resolution diffusion-weighted imaging in fixed human brain using diffusion-weighted steady state free precession. *NeuroImage, 46,* pp 775-785.

McKinney, M., Coyle, J.T. & Hedreen, J.C. (1983). Topographic analyses of the innervation of the rat neo-cortex and hippocampus by the basal forebrain cholinergic system. *The Journal of Comparative Neurology, 217*, pp 103-121.

McMackin, D., Cockburn, J., Anslow, P. & Gaffan, D. (1995). Correlation of fornix damage with memory impairment in six cases of colloid cyst removal. *Acta Neurochirurgica, 135,* pp 12-18.

Meibach, R. C. & Siegel, A. (1975). The origin of fornix fibres which project to the mammillary bodies in the rat: a horseradish peroxidase study. *Brain Research, 88,* pp 508-512.

Meibach, R. C. & Siegel, A. (1977a). Efferent connections of the hippocampal formation in the rat. *Brain Research, 124,* pp 197-224.

Meibach, R. C. & Siegel, A. (1977b). Thalamic projections of the hippocampal formation: evidence for an alternative pathway involving the internal capsule. *Brain Research, 134,* pp 1-12.

Mesulam, M. M. (1995). Cholinergic pathways and the ascending reticular activating system of the human brain. *Annals of the New York Academy of Sciences, 757,* pp 169-179.

Mesulam, M. M., Mufson, E. J., Levey, A. I. & Wainer, B. H. (1983). Cholinergic innervation of cortex by basal forebrain: cytochemistry and cortical connections of the septal area, diagonal band nuclei, nucleus basalis (substantia innominata), and hypothalamus in the rhesus monkey. *The Journal Comparative Neurology, 214,* pp 170-197.

Metzler-Baddeley, C., Caeyenberghs, K., Foley, S. & Jones, D. K. (2016). Task complexity and location specific changes of cortical thickness in executive and salience networks after working memory training. *NeuroImage, 130,* pp 48-62.

Metzler-Baddeley, C., Hunt, S., Jones, D. K., Leemans, A., Agggleton, J. P. & O'Sullivan, M. J. (2012a). Temporal association tracts and the breakdown of episodic memory in mild cognitive impairment. *Neurology, 79*, pp 2233-2240.

Metzler-Baddeley, C., Jones, D. K., Belaroussi, B., Aggleton, J. P. & O'Sullivan, M. J. (2011). Frontotemporal connections in episodic memory and aging: a diffusion MRI tractography study. *The Journal of Neuroscience, 31*, pp 13236-13245.

Metzler-Baddeley, C., O'Sullivan, M., Bells, S., Pasternak, O. & Jones, D. K. (2012b). How and how not to correct for CSF-contamination in diffusion MRI. *NeuroImage, 59*, pp 1394-1403.

Mian, M. K., Sheth, S. A., Patel, S. R., Spiliopoulos, K., Eskandar, E. N. & Williams, Z. M. (2014). Encoding of rules by neurons in the human dorsolateral prefrontal cortex. *Cerebral Cortex, 24*, pp 807-816.

Miller, E. K., Li, L. & Desimone, R. (1993). Activity of neurons in anterior inferior temporal cortex during a short-term memory task. *The Journal of Neuroscience, 13*, pp 1460-1478.

Miller, K. L., Stagg, C. J., Douaud, G., Jbabdi, S., Smith, S. M., Behrens, T. E., Jenkinson, M., Chance, S. A., Esiri, M. M., Voets, N. L., Jenkinson, N., Aziz, T. Z., Turner, M. R., Johansen-Berg, H. & McNab, J. A. (2011). Diffusion imaging of whole, post-mortem human brains on a clinical MRI scanner. *NeuroImage, 57*, pp 167-181.

Mink, J. W., Sinnamon, H. M. & Adams, D. B. (1983). Activity of basal forebrain neurons in the rat during motivated behaviors. *Behavioural Brain Research, 8*, pp 85-108.

Mioshi, E., Dawson, K., Mitchell, J., Arnold, R. & Hodges, J. R. (2006). The Addenbrooke's Cognitive Examination Revised (ACE-R): a brief cognitive test battery for dementia screening. *International Journal of Geriatric Psychiatry, 21*, pp 1078-1085.

Mishkin, M. (1978). Memory in monkeys severely impaired by combined but not by separate removal of the amygdala and the hippocampus. *Nature, 273*, pp 297-298.

Mitchell, A. S. & Dalrymple-Alford, J. C. (2005). Dissociable memory effects after medial thalamus lesions in the rat. *The European Journal of Neuroscience, 22*, pp 973-985.

Mitchell, A. S. & Dalrymple-Alford, J. C. (2006). Lateral and anterior thalamic lesions impair independent memory systems. *Learning & Memory, 13*, pp 388-396.

Momennejad, I. & Haynes, J. D. (2013). Encoding of prospective tasks in the human prefrontal cortex under varying task loads. *The Journal of Neuroscience, 33*, pp 17342-17349.

Moore, T. L., Schettler, S. P., Killiany, R. J., Rosene, D. L. & Moss, M. B. (2009). Effects on executive function following damage to the prefrontal cortex in the rhesus monkey (macaca mulatta). *Behavioural Neuroscience, 123*, pp 231-241.

Morris, J. C. (1993). The Clinical Dementia Rating (CDR): current version and scoring rules. *Neurology, 43,* pp 2412-2414.

Morris, R. G., Garrud, P., Rawlins, J. N. & O'Keefe, J. (1982). Place navigation impaired in rats with hippocampal lesions. *Nature, 297,* pp 681-683.

Morris, R. G., Schenk, F., Tweedie, F. & Jarrad, L. E. (1990). Ibotenate lesions of hippocampus and/or subiculum: Dissociating components of allocentric spatial learning. *The European Journal of Neuroscience, 2,* pp 1016-1028.

Moser, M. B., Moser, E., Forrest, E., Andersen, P. & Morris, R. G. (1995). Spatial learning with a minislab in the dorsal hippocampus. *Proceedings of the National Academy of Sciences of the United States of America, 92,* pp 9697-9701.

Moss, M., Mahut, H. & Zola-Morgan, S. (1981). Concurrent discrimination learning of monkeys after hippocampal, entorhinal, or fornix lesions. *The Journal of Neuroscience, 1,* pp 227-240.

Mueller, S. G. & Weiner, M. W. (2009). Selective effect of age, Apo e4, and Alzheimer's disease on hippocampal subfields. *Hippocampus, 19,* pp 558-564.

Mueller, S. G., Stables, L., Du, A. T., Schuff, N., Truran, D., Cashdollar, N. & Weiner, M. W. (2007). Measurement of hippocampal subfields and age-related changes with high resolution MRI at 4T. *Neurobiology of Aging, 28,* pp 719-726.

Mufson, E. J. & Pandya, D. N. (1984). Some observations on the course and composition of the cingulum bundle in the rhesus monkey. *The Journal of Comparative Neurology, 225,* pp 31-43.

Mufson, E. J., Binder, L., Counts, S. E., DeKosky, S. T., de Toledo-Morrell, L., Ginsberg, S. D., Ikonomovic, M. D., Perez, S. E. & Scheff, S. W. (2012). Mild cognitive impairment: pathology and mechanisms. *Acta Neuropathologica, 123,* pp 13-30.

Muftuler, L. T. & Nalcioglu, O. (2000). Improvement of temporal resolution in fMRI using slice phase encode reordered 3D EPI. *Magnetic Resonance in Medicine, 44,* pp 485-490.

Muir, J. L., Everitt, B. J. & Robbins, T. W. (1994). AMPA-induced excitotoxic lesions of the basal forebrain: a significant role for the cortical cholinergic system in attentional function. *The Journal of Neuroscience, 14,* pp 2313-2326.

Muller, R. U. & Kubie, J. L. (1989). The firing of hippocampal place cells predicts the future position of freely moving rats. *The Journal of Neuroscience, 9,* pp 4101-4110.

Mumby, D. G. (2001). Perspective on object-recognition memory following hippocampal damage: lessons from studies in rats. *Behavioural Brain Research, 127,* pp 159-181.

Mundy, M. E., Downing, P. E., Dwyer, D. M., Honey, R. C. & Graham, K. S. (2013). A critical role for the hippocampus and perirhinal cortex in perceptual learning of scenes and faces: complementary findings from amnesia and fMRI. *The Journal of Neuroscience,* 33, pp 10490-10502.

Muranishi, M., Inokawa, H., Yamada, H., Ueda, Y., Matsumoto, N., Nakagawa, M. & Kimura, M. (2011). Inactivation of the putamen selectively impairs rewards history-based action selection. *Experimental Brain Research, 209*, pp 235-246.

Murray, E. A. & Mishkin, M. (1998). Object recognition and location memory in monkeys with excitotoxic lesions of the amygdala and hippocampus. *The Journal of Neuroscience, 18,* pp 6568-6582.

Murray, E, A. & Richmond, B. J. (2001). Role of perirhinal cortex in object perception, memory, and associations. *Current Opinion in Neurobiology, 11,* pp 188-193.

Murray, E. A., Bussey, T. J. & Saksida, L. M. (2007). Visual perception and memory: a new view of medial temporal function in primates and rodents. *Annual Review of Neuroscience, 30,* pp 99-122.

Murray, E. A., Davidson, M., Gaffan, D., Olton, D. S. & Suomi, S. (1989). Effects of fornix transection and cingulate cortical ablation on spatial memory in rhesus monkeys. *Experimental Brain Research, 74*, pp 173-186.

Murty, V. P., Ritchey, M., Adcock, R. A. & LaBar, K. S. (2010). fMRI studies of successful emotional memory encoding: a quantitative meta-analysis. *Neuropsychologia, 48,* pp 3459-3469.

Naber, P. A. & Witter, M. P. (1998). Subicular efferents are organized mostly as parallel projections: a double-labeling, retrograde-tracing study in the rat. *The Journal of Comparative Neurology, 393*, pp 84-297.

Naber, P. A., Caballero-Bleda, M., Jorritsma-Byham, B. & Witter, M. P. (1997). Parallel input to the hippocampal memory system through peri- and postrhinal cortices. *Neuroreport, 8,* pp 2617-2621.

Naber, P. A., Lopes da Silva, F. H. & Witter, M. P. (2001a). Reciprocal connections between the entorhinal cortex and hippocampal fields CA1 and the subiculum are in register with the projections from CA1 to the subiculum. *Hippocampus, 11,* pp 99-104.

Naber, P. A., Witter, M. P., Lopes da Silva, F. H. (2000). Networks of the hippocampal memory system of the rat. The pivotal role of the subiculum. *Annals of the New York Academy of Sciences, 911,* pp 392-403.

Naber, P. A., Witter, M. P. & Lopes da Silva, F. H. (2001b). Evidence for a direct projection from the postrhinal cortex to the subiculum in the rat. *Hippocampus, 11,* pp 105-117.

Nakamura, N. H., Flasbeck, V., Maingret, N., Kitsukawa, T. & Sauvage, M. M. (2013) Proximodistal segregation of nonspatial information in CA3: preferential recruitment of

a proximal CA3-distal CA1 network in nonspatial recognition memory. *The Journal of Neuroscience, 33,* pp 11506-11514.

Nakazawa, Y., Pevzner, A., Tanaka, K. Z., Wiltgen, B. J. (2016). Memory retrieval along the proximodistal axis of CA1. *Hippocampus, 26,* pp 1140-1148.

Nauta, W. J. (1972). Neural associations of the frontal cortex. *Acta Neurobiologiae Experimentalis, 32,* pp 125-140.

Neave, N., Nagle, S. & Aggleton, J. P. (1997). Evidence for the involvement of the mammillary bodies and cingulum bundle in allocentric spatial processing by rats. *The European Journal of Neuroscience, 9,* pp 941-955.

Nelson, A. J. & Vann, S. D. (2014). Mammilliothalamic tract lesions disrupt tests of visuo-spatial memory. *Behavioral Neuroscience, 128,* pp 494-503.

Nelson, H. E. & Willison, J. (1991). *The National Adult Reading Test-Revised (NART-R): test manual (2nd Ed).* Windsor, UK: National Foundation for Educational Research–Nelson.

Nestor, P. G., Kubicki, M., Spencer, K. M., Niznikiewicz, M., McCarley, R. W. & Shenton, M. E. (2007). Attentional networks and cingulum bundle in chronic schizophrenia. *Schizophrenia Research, 90,* pp 308-315.

Neunuebel, J. P. & Knierim, J. J. (2014). CA3 retrieves coherent representations from degraded input: direct evidence for CA3 pattern completion and dentate gyrus pattern separation. *Neuron, 81,* pp 416-427.

Norman, K. A. (2010). How hippocampus and cortex contribute to recognition memory: revisiting the complementary learning systems model. *Hippocampus, 20,* pp 1217-1227.

O'Mara, S. M. (1995). Spatially selective firing properties of hippocampal formation neurons in rodents and primates. *Progress in Neurobiology, 45,* pp 253-274.

O'Mara, S. M. (2005). The subiculum: what it does, what it might do, and what neuroanatomy has yet to tell us. *Journal of Anatomy, 207,* pp 271-282.

O'Mara, S. M., Commins S., Anderson, M. & Gigg, J. (2001). The subiculum: a review of form, physiology and function. *Progress in Neurobiology, 64,* pp 129-155.

O'Mara, S. M., Rolls, E. T., Berthoz, A. & Kesner, R. P. (1994). Neurons responding to whole-body motion in the primate hippocampus. *The Journal of Neuroscience, 14,* pp 6511-6523.

O'Mara, S. M., Sanchez-Vives, M. V., Brotons-Mas, J. R. & O'Hare, E. O. (2009). Roles for the subiculum in spatial information processing, memory, motivation and the temporal control of behaviour. *Progress in Neuro-Psychopharmacology & Biological Psychiatry, 33,* pp 782-790.

Oberhuber, M., Jones, O. P., Hope, T. M. H., Prejawa, S., Seghier, M. L., Green, D. W. & Price, C. J. (2013). Functionally distinct contributions of the anterior and posterior putamen during sublexical and lexical reading. *Frontiers in Human Neuroscience, 7*, pp 1-10.

Oishi, K., Mielke, M. M., Albert, M., Lyketsos, C. G. & Mori, S. (2012). The fornix sign: a potential sign for Alzheimer's disease based on diffusion tensor imaging. *Journal of Neuroimaging, 22*, pp 365-374.

O'Keefe, J. (1979). A review of the hippocampal place cells. *Progress in Neurobiology, 13*, pp 419-439.

Olszewski, I. (1952). *The Thalamus of the Macaca mulatta. An atlas for use with the stereotaxic instrument.* New York, US: Karger.

Olton, D. S., Walker, J. A. & Gage, F. H. (1978). Hippocampal connections and spatial discrimination. *Brain Research, 139*, pp 295-308.

Papez, J. W. (1937). A proposed mechanism of emotion. *The Journal of Psychiatry and Clinical Neurosciences, 7*, pp 103-112.

Park, S. A., Hahn, J. H., Kim, J. I., Na, D. L. & Huh, K. (2000). Memory deficits after bilateral anterior fornix infarction. *Neurology, 54*, pp 1379-1382.

Parker, A. & Gaffan, D. (1997a). Mammillary body lesions in monkeys impair object-in-place memory: Functional unity of the fornix-mammillary system. *Journal of Cognitive Neuroscience, 9*, pp 512-521.

Parker, A. & Gaffan, D. (1997b). The effect of anterior thalamic and cingulate cortex lesions on object-in-place memory in monkeys. *Neuropsychologia, 35*, pp 1093-1102.

Parkinson, J. K., Murray, E. A. & Mishkin, M. (1988). A selective mnemonic role for the hippocampus in monkeys: memory for the location of objects. *The Journal of Neuroscience, 8*, pp 4159-4167.

Pasternak, O., Sochen, N., Gur, Y., Intrator, N. & Assaf, Y. (2009). Free water elimination and mapping from diffusion MRI. *Magnetic Resonance in Medicine, 62*, pp 717-730.

Paxinos, G. & Watson, C. (2004). *The Rat Brain in Stereotaxic Co-ordinates* (5th edition). Amsterdam, Netherlands: Elsevier Academic Press.

Paxinos, G., Huang, X., Petrides, M. & Toga, A. (2009). *The Rhesus monkey brain: in stereotaxic co-ordinates* (2nd edition). California, USA: Academic Press.

Penfield, W. & Milner, B. (1958). Memory deficit produced by bilateral lesions in the hippocampal zone. *AMA Archives of Neurology and Psychiatry, 79*, pp 475-497.

Penke, Z., Morice, E., Veyrac, A., Gros, A., Chagneau, C., LeBlanc, P., Samson, N., Baumgärtel, K., Mansuy, I. M., Davis, S. & Laroche, S. (2013). Zif268/Egr1 gain of function facilitates hippocampal synaptic plasticity and long-term spatial recognition memory. *Philosophical Transactions of the Royal Society of London Series B, Biological Sciences, 369,* doi:10.1098/rstb.2013.0159.

Perry, V. H. & Linden, R. (1982). Evidence for dendritic competition in the developing retina. *Nature, 297,* pp 683-685.

Petersen, R. C., Jack, C. R., Jr., Xu, Y. C., Waring, S. C., O'Brien, P. C., Smith, G. E., Ivnik, R. J., Tangalos, E. G., Boeve, B. E. & Kokmen, E. (2000). Memory and MRI-based hippocampal volumes in aging and AD. *Neurology, 54*, pp 581-587.

Petridou, N., Italiaander, M., van de Bank, B. L., Siero, J. C., Luijten, P. R. & Klomp, D. W. (2013). Pushing the limits of high-resolution functional MRI using a simple high-density multi-element coil design. *NMR in Biomedicine, 26,* pp 65-73.

Phelps, E. A. & LeDoux, J. E. (2005). Contributions of the amygdala to emotion processing: from animal models to human behavior. *Neuron, 48,* pp 175-187.

Pierpaoli, C. & Basser, P. J. (1996). Toward a quantitative assessment of diffusion anisotropy. *Magnetic Resonance in Medicine, 36,* pp 893-906.

Pierpaoli, C. (2011). Artifacts in Diffusion MRI. In D. K. Jones (Ed.), *Diffusion MRI: Theory, Methods and Applications* (pp 303-318). Oxford, UK: Oxford University Press.

Poirier, G. L., Amin, E., & Aggleton, J. P. (2008). Qualitatively different hippocampal subfield engagement emerges with mastery of a spatial memory task by rats. *The Journal of Neuroscience, 28,* pp 1034-1045.

van de Pol, L. A., Hensel, A., van der Flier, W. A., Visser, P. J., Pijnenburg, Y. A. L., Barkhof, F., Gertz, H. J. & Scheltens, P. (2006). Hippocampal atrophy on MRI in frontotemporal lobar degeneration and Alzheimer's disease. *Journal of Neurology, Neurosurgery and Psychiatry, 77,* pp 439-442.

Poletti, C. E. & Creswell, G. (1977). Fornix system efferent projections in the squirrel monkey: an experimental degeneration study. *The Journal of Comparative Neurology, 175,* pp 101-127.

Poletti, C. E. & Sujatanond, M. (1980). Evidence for a second hippocampal efferent pathway to hypothalamus and basal forebrain comparable to fornix system: a unit study in the awake monkey. *Journal of Neurophysiology, 44,* pp 514-531.

Poppenk, J., Evensmoen, H. R., Moscovitch, M. & Nadel, L. (2013). Long-axis specialization of the human hippocampus. *Trends in Cognitive Sciences, 17,* pp 230-240.

Poppenk, J. & Moscovitch, M. (2011). A hippocampal marker of recollection memory ability among healthy young adults: contributions of posterior and anterior segments. *Neuron, 72,* pp 931-937.

Poreh, A., Winocur, G., Moscovitch, M., Backon, M., Goshen, E., Ram, Z. & Feldman, Z. (2006). Anterograde and retrograde amnesia in a person with bilateral fornix lesions following removal of a colloid cyst. *Neuropsychologia, 44,* pp 2241-2248.

Potvin, O., Allen, K., Thibaudeau, G., Doré, F. Y. & Goulet, S. (2006). Performance on spatial working memory tasks after dorsal or ventral hippocampal lesions and adjacent damage to the subiculum. *Behavioral Neuroscience, 120,* pp 413-422.

Potvin, O., Doré, F. Y. & Goulet, S. (2007). Contributions of the dorsal hippocampus and the dorsal subiculum to processing of idiothetic information and spatial memory. *Neurobiology of Learning and Memory, 87,* pp 669-678.

Potvin, O., Doré, F. Y. & Goulet, S. (2009). Lesions of the dorsal subiculum and the dorsal hippocampus impaired pattern separation in a task using distinct and overlapping visual stimuli. *Neurobiology of Learning and Memory, 91,* pp 287-297.

Potvin, O., Lemay, F., Dion, M., Corado, G., Doré, F. Y. & Goulet, S. (2010). Contribution of the dorsal subiculum to memory for temporal order and novelty detection using objects, odors, or spatial locations in the rat. *Neurobiology of Learning and Memory, 93,* pp 330-336.

Powell, J., Lewis, P. A., Roberts, N., Garcia-Fiñana, M. & Dunbar, R. I. M. (2012). Orbital prefrontal cortex volume predicts social network size: An imaging study of individual differences in humans. *Proceedings of the Royal Society B - Biological Sciences, 279,* pp 2157-2162.

Powell, T. P. S., Guillery, R. W. & Cowan, W. M. (1957). A quantitative study of the fornixmamillo-thalamic system. *Journal of Anatomy, 91,* pp 419-437.

Ramnani, N., Elliott, R., Athwal, B. S. & Passingham, R. E. (2004). Prediction error for free monetary reward in the human prefrontal cortex. *NeuroImage, 23*, pp 777-786.

Ranganath, C. & Ritchey, M. (2012). Two cortical systems for memory-guided behaviour. *Nature Reviews Neuroscience, 13*, pp 713-726.

Randolph, C., Tierney, M. C., Mohr, E. & Chase, T. N. (1998). The repeatable battery for the assessment of neuropsychological status (RBANS): preliminary clinical validity. *Journal of Clinical and Experimental Neuropsychology, 20,* pp 310-319.

Ray, N. J., Metzler-Baddeley, C., Khondoker, M. R., Grothe, M. J., Teipel, S., Wright, P., Helmut, H., Jones, D. K., Aggleton, J. P. & O'Sullivan, M. J. (2015). Cholinergic basal forebrain structure influences the reconfiguration of white matter connections to support residual memory in Mild Cognitive Impairment. *The Journal of Neuroscience, 35*, pp 739-747.

Reverberi, C., Görgen, K. & Haynes, J. D. (2012). Compositionality of rule representations in human prefrontal cortex. *Cerebral Cortex, 22,* pp 1237-1246.

Ringo, J. L. (1996). Stimulus specific adaptation in inferior temporal and medial temporal cortex of the monkey. *Behavioural Brain Research, 76*, pp 191-197.

Risbrough, V., Bontempi, B. & Menzaghi, F. (2002). Selective immunolesioning of the basal forebrain cholinergic neurons in rats: effect on attention using the 5-choice serial reaction time task. *Psychopharmacology, 164,* pp 71-81.

Ritchey, M., Libby, L. A. & Ranganath, C. (2015). Cortico-hippocampal systems involved in memory and cognition: the PMAT framework. *Progress in Brain Research, 19,* pp 45-64.

Roitman, J. D. & Loriaux, A. L. (2014). Nucleus accumbens responses differentiate execution and restraint in reward-directed behavior. *Journal of Neurophysiology, 111*, pp 350-360.

Rolls, E. T. & O'Mara, S. M. (1995). View-responsive neurons in the primate hippocampal complex. *Hippocampus, 5,* pp 409-424.

Rolls, E. T. & Wilson, F. A. (1990). Learning and memory is reflected in the responses of reinforcement- related neurons in the primate basal forebrain. *The Journal of Neuroscience, 10*, pp 124-1267.

Rolls, E. T. & Xiang, J. Z. (2005). Reward-spatial view representations and learning in the primate hippocampus. *The Journal of Neuroscience, 25,* pp 6167-6174.

Rolls, E. T. & Xiang, J. Z. (2006). Spatial view cells in the primate hippocampus and memory recall. *Reviews in the Neurosciences, 17,* pp 175-200.

Rolls, E. T. (1990). A theory of emotion, and its application to understanding the neural basis of emotion. *Cognition and Emotion, 4,* pp 161-190.

Rolls, E. T., Miyashita, Y., Cahusac, P. M., Kesner, R. P., Niki, H., Feigenbaum, J. D. & Bach, L. (1989). Hippocampal neurons in the monkey with activity related to the place in which a stimulus is shown. *The Journal of Neuroscience, 9,* pp 1835-1845.

Rolls, E. T., Robertson, R. G. & Georges-François, P. (1997). Spatial view cells in the primate hippocampus. *The European Journal of Neuroscience, 9,* pp 1789-1794.

Rosene, D. L. & Van Hoesen, G. W. (1977). Hippocampal efferents reach widespread areas of cerebral cortex and amygdala in rhesus monkey. *Science, 198,* pp 315-317.

Rosene, D. L., Roy, N. J. & Davis, B. J. (1986). A cryoprotection method that facilitates cutting frozen sections of whole monkey brains for histological and histochemical processing without freezing artifact. *The Journal of Histochemistry and Cytochemistry, 34,* pp 1301-1315.

Rudebeck, S. R., Scholz, J., Millington, R., Rohenkohl, G., Johansen-Berg, H., & Lee, A. C. (2009). Fornix microstructure correlates with recollection but not familiarity memory. *The Journal of Neuroscience, 29,* pp 14987-14982.

Rugg, M. D., Vilberg, K. L., Mattson, J. T., Yu, S. S., Johnson, J. D. & Suzuki, M. (2012). Item memory, context memory and the hippocampus: fMRI evidence. *Neuropsychologia, 50,* pp 3070-3079.

Rupniak, N. M. J. & Gaffan, D. (1987). Monkey hippocampus and learning about spatially directed movements. *The Journal of Neuroscience, 7,* pp 2331-2337.

Ruth, R. E., Collier, T. J. & Routtenberg, A. (1982). Topography between the entorhinal cortex and the dentate septotemporal axis in the rats: I. Medial and intermediate entorhinal projecting cells. *The Journal of Comparative Neurology, 209,* pp 69-78.

Ruth, R. E., Collier, T. J. & Routtenberg, A. (1988). Topographical relationship between the entorhinal cortex and the septotemporal axis of the dentate gyrus in rats: II. Cells projecting from lateral entorhinal subdivisions. *The Journal of Comparative Neurology, 270,* pp 506-516.

Rye, D. B., Wainer, B. H., Mesulam, M. M., Mufson, E. J. & Saper, C. B. (1984). Cortical projections arising from the basal forebrain: a study of cholinergic and noncholinergic components employing combined retrograde tracing and immunohistochemical localization of choline acetyltransferase. *Neuroscience, 13,* pp 627-643.

Sakurai, Y. (2002). Coding of auditory temporal and pitch information by hippocampal individual cells and cell assemblies in the rat. *Neuroscience, 115,* pp 1153-1163.

Salamone, J. D. (1994). The involvement of nucleus accumbens dopamine in appetitive and aversive motivation. *Behavioural Brain Research, 61,* pp 117-133.

Salamone, J. D., Correa, M., Farrar, A. & Mingote, S. M. (2007). Effort-related functions of nucleus accumbens dopamine and associated forebrain circuits. *Psychopharmacology, 191,* pp 461-482.

Santín, L. J., Aguirre, J. A., Rubio, S., Begega, A., Miranda, R. & Arias, J. L. (2003). c-Fos expression in supramammillary and medial mammillary nuclei following spatial reference and working memory tasks. *Physiology & Behaviour, 78,* pp 733-739.

Sargolini, F., Fyhn, M., Hafting, T., McNaughton, B. L., Witter, M. P., Moser, M. B., Moser, E. I. (2006). Conjunctive representation of position, direction, and velocity in entorhinal cortex. *Science, 312,* pp 758-762.

Saunders, R. C. & Aggleton, J. P. (2007). Origin and topography of fibres contributing to the fornix in macaque monkeys. *Hippocampus, 17,* pp 396-411.

Saunders, R. C. & Rosene, D. L. (1988). A comparison of the efferents of the amygdala and the hippocampal formation in the rhesus monkey: I. Convergence in the entorhinal, prorhinal, and perirhinal cortices. *The Journal of Comparative Neurology, 271,* pp 153-184.

Saunders, R. C., Mishkin, M. & Aggleton, J. P. (2005). Projections from the entorhinal cortex, perirhinal cortex, presubiculum, and parasubiculum to the medial thalamus in macaque monkeys: identifying different pathways using disconnection techniques. *Experimental Brain Research, 167,* pp 1-16.

Saunders, R. C., Vann, S. D. & Aggleton, J. P. (2012). Projections from Gudden's tegmental nuclei to the mammillary body region in the cynomolgus monkey (Macaca fascicularis). *The Journal of Comparative Neurology, 520,* pp 1128-1145.

Schacter, D. L. (1987). Implicit memory: history and current status. *Journal of Experimental Psychology, 13,* pp 501-518.

Schlichting, M. L., Zeithamova, D. & Preston, A. R. (2014). CA1 subfield contributions to memory integration and inference. *Hippocampus, 24,* pp 1248-1260.

Schmahmann J. D. & Pandya, D. N. (2006). *Fibre pathways of the brain.* New York, US: Oxford University Press.

Schneider, C. A., Rasband, W. S. & Eliceiri, K. W. (2012). NIH Image to ImageJ: 25 years of image analysis. *Nature Methods, 9,* pp 671-675.

Schultz, H., Sommer, T. & Peters, J. (2012). Direct evidence for domain-sensitive functional subregions in human entorhinal cortex. *The Journal of Neuroscience, 32,* pp 4716-4723.

Scott, B. H., Leccese, P. A., Saleem, K. S., Kikuchi, Y., Mullarkey, M. P., Fukushima, M., Mishkin, M., & Saunders, R. C. (2015). Intrinsic connections of the core auditory cortical regions and rostral supratemporal plane in the macaque monkey. *Cerebral Cortex.* Advance online publication. pii:bhv277.

Scoville, W. M. & Milner, B. (1957). Loss of recent memory after bilateral hippocampal lesions. *Journal of Neurology, Neurosurgery and Psychiatry, 20*, pp 11-21.

Segal, M. & Landis, S. C. (1974). Afferents to the septal area of the rat studied with the method of retrograde axonal transport of horseradish peroxidase. *Brain Research, 82,* pp 263-268.

Seghier, M. L. & Price, C. J. (2010). Reading aloud boosts connectivity through the putamen. *Cerebral Cortex, 20,* pp 570-582.

Sergerie, K., Chochol, C. & Armony, J. L. (2008). The role of the amygdala in emotional processing: a quantitative meta-analysis of functional neuroimaging studies. *Neuroscience and Biobehavioral Reviews, 32,* pp 811-830.

Sesack, S. R., Deutch, A. Y., Roth, R. H. & Bunney, B. S. (1989). Topographical organization of the efferent projections of the medial prefrontal cortex in the rat: an anterograde tract-tracing study with Phaseolusulgaris vulgaris leucoagglutinin. *The Journal of Comparative Neurology, 290,* pp 213–242.

Sexton, C. E., Mackay, C. E., Lonie, J. A., Bastin, M. E., Terrière, E., O'Carroll, R. E. & Ebmeier, K. P. (2010). MRI correlates of episodic memory in Alzheimer's disease, mild cognitive impairment, and healthy aging. *Psychiatry Research, 184,* pp 57-62.

Shah, A., Jhawar, S. S. & Goel, A. (2012). Analysis of the anatomy of the Papez circuit and adjoining limbic system by fibre dissection techniques. *Journal of Clinical Neuroscience, 19,* pp 289-298.

Sharp, P. E. & Green, C. (1994). Spatial correlates of firing patterns of single cells in the subiculum of the freely moving rat. *The Journal of Neuroscience, 14*, pp 2339-2356.

Sheikh, J. I. & Yesavage, J. A. (1986). Geriatric Depression Scale (GDS): recent evidence and development of a shorter version. In T. L. Brink (Ed.) *Clinical gerontology: a guide to assessment and intervention* (pp 165-173). New York, US: Haworth.

Sheng, M. & Greenberg, M. E. (1990). The regulation and function of c-fos and other immediate early genes in the nervous system. *Neuron, 4*, pp 477-485.

Shenhav, A., Barrett, L. F. & Bar, M. (2013). Affective value and associative processing share a cortical substrate. *Cognitive, Affective, and Behavioral Neuroscience, 13*, pp 46-59.

Shi, C., Xie, G., Zhang, X., Su, S., Zhang, Y., Zhang, L., Qiu, B. & Liu, X. (2015). High spatiotemporal resolution fMRI using partial separability model. *Bio-medical Materials and Engineering, 26*, pp 1439-1446.

Shibata, H. (1992). Topographic organization of subcortical projections to the anterior thalamic nuclei in the rat. *The Journal of Comparative Neurology, 323*, pp 117-127.

Shibata, H. (1993a). Efferent projections from the anterior thalamic nuclei to the cingulate cortex in the rat. *The Journal of Comparative Neurology, 330*, pp 533-542.

Shibata, H. (1993b). Direct projections from the anterior thalamic nuclei to the retrohippocampal region in the rat. *The Journal of Comparative Neurology, 337,* pp 431-445.

Shipton, O. A., El-Gabv, M., Apergis-Schoute, J., Deisseroth, K., Bannerman, D. M., Paulsen, O. & Kohl, M. M. (2014). Left-right dissociation of hippocampal memory processes in mice. *Proceedings of the National Academy of Sciences of the United States of America, 111,* pp 15238-15243.

Sikes, R. W., Chronister, R. B., White, J. R. (1977). Origin of the direct hippocampus-anterior thalamic bundle in the rat: a combined horseradish peroxidase-Golgi analysis. *Experimental Neurology, 57,* pp 379-395.

Simons, J. S. & Spiers, H. J. (2003). Prefrontal and medial temporal lobe interactions in long-term memory. *Nature Review Neuroscience, 4,* pp 637-648.

Smith, C. D., Lori, N. F., Akbudak, E., Sorar, E., Gultepe, E., Shimony, J. S., McKinstry, R. C. & Conturo, T. E. (2009). MRI diffusion tensor tracking of a new amygdalo-fusiform and hippocampo-fusiform pathway system in humans. *Journal of Magnetic Resonance Imaging, 29,* pp 1248–1261.

Smith, M. L. & Milner, B. (1981). The role of the right hippocampus in the recall of spatial location. *Neuropsychologia, 19,* pp 781-793.

Smith, S. M., De Stefano, N., Jenkinson, N. & Matthews, P. M. (2001). Normalised accurate measurement of longitudinal brain change. *Journal of Computer Assisted Tomography, 25,* pp 466-475.

Smith, S. M., Jenkinson, M., Woolrich, M. W., Beckmann, C. F., Behrens, T. E., Johansen-Berg, H., Bannister, P. R., De Luca, M., Drobnjak, I., Flitney, D. E., Niazy, R. K., Saunders, J., Vickers, J., Zhang, Y., De Stefano, N., Brady, J. M. & Matthews, P. M. (2004). Advances in functional and structural MR image analysis and implementation as FSL. *NeuroImage, 23,* pp 208-219.

Smith, S. M., Zhang, Y., Jenkinson, M., Chen, J., Matthews, P. M., Federico, A. & De Stefano, N. (2002). Accurate, robust and automated longitudinal and cross-sectional brain change analysis. *NeuroImage, 17,* pp 479-489.

Sobotka, S. & Ringo, J. L. (1993). Investigations of long-term recognition and association memory in unit responses from inferotemporal cortex. *Experimental Brain Research, 96,* pp 28-38.

Solstad, T., Boccara, C. N., Kropff, E., Moser, M. B., & Moser, E. I. (2008). Representation of geometric borders in the entorhinal cortex. *Science, 322,* pp 1865-1868.

Spiers, H. J., Maguire, E. A. & Burgess, N. (2001). Hippocampal amnesia. *Neurocase, 7,* pp 357-382.

Stenson, S. M. & Roth, B. L. (2014). Chemogenetic tools to interrogate brain functions. *Annual Review of Neuroscience, 37,* pp 387-407.

Stern, C. E. & Passingham, R. E. (1995). The nucleus accumbens in monkeys (macaca fascicularis). III. Reversal Learning. *Experimental Brain Research, 106*, pp 239-247.

Storey, J. D. (2003). The positive false discovery rate: a Bayesian interpretation and the *q*-value. *Annals of Statistics, 31,* pp 2013-2035.

Strange, B. A., Witter, M. P., Lein, E. S. & Moser, E. I. (2014). Functional organization of the hippocampal longitudinal axis. *Nature Reviews Neuroscience, 15,* pp 655-669.

van Strien, N. M., Cappaert, N. L. & Witter, M. P. (2009). The anatomy of memory: an interactive overview of the parahippocampal-hippocampal network. *Nature Reviews Neuroscience, 10,* pp 272–282.

Suthana, N. A., Donix, M., Wozny, D. R., Bazih, A., Jones, M., Heidemann, R. M., Trampel, R., Ekstrom, A. D., Scharf, M., Knowlton, B., Turner, R. & Bookheimer, S. Y. (2015). High-resolution 7T fMRI of human hippocampal subfields during associative learning. *Journal of Cognitive Neuroscience, 27,* pp 1194-1206.

Suthana, N. A., Ekstrom, A. D., Moshirvaziri, S., Knowlton, B. & Bookheimer, S. Y. (2009). Human hippocampal CA1 involvement during allocentric encoding of spatial information. *The Journal of Neuroscience, 29,* pp 10512–10519.

Sutherland, R. J. & Rodriguez, A. J. (1989). The role of the fornix/fimbria and some related subcortical structures in place learning and memory. *Behavioural Brain Research, 32,* pp 265-277.

Suzuki, W. A. & Amaral, D. G. (1990). Cortical inputs to the CA1 field of the monkey hippocampus originate from the perirhinal and parahippocampal cortex but not from area TE. *Neuroscience Letters, 115*, pp 43-48.

Swanson, L. W. & Cowan, W. M. (1977). An autoradiographic study of the organization of the efferent connections of the hippocampal formation in the rat. *The Journal of Comparative Neurology, 172,* pp 49-84.

Swanson, L. W. (1977). The anatomical organization of septo-hippocampal projections. *Ciba Foundation Symposium, 58,* pp 25-48.

Swanson, L. W. (1992). *Structure of the rat brain. Brain maps.* Amsterdam: Elsevier.

Swanson, L. W., Kohler, C. & Bjorklund, A. (1987). The limbic region. I: the septohippocampal system. In Bjorklund, A., Hokfelt, T. & Swanson, L. W. (Eds.), *Handbook of Chemical Neuroanatomy, vol 5. Integrated Systems of the CNS, Part 1* (pp 125-277). Amsterdam: Elsevier.

Sziklas, V. & Petrides, M. (2002). Effects of lesions to the hippocampus or the fornix on allocentric conditional associative learning in rats. *Hippocampus, 12,* pp 543–550.

Sziklas, V., Lebel, S., & Petrides, M. (1998). Conditional associative learning and the hippocampal system. *Hippocampus, 8,* pp 131-137.

Takagishi, M. & Chiba, T. (1991). Efferent projections of the infralimbic (area 25) region of the medial prefrontal cortex in the rat: an anterograde tracer PHA-L study. *Brain Research, 566,* pp 26–39.

Tanaka, H., Hoshino, Y., Watanabe, Y., Sakurai, K., Takekawa, H. & Hirata, K. (2012). A case of strategic-infarct mild cognitive impairment. *Neurologist, 18*, pp 211-213.

Tanaka, Y., Miyazawa, Y., Akaoka, F. & Yamada, T. (1997). Amnesia following damage to the mammillary bodies. *Neurology, 48,* pp 160-165.

Taube, J. S. (2007). The head direction signal: origins and sensory-motor integration. *Annual Review of Neuroscience, 30,* pp 181-207.

Tischmeyer, W. & Grimm, R. (1999). Activation of immediate early genes and memory formation. *Cellular and Molecular Life Sciences, 55,* pp 564-574.

Thiebaut de Schotten, M., Ffytche, D. H., Bizzi, A, Dell'Acqua, F., Allin, M., Walshe, M., Murray, R., Williams, S. C., Murphy, D. G. & Catani M. (2011). Atlasing location, asymmetry and inter-subject variability of white matter tracts in the human brain with MR diffusion tractography. *NeuroImage, 54,* pp 49-59.

Thomas, G. J. (1978). Delayed alternation in rats after pre- or postcommissural fornicotomy. *Journal of Comparative and Physiological Psychology, 92*, pp 1128-1136.

de Toledo-Morrell, L., Dickerson, B., Sullivan, M. P., Spanovic, C., Wilson, R. & Bennett, D. A. (2000). Hemispheric differences in hippocampal volume predict verbal and spatial memory performance in patients with Alzheimer's disease. *Hippocampus, 10,* pp 136-42.

Toscano, C. D., McGlothan, J. L. & Guilarte, T. R. (2006). Experience-dependent regulation of zif268 gene expression and spatial learning. *Experimental Neurology, 200,* pp 209-215.

Tournier, J. D., Calamante, F. & Connelly, A. (2007). Robust determination of the fibre orientation distribution in diffusion MRI: non-negativity constrained super-resolved spherical deconvolution. *NeuroImage, 35,* pp 1459-1472.

Tournier, J. D., Calamante, F. & Connelly, A. (2013). Determination of the appropriate b value and number of gradient directions for high-angular-resolution diffusion-weighted imaging. *NMR in Biomedicine, 26,* pp 1775-1786.

Tournier, J. D., Calamante, F., Gadian, D. G. & Connelly, A. (2004). Direct estimation of the fibre orientation density function from diffusion-weighted MRI data using spherical deconvolution. *NeuroImage, 23*, pp 1176-1185.

Tournier, J. D., Yeh, C. H., Calamante, F., Cho, K. H., Connelly, A. & Lin, C. P. (2008). Resolving crossing fibres using constrained spherical deconvolution: validation using diffusion-weighted imaging phantom data. *NeuroImage, 42,* pp 617-625.

Trenerry, M. R., Crosson, B., DeBoe, J. & Leber, W. R. (1989). *Stroop Neuropsychological Screening Test.* Florida, USA: Psychological Assessment Resources.

Trenerry, M. R., Jack, C. R., Jr., Ivnik, R. J., Sharbrough, F. W., Cascino, G. D., Hirschorn, K. A., Marsh, W. R., Kelly, P. J. & Meyer, F. B. (1993). MRI hippocampal volumes and memory function before and after temporal lobectomy. *Neurology, 43*, pp 1800-1805.

Tsanov, M., Chah, E., Vann, S. D., Reilly, R. B., Erichsen, J. T., Aggleton, J. P. & O'Mara, S. M. (2011). Theta-modulated head direction cells in the rat anterior thalamus. *The Journal of Neuroscience, 31*, pp 9489-502.

Tsivilis, D., Vann, S. D., Denby, C., Roberts, N., Mayes, A. R., Montaldi, D. & Aggleton, J. P. (2008). A disproportionate role for the fornix and mammillary bodies in recall versus recognition memory. *Nature Neuroscience, 11*, pp 834-842.

Tuch, D. S., Reese, T. G., Wiegell, M. R., Makris, N., Belliveau, J. W. & Wedeen, V. J. (2002). High angular resolution diffusion imaging reveals intravoxel white matter fibre heterogeneity. *Magnetic Resonance in Medicine, 48,* pp 577-582.

Tulving, E. & Markowitsch, H. J. (1998). Episodic and declarative memory: role of the hippocampus. *Hippocampus, 8*, pp 198-204.

Tulving, E. (1972). Episodic and semantic memory In Tulving, E. & Donaldson, W. (Eds.), *Organization of Memory* (pp 381-402). New York, US: Academic Press.

Turriziani, P., Serra, L., Fadda, L., Caltagirone, C. & Carlesimo, G. A. (2008). Recollection and familiarity in hippocampal amnesia. *Hippocampus, 18,* pp 469-480.

Tyler, A. L., Mahoney, J. M., Richard, G. R., Holmes, G. L., Lenck-Santini, P. P. & Scott, R. C. (2012). Functional network changes in hippocampal CA1 after status epilepticus predict spatial memory deficits in rats. *The Journal of Neuroscience, 32,* pp 11365-11376.

Uğurbil, K., Xu, J., Auerbach, E. J., Moeller, S., Vu, A. T., Duarte-Carvajalino, J. M., Lenglet, C., Wu, X., Schmitter, S., Van de Moortele, P. F., Strupp, J., Sapiro, G., De Martino, F., Wang, D., Harel, N., Garwood, M., Chen, L., Feinberg, D. A., Smith, S. M., Miller, K. L., Sotiropoulos, S. N., Jbabdi, S., Andersson, J. L., Behrens, T. E., Glasser, M. F., Van Essen, D. C., Yacoub, E., WU-Minn HCP Consortium. (2013). Pushing spatial and temporal resolution for functional and diffusion MRI in the Human Connectome Project. *NeuroImage, 80,* pp 80-104.

Van Hoesen, G. W., Rosene, D. L. & Mesulam, M. M. (1979). Subicular input from temporal cortex in the rhesus monkey. *Science, 205,* pp 608-610.

Van Leemput, K., Bakkour, A., Benner, T., Wiggins, G., Wald, L. L., Augustinack, J., Dickerson, B. C., Golland, P. & Fischl, B. (2009). Automated segmentation of hippocampal subfields from ultra-high resolution in vivo MRI. *Hippocampus, 19,* pp 549-557.

Van der Werf, Y. D., Scheltens, P., Lindeboom, J., Witter, M. P., Uylings, H. B. M. & Jolles, J. (2003). Deficits of memory, executive functioning and attention following infarction in the thalamus; a study of 22 cases with localised lesions. *Neuropsychologia, 41*, pp 1330-1344.

Van der Werf, Y. D., Witter, M. P., Uijlings, H. B. M. & Jolles, J. (2000). Neuropsychology of infarctions in the thalamus: a review. *Neuropsychologia, 38*, pp 613–627.

Vann, S. D. & Aggleton, J. P. (2003). Evidence of a spatial encoding deficit in rats with lesions of the mammillary bodies or mammillothalamic tract. *The Journal of Neuroscience, 23*, pp 3506-3514.

Vann, S. D. & Aggleton, J. P. (2004). The mammillary bodies: two memory systems in one? *Nature Reviews Neuroscience, 5*, pp 35-44.

Vann, S. D. & Nelson, A. J. D. (2015). The mammillary bodies and memory: more than a hippocampal relay. *Progress in Brain Research, 219*, pp 163-185.

Vann, S. D. (2005). Transient spatial deficit associated with bilateral lesions of the lateral mammillary nuclei. *The European Journal of Neuroscience, 21*, pp 820-824.

Vann, S. D. (2010). Re-evaluating the role of the mammillary bodies in memory. *Neuropsychologia, 48*, pp 2316–2327.

Vann, S. D. (2013). Dismantling the Papez circuit for memory in rats. *Elife, 2*, doi: 10.7554/eLife.00736.

Vann, S. D., Aggleton, J. P. & Maguire, E. A. (2009a). What does the retrosplenial cortex do? *Nature Reviews Neuroscience, 10*, pp 792-802.

Vann, S. D., Brown, M. W. & Aggleton, J. P. (2000a). Fos expression in the rostral thalamic nuclei and associated cortical regions in response to different spatial memory tests. *Neuroscience, 101*, pp 983-991.

Vann, S. D., Brown, M. W., Erichsen, J. T. & Aggleton J. P. (2000b). Fos imaging reveals differential patterns of hippocampal and parahippocampal subfield activation in rats in response to different spatial memory tasks. *The Journal of Neuroscience, 20*, pp 2711–2718.

Vann, S. D., Denby, C., Love, S., Montaldi, D., Renowden, S., & Coakham, H. B. (2008). Memory loss resulting from fornix and septal damage: impaired supra-span recall but preserved recognition over a 24-hour delay. *Neuropsychology, 22*, pp 658-668.

Vann, S. D., Erichsen, J. T., O'Mara, S. M. & Aggleton, J. P. (2011). Selective disconnection of the hippocampal formation projections to the mammillary bodies produces only mild deficits on spatial memory tasks: implications for fornix function. *Hippocampus, 21*, pp 945-957.

Vann, S. D., Saunders, R. C. & Aggleton, J. P. (2007). Distinct, parallel pathways link the medial mammillary bodies to the anterior thalamus in macaque monkeys. *The European Journal of Neuroscience, 26,* pp 1575-1586.

Vann, S. D., Tsivilis, D., Denby, C. E., Quamme, J. R., Yonelinas, A. P., Aggleton, J. P., Montaldi, D. & Mayes, A. R. (2009b). Impaired recollection but spared familiarity in patients with extended hippocampal system damage revealed by 3 convergent methods. *Proceedings of the National Academy of Sciences, 106,* pp 5442-5447.

Veazey, R. B., Amaral, D. G. & Cowan, W. M. (1982). The morphology and connections of the posterior hypothalamus in the cynomolgus monkey (Macaca fascicularis). I. Cytoarchitectonic organization. *The Journal of Comparative Neurology, 207,* pp 114-134.

Vertes, R. P., Albo, Z. & Viana Di Prisco, G. (2001). Theta-rhythmically firing neurons in the anterior thalamus: implications for mnemonic functions of Papez's circuit. *Neuroscience, 104,* pp 619-625.

Vertes, R. P., Hoover, W. B. & Viana Di Prisco, G. (2004). Theta rhythm of the hippocampus: subcortical control and functional significance. *Behavioral and Cognitive Neuroscience Reviews, 3,* pp 173-200.

Veyrac, A., Besnard, A., Caboche, J., Davis, S. & Laroche, S. (2014). The transcription factor Zif268/Egr1, brain plasticity, and memory. *Progress in Molecular Biology and Translational Science, 122,* pp 89-129.

Victor, M., Adams, R. D. & Collins, G, H. (1971). The Wernicke-Korsakoff syndrome: a clinical and pathological study of 245 patients, 82 with post-mortem examinations. *Contemporary Neurology Series,* 7, pp 1-206.

Voytko, M. L., Olton, D. S., Richardson, R. T., Gorman, L. K., Tobin, J. R. & Price, D. L. (1994). Basal forebrain lesions in monkeys disrupt attention but not learning and memory. *The Journal of Neuroscience, 14*, pp 167-186.

Wall, P. M. & Messier, C. (2001). The hippocampal formation - orbitomedial prefrontal cortex circuit in the attentional control of active memory. *Behavioural Brain Research, 127,* pp 99-117.

Waltz, J. A., Knowlton, B. J., Holyoak, K. J., Boone, K. B., Mishkin, F. S., De Menezes Santos, M., Thomas, C. R. & Miller, B. L. (1999). A system for relational reasoning in human prefrontal cortex. *Psychological Science, 10*, pp 119-125.

Wan, H., Aggleton, J. P. & Brown, M. W. (1999). Different contributions of the hippocampus and perirhinal cortex to recognition memory. *The Journal of Neuroscience. 19,* pp 1142-1148.

Warburton, E. C., Morgan, A., Baird, A., Muir, J. L. & Aggleton, J. P. (2001). The conjoint importance of the hippocampus and anterior thalamic nuclei for allocentric spatial learning: evidence from a disconnection study in the rat. *The Journal of Neuroscience, 21,* pp 7323-7330.

Watanabe, K. & Kawana, E. (1980). A horseradish peroxidase study on the mammillothalamic tract in the rat. *Acta Anatomica, 108,* pp 394-401.

Wechsler, D. (1997). *Wechsler Memory Scale* (3rd edition). Texas, US: The Psychological Corporation.

Wible, C. G., Shiber, J. R. & Olton, D. S. (1992). Hippocampus, fimbria-fornix, amygdala, and memory: Object discrimination in rats. *Behavioural Neuroscience, 106,* pp 751-761.

Wieshmann, U. C., Clark, C. A., Symms, M. R., Franconi, F., Barker, G. J. & Shorvon, S. D. (1999). Reduced anisotropy of water diffusion in structural cerebral abnormalities demonstrated with diffusion tensor imaging. *Magnetic Resonance Imaging, 17,* pp 1269-1274.

Wilson, C. R. E., Charles, D. P., Buckley, M. J. & Gaffan, D. (2007). Fornix transection impairs learning of randomly changing object discriminations. *The Journal of Neuroscience, 27*, pp 12868-12873.

Wilson, D. I., Langston, R. F., Schlesiger, M. D., Wagner, M., Watanabe, S. & Ainge, J. A. (2013). Lateral entorhinal cortex is critical for novel object-context recognition. *Hippocampus, 23,* pp 352-366.

Winecoff, A., Clithero, J. A., Carter, R. M., Bergman, S. R., Wang, L. & Huettel, S. A. (2013). Ventromedial prefrontal cortex encodes emotional value. *The Journal of Neuroscience, 33,* pp 11032-11039.

Winters, B. D., Saksida, L. M. & Bussey, T. J. (2008). Object recognition memory: neurobiological mechanisms of encoding, consolidation and retrieval. *Neuroscience and Biobehavioral Reviews, 32,* pp 1055-1070.

Wintzer, M. E., Boehringer, R., Polygalov, D. & McHugh, T. J. (2014). The hippocampal CA2 ensemble is sensitive to contextual change. *The Journal of Neuroscience, 34,* pp 3056-3066.

Wirth, S., Yanike, M., Frank, L. M., Smith, A. C., Brown, E. N. & Suzuki, W. A. (2003). Single neurons in the monkey hippocampus and learning of new associations. *Science, 300,* pp 1578-1581.

Wisden, W., Errington, M. L., Williams, S., Dunnett, S. B., Waters, C., Hitchcock, D., Evan, G., Bliss, T. V. & Hunt, S. P. (1990). Differential expression of immediate early genes in the hippocampus and spinal cord. *Neuron, 4,* pp 603-614.

Witter, M. P. & Amaral, D. G. (1991). Entorhinal cortex of the monkey: V. Projections to the dentate gyrus, hippocampus, and subicular complex. *The Journal of Comparative Neurology, 307,* pp 437-459.

Witter, M. P. (1986). A survey of the anatomy of the hippocampal formation, with emphasis on the septotemporal organization of its intrinsic and extrinsic connections. *Advances in Experimental Medicine and Biology, 203,* pp 67-82.

Witter, M. P. (1989). Connectivity of the rat hippocampus. In (Chan-Palay, V. & Kohler, C. (Eds.), *The Hippocampus - New Vistas (Neurology and Neurobiology)* (pp 67-82). New York, US: Alan Liss Inc.

Witter, M. P. (2006). Connections of the subiculum of the rat: topography in relation to columnar and laminar organization. *Behavioural Brain Research, 174,* pp 251-264.

Witter, M. P., Naber, P. A., van Haeften, T., Machielsen, W. C., Rombouts, S. A., Barkhof, F., Scheltens, P. & Lopes da Silva, F. H. (2000a). Cortico-hippocampal communication by way of parallel parahippocampal-subicular pathways. *Hippocampus, 10,* pp 398-410.

Witter, M. P., Ostendorf, R. H. & Groenewegen, H. J. (1990). Heterogeneity in the dorsal subiculum of the rat. Distinct neuronal zones project to different cortical and subcortical targets. *The European Journal of Neuroscience, 2,* pp 718-725.

Witter, M. P., Wouterlood, F. G., Naber, P. A. & Van Haeften, T. (2000b). Anatomical organization of the parahippocampal-hippocampal network. *Annals of the New York Academy of Sciences, 911,* pp 1-24.

Wixted, J. T. & Squire, L. R. (2010). The role of the human hippocampus in familiarity-based and recollection-based recognition memory. *Behavioural Brain Research, 215,* pp 197-208.

Woollett, K., Spiers, H. J. & Maguire, E. A. (2009). Talent in the taxi: a model system for exploring expertise. *Philosophical Transactions of the Royal Society B, 3674,* pp 1407-1416.

Wright, N. F., Erichsen, J. T., Vann, S. D., O'Mara, S. M. and Aggleton, J. P. (2010). Parallel but separate inputs from limbic cortices to the mammillary bodies and anterior thalamic nuclei in the rat. *The Journal of Comparative Neurology, 518,* pp 2334-2354.

Wright, N. F., Vann, S. D., Erichsen, J. T., O'Mara, S. M. & Aggleton, J. P. (2013). Segregation of parallel inputs to the anteromedial and anteroventral thalamic nuclei of the rat. *The Journal of Comparative Neurology, 521,* pp 2966-2986.

Wu, D., Xu, J., McMahon, M. T., van Zijl, P. C., Mori, S., Northington, F. J. & Zhang, J. (2013). In vivo high-resolution diffusion tensor imaging of the mouse brain. *NeuroImage, 83,* pp 18-26.

Wymbs, N. F., Bassett, D. S., Mucha, P. J., Porter, M. A. & Grafton, S. T. (2012). Differential recruitment of the sensorimotor putamen and frontoparietal cortex during motor chunking in humans. *Neuron, 74,* pp 936-946.

Wyss, J. M., Swanson L. W. & Cowan, W. M. (1980), The organization of the fimbria, dorsal fornix and ventral hippocampal commissure in the rat. *Anatomy and Embryology, 158,* pp 303-316.

Xiang, J. Z. & Brown, M. W. (1998). Differential neuronal encoding of novelty, familiarity and recency in regions of the anterior temporal lobe. *Neuropharmacology, 37,* pp 657-676.

Xiao, D. & Barbas, H. (2002a). Pathways for emotions and memory. I. Input and output zones linking the anterior thalamic nuclei with prefrontal cortices in the rhesus monkey. *Thalamus & Related Systems, 2,* pp 21-32.

Xiao, D. & Barbas, H. (2002b). Pathways for emotions and memory. II. Afferent input to the anterior thalamic nuclei from prefrontal, temporal, hypothalamic areas and the basal ganglia in the rhesus monkey. *Thalamus & Related Systems, 2,* pp 33-48.

Yamada, H., Matsumoto, N. & Kimura, M. (2004). Tonically active neurons in the primate caudate nucleus and putamen differentially encode instructed motivational outcomes of action. *The Journal of Neuroscience, 24,* pp 3500–3510.

Yassa, M. A. & Stark, C. E. (2011). Pattern separation in the hippocampus. *Trends in Neurosciences, 34,* pp 515-525.

Yeterian, E. H. & Pandya, D. N. (1988). Corticothalamic connections of paralimbic regions in the rhesus monkey. *The Journal of Comparative Neurology, 269,* pp 130-146.

Yeo, S. S., Seo, J. P., Kwon, Y. H. & Jang, S. H. (2013). Precommissural fornix in the human brain: a diffusion tensor tractography study. *Yonsei Medical Journal, 54,* pp 315-320.

Yoder, R. M. & Taube, J. S. (2011) Projections to the anterodorsal thalamic nucleus and lateral mammillary nuclei arise from different cell populations within the postsubiculum: implications for the control of head direction cells. *Hippocampus, 21,* pp 1062-1073.

Yu, Y., FitzGerald, T. H. B. & Friston, K. J. (2013). Working memory and anticipatory set modulate midbrain and putamen activity. *The Journal of Neuroscience, 33*, pp 14040-14047.

Yukie, M. (2000). Connections between the medial temporal cortex and the CA1 subfield of the hippocampal formation in the Japanese monkey (Macaca fuscata). *The Journal of Comparative Neurology, 423,* pp 282-298.

Zahr, N. M., Rohlfing, T., Pfefferbaum, A., Sullivan, E. V. (2009). Problem solving, working memory, and motor correlates of association and commissural fibre bundles in normal aging: a quantitative fibre tracking study. *NeuroImage, 44*, pp 1050-1062.

Zangenehpour, S. & Chaudhuri, A. (2002). Differential induction and decay curves of c-fos and zif268 revealed through dual activity maps. *Molecular Brain Research, 109,* 221–225.

Zeidman, P. & Maguire, E. A. (2016). Anterior hippocampus: the anatomy of perception, imagination and episodic memory. *Nature Reviews Neuroscience, 17,* pp 173-182.

Zeidman, P., Mullally, S. L. & Maguire, E. A. (2015). Constructing, perceiving, and maintaining scenes: hippocampal activity and connectivity. *Cerebral Cortex, 25,* pp 3836-3855.

Zhang, J., McQuade, J. M., Vorhees, C. V. & Xu, M. (2002). Hippocampal expression of c-fos is not essential for spatial learning. *Synapse, 46,* pp 91-99.

Zhu, X. O., Brown, M. W. & Aggleton, J. P. (1995a). Neuronal signalling of information important to visual recognition memory in rat rhinal and neighbouring cortices. *The European Journal of Neuroscience, 7,* pp 753-765.

Zhu, X. O., Brown, M. W., McCabe, B. J. & Aggleton, J. P. (1995b). Effects of the novelty or familiarity of visual stimuli on the expression of the immediate early gene c-fos in rat brain. *Neuroscience, 69,* pp 821-829.

Zhu, X. O., McCabe, B. J., Aggleton, J. P. & Brown, M. W. (1996). Mapping visual recognition memory through expression of the immediate early gene c-fos. *Neuroreport, 7,* pp 1871-1875.

Zhuang, L., Wen, W., Trollor, J. N., Kochan, N. A., Reppermund, S., Brodaty, H. & Sachdev, P. (2012). Abnormalities of the fornix in mild cognitive impairment are related to episodic memory loss. *Journal of Alzheimer's Disease, 29,* pp 629-639.

Zola, S. M., Squire, L. R., Teng, E., Stefanacci, L., Buffalo, E. A. & Clark, R. E. (2000). Impaired recognition memory in monkeys after damage limited to the hippocampal region. *The Journal of Neuroscience, 20,* pp 451-463.

Zola-Morgan, S., Squire, L. R. & Amaral, D. G. (1986). Human amnesia and the medial temporal region: enduring memory impairment following a bilateral lesion limited to field CA1 of the hippocampus. *The Journal of Neuroscience, 6,* pp 2950-2967.

Zola-Morgan, S., Squire, L. R. & Amaral, D. G. (1989). Lesions of the hippocampal formation but not lesions of the fornix or the mammillary nuclei produce long-lasting memory impairment in monkeys. *The Journal of Neuroscience, 9,* pp 898-913.

Zola-Morgan, S., Squire, L. R., Rempel, N. L., Clower, R. P. & Amaral, D. G. (1992). Enduring memory impairment in monkeys after ischemic damage to the hippocampus. *The Journal of Neuroscience, 12,* pp 2582-2596.